DEVELOPMENT OF THERMAL ENERGY STORAGE AND COOKER MODULE FOR THE INTEGRATED SOLAR ENERGY PROJECT

by

Abdulsalam S.A. Sulaiman

Submitted in fulfilment of the academic requirements for the degree of

Master of Science in Engineering

at

The University of KwaZulu-Natal

School of Mechanical Engineering

Supervisor: Dr. F. L. Inambao

2008

Declaration

I, hereby declare that the thesis entitled Development of Thermal Energy Storage and Cooker Module for the Integrated Solar Energy Project is the result of my own investigation and research except where due acknowledgement is made to others, and that it has not been submitted in part or in full for any degree to any other University.

Abdusalam Sulaiman 2008

ACKNOWLEDGEMENTS

I would like to express my heart-felt and most profound gratitude's to my Supervisor, Dr. F. L. Inambao, for his priceless support (across the spectrum) and indispensable guidance throughout the course of this work. His vast and in-depth experience in Solar Energy and Heat Transfer has been a unique resource which I couldn't do without. Discussions with him always left me refreshed with new energy and inspiration to put into further work. May God Bless you!

I would like to express my deep and sincere gratitude to my current and former (Mr. G.L. Reinhardt) supervisors for their understanding, encouragement and personal guidance which enabled me to complete this thesis.

Lastly, I owe my loving thanks to my wife Zainab Sawehli and my three sons Abdulrahman, Taha and Elsadiq who have sacrificed so much to remain with me throughout this period abroad. Without their encouragement and understanding it would have been impossible for me to finish this work. My special gratitude is due to my parents and family in Libya for their loving support.

Abstract

Large percentages of the South African population have no access to grid power and are located at distances that make provision for such facility uneconomical. Also traditional fuels are under pressure. Most areas in South Africa receive 300 days of sunshine per year. The proposed solar system addresses the needs of such communities.

A solar thermal energy storage system utilizing phase change material has been proposed that can overcome the time mismatch between solar availability and demand. The system consists of two types of thermal heat storage. The latent heat storage used Phase Change Materials (PCM) which melts at a sufficiently high temperature for cooking a variety of food types. By choosing a suitable PCM to take advantage of the latent heat absorbed during phase changes. Heat losses from both the latent heat storage and condenser are captured in the surrounding sensible heat store.

The objective of this project to develop a prototype modules which together as a system could provide the essential domestic power requirements of the target groups. This includes power for cooking, hot water and in addition a limited electrical power supply for the system itself as well as for other minor loads.

CONTENTS

LIST OF FIGURES

LIST OF TABLES

NOMENCLATURE

A	Cross-sectional area through the heat conducting, Surface area of the object, Contact Area
A/D	Analogue to Digital
ASME	American Society of Mechanical Engineering
C_p	Specific heat (isobaric) (J/kg°C).
$\overline{C}_{p_l}$	Average specific heat between T_m and T_2
$\overline{C}_{p_s}$	Average specific heat between T_i and T_m
D	Duct
d	Diameter
ETSC	Evacuated Tube Solar Collector
HSU	Heat Storage Unit
HTF	Heat Transfer Fluid
HTS	Heat Transfer Salts
ΔH_m	Latent heat of fusion per unit mass (kJ/kg)
h_f	Film coefficient
h_t	Contact resistance, Contact Coefficient
I	Incident radiation
IR	Infrared
kWh	Kilowatt-hours
L	Liquid state
LHS	Latent Heat Storage
LPG	Liquid Petroleum Gas
M	Paraboloidal mirror
m	Mass of heat storage medium (kg)
m_a	Mass Fraction melted
n.a.	Not available
OTEC	Ocean Thermal Energy Conversion
P	Pebble-bed heat storage unit.
PC	Personal Computer
PCM	Phase Change Material

PV	Photovoltaic
q	Heat transfer rate
q"	Heat flux
$q_{absorbed}$	Heat absorbed by the surface
$q_{conduction}$	Heat transfer by conduction
$q_{convection}$	Heat transfer from a surface by convection
$q_{emitted}$	Heat radiation emitted by an object
Q	Quantity of heat stored (J), Thermal energy
R	Receiver
RTD	Resistance Thermometer Detector
S	Solid state
S_1	Lower Stand houses the main axis drive motor
S_2	Upper stand houses
SHS	Sensible Heat Storage
T_i	Temperature (°C), i-indicating specific position or object.
T_∞	Ambient or fluid temperature
TES	Thermal Energy Storage
T_m	Melting temperature
$T_{Surface}$	Surface temperature
UKZN	University of Kwazulu-Natal
UV	Ultraviolet
v	Volume of heat storage medium (m^3), Fluid velocity
W	Counterweight
w	Wall temperature

Greek symbols

μ	Viscosity
κ	Thermal conductivity
α	Absorptivity, Thermal diffusivity
ε	Emissivity
σ	Stefan-Boltzmann constant
ρ	Density (kg/ m^3)

CHAPTER 1
INTRODUCTION

1.1 Solar Energy

The most abundant source of energy to be found on the planet is solar energy, and in comparison to other energy sources derived from oil, coal and nuclear reaction, solar energy is also much cleaner. Solar energy is usually harnessed and transferred to thermal energy for the purposes of heating homes and water, or to generate electricity.

Since the availability of solar energy is dependent on various conditions such as time, weather conditions, latitude, and the fluctuating demand for electricity over long periods, the originally harnessed energy needs to be stored. This energy can be stored as thermal energy or electricity, but thermal energy storage is considered the more economical method [1].

There are diverse forms of renewable energy sources including solar, geothermal, wind, tidal, wave, hydroelectric, and ocean thermal energy conversion (OTEC). Although some of these examples have been applied successfully in practice, many are contingent on climatic conditions, and more importantly, some are cyclic in nature. In addition to this, the demand for energy is also time-based which means that people's need for energy varies from season to season, and from day to night. It is this cyclic nature of both the supply and demand for energy that has created the need for energy storage. By using energy storage the supply and demand curves can be shifted with respect to each other in a given time frame, to allow supply and demand peaks to fall in phase. Alternatively, storage can be used to flatten-out the valleys and peaks which occur in the demand and supply curves, thus making the matching of the two curves an easy task [2].

The industrial usage of thermal energy storage systems was first initiated in the mid-nineteenth century, when ceramic regenerators were used to recover waste heat from high temperature flue gasses. Thermo-chemical storage systems were also used to provide mechanical energy for the propulsion of steam-driven vehicles as early as 1880. The principle involved the absorption of waste steam using sodium hydroxide (NaOH), which subsequently liberated sufficient energy to evaporate the water in the boilers. The NaOH was then re-concentrated by the evaporation of the water [3].

In more recent times, Stirling engines using thermal energy storage (TES) units with high temperature phase change materials have been proposed for buses and passenger vehicles in

Europe and the USA. Latent heat TES is presently being utilized in certain Volkswagen vehicles to reduce engine wear. Under cold starting conditions, the engine is rapidly brought to operating temperature through the use of a modified cooling circuit that transfers heat from a TES unit to the cold engine. This also has the advantage of providing instantaneous hot air for the passenger compartments. The TES unit is charged once the engine has reached operating temperature.

There are a great many possible uses for thermal energy storage, and the ongoing research into this field will have profound implications in the future. In industry, TES can improve plant efficiency by providing a thermal buffer which minimizes the imbalances between the demand and supply of thermal energy in the system. In batch processes, TES is particularly useful for capturing the waste heat from one batch for re-use at a later stage. Many building designs include TES to assist with the cooling and heating loads on a daily and seasonal basis. A common domestic application is the storage of heat from solar collectors and air conditioners in TES units for water heating purposes. Thermal energy storage using phase change materials (PCM) can also be found in many applications in the space industry. The Apollo 15 lunar vehicles used paraffin wax to store the heat from the onboard electronics, while the temperature on the Skylab was controlled using phase change materials. TES will also be required for the solar-driven power systems of satellites, especially when their path is eclipsed by the earth. These power systems are either Brayton or Stirling cycles which require very high temperature heat storage [4].

The Southern African region as a whole receives an average of more than 2,500 hours of sunshine per year, and the average daily solar radiation levels range between 4.5 and 6.5 kilowatt-hours (kWh) per square meter. The annual 24 hour global solar radiation average is about 220 watts per square meter for South Africa, compared to about 150 watts per square meter for parts of the United States and about 100 watts per square meter for Europe [5].

Solar thermal energy finds its simplest application in the form of solar cooking, which in itself has enormous potential for reducing dependence on conventional fuels in the domestic sector. The different types of solar cookers developed for cooking are a box type, a concentrator type and an indirect type. The detailed design, test procedures, theory and utility of solar cookers are well developed. An indirect solar cooker uses a fluid to transfer heat from a solar collector to the cooking pots, but it has more advantages than a box type or concentrator cookers because it provides high thermal power and temperatures without

tracking and allows cooking in the shade or even in a conventional kitchen. One exception is that cooking of food is not possible in the evening. If storage of solar energy can be provided in a solar cooker, then there is the possibility of cooking food during overcast conditions or in the evening and the storage will increase the utility and reliability of the solar cooker. These attractions led us to study the problem of cooking in the evening or during low intensity solar radiation periods [6].

1.2 Problem Statement

In developing countries, most rural villagers are accustomed to earning a low and sporadic income which has a direct bearing on how they select energy services in at least three ways. Firstly, households in this category don't have the financial means to afford expensive fuels and energy carriers or even modern end-user appliances, such as efficient and low-pollution stoves. This situation can clearly be witnessed in South Africa, where low-income households have been provided with access to electricity through subsidized electrification programmes, only to be disconnected at a later stage because they have been unable to pay their bills [7]. Secondly, in the competition for the market share, those services that are available in small, discrete quantities will be favored. Thus fuels such as paraffin often diffuse more rapidly than liquefied petroleum gas (LPG) because the latter is economical only when purchased in full tanks. Thirdly, the capital requirements for modern energy appliances such as modern stoves and lanterns can be prohibitively costly [8].

A clear feature of low incomes and the uneven availability of fuels is that these households often meet the same energy service, such as cooking, with a variety of energy carriers [9]. Models must therefore estimate energy services separately from appliance and fuel choices. In the village survey that is used to calibrate the model in this paper, for example, biomass and paraffin are the most common fuels used for cooking. Most households used both, with wood as the primary fuel and paraffin as the second choice for quick-start and small batch cooking. (Even in other villages where electricity is available, expensive electrons are rarely used for cooking by households in the lowest income group.) The choice and quantity of fuel also varies with appliance. Households in the case study typically deploy two fuels for lighting namely wax (as candles) and paraffin- but they are given the freedom to switch to other devices, such as efficient pressurized ('primus') devices for lighting. The switch allows the same energy service (lumens) to be supplied even as the total fuel consumed (joules) declines.

The final selection of service in terms of appliance and fuel have additional effects, namely pollution and other hazards that to date have not been thoroughly analyzed. Most low-income households in South Africa burn wood, coal and other fuels within or near the home dwelling, which exposes occupants to damaging emissions such as carbon monoxide and particulates. The second highest cause of infant mortality in South Africa is respiratory disease, of which the major cause is indoor air pollution from fuel burning [10]. The problem of solar cooking in the evening or during low intensity solar radiation periods also leads to solar energy storage problems.

1.3 Proposed Investigation

At the University of KwaZulu-Natal (UKZN), two specific proposals have been made. The first one is the development of a small solar concentrating system with heat storage for rural food preparation as shown in Figure 1.1.

As the diagram illustrates, a paraboloidal mirror (M) is used to concentrate the incident solar radiation on the absorber mounted inside the ''open volumetric receiver'' (R). Air is then heated to temperatures as high as 400°C as it is forced to flow through the absorber and into duct (D1) at the top of the pebble-bed storage (P). Starting with (P) at ambient temperature, the air transfers heat to the pebbles as it is flows through (P) during the ''charging'' operation, and if the heat transfer between the air and the pebbles were perfect, a step temperature profile (at the inlet temperature) would propagate toward the bottom of the storage leading to cold air emerging from the bottom layer of the pebbles until the bed is ''fully charged''. This then results in a sudden increase in outlet temperature at (D2), and if the flow were interrupted at any time, a perfectly ''stratified'' temperature profile would thus be obtained - i.e. hot and cold layers of pebbles would be distinctly separated.

When it comes to utilizing the thermal energy stored in (P), the direction of the airflow is reversed during the ''discharging'' process, so that cold air enters the bottom of the storage at (D2). Consequently, the heat exchange between the incoming air and the pebbles leads to the temperature profiles being pushed upward, and in the ideal case of optimum heat transfer and perfect insulation, the air then emerges from (D1) at the top of the bed at the original charging temperature until the storage is completely discharged. In practical pebble-bed storage systems the thermal stratification is not ideal and the front of the temperature profile is not very sharp, especially after repeated ''charging'' and

''discharging'' cycles. The temperature profile tends to increase gradually along the bed. The conceptual diagram shows a range of appliances (U), which can utilize the solar thermal energy stored in (P) [11].

The system, which consists of a parabolic reflector mounted on a polar axis tracker, has been designed and built. Air at atmospheric pressure is heated by the concentrated solar radiation to temperatures of up to 400°C as it sucked through the receiver and into the pebble-bed heat storage unit, by means of a fan at the bottom of the storage. The stored heat is recovered by the reversal of the fan and the resulting hot air can be used in a convection oven and other appliances.

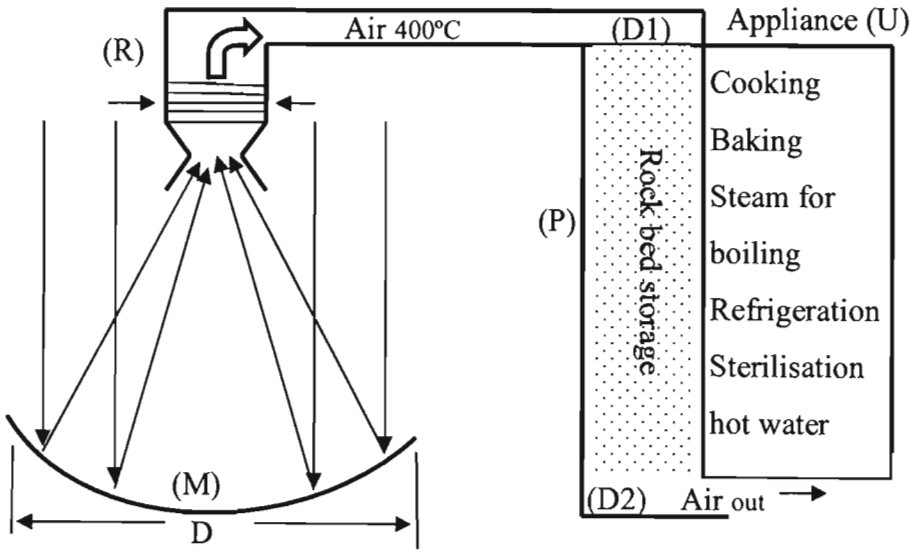

Figure 1.1 Conceptual Diagram of Concentrating System with Potential Appliances Indicated [11].

W	Counterweight
R	Receiver
D	Duct
S1	Lower Stand houses the main axis drive motor
S2	Upper stand houses
P	pebble-bed heat storage unit.
M	Paraboloidal mirror

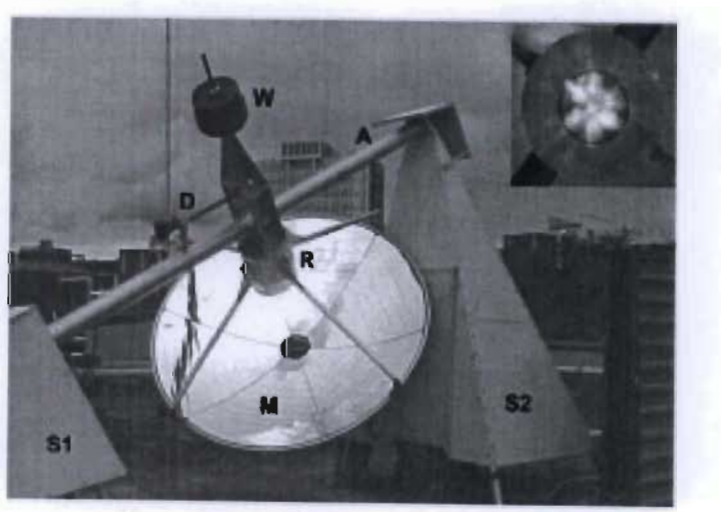

Figure 1.2 Prototype Solar Thermal Concentrating System [11].

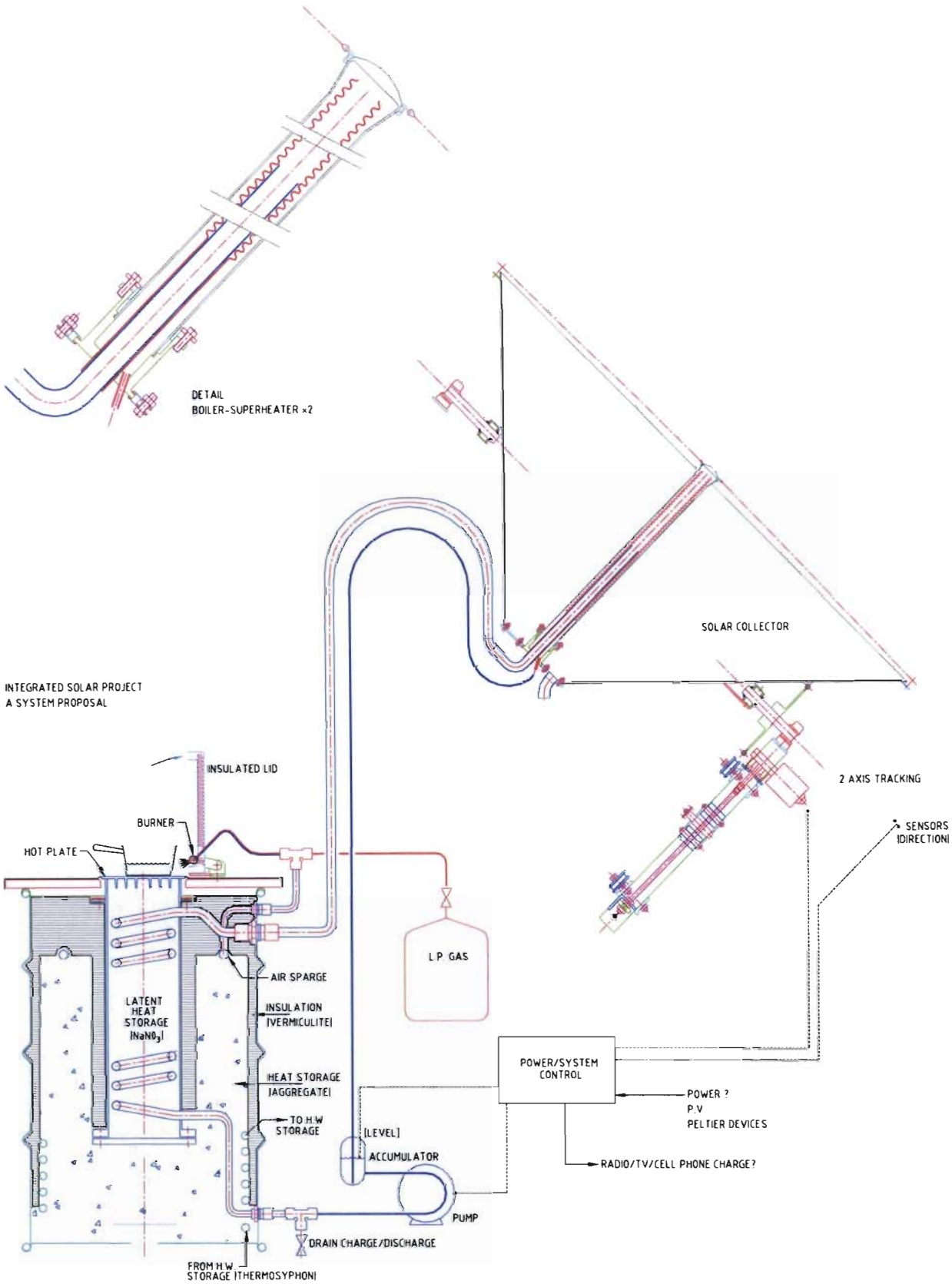

Figure 1.3 Integrated Storage Cooker System (Author design with supervisors assist).

The second system Integrated storage/cooker is shown in Figure 1.3. This system consists of a solar collector and two types of thermal heat storage, the latent heat storage used Phase Change Materials (PCM) which melts at a sufficiently high temperature for cooking a variety of food types. The proposed heat transfer fluid is either water or Dowtherm A., which is circulated, in a hermitically sealed circuit, to transfer the heat to PCM vessel. By choosing a suitable PCM to take advantage of the latent heat absorbed during phase of the material from solid form to liquid form, a large quantity of daytime solar energy can be stored and used later. Heat losses from both the latent heat storage and condenser are captured in the surrounding sensible heat store. The air in this can be used as an economizer for the back-up burner.

1.4 Aim and Objectives

The aim of this research is to develop prototype modules, which together as a system provide the essential domestic power requirements of family remote from the national grid. This includes power for cooking and hot water.

The specific and main objectives of the project are to:

- Design a set of experiments to compare the proposed system to that of commercially available, electric hot plates and ovens.
- Determine the physical properties of locally available industrial grade heat storage materials, specifically temperatures, latent heat of fusion and thermal conductivity for each.
- Design an experiment to determine the heat transfer characteristics of the proposed design.
- Use the model to predict suitable design parameters.
- Build and test the optimized model.
- Draw conclusions.

New latent heat thermal energy storage with heat pipe exchanger was designed and manufactured. The performance of the unit under various possible operation modes was investigated experimentally.

1.5 Structure of the Thesis

Chapter 1 gives an introduction to solar energy, contains a problem statement, proposed investigation, aims and objectives. Chapter 2 contains an overview on thermal energy

storage, heat transfer analysis, applications and previous work carried out on the solar heat storage and solar cooking system. Chapter 3 gives a review of PCM heat transfer analysis and application. The chapter 3 also gives a review of heat transfer fluids. Chapter 4 gives details of the heat storage salts. Chapter 5 gives details of the experimental instruments and equipment and procedure. Chapter 6 describes the energy consideration and material selection. Chapter 7 gives details of the experimental design and setup. Chapter 8 gives a detailed description of the experimental results and discussion. The conclusion and relevant recommendations are in chapter 9.

1.6 Summary

An introduction to solar energy, its usage of thermal energy storage and its application in the form of solar cooking are discussed in this chapter. The chapter concentrates on the problem statement, proposed investigation and the objectives of the research project.

The discussion of this chapter is based on the fact that the Southern African region as a whole receives an average of more than 2,500 hours of sunshine per year, and the average daily solar radiation levels range between 4.5 and 6.5 kilowatt-hours (kWh) per square meter. In the general context of using solar energy generators and in terms of their operating requirements, two components are required to have a functional solar energy unit, namely a collector and a storage unit. The collector simply collects the radiation that falls on it and converts a fraction of it to other forms of energy (either electricity and heat or heat alone).

The storage unit is required due to the non-constant nature of solar energy; at certain times only a very small amount of radiation will be received. At night or during heavy cloud cover, for example, the amount of energy produced by the collector will be quite small. The storage unit can hold the excess energy produced during the periods of maximum productivity, and release it when the productivity drops.

CHAPTER 2
AN OVERVIEW OF THERMAL ENERGY STORAGE

2.1 An Overview

Due to the fact that solar energy is a time-dependent energy resource, it requires appropriate storage and utilization in terms of daily energy requirements. Assessing energy storage needs an awareness of a solar process system, the major components of which are the solar collector, storage units, conversion devices (such as air conditioners or engines), loads, auxiliary (supplemental) energy supplies, and control systems. The performance of each of these components is related to that of the other. The dependence of the collector performance on temperature makes the whole system performance sensitive to temperature. The optimum capacity of an energy storage system depends on the expected time dependence of solar radiation availability, the nature of loads to be expected on the process, degree of reliability, the manner in which auxiliary energy is supplied, and an economic analysis weighing the relative use of solar and auxiliary energy [12].

One of the main benefits of solar energy as an alternative energy source is that it is pollution free. Conversion into thermal energy or directly to electricity (by photovoltaic conversion) can readily be done. The thermal energy conversion , divided into three categories, can be grouped as (i) low (<10°C), which deals with solar cooling , medium (10-150°C), which includes flat plate collectors, air heathers , solar distillation system, swimming pool and greenhouse heating etc. (iii) high (>150°C) which includes the concentrator, used in power generation or cooking systems [13].

Solar cooking systems have evolved in various guises beginning from hot box ovens to focusing dish cookers; solar cookers in which the cooking pot is placed at the focus of a concentrating mirror have not been widely embraced due to the necessity of having to continually adjust the orientation of the concentrator [14].

The physical or chemical process which occurs in the store during the charge and discharge operation is referred to as thermal energy storage (TES). The store consists of the storage vessel (tank) which is usually thermally insulated, the storage, the storage medium, the charging and discharging devices, and the auxiliaries. The manner in which energy for charging the accumulator is extracted from the energy source and in which energy is discharged from the accumulator determines the design of the storage system, and is in many cases, transformed into the required form of energy [13].

2.2 Advantages of Solar Thermal Energy [15]

1. Solar thermal energy makes use of a renewable natural resource which is readily available in most parts of the world.
2. Solar energy used by it creates no carbon dioxide or other toxic emissions.
3. The heated fluid can be stored in insulated tanks allowing energy to be used during brief cloudy or overcast periods.
4. New equipment and technological advances have reduced the cost of solar thermal power to a level that can be competitive with fossil-fuel generated electricity in some areas.
5. Use of solar thermal energy to heat water or generate electricity will help reduce the dependence on imported fossil fuels.
6. Solar water heaters are an established technology, readily available on the commercial market, and simple enough to build, install and maintain by yourself.

2.3 Disadvantages of Solar Thermal System [15]

1. Solar thermal systems are not cost-effective in areas which have long periods of cloudy weather or short daylight hours. Efficiency is also reduced by atmospheric haze or dust.
2. In cooler climates, freezing can damage collecting system components, such as pipes.
3. The arrays of collecting devices for large power production systems cover extensive land areas. This land could be used for agricultural, residential, resort or commercial purposes.
4. The reflective surfaces of some collectors may be disturbing or undesirable in certain areas.
5. These systems only work with sunshine and do not operate at night or in inclement weather. Storage of hot water for domestic or commercial use is simple, using insulated tanks, but storage of fluids at the higher temperatures needed-for electrical generation, or storage of electricity itself, needs further technical development.

2.4 Areas of Research

The various areas of research in thermal storage systems can be classified as are shown in Figure 2.1. The present considerations for the design and develop prototype modules, which together as a system provide the essential domestic power requirements of family remote from the national grid, includes power for cooking and hot water were materials research, selection of materials, thermal storage materials, construction of materials, thermo physical properties, short term behavior, long term behavior, thermal cycle, useful life and heat exchanger development , selection of type of heat exchanger, experimental research, thermal analysis. The green colour in Figure 2.1 and in Figure 2.2 represents the areas of author's participation.

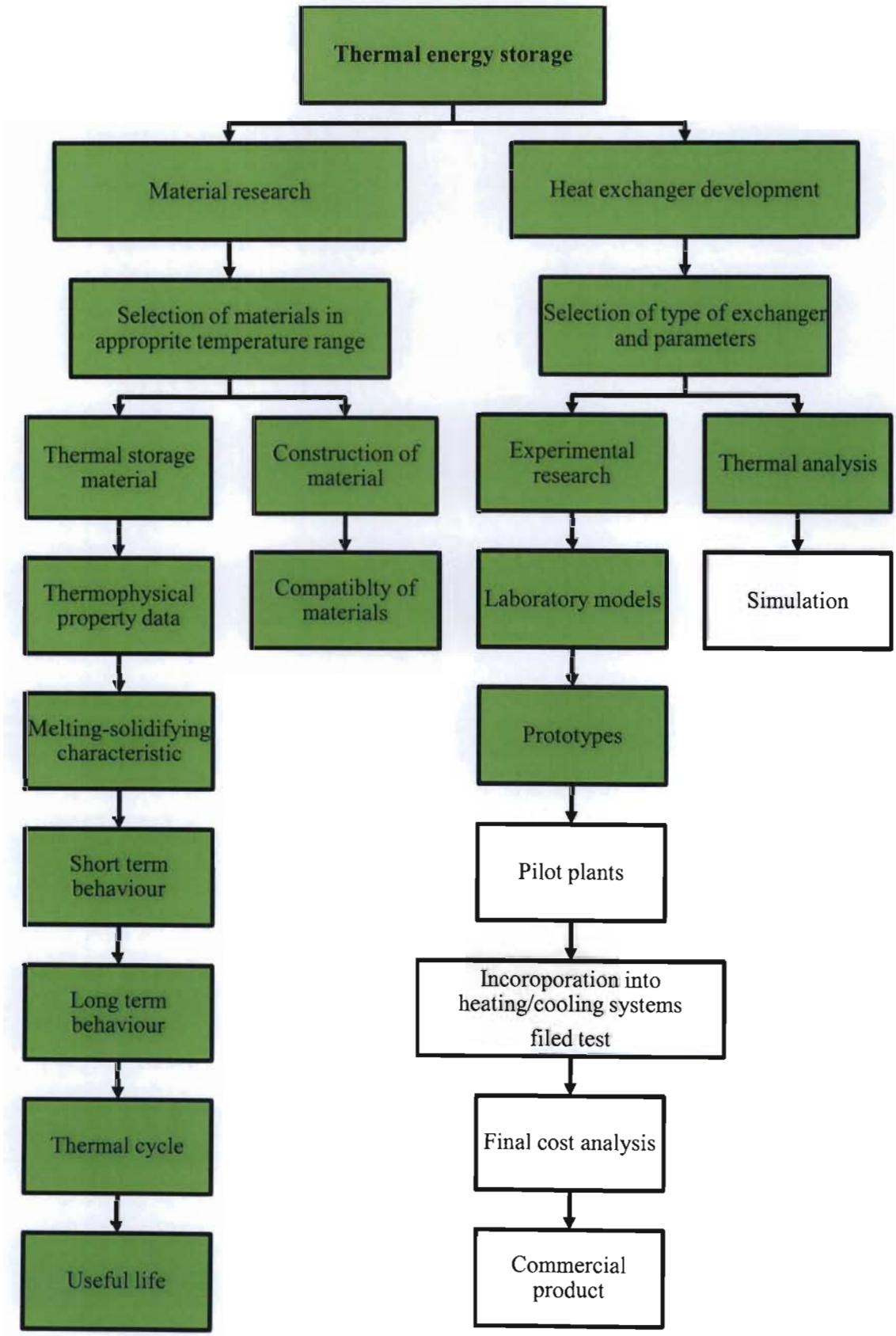

Figure 2.1 Areas of Research in Thermal Storage Systems [16].

2.5 Classification of the Substances Used for TES

The classification of the substances used for TES and complete review of the types of material which have been used, their classification, characteristics, advantages and disadvantages and the various experimental techniques used to determine the behaviour of these materials in melting and solidification are well described in references [16-20]. Classification of the substances used for TES, shown in Figure 2.2. In this research project, Materials, Sensible heat, Latent heat, Solid-Liquid phase, Inorganic, Mixtures Temperature intervals and Hydrated Salts have been considered.

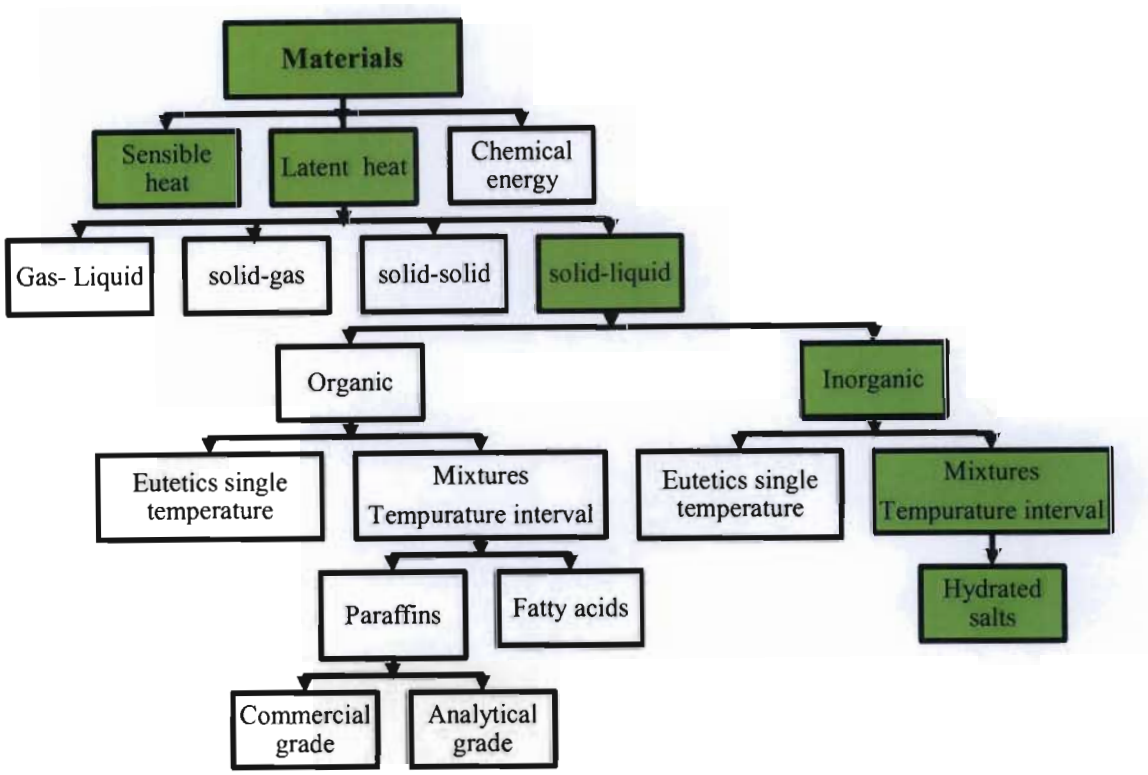

Figure 2.2 Classifications of Energy Storage Materials [16].

2.6 Sensible Heat Storage

Sensible heat and latent heat are the two available choices when it comes to storing thermal energy. Sensible heat storage systems utilize the heat capacity and the change in temperature of the material during the process of charging and discharging. The temperature of the storage material increases when energy is absorbed and decreases when energy is withdrawn. The charging and discharging operations, in a sensible heat storage system, can be assumed to be completely reversible for an unlimited number of cycles, over the life-span. The sensible heat Q gained or lost by a material in changing temperature from T_1 to T_2 is:

$$Q = m\int_{T_1}^{T_2} C_p dT = v\int_{T_1}^{T_2} \rho C_p dT \quad \text{..... 2.1}$$

Where Q = Quantity of heat stored (J),

m = Mass of heat storage medium (kg),

T = Temperature (°C),

T_I = Initial temperature (°C),

v = Volume of heat storage medium (m^3),

T_2 = Final temperature (°C),

ρ = Density of heat storage medium (kg/ m^3),

C_P = Specific heat (J/kg°C).

Equation 2.1 clearly shows the higher the specific heat and density of the material, the higher the energy stored in a given volume of the material will be. However, there are several other parameters affecting the performance of the system, viz., the operating temperature, thermal conductivity, thermal diffusivity, vapor pressure, compatibility between the storage material and the container, stability of the material at the highest temperature of the cycle and the cost of the system [13].

Increasing the temperature of the storage medium has a direct effect on sensible heat storage. As a result, it is desirable for the storage medium to have high specific heat capacity, long term stability under thermal cycling, compatibility with its containment and, most importantly, low cost. Sensible heat storage may be classified on the basis of the heal storage media as Liquid media storage (like water, oil based fluids, molten salts etc.) and Solid media storage (like rocks, metals etc.) [21].

Table 2.1 illustrates the differences between the sensible heat storage using a rock bed and water tank and the latent heat storage using organic and non organic compounds. The advantage of the latent heat over the sensible heat is clear from the comparison of the volume and mass of the storage unit required for storing a certain amount of heat. It is also clear from Table 2.1 that inorganic compounds, such as hydrated salts, have a volumetric thermal storage density, which is higher than that of most organic compounds due to their higher latent heat and density.

2.6.1 Liquid Media Storage

Heat storage liquids are abundant as well as economically viable. At low temperature storage in water is one of the best storage media. It has higher specific heat than other materials, and it is cheap and widely available. However, due to its high vapor pressure, it requires costly insulation and pressure withstanding containment for high temperature applications. Water can be used over a

wide range of temperature, say 25-90°C. For a 60°C temperature change, water will store 250 kJ/kg. Hot water is required for washing, bathing etc.. and it is commonly employed in radiators for space heating. Water can be used as storage and as a transport medium of energy, for example, in a solar energy system. Consequently, it is the most widely used storage medium today for solar based warm water and space healing applications [1, 22]. Because of its simplicity, a large amount of published data is available on the design criteria for water storage media.

Table 2.1 Comparison of Various Heat Storage Media [20].

Property	Sensible heat storage		Phase Change Materials	
	Rock	Water	Organic	Inorganic
Latent heat of fusion (kJ/kg)	*	*	190	230
Specific heat (kJ/ kg)	1.0	4.2	2.0	2.0
Density (kg/m^3)	2240	1000	800	1600
Storage mass for storing (10^6 J/kg)	67000	16000	5300	4350
Relative mass**	15	4	1.25	1.0
Storage volume for storing (10^6 J/kg)	30	16	6.6	2.7
Relative volume**	11	6	2.5	1.0

*Latent heat of fusion is not of interest for sensible heal storage,

**Relative mass and volume are based on latent heat storage in inorganic phase change materials

Thermal stratification or thermocline in a solar water heat storage tank can be established due to the buoyancy forces, which ensure the highest temperature at the top and the lowest temperature at the bottom of the tank. Stratification is achieved through the elimination of mixing during storage, whereby a two-fold advantage is gained:

(i) The efficiency with which the energy can be used will be improved if it is supplied to the load at the temperature it was collected rather than at a lower mixed storage temperature.

(ii) The amount of energy collected may be increased if the collector inlet fluid temperature is lower than the mixed storage temperature.

Steel, aluminum, reinforced concrete and fiber glass are all usable materials from which water storage tanks can be built. The tanks are insulated with glass wool, mineral wool or poly-urethane. The sizes of the tanks used vary from a few hundred liters to a few thousand cubic meters. For large scale storage applications, underground natural aquifers have been considered. Aquifers are geological formations containing ground water, offering a potential way of storing heat for long periods of time.

2.6.2 Solid Media Storage

Solid materials such as rocks, metals, concrete, sand, bricks etc. can be used in the case of both low and high temperature thermal energy storage. In this instance, the energy can be stored at low or high temperatures, since these materials will not freeze or boil. The difficulties of the high vapor pressure of water and the limitations of other liquids can be avoided by storing thermal energy as sensible heat in solids. Moreover, solids do not leak from their container.

The highest product in the list of solid materials for sensible heat storage is cast iron, which exceeds the energy density level of water storage. However, cast iron is more expensive than stone or brick and, hence, the payback period is much longer. Pebble beds or rock piles are generally preferred as the storage material due to their low cost.

2.6.2.1 Storage in Rocks.

Rock piles or pebble beds are made of a layer of roughly packed rock material which facilitates the flow of the heat transport fluid. The thermal energy is stored in the packed bed by forcing heated air into the bed and utilized again by re-circulating ambient air into the heated bed. The energy stored in a packed bed storage system depends, apart from the thermo physical properties of the material, on several parameters, including rock size and shape, packing density, heat transfer fluid etc.

A further storage option for solar energy is the use of rocks or pebbles (packed in insulated vessels), which makes it convenient to install in buildings. This type of storage is used very often for temperatures up to 100°C in conjunction with solar air heaters. Typically, the characteristic size of the pieces of rock used varies from 1 to 5 cm. An approximate thumb rule followed for sizing is to use 300-500 kg of rock per square meter of solar collector area for space heating applications. For a temperature change of 50°C, rocks and concrete will store around 36 kJ/kg. Rock or pebble bed storage can also be used for much higher temperatures, up to 1000°C. King and Burns in 1981 use a number of characteristics, typically particle size, void fraction, bed cross-sectional area and bed length, superficial air velocity and Reynolds number, in order to describe the thermal and geometric properties of packed beds. Like rock beds, fluidized beds can be utilized for low, intermediate and high temperature solar applications [1, 22].

Furthermore, the rate of heat exchange between the heat carrying fluid and the storage medium is comparatively faster in fluidized beds than in rock beds, which can be an advantage in several applications. The fluidized bed thermal storage can also be used for waste heat recovery purposes.

2.6.2.2 Storage in Metals.

The majority of materials put forward for use in high temperature (120-1400°C) energy storage are either inorganic salts or metals. Aluminium, magnesium and zinc have been mentioned as suitable examples of metals. The use of metal media may be advantageous where high thermal conductivity is required and where cost is of secondary importance [13]. Solid industrial wastes like copper slag, iron slag, cast iron slag, aluminium slag and copper chips could be used as storage material for energy storage. The design of sensible heat storage units is well described in textbooks [1, 13, 22]

2.6.3 Latent Heat Storage

A distinctly advantageous feature of latent heat storage is the fact that it provides a high energy storage density and has the capacity to store heat as latent heat of fusion at a constant temperature corresponding to the phase transition temperature of the phase change materials (PCMs). For example, in the case of water, 80 times as much energy is required to melt 1 kg of ice as to raise the temperature of 1 kg of water by l° C [23]. This means that a much smaller weight and volume of material is needed to store a certain amount of energy.

2.7 Phase Change Materials (PCMs)

In comparison to sensible-heat storage systems such as rock beds or water tanks, latent-heat storage systems provide greater storage capacity per unit weight or volume, less control complexity, and greater system efficiency.

Additionally, latent-heat systems further utilize some sensible-heat storage above and below the PCM melting point. In the following equations, the first term represents the latent heat; the second term, the sensible heat below the melting point; and the third term, the sensible heat above the melting point. In practical PCM systems the latent-heat term predominates.

$$Q = m\, a_m\, \Delta h_m + \int_{T_i}^{T_m} m\, C_p\, dT + \int_{T_m}^{T_2} m\, C_p\, dT$$

$$Q = m\, [a_m\, \Delta h_m + \bar{C}_{ps}\, (T_m - T_i) + \bar{C}_{pi}\, (T_2 - T_m)] \quad \text{..... 2.2}$$

Where Q = Quantity of heat stored

m = Mass of heat storage medium

a_m = Fraction melted

Δh_m = Heat of fusion per unit mass

T = Temperature

T_i = Initial temperature

T_m = Melting temperature

T_2 = Final temperature

C_P = Specific heat (isobaric)

$\overline{C}_{p_s}$ = Average specific heat between T_i and T_m

$\overline{C}_{p_l}$ = Average specific heat between T_m and T_2

When it comes to systems using solar collectors, either air- or water-cooled, an additional merit of PCM storage is the fact that as the operating temperature of a collector increases, the collection efficiency drops. PCM systems maintain lower collector temperatures with improved efficiency. When used as the heat source-heat sink with heat pumps, PCMs have another advantage. Since PCM storage is isothermal, a heat pump can be configured to operate at maximum efficiency at the PCM melting point. High values of Coefficient of Performance (COP) have been obtained for such systems [24].

2.7.1 Requirements for PCMs [18].

For the present research project the most important criteria for selecting a practical PCM were thermal properties, physical properties, kinetic properties and economic which listed as follows:

2.7.1.1 Thermal Properties

- Suitable phase-transition temperature
- High latent heat of transition
- Good heat transfer

2.7.1.2 Physical Properties

- Favorable phase equilibrium
- Low vapor pressure
- Small volume change
- High density

2.7.1.3 Kinetic Properties

- No super cooling
- Sufficient crystallization rate

2.7.1.4 Chemical Term Properties

- Long- chemical stability
- Compatibility with materials of construction
- No toxicity
- No fire hazard

2.7.1.5 Economics

- Abundance
- Availability
- Cost-effectiveness

The different factors have their own various merits, and the leading issues in research and development have been phase-transition temperature, super cooling, phase-equilibrium behavior, materials of construction, heat transfer technology.

2.7.2 Temperature

When it comes to choosing a PCM for a particular use, it's essential that the operating temperature of the heating or cooling system corresponds to the transition temperature of the storage material. In doing so, the PCM melting point must be chosen at a temperature interval above the operating temperature. This interval must be large enough to provide a sufficient temperature gradient for a satisfactory heat withdrawal rate. However, the temperature interval should not be excessive, since heat losses will increase and system efficiency will decrease. An interval of 5 to 10°C has been employed for many systems [24].

2.7.3 Stability to Segregation

During the early phases of PCM development, the majority of the salt hydrates used for study purposes used to segregate in the process of freezing and melting, leaving denser material to settle to the bottom of the container, thereby significantly reducing the heat storage capacity.
This phenomenon has been a considerable impediment to PCM heat storage development. Because segregation is critical, PCM phase-equilibrium studies have been very important and will be discussed more fully in a later section.

2.7.4 Density

Density and the change in density during phase transition are two critical physical properties for PCMs. High density is preferable to allow a smaller size of storage container. However, lower hydrates, with fewer water molecules coordinated to the inorganic salt, are more dense than materials with higher hydration levels, yet they have lower heats of fusion, i.e., less storage capacity. The two factors must be balanced in choosing a storage material.

PCM heat storage systems encounter difficulties when there is density change during phase transition. Storage containers need to be strong enough to withstand the forces of expansion and contraction. The melting process consists of disruption of the crystal lattice of a compound,

destroying the long-range order of the molecules. The energy needed for this disruption is the fusion energy, which is useful for heat storage. This process is necessarily associated with a change in density as the molecules become more disordered. The density change and the energy absorbed generally rise and fall together, although the relationship has many exceptions [24].

2.7.5 Heat Storage Capacity

It is a requirement that the transition heat be as high as possible, particularly on a volumetric basis, to minimize the physical size of the heat store. However, other factors can be more important, For example, because incongruent melting materials lose storage capacity rapidly and are difficult to stabilize, it is always preferable to choose a stable, congruent melting PCM, even if the heat of fusion is somewhat lower.

2.7.6 Phase-Transition Kinetics

The inherently low crystallization rates of certain salt hydrates which in other respects are promising as heat storage PCMs, are too low to provide a sufficient rate of heat withdrawal in a practical thermal storage system. While some methods of accelerating the crystallization process are known, usually little can be done to convert these salt hydrates into suitable PCMs.

Supercooling is a problematic issue which has raised a high degree of interest. Most salt hydrates drop many degrees below the melting point before crystallization begin. When crystallization begins, the temperature rises to the melting point until freezing is complete. Supercooling is undesirable for PCMs since it interferes with heat withdrawal. For most salt hydrate PCMs, supercooling has been mitigated by adding nucleators, chemicals to initiate the freezing process.

2.7.7 Chemical Stability and Safety

Excluding the problematic issues just discussed, PCMs can also be adversely affected by loss or gain of water of hydration, chemical decomposition, or incompatibility with materials of construction. To prevent alteration in degree of hydration in salt hydrate PCMs, the encapsulating material must be of sufficient thickness and impermeability to prevent in- or out-migration of water vapor. PCMs, especially organic materials, can also degrade by thermal decomposition, hydrolysis, or oxidation.

2.8 Phase Equilibrium Properties [24]

Two general categories of salt hydrates exist with subdivisions on the basis of their phase equilibrium behavior:

1. Segregating hydrates
    - Semicongruent melting
    - Incongruent melting

2. Nonsegregating hydrates
    - Congruent melting
    - Quasi-congruent melting
    - Congruent isomorphous
    - Eutectic

Due to the fact that segregation has caused a wide array of problems for PCM systems, and phase-segregation behavior is determined by which category the system falls in, it is important to era-ploy these terms with technical precision. Regrettably, out of all the salt hydrates the segregating type is more common than the non-segregating variety, so the selection of stable materials is restricted. If a non-segregating hydrate is available with the correct melting point and other properties, it should be selected in preference to a segregating material.

2.8.1 Congruent Melting

Congruent-melting mixtures hold the features of when at the stage of melting or freezing at equilibrium, have precisely the same composition in the liquid and solid phases.

2.8.2 Isomorphous Compositions

Component crystals of isomorphous mixtures are both soluble and form solid solutions. This can take place when lattice parameters of the components are nearly identical and the chemical makeup is similar. Isomorphous mixtures can be either incongruent or congruent melting. In the latter case, segregation does not occur during melting or freezing.

2.8.3 Quasi-Congruent Melting

Quasi-congruent refers to materials which in a technical sense are semi congruent melting but melt and freeze as if they were congruent-melting. In this case kinetics, not equilibrium, determines the behavior of the material, and segregation does not occur. These materials are always suspected since segregation could begin after a long period of desirable behavior.

2.8.4 Semi congruent Melting

With respect to semi congruent melting materials, the liquid and solid phases in equilibrium during a phase transition have different compositions because of conversion of the hydrate to a lower hydrated material through loss of water. This conversion is termed a peritectic reaction.

2.8.5 Incongruent Melting

The behavior during phase-transition of incongruent melting salt hydrates reflects that of semi-congruent materials, except that the peritectic reaction forms an anhydrous salt instead of a lower hydrate. Incongruent-melting PCMs also usually are thickened or gelled to impede the segregation, with varying success. They are more difficult to stabilize than are semi-congruent-melting materials.

2.8.6 Eutectics

A minimum-melting composition of two or more components is called a eutectic. When the components melt and freeze congruently, they form a mixture of the component crystals during crystallization. Eutectics nearly always melt and freeze without segregation since they freeze to an intimate mixture of crystals, leaving little opportunity for the components to separate. On melting both components liquefy simultaneously, again with separation unlikely.

2.9 Nucleation and Crystallization

In the field of PCM technology, the processes of nucleation (i.e., the initiation of crystal formation) and crystallization (i.e., crystal growth) are of great importance. Nearly all salt hydrates super cool before they freeze; that is, when they are cooled, the temperature drops below the equilibrium melting-freezing temperature before freezing begins. Once crystallization has been initiated, the temperature rebounds to the equilibrium melting-freezing temperature and is maintained until freezing is complete [24, 25].

2.9.1 Super-cooling

A well-disciplined PCM should preferably exhibit a minimum of super-cooling - ideally, none. Great efforts have been made to eliminate super-cooling in salt hydrate PCMs. Super-cooling is a natural phenomenon in most materials, and salt hydrates are especially prone to it. The reduction of super-cooling to a minimum in heat storage systems is vital since it interferes with the ability to withdraw stored heat. For example, if one attempts to withdraw heat from a PCM store melting at 27°C, using air heat-transfer fluid at 22°C, more than 5°C super-cooling will not allow any crystallization and thus no heat withdrawal.

2.9.2 Nucleators

The growth of crystals appears at tiny centers where nucleation occurs. Without the presence of such sites, pure salt hydrates super-cool to 50 to 100°C below their melting points. Few materials display this extent of super-cooling since spots on the container wall, tiny particles of dust, or impurities can serve as nucleation centers, often reducing the amount of super-cooling to about 10 to 20°C. Also, super-cooling tends to be lessened as the container size increases since there is a

higher probability of incidental nucleating centers being present. For small, encapsulated PCM masses, super-cooling can be a significant problem [25].

2.9.3 Crystal Growth

For a PCM to be functional, a salt hydrate, once nucleated, needs to crystallize at an adequate rate in order to release energy fast enough to provide the necessary heat input to the system. Most salt hydrates are adequate in this regard, although there are some notable failures, such as calcium nitrate tetra-hydrate. If crystallization proves to be too slow, such as when the hydrate melt is highly viscous, preventing ions from moving to the crystallizing surface, a viscosity reduction additive might be helpful. Most often, however, the material must be abandoned as a PCM.

2.10 PCM Encapsulation

The vast majority of PCMs, including salt hydrate PCMs, need to be encapsulated to ensure their energy storage practicability. The discrete masses of PCM that are surrounded by encapsulation media can range from a hefty chunk weighing a ton or more, contained in a large tank with heat exchanger, down to particles a few micrometers in diameter.

The difficulties of PCM encapsulation are quite complex, due to the fact that the capsule functions not only as a container for the melted PCM but also as a heat-transfer surface, vapor barrier, and structural member and often as a decorative element. Encapsulants thus have rather stringent requirements, and more than one commercial entry has foundered, not because the PCM was inadequate, but because the package was improperly designed [26]. PCM encapsulation has prompted the interest of several researchers. Pros and cons of the different geometries of PCM encapsulation with different materials and their compatibility was discussed by Lane [17, 18].

2.10.1 Requirements

Metal containers are often used for encapsulation because they seal easily, have good physical strength, possess good heat-transfer properties, and are readily available at a low cost. However, since some salt hydrate-metal combinations tend to corrode, a metal encapsulant should be chosen carefully in such systems. Aluminum is not suitable with most salt hydrates. Usually, mild steel can be used if air is excluded from the interior, since oxygen accelerates the attack of many salts on steel. Some nitrate salts cause stress crack corrosion in mild steel. Stainless steel cannot be used with chloride salts, again because of stress crack corrosion. In most cases, organic PCMs are compatible with metal encapsulants but there are exceptions. For example, fatty acid PCMs attack both aluminum and steel. The most important physical properties of the encapsulant are container strength and flexibility, temperature resistance, ultraviolet (UV) stability, and vapor barrier properties.

The majority of PCMs are subject to a significant volume increase during melting and shrinkage during freezing. This causes pressure changes in the air space above the PCM in the sealed container, imposing a stress on the encapsulant. Also, localized, unrelieved volume increases frequently occur during melting, causing further stress. Metal containers must be of sufficient thickness and strength to withstand these stresses. Plastic encapsulants accommodate these stresses through a combination of strength and flexibility [27].

2.10.2 Bulk Storage in Tanks

In the case of when the PCM is contained in a single large mass, as in a tank, the tank itself rarely is the heat-transfer surface; rather, a heat exchanger is immersed in the PCM. While this is analogous to a heat storage water tank, there are important differences. Since a PCM tank stores much more heat in a given volume, it must also contain proportionately more heat-transfer surface to provide a given rate of heat withdrawal. In addition, solid buildup on the heat exchanger further reduces the heat-transfer rate, requiring more surface area.

In direct contrast where water storage tanks are shipped empty to the site, installed, and then filled, PCM tanks are best filled at the factory and shipped full. They must be sufficiently rugged to withstand the additional stresses of this treatment. In spite of the extra complexity and cost of the PCM tank, the space conservation has proven to be well worth the price, particularly in commercial installations. To enlarge the heat transfer rate, the technique of direct-contact heat transfer has been applied to bulk tank storage. While this involves increased mechanical complexity, the size of the heat exchanger is minimized.

2.10.3 Macro-encapsulation

PCM macro capsule sizes differ greatly, at one end from plastic pipes several inches in diameter and several feet long to the other end with shapes the size of an aspirin tablet. As opposed to the bulk storage tank, the PCM macro capsule incorporates no moving mechanical equipment and uses its own surface for the heat-transfer process. Macro encapsulated systems can use either liquid or air for heat transfer. Macro capsules are quite amenable to mass production and shipping [28].

2.10.4 Micro-encapsulation

The defining characteristics of Microencapsulated PCM systems are small, individual particles of PCM, with an encapsulant surrounding. Most of the time, the encapsulant forms a continuous web throughout the PCM mass. Ideally, the encapsulant matrix functions as the physical containment, moisture barrier, and heat transfer surface.

Micro-encapsulation is a complex but promising technology because it makes it possible to fabricate structural, functional, or decorative materials directly out of PCM. At present, very few microencapsulated systems are on the market, although a cement-encapsulated Glauber's salt product is available, further encapsulated in a stainless-steel pipe [24].

2.11 Available Commercial PCMs

As mentioned earlier, a variety of PCMs is required to meet the different applications for energy storage. The melting point of the PCM is matched with the needs of the application. At higher temperatures, the use of PCM heat storage for industrial processing and solar electric power applications is an interesting and attractive field. Fused-salt PCMs are available with melting points ranging up to several hundred degrees. A list of the commercial PCMs available in the market with their thermo physical properties as given by the companies (melting point, heat of fusion and density), and the company which is producing them are shown in Table T.1 and Table T.2 in Appendix T.

2.11.1 Non-Commercial/Commercial Materials

Although a wide range of substances have been studied as potential PCMs, only a few of them have found commercial application. Tables T.3 – T.12 in Appendix T present the different substances, eutectics and mixtures (inorganic, organic and fatty acids), that have been studied by different researchers for their potential use as PCMs. Some of their thermo physical properties are included (melting point, heat of fusion, thermal conductivity and density), although some authors give further information (congruent/incongruent melting, volume change, specific heat, etc.).

2.11.2. Organic/Inorganic Materials

A comparative table of organic and inorganic materials is shown in Appendix T.10. Prominent among inorganic materials are hydrated salts and their multiple applications in the field of solar energy storage, with regard to the storage temperature or phase change, the heat transfer in accumulators can be improved choosing the PCM in such a way that its phase change temperature optimizes the thermal gradient with respect to the substance with which the heat is being exchanged.

2.12 Summary

This chapter has analyzed two modes of thermal energy storage (TES), namely sensible heat storage (SHS) and latent heat storage (LHS). SHS refers to energy systems that store thermal energy without phase change and this mode occurs by adding heat to the storage medium and increasing its temperature. Thermal stratification is important for the SHS as heat is added from a heat source to the liquid or solid storage medium.

Conversely, heating of a material that undergoes a phase change (usually melting) is called LHS. The amount of energy stored in the LHS depends upon the mass and latent heat of the material, and with LHS, the storage operates isothermally at the phase change of the material.

An overview of thermal energy storage, including the advantages and disadvantages of solar thermal energy has been discussed in this chapter. A flow diagram of the area of research and classification of substances used for thermal energy storage have also been presented.

Details on sensible heat storage as a liquid media store, solid media storage, latent heat storage, phase change materials (PCMs), requirements for PCMs and its thermal, physical, kinetic and chemical properties have also been mentioned. This chapter focus on PCMs stability, heat storage capacity, chemical stability, safety, phase equilibrium properties and available PCMs. Lastly, a comparison of a table of organic and inorganic heat storage materials is given.

The thermal stratification is important for the SHS. Heating of a material that undergoes a phase change (usually melting) is called the LHS. The amount of energy stored in the LHS depends upon the mass and latent heat of the material. In the LHS, the storage operates isothermally at the phase change of the material.

CHAPTER 3

HEAT TRANSFER FLUIDS ANALYSIS AND APPLICATIONS

3.1 Heat transfer

3.1.1. Moving boundary problems

A moving boundary problem is a problem in which one of the domain boundaries is an unknown. The classic example is the Stefan melting problem [29], a heat transfer problem requiring the tracking of the a priori unknown melting front. Since the melt front position needs to be determined as part of the solution the problem formulation requires an additional boundary condition the Stefan condition, obtained by balancing the net heat flux arriving at the melting front with the rate of evolution of latent heat.

Typically moving boundary problems only have a limited number of analytical solutions [30] and as a result, from the advent of digital computers (see Price and Slack [31] and Eyres el al [32]), there has been extensive development of numerical methods. Practically analyzing heat transfer problems with regard to melting and solidification processes (scientifically referred to as moving boundary problems) , is particularly difficult because the solid–liquid boundary moves depending on the speed at which the latent heat is absorbed or lost at the boundary, so that the position of the boundary is unknown from what goes before and forms part of the solution.

A review on analytical/numerical and experimental work in the area of phase change, specifically freezing and melting processes was carried out by Eckert et al. in 1994 [33]. They divided the review in melting and freezing of spheres, cylinders and slabs; Stefan problems; ice formation in porous materials; contact melting; and solidification during casting. When the substance that solidifies is pure, the solidification occurs at a single temperature, while in the opposite case (with mixtures, alloys and impure materials) the solidification takes place over a range of temperatures, and therefore there appears a two-phase zone (a ''mushy region'') between the solid and liquid zones. In this latter case, it is appropriate to consider the energy equation in terms of enthalpy which, if the advective movements in the inner of the liquid are disregarded.

3.1.2. Numerical solution considering only conduction

Even though the primary heat transfers mechanisms are conduction and natural convection in liquid phase, the earliest literature analyses heat transfer basically by considering one-

dimensional conduction in pure substances. In 1943, London and Seban [34] analysed the process of ice formation for different geometries (cylinder, sphere, and flat plate). This study is very interesting although it was later disputed by Shamsundar [35] who asserted that London's one-dimensional formulation led to errors increasing with the progress of the solidification process and proposed a two-dimensional formulation for cylinders.

A study was presented in 1970 by Lasaridis [36] showing relative importance of conduction and convection. Shamsundar and Sparrow [37] demonstrated the equivalence between the energy conversation equation applied in the three zones (solid, liquid, and solid/liquid) and the enthalpy model. These are solved through a finite differential method and the solidification is analysed in a square plate cooled by means of convection. This method is valid both for phase change in a single temperature and for phase change in a range of temperatures (mixtures or alloys). Among the hypotheses in this work, it can be pointed out that the authors do not consider convection in the melting phase and assume the solid and liquid densities to be equal and uniform. Later, they evaluated the effects of density change [38]. In their conclusions, the relation between the heat transfer speed and the Biot number, linked with convection of the heat-carrier fluid, was already presented. Goodling [39] resolved a one-dimensional geometry outward solidification in a cylinder with a constant heat flow in the inner wall, the solution being given by the finite difference method applied to the temperature.

The problem of phase change conduction was studied by Meyer [40], who established that the classic Stefan problem implied the resolution of the temperature range and carrying out a review and comparison of explicit and implicit methods. The same year, Marshall published [41] a work studying natural convection effects in an annular geometry using hydrated salts and waxes/paraffins. He showed that the existence of natural convection significantly reduced the time necessary for melting, and gave recommendations for making use of natural convection especially with substances of low thermal conductivity (paraffins).

Bathelt [42] experimented with heptadecane (C_{17} H_{36}) and studied solidification around a horizontal cylinder. Using photographs, he showed the important role of natural convection, which increases with time and produces an increase in the average radius of solidification (non-concentric). This two-dimensional behaviour for this geometry has also been confirmed by other authors. Shamsundar and Srinivasan in 1978 [35] analysed a heat exchanger of shell

and tubes, and proposed a two-dimensional analysis, also taking into consideration the axial variation of the temperature, thus approaching a three-dimensional analysis. In 1981 Sparrow [43] analysed solidification on the outside of a tube carrying coolant inside, and confirmed the influence of the axial temperature variation of the coolant. He proposed an analytical solution providing initial values for the numerical method in which the moving boundary is immobilized by a transformation of co- ordinates. As a continuation of previous works, Shamsundar in 1981 [44] studied the influence of change in volume on phase change in the range of 10–20%. This involves the formation of cavities in the top part through which it is supposed there is no heat transfer (an additional adiabatic wall), so the usefulness of the methodology is therefore justified although there is density change in the solidification. The same author in 1982 [45] developed analytical solutions and evaluated the resulting formulation using results obtained with numerical methods.

In 1983 Achard [46] carried out a thermal storage experimental study on a test bench, using an immersed tubular heat exchanger in the PCM, both with salt hydrates and with fatty acids. They also developed a theoretical study using the enthalpy method and solved by means of finite differences, disregarding the convection effect. In the conclusion the theoretical and experimental results were compared and significant discrepancies found in the melting. It was therefore deduced that it is necessary to consider natural convection in the liquid.

Hunter in 1989 [47] and Amdjadi in 1990 [48] confirmed that the enthalpy method is the most suitable for real substances provided that there is no alteration to the numerical scheme in the boundary. Amdjadi added that if the material has hysteresis, it is necessary to rearrange or adjust the method. In this later work the finite differences method is used with a variable time step, adjusting it at each moment according to the stage of the phase change process. In 1999, Banaszek [49] studied experimentally and numerically solid–liquid phase change in a spiral TES unit.

3.1.3. Numerical Solution considering also Convection

The earliest publications that make reference to the convection heat transfer mechanism are Sparrow and Bathelt [50]. An interesting article about convection is by Gobin [51] whose objective is to determine the influence of natural convection on the melting process. To model these processes, some articles include the influence of the convection considering an effective thermal conductivity. Ozisik [52] includes a classification of the various solution methods:

1. Exact solutions, limited to a few idealized situations.
2. Integral method. One-dimensional: solution of an integral equation to localise the boundary.
3. Heat moving source method.
4. Perturbation method.
5. Electrical analogy (this is being replaced by numerical methods owing to the availability of powerful computers).
6. Finite differences method.
7. Finite elements method.

Completing this classification, Ismail [53] compared the results obtained with four different numerical methods, that is, the continuous solid phase models, the single phase models and the thermal diffusion models or models with thermal gradient inside the particles. The authors evaluate the models in relation to the computational time consumed to solve a specific test problem and then compare them in relation to the influence to different factors. Also Ismail in another publication [54] divides the numerical methods for the solution of phase change problems into two groups: fixed grid methods based on the enthalpy concept, and moving grid methods utilizing the interface immobilization technique. Furzerland [55] compared the two methods for the solution of a specific test problem of one dimension and heat transfer by pure convection. One of this conclusions is that the enthalpy method is easy to program and more suitable for PCM with a range of fusion temperatures.

3.1.4. Numerical Simulation in Different Heat Exchanger Geometries

Dincer and Rosen [19] manage the problems of heat transfer with phase change materials in simple and complex geometries and around isothermal finned cylinders. The results are presented and validated with actual and existing data.

3.2. Heat Transfer Enhancement

Numerous methods are available to improve the heat transfer in a latent heat thermal store. The use of finned tubes with different configurations has been proposed by various researchers such as Abhat, Morcos, Sadasuke, Costa, Padmanabham [56]. Velraj and Ismail [57] use finned tubes in thermal storage systems. Several other heat transfer enhancement techniques have been reported.

3.3 Heat Transfer Fluids

Choosing a high-temperature heat-transfer fluid for a particular application starts with the definition of general parameters for fluid selection and the assembling of information on different available fluids. Regrettably, there are a number of methods for presenting fluid physical and stability data. Units of measurement and the methods for measuring fluid characteristics may not be directly comparable. Before an informed selection can be made, there must be some assurance that important specifications can be compared and evaluated accurately.

3.3.1 Process Temperature Range

When it comes to fluid selection, the primary concern is the process temperature range. Before delving into the process of selecting a high-temperature organic heat-transfer fluid, one should be sure that the application conditions warrant the cost of an organic fluid. Some of the alternatives and points to consider are discussed below [24].

For temperatures between 0 and 177°C, water is the most economical and efficient heat-transfer fluid. Even occasional freezing temperatures can often be tolerated. For example, if system shutdown would be required should ambient conditions fall below the freezing point; freeze protection can be provided by heat tracing piping for equipment exposed to these low temperatures. If the application involves chilling, freezing, or frequent ambient conditions well below freezing, the most common heat-transfer fluids are vapor compression refrigerants, brines, and glycol-water solutions. A citrus derivative, Dlimonene, has been found to be a useful low-temperature heat-transfer fluid in the temperature range from -95.5 to 81.6°C.

Refrigerants of the vapor compression variety are useful in many chilling and freezing applications. Brines are an inexpensive solution for many low-temperature applications. Unfortunately they are also corrosive to most inexpensive, commonly used metals. To render them less corrosive, toxic inhibitors such as chromates are commonly added. Because of these factors, care must be exercised in the use of brine and in the selection of equipment materials for construction. An alternative low-cost option for applications requiring temperatures in the range of -51 to 121°C are glycol-water solutions. Glycol alone can be corrosive in contact with air, so a low toxicity corrosion inhibitor is generally included in the glycol formulation. Some inhibited glycols are specifically designed for applications where accidental contact with food or potable water must be considered.

Brines and glycols provide equally good low-temperature capabilities although they are unstable or corrosive at temperatures high above the boiling point of water. Even the use of steam as a heat-transfer fluid has some limitations above 177°C because both the vapor pressure of water and the associated process equipment costs increase significantly.

The majority of organic heat-transfer fluids, at 343°C, have vapor pressures between 0 to 2 bars. This low vapor pressure makes these special fluids more attractive for high-temperature applications. In fact, low vapor pressure at high temperatures is the major reason for choosing an organic fluid over steam. Organic fluids also provide benefits at temperatures below the freezing point of water. Some high-temperature fluids may be practical to pump down to - 73°C. In situations which require both low and high-temperature capabilities, high-temperature organic heat-transfer fluids can often be the optimum choice.

The low-temperature properties of organic fluids might warrant consideration even when the process normally requires only high-temperature capabilities. For example, in geographic locations where seasonal temperatures can drop well below freezing, low-temperature capabilities become equally important to prevent a system shutdown. Setting the fluid temperature range is just the starting point in the procedure of selecting a fluid. A number of other factors, including fluid vapor pressure, flammability, corrosion, toxicity, engineering properties, thermal stability, and cost must also be considered.

3.3.2 Vapor Pressure

For existing operational systems, their pressure capabilities should be considered when it comes to the selection of a replacement heat-transfer fluid. In the design of new systems, the fluid can dictate the system pressure parameters. Normally the equipment with the lowest pressure rating in a heat-transfer system is the expansion tank or process vessels. The expansion tank should have pressure capabilities sufficient to take into account the pressure created when the fluid thermally degrades or if water or other contaminants enter the system. In the majority of cases, an inert gas such as nitrogen is used to blanket the air space above the heat-transfer fluid. The expansion tank should be selected to withstand the inert gas pressure in addition to the other possible sources of pressure mentioned.

3.3.3 Flammability

The majority of organic heat-transfer fluids are volatile in terms of flammability when the temperature is sufficiently high and a source of ignition is present. At the flash point, the

fluid momentarily ignites on application of a flame or spark. At the fire point, vapor is generated at a rate sufficient to sustain combustion. At the auto-ignition temperature, no ignition source is required to initiate combustion. The auto-ignition temperature of most organic fluids is far above their maximum recommended use temperatures. In all cases, air must be present at sufficient concentrations to support combustion.

3.3.4 Corrosion

The heat-transfer fluids mentioned in Tables T.13 and T.14 in Appendix T are all non corrosive to mild steel, so material selection can generally be based on operating temperatures and pressures of the process medium. For example, at low temperatures stainless steel may be required for strength, even though neither the process fluid nor the heat-transfer fluid is corrosive. Specific material compatibility is available from most fluid and heat-transfer equipment manufacturers.

3.3.5 Toxicological and Environmental Concerns

The majorities of commercially available heat-transfer fluids are moderately toxic but should present no grave risk to operating personnel if normal operating precautions are taken. Product warning information is provided giving detailed information on how to handle a spill or leakage from the system.

3.3.6 Pump ability and Engineering Efficiency

The selected fluid should have temperature capabilities that extend beyond those of the process at both the high and the low ends of the range. It is desirable to select a fluid with higher temperature capabilities than required in order to safeguard the system against unexpected overheating and degradation of the fluid.

The lowest operating temperature required for the system's fluid may be dictated by either the process or the ambient conditions. When low process temperatures are not applicable, the fluid should remain pump able at the lowest ambient temperature of the geographic location in the event of an extended shutdown. It is possible to steam or to trace heat-transfer lines electrically in order to keep fluid pump able for cold weather startups, but a fluid that remains pump able without tracing will generally prove more economical in the long run.

It is crucial to differentiate between pour point and minimum pumping temperature when comparing fluids. The pour point is determined by the ASTM D97-66 procedure. In this test

procedure, the fluid is cooled to the temperature where the fluid will not flow when the container is tilted on its side. For determining pump ability, the viscosity is a major factor to evaluate the minimum pumping temperature is governed by the temperature at which the fluid viscosity reaches 1000 cp. A standard centrifugal pump, designed for normal operating conditions, will experience a significant reduction in flow rate when the viscosity increases above this limit. Pump and heater bypass loops can be designed into the system, but they also become ineffective as the viscosity rises.

3.3.7 Engineering Properties

Table T.13 in Appendix T shows some of the most commonly used heat-transfer fluids and their typical properties. Included are reported use range, minimum pumping temperature, flammability characteristics, thermal properties, and relative price range. This table is based on the conversion of manufacturers' reported data to U.S. customary units with metric conversions as required. In Table T.14 in Appendix T the relative heat-transfer coefficient and the pressure drop for each fluid, as calculated from the data of Table T.13 in Appendix T, are presented.

3.4 Fluid Thermal Stability

The most crucial point when it comes to selecting a high-temperature heat-transfer and its dominant effect on long-term performance and operating costs is the thermal stability. Low thermal stability will cause premature degradation of the heat-transfer fluid, possibly resulting in loss of fluid, shortening of fluid life, loss of heat-transfer efficiency, increase in viscosity and pumping costs, system fouling, and equipment damage.

The choice of a fluid with an operating temperature range that matches the process temperature range is insufficient. Consideration needs to be given to conditions that can cause temporary fluid overheating such as equipment malfunctions or temperature control fluctuations.

As a consequence of selecting a fluid with high thermal stability, most problems associated with localized or temporary temperature excursions beyond the upper process temperature limit are prevented. In addition to minimizing problems associated with fluid overheating, a high-stability fluid will result in better efficiency and less frequent fluid replacement than a lower-stability fluid.

3.5 Relative Film Coefficients

Numerous studies have been undertaken to clearly show correlations between the film coefficient h_f and the fluid's physical properties. The Sieder and Tate Correlation [24] gives reliable coefficients for organic fluids. It is expressed by

$$h_f = 0.023\frac{k}{d}\left(\frac{dv\rho}{\mu}\right)^{0.8}\left(\frac{C_p\mu}{k}\right)^{1/3}\left(\frac{\mu}{\mu_w}\right)^{0.14} \quad \text{.....4.1}$$

Where C_p = Specific Heat

d = Diameter

k = Thermal conductivity

v = Fluid velocity

w = Wall temperature

μ = Viscosity

ρ = Density

Taking the physical properties from Table T.13 in Appendix T into account, the film coefficient has been calculated for each fluid and tabulated in Table T.14 in Appendix T. This relative study is for 600°F (315.5°C) and for fluid velocities of 5 and 7 ft/s (1.52 and 2.13 m/s). The optimum velocity, in any given case, will be an economic balance between cost of power and cost of heating surface. The two velocities selected are within the range of typical heat exchangers.

3.6 Overall Considerations for Fluid Selection

When choosing an organic heat-transfer fluid for a high-temperature process, the operating and ambient temperature requirements are first determined. If moderate temperatures are required below 260°C, then multiple fluids are available. When low-temperature pump ability or high-temperature requirements are needed, then the fluid selection is restricted.

After the system temperatures are defined, a review by product can be made. Thermal stability is recognized as the most critical factor in fluid selection. If the fluid cannot pass this screening, then it need not be evaluated for engineering properties, flammability, toxicity, and cost.

3.7 Solar Cooking with PCM Storage

The team of Morrison and Mills [14] engineered a hot plate cooking system powered by solar thermal energy. The system uses a concentrating evacuated tubular collector to supply

thermal energy to a high temperature store so that heat can be supplied for cooking at any time of day. The system incorporates a passive downward energy transfer system between the solar collector and the store. The cooking system can be installed indoors and the collectors mounted on any convenient roof, without the need for pumps or thermosyphon loops to transport energy from the solar collector to the store.

Morrison cooking tests are shown in Table 3.1. These tests show that for effective frying the energy store temperature must be higher man 160°C. Boiling or steaming cooking operations can be carried out in times similar to a conventional electric hot plate for store temperatures down to 130°C.

Table 3.1 Cooking Times for Steam Heated Cook Top [14]

Cooking operation	Energy store Temperature	Time required Minutes
Cook 0.5kg rice in 0.75kg water	150°C	17
Fry 3 eggs and 0.25kg onions	150°C	8
Steam 1 kg rice in 1.3kg water	160°C	17
Fry 0.5kg rice, 0.25kg green beans and 0.25kg shrimps	175°C	8
Fry 1kg sausages	175°C	10
Fry 4 eggs and 0.25kg onions	175°C	9
Fry 0.8kg beef	180°C	9
Fry omelette, 3 eggs, 0.25kg onions	180°C	8

Solar cookers are thought to have great potential in countries with a hot climate and they were the subject of intensive investigations [26, 58–85]. The application of solar cookers is restricted if they are not equipped with a heat storage system since it is impossible to use them in cloudy conditions or evenings.

Domanski et al. [79] were the first to experimentally investigate the possibility of cooking during off-sunshine hours using PCMs. In their investigation, they used a non-conventional design of a box-type solar cooker with multi-step inner reflectors, as illustrated in Figure 3.1. The storage-cooking unit consisted of two aluminium concentric cylindrical vessels with the 1.5 mm thick walls, which were connected together at their tops using four screws to form a

double-wall vessel with a gap between the outer and inner walls. The outer vessel had a diameter of 180mm and height of 120 mm, while the inner vessel had a diameter of 140mm and height of 100 mm. The annular gap between the outer and inner vessels was 20 mm. The outside surface of the outer vessel and covers were painted using a conventional black paint. The gap between the outer and inner vessels was filled with kg of 95% commercial stearic acid, or 2 kg of magnesium nitrate hexahydrate, produced by Aldrich Co. It was established that the heat discharging time tends to increase with increasing the initial temperature of the cooking medium and the degree of superheating of the liquid PCM, but it decreased as the mass of the cooking medium increased.

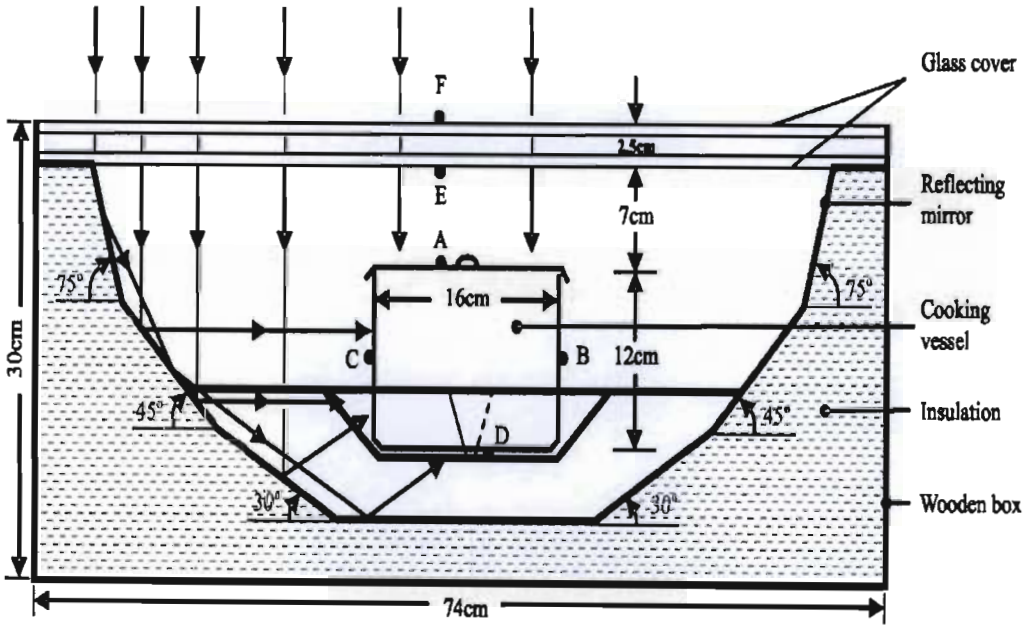

Figure 3.1 A schematic Diagram of the Solar Cooker by Domanski et al. [79].

The resulting values of the overall utilisation efficiency of the cooker were about 3-4 times greater than those for steam and heat-pipe solar cookers which could be used for indoor cooking. The cooker under investigation could achieve higher temperatures by using PCMs when the melting point exceeds 100 °C (for instance, magnesium chloride hexahydrate has the melting temperature of 116.7°C).

Buddhi and Sahoo [80] also proposed to use a PCM in solar cookers. The commercial stearic acid with the melting point of 55.1°C and the heat of fusion of 160 kJ/kg was used as a latent heat storage material. A similar cooker in the form of the aluminium cooking pot, which is 0.16m in diameter and 0.06m in height with the lid, is widely used in India to cook rice. The

solar cooker contained about 3.2 kg of stearic acid and although experiments indicated that this design allowed users some time to cook when there was no sunshine, the amount of the stored heat was inadequate and the melting temperature of the PCM was not sufficiently high.

In 2000, Sharma et al. [59] reported that they had developed a much-improved design of solar cooker using a latent heat storage material. As a PCM, they tested the commercially available acetamide with the melting point of 82°C and the heat of fusion of 263 kJ/kg. Experiments demonstrated that such a cylindrical latent HSU with a cooking pot was capable of storing energy which then was used in the evenings. To make this possible, the melting point of the PCM must be between 105 and 110°C. Experience gained demonstrated that solar cookers without concentrating systems or high quality solar collectors could have a very limited application.

Therefore, to increase the performance of a box-type solar cooker, Buddhi et al. [60] suggested using three plane adjustable reflectors. This technique made it possible to use as a latent heat storage material a commercial grade of acetanilide with a melting temperature of 118.9°C and a heat of fusion of 222 kJ/kg. Even then, the technical performance of the box-type solar cookers was quite poor, since it was possible to cook only 0.3–0.4 kg of rice over a 2-h period. Therefore, in order to improve the performance of solar cookers, it has been suggested that they were coupled with evacuated tube solar collectors (Balzar et al. [65] and Kumar et al. [72]) and concentrating systems (Mullick et al. [73], Habeebullah et al.[69] and Ozturk [81]).

Schwarzer and de Silva [80] tested a collector with reflectors using pebbles as the thermal storage for cooking purposes. Sharma and Sagara [83] and Sagara et al. [84, 85] tried out evacuated tube solar collectors to develop a solar cooker with latent heat storage. Thus, they used two vacuum-tube collector units having a net absorbing area of 1.82m^2 each and erythritol as a latent heat storage material with the melting point of 122°C and the heat of fusion of 338.8 kJ/kg. The storage unit had two hollow concentric aluminum cylinders, and its inner and outer diameters were 304 and 441 mm, respectively, and it was filled with 45 kg erythritol, which was used as a PCM. The cooking vessel itself was 297mm in diameter and 300mm in height and could be easily placed inside the PCM storage unit. Cooking experiments demonstrated that the developed Heat Storage Unit (HSU) was able to store an adequate amount of heat to cook in the day and the evening.

This type of solar cookers with a latent heat storage system is quite expensive but it has a good potential for community applications. At present further research is in progress on new PCMs which could be used effectively in solar cooking applications.

3.8 Summary

A review on analytical/numerical and experimental work in the area of phase change, specifically freezing and melting processes was carried out. This review was based on the past distinct stages in the development of works dealing with thermal energy storage using phase change. The review has been organized chronologically, but at the same time the material has been arranged within the main areas of Phase change materials, heat transfer analysis and applications. This chapter is concerned with moving boundary problems, numerical solution considering only conduction, numerical solution considering also convection, numerical simulation in different heat exchanger geometries, heat transfer enhancement, heat transfer fluids, process temperature range, vapour pressure, flammability, corrosion, toxicological and environmental concerns, pump ability and engineering efficiency, engineering properties, fluid thermal stability, relative film coefficients, overall considerations for fluid selection and solar cooking with PCM storage.

CHAPTER 4
HEAT STORAGE SALTS

In the 1930's a mixture was developed which has been the most widely used ever since. It contains a blend of potassium nitrate, sodium nitrite, and sodium nitrate (53/40/7 percent by weight, respectively). It melts at 288°F (142°C) and can be used up to 900°F (482°C). This mixture is the eutectic or lowest melting formulation of these salts. It is best known as Hitec, a trademarked product of Coastal Chemical. This and similar compositions are called heat transfer salts (HTS). The HTS designation is also used with other formulations, even those chemically incompatible with Hitec [86].

Another variety is Drawsalt, 60/40 percent by weight sodium nitrate and potassium nitrate, which can be used if the lower melting point of HTS can be sacrificed to obtain higher thermal stability and lower cost. It melts from 432 to 473°F (222 to 245 °C) and can be used to 1050°F (566°C). Drawsalt has had extensive testing for solar power applications. The more expensive eutectic (46/54 percent by weight) melts at 432°F (222°C). Often also referred to as drawsalt, it will be referred to here as eutectic drawsalt [87].

For other applications, different salts are routinely used, but nitrate and nitrite salts so dominate thermal transfer and storage that this chapter deals with them exclusively. Janz and others [88, 89] discuss salts outside the scope defined here. Salt mixtures and their warning labels, even for thermal transfer or energy engineering may include mixtures which are explosive and should carry warning labels. No mixture of oxidizing salts with reducing salts, liquid or powdered metals, or organic materials should be used for thermal transfer media. Mixtures of nitrate or nitrite salts (both are oxidizing) with ammonium salts, with organic materials such as urea, or with cyanide, cyanate, thiocyanide, thiocyanate, sulfide, polysulfide, sulfite, or thiosulfate salts, or with sulfur should be avoided.

Molten salts have their own innate advantages which are high heat capacity and other good physical properties, excellent thermal stability, low cost, good materials compatibility, negligible vapor pressure or flash point problems, decades of industrial experience, and multiple supply sources. The option of using a water dilution system for HTS is another advantage. Available from American Hydrotherm, New York, it retains the HTS upper temperature limit, but allows system cooling with a liquid medium (of changing composition) to much lower temperatures, such as 100°F (38°C).

Disadvantages include high melting points in the anhydrous systems, a tendency for the melting point of HTS to drift upward with slow oxidation, the advisability of using a nitrogen blanket on HTS to retard deterioration, the propensity of molten salts to leak around seals, and an increase in corrosive aggressiveness if the salt is contaminated or deteriorates. In contrast to HTS, drawsalt is not used with a nitrogen blanket since it has a stable melting range.

4.1 Physical Properties

Information relating to physical property includes melting behavior, viscosity, density, heat capacity, and thermal conductivity. Vapor pressure, as usually defined, is negligible. The salt does attempt to equilibrate with some components of its cover gas and can generate significant pressures of oxygen and/or nitrogen oxides under thermal or chemical degradation. Within an operating system, the relative amounts of nitrates and nitrites can vary considerably over time. The physical properties that depend significantly on the nitrite content are melting behavior and density.

Further elucidation regarding the melting behavior is warranted. Eutectics have a melting point, which is the temperature at which the mixture melts completely. Noneutectic mixtures have a melting range. At the lower temperature, or solidus, melting begins. For compositions near the eutectic, the most melting occurs at the solidus. At the liquidus, or higher temperature of the range, the mixture becomes entirely liquid. The liquidus is the key temperature for thermal transfer considerations. Note that as HTS degrades, it changes from eutectic to noneutectic. Table T.15 in Appendix T shows physical Properties of Molten HTS and Drawsalt, equations which relate physical properties to temperature and composition.

4.2 Chemical Properties

Reaction-wise, the most significant one occurring in molten nitrate-nitrite salt mixtures is the drive toward equilibrium with oxygen in the cover gas. Nitrite and its equilibrium concentration differs as the square root of the oxygen partial pressure, and ranges from tens of parts per million to a few tenths of a percent for atmospheric oxygen partial pressure throughout the temperature range of use (to perhaps a percent near the upper range of draw salt) [90]. This reaction is rather benign since both nitrate and nitrite are soluble in the melt, noncorrosive, and stable. The consequence of this reaction for drawsalt is a slight decrease in the liquids due to a slight increase in the nitrite content.

4.3 Material Compatibility

Drawsalt or HTS used at sub 800°F (427°C) is compatible with most materials of construction. However, no contact should be permitted with organic materials, carbon, sulfur, with reactive metals such as aluminum, magnesium, or their alloys, or with powdered iron. Use with cast iron or copper is not recommended. At higher temperatures low-carbon stainless steels are recommended, such as SS 316L or SS 304L. Steels containing molybdenum, such as SS 347L, are somewhat less desirable. The low-carbon designation is critical at temperatures over 850°F (454°C) and in thin performance parts, such as in valves. Verification is important since low- and normal-carbon steels are sometimes interchanged by suppliers. Code restrictions may need special consideration when specifying the low-carbon steels [91].

In situations of high heat flux at the higher temperatures, high nickel alloys such as Incoloy 800 should be used. Where contamination is sometimes unavoidable, critical surfaces may require more costly materials, such as the Hastelloys. Usually this is not specified initially, but it may be considered after actual lifetime information on the alternatives has been obtained.

When dealing with salts which are occasionally contaminated in use by chloride or sulfate, it may be necessary to use the high-nickel alloys even at lower temperatures. Even then, salt contamination should be corrected. Quartz and glass are prone to etching if the salt temperature or the alkalinity is high. Alumina and magnesia (the oxide ceramics) appear to withstand almost the entire gamut of salt conditions.

4.4 Design and Construction

When dealing with the melting point of HTS, steam tracing of pipes, valves, and flanges is the usual method. For draw-salt, electric heat tracing is needed. With electric heat tracing, it is important to make it almost impossible for molten salt to leak onto the heaters or wiring, even in the smallest amounts. This requires great care, since molten salt can leak through the smallest joints, holes, and seals, and will "creep" up surfaces hot enough to keep it molten. Venting from the system should be directed safely outside since it may contain fine salt particles.

In cases where avoidance of salt leaks is important, welding should be used for pipe bends and connections. Exposed salt lines and valves should be insulated. At high temperatures,

valves may need radiation fins to protect the packing glands. It is important that no leakage occur onto solid fuel or built up carbon or soot. Bearings or rotary seals should not be in contact with the salt [23] cantilever pumps that permit no contact of the molten salt with the packing gland can be used for circulation. Manually operated steel gate valves and automatic valves can be used if they are installed so that they can drain freely. It is prudent to configure the system so that it can drain completely from top to bottom, via gravity, into the sump in the event of total system failure. A bypass around the cold-side heat exchanger will allow drainage even if the exchanger is plugged and will facilitate a gradual system startup.

HTS has been used successfully with metallic asbestos gaskets, asbestos sheet gaskets, and asbestos packing. Organic valve-packing lubricants or excessive pipe dope should be avoided. Graphite-lubricated asbestos is satisfactory if the graphite content is minimal.
Try not to have high heat fluxes at heater tubes or hot-side heat exchanger surfaces in systems working near the upper temperature range of the salt or when bringing a system up to its operating temperature. There will be a "burn-in" period during startup of a system. At this stage, the initial salt decomposition rate will be relatively high, as will be the formation of nitrogen oxides. Such behavior may also occur in the event of temperature excursions or process stream leaks. In normal operation the hottest surface seen by the salt should be no more than 100°F (38°C) above the nominal rated bulk upper temperature limit.

As for worst-case scenarios (leaks, loss of circulation, plugging, etc.) one should never allow salt to contact a surface hotter than 1150°F (621°C) for HTS or 1250°F (677°C) for drawsalt, as violent reaction with the surface material may result. Since molten salt is a good electrical conductor, this possible additional source of inadvertent heating should be considered.

Methods for controlling fires in the vicinity of a molten salt unit can include carbon dioxide and approved dry powder-type extinguishers. Vaporizing liquid (carbon tetrachloride) or water extinguishers (other than fine spray sprinklers or low-velocity fog nozzles) should not be used. Note that even small amounts of water can cause violent steam explosions if they penetrate the surface of molten salt. Clean, dry sand is useful for slagging and diking spills of molten salt.

4.5 Salt Charging

It is feasible for salt to be charged molten if delivered that way, although it is more common is to first charge to a portable melter or directly to a sump equipped with immersion heaters

or steam coils adequate to melt the salts and bring them up to a high enough temperature to circulate. With HTS, a water dilution system can be used. Small amounts of water can aid in melting the salt, but with some pumps the water vapor may cause pump cavitation until the salt becomes rather dry at about 400°F (204°C). A nitrogen sparge can be used to speed the drying of the melt after "boiling" stops.

Intrinsic to the salt heaters design should be a feature to prevent localized overheating during startup. The salt freezes with volume contraction, so re melting should be done in such a way as to prevent entrapped melting. For this reason, heaters in the sump should penetrate the salt surface to deal with a drain-down and freeze problem. This will also avoid the settling of sludge onto heated surfaces, which impedes the flow of heat and can cause disastrous local overheating.

Since HTS is hygroscopic, old bags or opened drums may become solidly caked. Additional effort should then be planned to deal with breaking the cake. Care must always be used to prevent splashing of the molten salt since the high heat capacity results in extremely severe burns. High-temperature protective gloves as well as face shields and protective clothing and boots should be worn.

4.6 Salt Maintenance

At the very least, regular testing of the melting range and total alkalinity should be done, perhaps monthly. Less frequent tests of sulfate, chloride, and any other likely contaminants should also be performed. Analyses sampling necessitates special care. The sample should be taken molten into a vessel of about the needed sample size (nickel or stainless steel is acceptable). When cool, the entire sample must be ground and mixed since it does not freeze uniformly.

The most routine form of maintenance for HTS is to restore its melting point by replacing some of the salt with a "butting salt" of high nitrite content and the correct sodium-to-potassium ratio. The replacement amount is chosen to bring the nitrite of the final mixture to 40 percent by weight expressed as sodium nitrite. Note that bringing up the nitrite by adding sodium nitrite alone is not satisfactory. Following this procedure with the usual butting salt (54 percent potassium nitrate and 46 percent sodium nitrite by weight), a substantial portion of the existing salt may need to be replaced. Note that this will dilute contaminants, improving their levels as well. However, if impurities and total alkalinity are low, it may be

more cost-effective to replace a smaller fraction of the salt with a more expensive all-nitrite butting mixture of 50 percent potassium nitrite and 50 percent sodium nitrite by weight.

4.6 Summary

The main aim of this chapter was focused on heat storage salts as a mixture which was developed in 1930's and which has been the most widely used ever since. The heat transfer fluids known as molten salts are solid chemical; its physical properties, chemical properties, material compatibility, design and construction, salt charging and salt maintenance were described.

CHAPTER 5
EXPERIMENTAL INSTRUMENTS AND EQUIPMENTS

5.1 Temperature Measurement

Temperature can be measured via a diverse array of sensors. All of them infer temperature by sensing some change in a physical characteristic. Six types with which the engineer is likely to come into contact are: thermocouples, resistive temperature devices (RTDs), infrared radiators, bimetallic devices, liquid expansion devices, and change-of-state devices.

5.1.1 Thermocouples

Any pair of thermoelectrically dissimilar materials can be used as a thermocouple. The pair need only be joined together at one end and connected to a voltage-measuring instrument at the other to form a usable system. A thermocouple develops its signal in response to the temperature difference from one end of the pair to the other. The temperature at one end, known as the reference junction end, must be known accurately before the temperature at the other end can be deduced from the voltage.

Thermocouples are the most commonly used electrical output sensors for temperature measurement. With different materials for different ranges, thermocouples have been used from cryogenic temperatures (a few Kelvin) to over 3000 K. In the moderate temperature range, ambient to 1200°C, manufacturer's quoted calibration accuracy can be as good as ±3% of reading (referred to 0°C) for precision-grade base metal thermocouples. Broader tolerances apply at very high temperature and very low temperatures.

Thermocouple signals are DC voltages in the range from a few microvolt's to a few tens of micro volts per degree C. Because of their low signal levels, thermocouple circuits must be protected from ground loops, galvanic effects, and from pickup due to electrostatic or electromagnetic interactions with their surroundings. Thermocouples are low-impedance devices. Multiple channels of thermocouples can be fed to a single voltage reader using low-noise-level scanners or preamplifiers and electronic multiplexers.

5.1.1.1 Thermocouple Usage

Thermocouples are the most frequently used type of temperature sensor in industrial applications for these reasons:

- They provide a degree of accuracy acceptable to most industrial processes.
- Higher degrees of accuracy may be obtained, when required, by selectively matching the positive and negative thermo elements.
- Temperature measurements from -270 to 1820°C can be measured by selecting the proper type of thermocouple.
- Properly constructed thermocouples are the most rugged industrial temperature sensors.
- Because thermocouples can be manufactured variety of configurations, they can be designed to match unique process requirements. Thermocouples can be the most cost-effect measuring sensors for many industrial applications.

5.1.1.2 Thermocouple Standards

The Instrument Society of America (ISA) and ASTM1 have standardized eight types of thermocouple and assigned letter designations. Five of these types, J, K, N, T, and E are base-metal thermocouples. The remaining types, R, S and B are noble-metal thermocouples. Table T.16 in Appendix T shows the IEC-ISA-designated thermocouple alloys of the positive and negative thermo elements of these thermocouples, the base compositions, and the range of applications. Types J and K are the most frequently used thermocouples in general industry.

5.1.1.2.1 Type J

Type J thermocouples may be employed continuously in either oxidizing or reducing atmospheres up to a temperature of 750°C. The positive and negative thermo elements are, respectively, iron and a copper-nickel alloy commonly known as Constantan. Thermocouples of this type are used extensively in heat-treating furnaces where the couples are exposed directly to the furnace atmosphere. They also find wide usage in plastics processing and general industry for measurements in the 0 to 760°C range.

5.1.1.2.2 Type K

Type K is one of two base-metal thermocouples capable of measuring temperatures to 1250°C. The positive thermo element is Ni-10%Cr alloy; the negative, a Ni-5% (Mn AlSi) alloy. At elevated temperatures, type K couples should be used only in an oxidizing atmosphere. Type N was developed to essentially eliminate the high-temperature drift seen in type K thermocouples. As a result of their high-temperature capabilities, type K thermocouples are used extensively to measure temperatures in heat-treating furnaces, jet engines, boiler tubes, and in many applications in chemical and power plants. All the

temperatures required inside the TES unit, and at the inlet and outlet to the TES, were measured using J-type (iron/constantan) solid core thermocouple. The fundamental principle on which thermocouple is based is known as the Seebeck effect.

The Seebeck effect describes the voltage or electromotive force (emf) induced by the temperature difference (gradient) along the wire. The change in material EMF with respect to a change in temperature is called the Seebeck coefficient or thermoelectric sensitivity. This coefficient is usually a nonlinear function of temperature.

The emf generated by the thermocouple was measured using an analogue-to-digital PC card and Data logger. Hence the junctions of two dissimilar metal wires form a closed loop and are exposed to different temperatures, a net emf is generated which induces an electrical current. It was Antoine Cesare Becquerel who first used this effect to measure temperature. Later Jean Peltier discovered that the thermocouple junction acted like a heat sink when a small electric current was passed across it. This was in effect the reversal of the phenomenon observed by Thomas Seebeck. Figure 5.1 shows the basic circuit required to measure the temperature of a thermocouple junction.

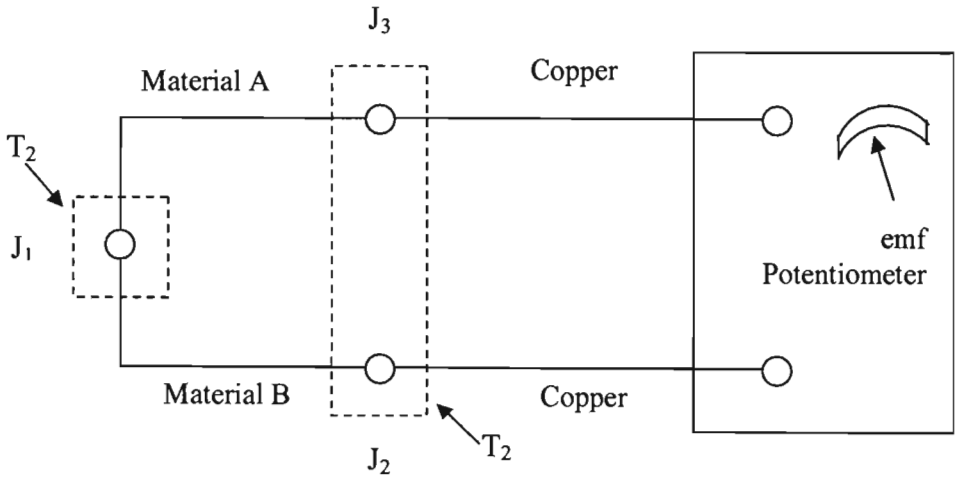

Figure 5.1 Typical thermocouple measurement circuit.

When an attempt is made to measure the thermocouple voltage, two further junctions are produced. When junctions J2 and J3 are at the same temperature, the effects of the copper leads cancel each other out. This combined junction is known as the cold, or reference, junction. The potentiometer effectively measures the emf generated between J_1 and this reference junction. If the reference junction is held at 0°C (in an ice bath), then the emf

generated can be applied directly to published tables or equations, to obtain the temperature at J_1. Compensation is necessary for all reference temperatures not equal to 0°C.

An equivalent emf is calculated for this temperature and added to the potentiometer reading. This total value is then applied as if the reference temperature were 0°C. As the Seebeck coefficients for thermocouple vary over their usable measuring range, a form of linearisation is required to calculate the correct temperature accurately, if tables are not used. Table T.17 in Appendix T Shows Seebeck coefficient for various thermocouples.

For example the coefficients for J-type thermocouple range between 22μV/°C at -200°C and 64μV/°C at 750°C. Two methods of linearization are commonly used. The first method utilises tables of temperature versus voltage measured. Although rapidly accomplished with a computer, this technique requires vast amounts of memory. It is also difficult to compensate for the reference junction temperature. A more memory efficient technique uses a polynomial approximation of the function of the emf generated versus temperature.

The order of the polynomial used is dependent on the temperature range measured, the type of thermocouple used and the accuracy required. A J-type thermocouple can be approximated to within 0.1°C over 0 to 750°C by a fifth order polynomial. The cold junction temperature can be similarly converted to a voltage using a polynomial. Often, extension wires which have similar properties to the thermocouple wires are inserted between the measuring junction and the reference junction. These wires are less pure and therefore less expensive. The disadvantage is that they can result in a maximum uncertainty of 2.2 °C, depending on the temperatures at the end of the wires.

Thermocouples were chosen for their cost-effectiveness and ease of installation when compared to RTD probes. J-Type thermocouple were selected due to their lower cost, relatively high Seebeck coefficient, and good linearity in the 0-100°C range when compared to types-E,K,R,S and T. The thermocouples inside the TES unit were attached to the outer surface of the tube with stainless steel fitting.

5.2 Analogue to Digital Conversion Tools

5.2.1 PCI-773 Thermocouple/Rtd Input Board.

The PCI-773 is a low cost thermocouple measurement sub-system for an IBM compatible PC. It consists of a half size board which plugs into the PC and contains the A/D converter, processing and control components. There is also an external screw terminal board which

provides a connecting point for the thermocouple. This board was connected to the PC plug in board via a 25 core ribbon cable.

The analogue input from the thermocouple was fed into an differential amplifier and then converted into a 12-bit digital code using a monolithic analogue to digital converter. The temperature sensor on the terminal board used for the cold junction compensation was not amplified, but fed directly to the A/D converter. It had a constant scale factor of 10 mV/°C over the entire operating range.

As a result of the need to amplify the signal, the card had a maximum throughput rate of only 30 Hz; approximately 2.5 seconds elapsed between the first and final temperature readings. As the channels were read in the same sequence each time, a similar data capture interval existed between the same channel readings. Software which formed part of the overall data acquisition program was used to access the three PCI-773 cards via four 8-bit registers. Their locations were set using switches on the card itself.

The accuracy of the measuring system was dependent on three factors:

(i) The accuracy of the PCI-773 card with a gain setting of 500, the uncertainty associated with the amplifier and D/A conversion was ±0.05°C.

(ii) The uncertainty of the cold junction temperature measurement was ± 1.0°C.

(iii) The uncertainty due to linearization was ±0.1 °C for a type J thermocouple above 0°C.

From the above it can deduced that the thermocouple were the limiting factor in the accuracy of the measurement.

5.2.2 Data logger

A data logger is any device that can be used to store data. This includes many data acquisition devices such as plug-in boards or serial communication systems which use a computer as a real time data recording system. However, most instrument manufacturers consider a data logger a standalone device that can read various types of electrical signals and store the data in internal memory for later download to a computer.

A data logger is an electronic instrument which connects to real world devices for the purpose of collecting information. Data logger can be pictured as a black box recorder in

airplanes. These data loggers record mainly voice and the plane stats data information. A data logger could be used for the following:

- Temperature sensors
- Pressure sensors & strain gauges
- Flow and speed sensors
- Current loop transmitters
- Weather & hydrological sensors
- Laboratory analytical instruments

The advantage of data loggers is that they can operate independently of a computer, unlike many other types of data acquisition devices. In this project experiments Rustrak ranger IV data logger as shown in Figure 5.2 and Data Taker DT600 as shown in Figure 5.3 were used to record the reading of the temperature sensors during both charging and discharging the heat storage system.

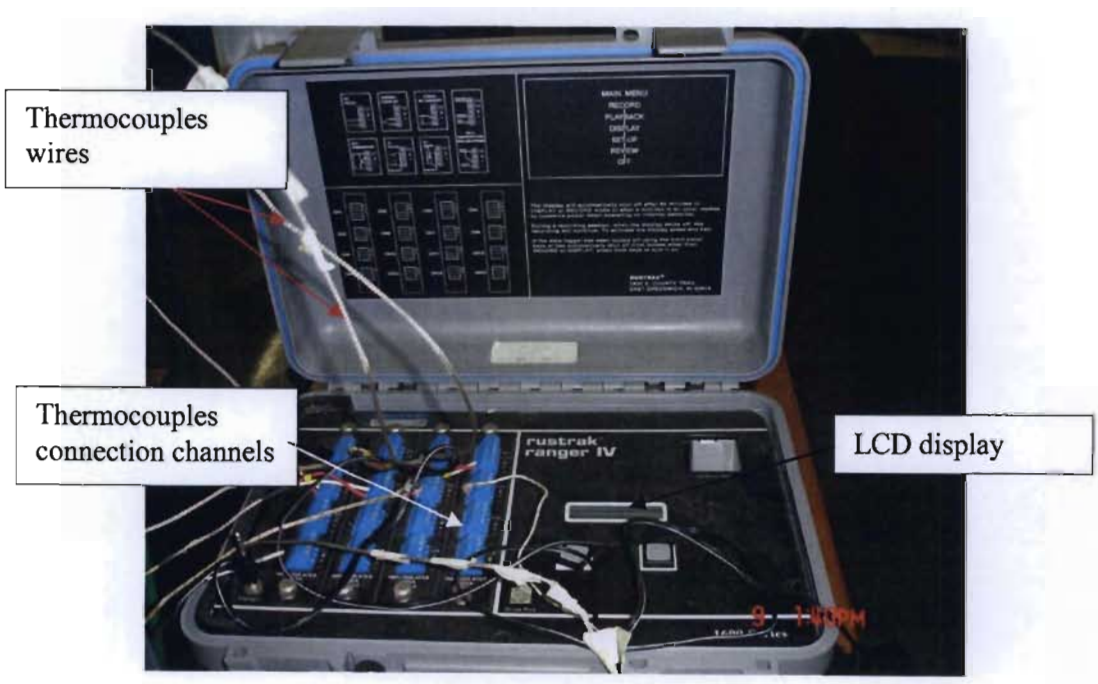

Figure 5.2 Rustrak ranger IV data logger

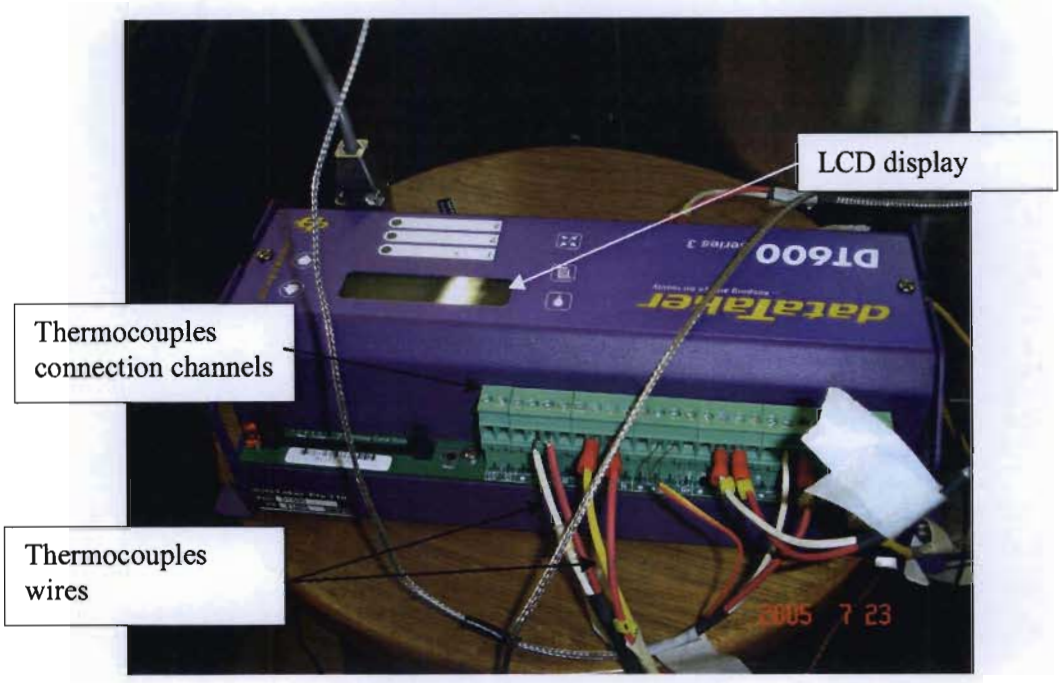

Figure 5.3 Data Taker DT600

5.2.3 Thermocouple Thermometer Type J/K Dual Input

Thermocouple thermometer with Alarm Type J/K Dual Input features: Dual Type J or K input with dual display; with highest 0.05% accuracy; dual LCD displays T_1, T_2 or T_1-T_2, It is an instrument used to measure and receive the temperature reading from thermocouples during charging and discharging process as shown in Figure 5.4

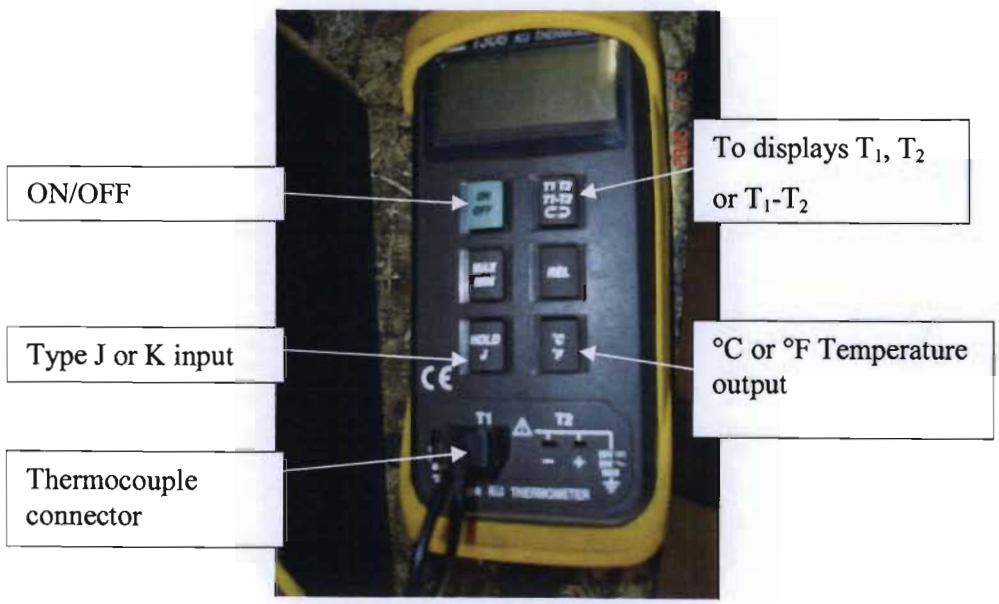

Figure 5.4 Thermocouple Thermometer

5.2.4 Calibration of Instruments

5.2.4.1 PC-773 Thermocouple Card

It was found that the cards drifted and needed re-calibrating each week to ensure that the temperatures measured were accurate. The calibration procedures were followed whenever the thermocouple was reconnected. Before any adjustments were made, the PC and the cards were warmed up for half an hour. A millivolt source having an accuracy of 0.05% of the setting was used to provide the necessary inputs. The source itself was also checked and found to be accurate within the above specification. The A/D calibration was carried out by adjusting the two trimpots for gain and offset. The source was connected to channel zero, while the output code was displayed on the PC monitor. Zero volts were applied and the offset trimpot was adjusted until the value read by the PC lay between -2 and + 2. It was not possible to adjust the trimpot for a value of zero; this was possibly due to electrical interference from surrounding sources, for example, the computer transformer or the fluorescent lights. Similarly, the gain was set by allowing the output code to fluctuate between 4093 and 4095 while an input of 8.189 mV was applied to the channel. The above two steps were repeated until no further adjustments were required.

5.2.4.2 Thermocouples

Although the thermocouple card was calibrated as accurately as possible, the temperature measurements made at the melting and boiling points of water were found to vary by ±1°C of the true value. It was felt that the uncertainty of the temperature measurements could be reduced by calibrating individual thermocouple in a similar way to the RTD probe. However, it was not possible to calibrate individual thermocouple in the core of the TES unit, as these were already attached to the tubes. Although calibrations prior to attachment have been carried out, these have required the disconnection of the thermocouple from the card before the core was inserted into the heat storage unit. This also has led to de-calibration of the measurement, as a new junction, with its own slightly different characteristics, would be formed upon reconnection to the Thermocouples card.

The calibration equipment is shown Figure 5.5. The thermocouples were inserted into test tubes in order to electrically isolate them from one another. The test tubes were filled with oil. It was realized that calibration would be carried out for a particular cold junction temperature, which did not necessarily remain constant during a test run, as it was determined by the ambient conditions. Even with these factors taken into account, it was

found that accuracy improved to ±0.5°C at both melting and boiling point of water for a range of ambient conditions. Consequently, an uncertainty of ±0.5°C for all temperatures measured by the inlet and outlet thermocouple was considered acceptable.

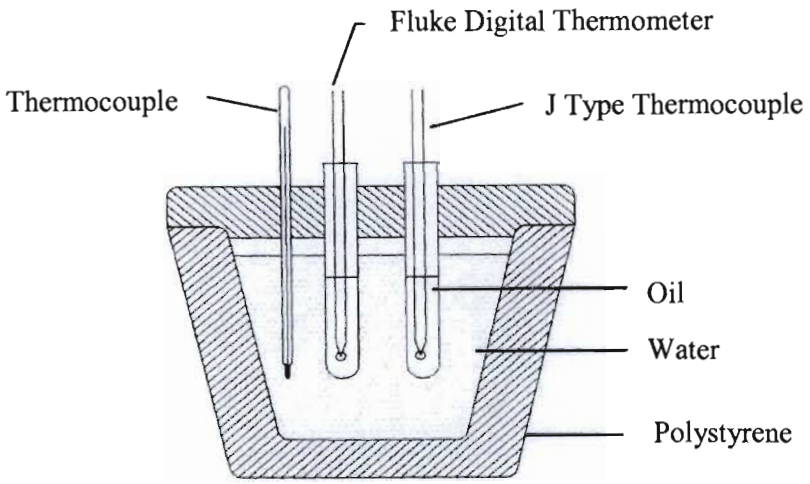

Figure 5.5 Thermocouple Calibration Equipment

5.3 Electrical Instruments and Equipments

5.3.1 Voltage Variance

The voltage variance is an instrument to vary power to an electrical appliance as shown in Figure 5.6. The voltage variance was used to vary power to heating element and through the welding machine.

5.3.2 Voltmeter

The voltmeter is an instrument was used to measure the volts during charging and discharging the heat storage systems as shown in Figure 5.6

Figure 5.6 Voltages Variance and Voltmeter

5.3.3 Digital Multimeter DT9205

It is an instrument used to measure the volts and current flow during electric heating process as shown in Figure 5.7

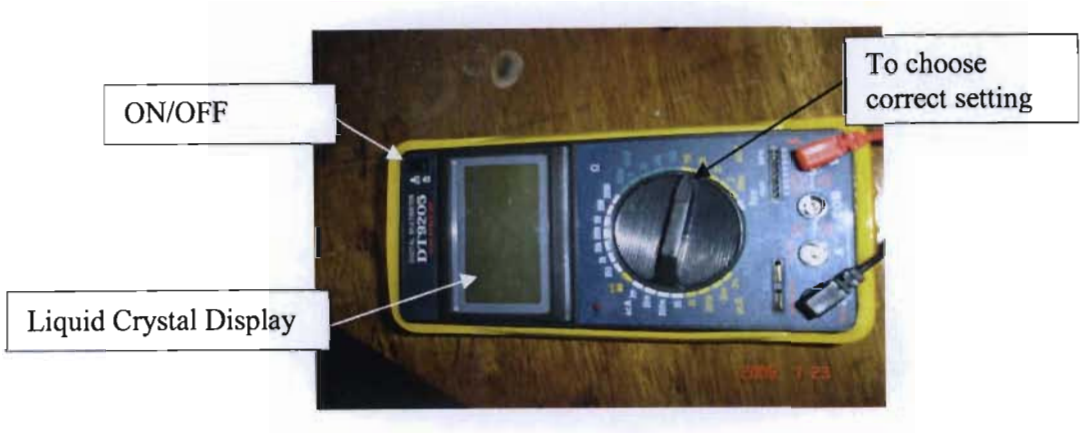

Figure 5.7 Digital Multimeter DT9205

5.3.4 Electric Resistance Heaters

Electric resistance heating converts nearly 100% of the energy in the electricity to heat by resisting the free flow of electric current. However, most electricity is produced from oil, gas, or coal generators that convert only about 30% of the fuel's energy into electricity. Because of electricity's generation and transmission losses, electric heat is often more expensive than heat produced in the home with combustion appliances, such as natural gas, propane, and oil furnaces [92].

Electric heating has several advantages: it can be precisely controlled to allow a uniformity of temperature within very narrow limits; it is cleaner than other methods of heating because it does not involve any combustion; it is considered safe because it is protected from overloading by automatic breakers; it is quick to use and to adjust; and it is relatively quiet. For these reasons, electric heat is chosen to be use.

Resistance heaters produce heat by passing an electric current through a resistance coil, wire, or other obstacle which impedes current and causes it to give off heat. Heaters of this kind have an inherent efficiency of 100% in converting electric energy into heat. Devices such as electric ranges, ovens, hot-water heaters, sterilizers, stills, baths, furnaces, and space heaters are part of the long list of resistance heating equipment.

5.3.4.1 Finned Tubular Heaters

Finned tubular heaters consist of a tubular heating element with a series of fins attached to the heating element's steel sheath to increase the surface area.

Typical Applications: Process gas and air applications, including drying and gas heating, are common.

Temperature Range	:	Up to 1200°F (649°C) with a stainless-steel sheath, or as limited by the fin-attaching braze material, is recommended.
Watt-Density Range	:	Up to 80 W/in^2 (12.4 W/cm^2) is recommended.
Thermal Response	:	This is better than that obtained with no finned units, allowing increased watt density and lower operation temperatures.
Efficiency	:	Efficiency is 100 percent when gas is heated.

5.3.4.2 Immersion Heaters-Tubular

Immersion heaters consist of hairpin or straight tubular heating elements brazed, welded, or mechanically fastened into a plug, fitting, to be plumbed into a fluid flow system for fluid heating as shown in Figure 5.8.

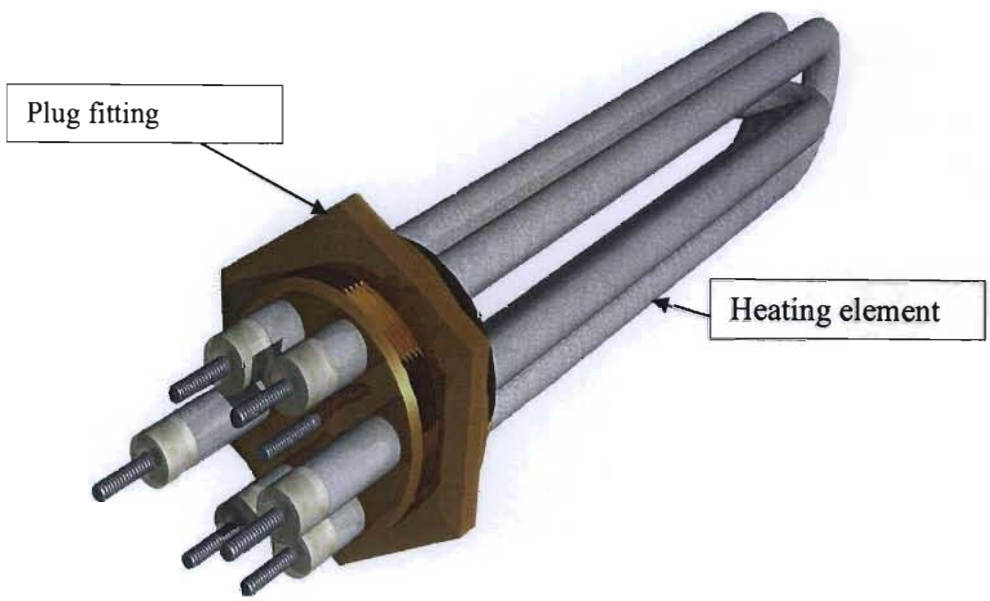

Figure 5.8 Immersion Heater

Tubular immersion heaters are used in applications requiring the heating of fluids or highly viscous materials. Electric immersion heaters are especially suitable for heating fluids via natural or forced convection. They are mainly used for water heaters, heating tanks and for

fluid circulation heaters. Depending on the application, they exist in different materials. The layout of heating elements allows an optimum heat exchange [92].

5.3.4.2 Variable Frequency Drive

A variable frequency drive is an electronic controller that adjusts the speed of an electric motor by regulating the power being delivered. Variable-frequency drives provide continuous control, matching motor speed to the specific demands of the work being performed.

Single-speed drives start motors abruptly, subjecting the motor to high torque and current surges up to 10 times the full-load current. Variable frequency drives offer a soft start, gradually ramping up a motor to operating speed. The variable frequency lessens mechanical and electrical stress on the motors and can reduce maintenance and repair costs and extend the motor life. Vector inverter CFW^{08} Variable Frequency Drive as shown in Figure 5.9 is used during charging the oil heating storage system experiments to control fluid flow rates by adjusts the oil pump speed to get the desired rate.

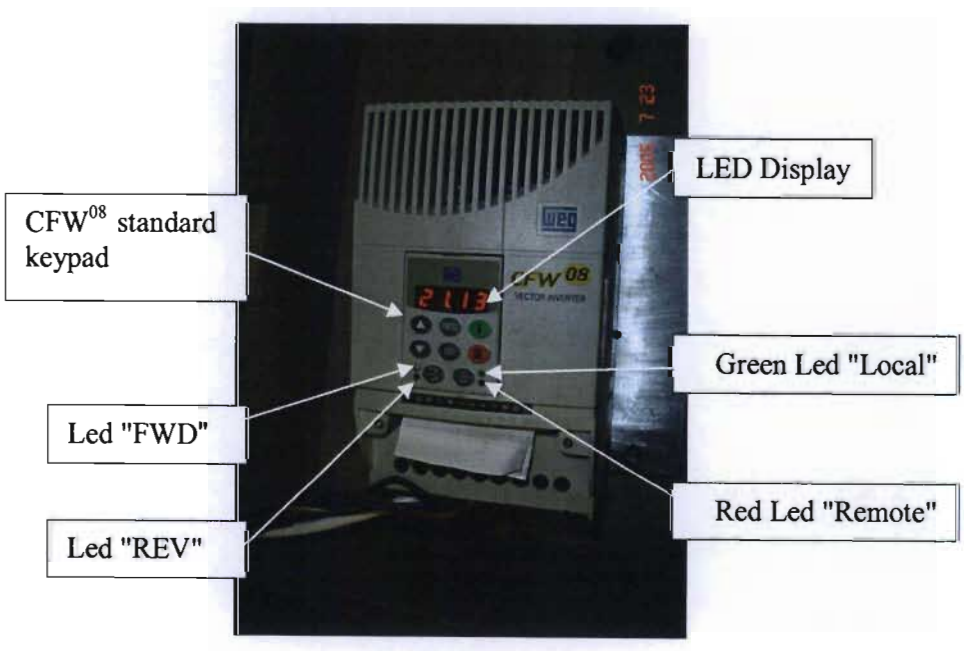

Figure 5.9 Vector inverter CFW^{08} Variable Frequency Drive

5.4 Summary

In this chapter experimental instruments and equipment have been discussed. Details of temperature measurement, thermocouples, thermocouple usage, thermocouple standards, type j, and type k have been given.

Some details of analogue to digital conversion tools, pci-773 thermocouple/rtd input board, data logger, thermocouple thermometer, calibration of instruments, pc-733 thermocouple card, and electrical instruments were included discussed.

CHAPTER 6
ENERGY CONSIDERATION AND MATERIAL SELECTION

6.1 Energy Required for Cooking

The intrinsic design feature of a solar cooker is the means to covey heat to foodstuffs thereby increasing their temperature so that they may be cooked via the raised temperature and the associated chemical changes involved in the cooking process. Numerous cooking methods exist throughout the world; however the principal ones are outlined below.

During the processes of boiling and frying, heat is transferred from the heated liquid to the solid food, whereas in baking and roasting heat is transferred both by convection from the surrounding hot air and sometimes by radiation from hot surfaces.

6.1.1 Heat Transfer

A close relationship exists between thermal energy and the temperature of matter. As a general principle for any particular material and mass; the higher the temperature, the greater its thermal energy. The study of heat transfer focuses on the exchange of thermal energy through a body or between bodies which occurs when there a temperature difference exists. In the case of two bodies which are at different temperatures, thermal energy transfers from the one with higher temperature to the one with lower temperature. Heat always transfers from hot to cold.

Displayed in Table 6.1 are the standard SI and English units and conversion factors to describe heat and heat transfer rates. The symbol Q typically represents heat, and is expressed in joules (J) in SI units. The rate of heat transfer is measured in watts (W), equal to joules per second, and is denoted by q. The heat flux, or the rate of heat transfer per unit area, is measured in watts per area (W/m^2), and uses q'' for the symbol.

Table 6.1 Units and Conversion Factors for Heat Measurements

	SI Units	English Units
Thermal Energy (Q)	1 J	9.4787×10^{-4} Btu
Heat Transfer Rate (q)	1 J/s or 1 W	3.4123 Btu/h
Heat Flux (q'')	1 W/m^2	0.3171 Btu/h ft^2

6.1.2 Three Modes of Heat Transfer

Heat transfer can occur in 3 different modes, namely conduction, convection, and radiation. Any exchange of energy between bodies takes place through one of these modes or a combination of them. The transfer of heat through solids or stationery fluids is referred to as conduction. Convection utilizes the movement of fluids to transfer heat but radiation does not require a medium for transferring heat; instead this mode uses the electromagnetic radiation emitted by an object for exchanging heat [93].

6.1.2.1 Conduction

The transfer of heat through solids or stationery fluids occurs through conduction. When you touch a hot object, the heat you feel is transferred through your skin via this process which involves two mechanisms, namely lattice vibration and particle collision. Conduction through solids occurs by a combination of the two mechanisms; heat is conducted through stationery fluids mainly by molecular collisions.

The nature of solids is such that atoms are bound to each other by a series of bonds, comparable to springs as shown in Figure 6.1 When there is a temperature difference in the solid, the hot side of the solid undergoes more vigorous atomic movements. These vibrations are transmitted through the springs to the cooler side of the solid. Finally, they reach an equilibrium, whereby all the atoms are vibrating with the same energy.

Out of all solids, metal in particular has free electrons, which are not bound to any particular atom and can freely move about the solid. The electrons in the hot side of the solid move more quickly than those on the cooler side. This occurrence is illustrated in Figure 6.2. As the electrons are subject to a series of collisions, the faster electrons give off some of their energy to the slower electrons. Finally, after a series of random collisions, a sete of equilibrium is reached, where the electrons are moving at the same average velocity.

Comparatively speaking, conduction through electron collision is more effective than through lattice vibration; this is why metals generally are better heat conductors than ceramic materials, which do not have many free electrons. In fluids, conduction takes place through collisions between freely moving molecules. The mechanism is exactly the same as the electron collisions in metals.

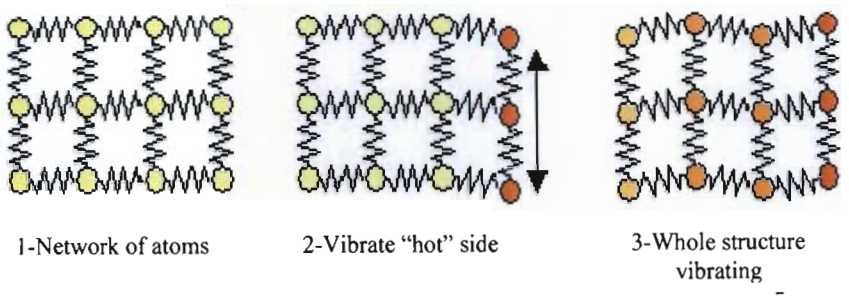

Figure 6.1 Conduction by lattice vibration

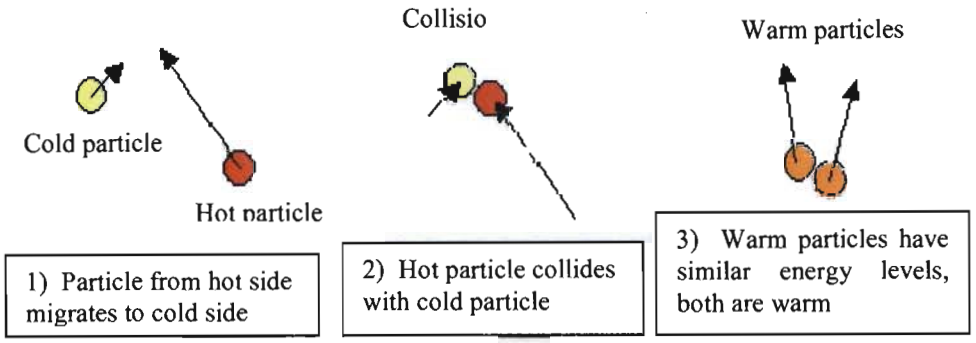

Figure 6.2 Conduction by particle collision

Thermal conductivity measures the effectiveness by which heat is transferred through a given material, *k*. A good conductor, for example copper, has a high conductivity; a poor conductor, or an insulator, has a low conductivity. Conductivity is measured in watts per meter per Kelvin (W/m/K). The rate of heat transfer by conduction is given by:

$$q_{conduction} = -kA\frac{\Delta T}{\Delta x} \quad \text{.....6.1}$$

Where A = Cross-sectional area through the heat conducting,

T = Temperature difference between the two surfaces

Δx = Distance

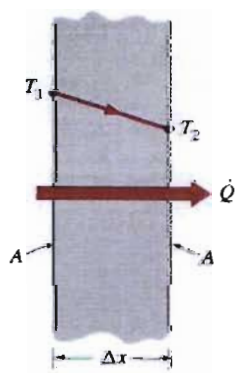

Figure 6.3 Heat Conduction through a Large Plane Wall

6.1.2.2 Convection

The motion of fluids is used in convection to transfer heat. A typical convective heat transfer involves a hot surface heating the surrounding fluid, which is then carried away by fluid movement such as wind. The warm fluid is substituted by cooler fluid, which can retract more heat away from the surface. Because the heated fluid is constantly replaced by cooler fluid, the rate of heat transfer is magnified. In the case of natural convection (or free convection), the fluid movement is generated by the warm fluid itself. The density of fluids decrease as they are heated which means that hot fluids are lighter than cool fluids. Warm fluid surrounding a hot objects rises, and is replaced by cooler fluid. The result is a circulation of air above the warm surface, as depicted in Figure 6.4.

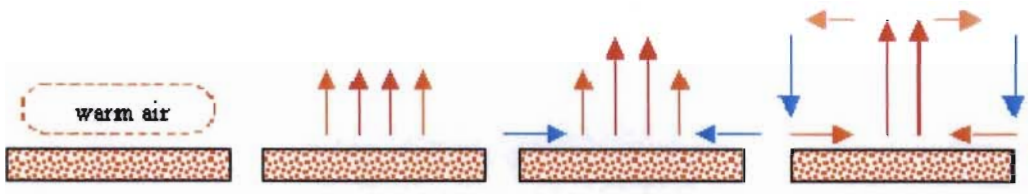

Figure 6.4 Natural convection

The main feature of forced convection is its use of external means to produce fluid movement. This phenomenon is what makes a windy, winter day feel much colder than a calm day with same temperature. The heat loss from your body is exacerbated due to the constant replenishment of cold air by the wind. Natural wind and fans are the two most common sources of forced convection.

Convection coefficient H, is the measure of how effectively a fluid transfers heat via the convection process. It is measured in W/m^2K, and is determined by factors including fluid density, viscosity, and velocity. Wind blowing at 5 mph has a lower h than wind at the same temperature blowing at 30 mph. The rate of heat transfer from a surface by convection is given by:

$$q_{convection} = -kA(T_{surface} - T_{\infty}) \quad \text{.....6.2}$$

Where A = The surface area of the object,

$T_{surface}$ = Surface temperature

T_{∞} = Ambient or fluid temperature

6.1.2.3 Radiation

The transfer of radiative heat does not need a medium to pass through it and so as a result, it is the only form of heat transfer present in vacuum. It uses electromagnetic radiation (photons), which travels at the speed of light and is emitted by any matter with temperature above 0 degrees Kelvin (-273 °C). Radiative heat transfer occurs when the emitted radiation strikes another body and is absorbed. Everyone experiences radiative heat transfer on a daily basis; solar radiation, absorbed by our skin, is why we feel warmer in the sun than in the shade [93].

According to the electromagnetic spectrum, radiation is classified based on wavelengths of the radiation. The main types of radiation are (from short to long wavelengths): gamma rays, x-rays, ultraviolet (UV), visible light, infrared (IR), microwaves, and radio waves.

Radiation containing shorter wavelengths is more energetic and holds more heat. X-rays, having wavelengths ~10-9 m, are very energetic and can be harmful to humans, while visible light with wavelengths ~10-7 m contain less energy and therefore have little effect on life. An additional characteristic with subsequent significance is that radiation with longer wavelengths generally can penetrate through thicker solids. Visible light, as is generally known, cannot penetrate a wall. However, radio waves, having wavelengths on the order of meters, can easily pass through concrete walls [93].

Radiation is emitted from anybody with a temperature above 0 Kelvin, and the emitted radiation type is determined to a greater degree by the temperature of the body. Most "hot" objects, from a cooking standpoint, emit infrared radiation. Hotter objects, such as the sun at ~5800 K, emits more energetic radiation including visible and UV. The visible portion is evident from the bright glare of the sun; the UV radiation causes skin to tan and burn.

The following equation shows the amount of radiation emitted by an object:

$$q_{emitted} = \varepsilon\sigma . AT^4 \quad \text{.....6.3}$$

Where A = The surface area of the object,

$T_{surface}$ = Surface temperature

σ = Stefan-Boltzmann constant, equal to 5.67×10^{-8} W/m^{2}k^4

ε = Emissivity

The emissivity has a value between zero and 1, and is a measure of how efficiently a surface emits radiation. It is the ratio of the radiation emitted by a surface to the radiation emitted by a perfect emitter at the same temperature.

The radiation which is emitted strikes a second surface, whereupon it is reflected, absorbed, or transmitted Figure 6.5. The segment that contributes to the heating of the surface is the absorbed radiation. The percentage of the incident radiation that is absorbed is called the absorptivity, a. The amount of heat absorbed by the surface is given by:

$$q_{absorbed} = \alpha . I \quad \text{.....6.4}$$

Where α = Absorptivity,

I = Incident radiation

The incident radiation is determined by the amount of radiation emitted by the object and how much of the emitted radiation actually makes contact with the surface. The latter is given by the shape factor, F, which is the percentage of the emitted radiation reaching the surface.

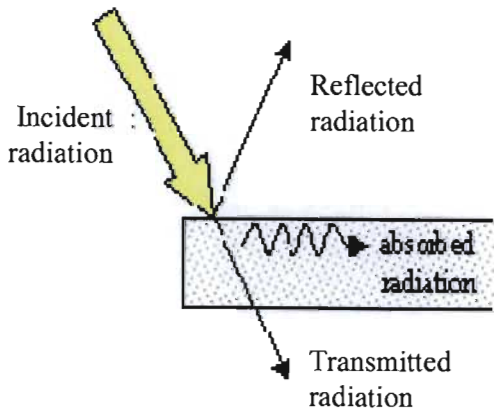

Figure 6.5 Interaction between a surface and incident radiation

6.2 Cooking Methods

Cooking methods can be characterized into two main types: dry heat cooking and moist heat cooking. Dry heat cooking heats foods in the absence of water, and includes methods such as baking and roasting, broiling, and pan-frying. A moist heat cooking use water to heat food, and includes boiling, simmering, braising, and steaming.

6.2.1 Dry Heat Cooking

Ovens are used in many dry heat methods. Electric ovens use two heating coils, located at the top and bottom of the oven. The bottom coil is used for baking and roasting; the top is used for broiling. The heating coils are simply resistive elements which are heated by passing an electric current through them [94].

In traditional ovens, when bottom coil is heated, the air inside the oven is heated primarily by conduction and natural convection. The heat is then transferred to the food, which is heated by the natural convection current. In a convection oven, the heat transfer is enhanced by the use of a fan. The fan creates forced convection within the oven, which not only heats the food faster but also encourages even distribution of heat.

Heat transfer inside an oven is actually more complicated than simply conduction and convection. The heating element emits a considerable amount of radiation which also contributes to the heating of the food. In addition, the walls of the oven become heated as well, emitting their own radiation. Broiling takes advantage of the radiation from the coil to rapidly heat the top of the food. Broiling uses only the top coil, which suppresses the natural convection current since the hot air is blocked by the ceiling of the oven. The radiation from the top coil (which is often set to a very high temperature) heats the surface of the food to high temperatures, promoting browning [95].

Cooking on the stovetop utilizes conduction through a pan to heat the contents. In dry heat cooking, heat is conducted directly from the pan to the food, as shown in Figure 6.6. The heat is generated by resistive elements on electric stovetops.

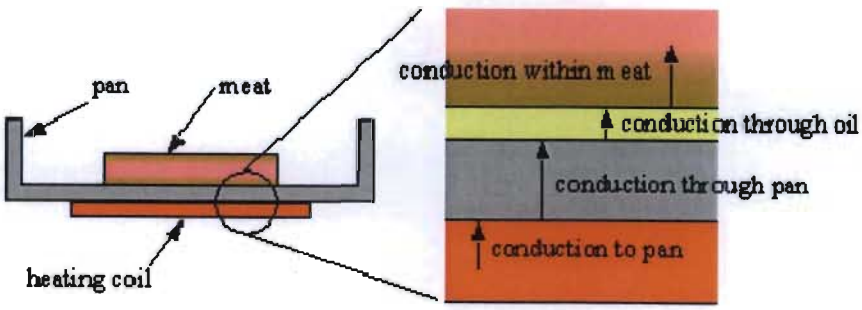

Figure 6.6 Dry Heats Cooking on the Stovetop

6.2.2 Moist Heat Cooking

Moist heat methods use water in various states to heat food. The most common state is boiling, where water is heated by conduction through a pot on stovetop, and the heat is

transferred to the food through convection as shown in Figure 6.7. Water boils at 100 °C at sea level; therefore, boiling allows the food to cook at a constant temperature of 100°C. Although this provides a convenient, consistent cooking medium, one major disadvantage is the lack of browning and the flavors that accompany the browning reaction. Browning of food occurs at temperatures above ~150°C, which cannot be reached by moist cooking methods. The boiling point of water can be raised slightly to reduce the cooking time. Impurities, such as salt, increase the boiling temperature by a few degrees. Pressure cookers also effectively raise the temperature of boiling water by increasing the pressure inside the pot. The relationship between pressure and boiling point is discussed in greater detail later on in the course.

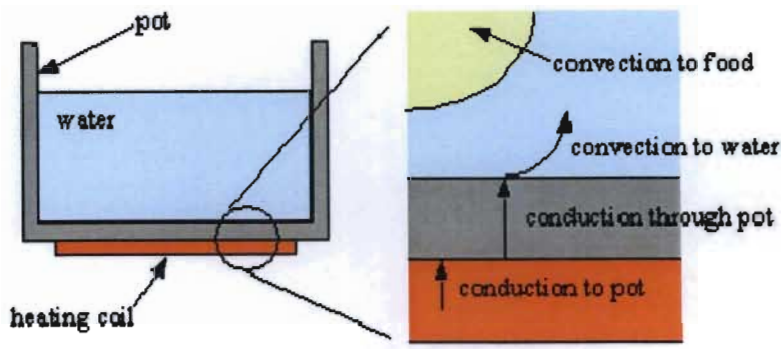

Figure 6.7 Moist heat cooking

Various states of water are used for cooking, and there are special names for some of them. Poaching uses warm water just before boiling. Simmering refers to cooking in water when it has just begun to boil. Boiling uses vigorously boiling water. Steaming uses the water in vapor phase to heat the food. The temperature of steam is typically a few degrees hotter than the temperature of boiling water.

6.2.3 Other Methods [96]

Deep frying is classified as a dry heat method, although the food is heated indirectly by convection through the oil. Oils can reach a higher temperature than water; this is why the food can be browned during frying but not in boiling. Typical frying temperatures range between 180°C and 200°C.

Microwave has become a popular cooking appliance, mainly because of its ability to heat foods quickly. It uses electromagnetic radiation to agitate water molecules, which then produce heat due to friction. You will study more about microwave ovens later on in the course.

6.3 Cooking Materials

Most cooking containers are metal or ceramic, due to their ability to withstand high temperatures. Common metals are aluminum, copper, tin, stainless steel, and cast iron. Ceramics include glass, porcelain, earthenware, and stoneware. In addition, non-stick coatings and enamel coatings may be used on the surfaces to improve the properties.

Thermal conductivity, density, and specific heat are three very important factors in determining what cooking material is best suited for the kitchen. A high conductivity material tends to have a more even temperature distribution than one with a low thermal conductivity. A material with low specific heat requires less thermal energy to heat; therefore, it heats faster than one with a high specific heat. Thermal diffusivity (a) is the combination of the three properties:

$$\alpha = \frac{k}{\rho . C_p} \quad \text{.....6.5}$$

Where k = Thermal conductivity,

C_p = Specific heat

a = Thermal diffusivity

ρ = Density

Thermal diffusivity measures the effectiveness by which a material conducts thermal energy with respect to its ability to store thermal energy. A material with high a is characterized by a quick response to the changes in surrounding temperatures. A material with low a takes longer to reach a steady state condition, but is excellent at retaining heat once heated.

In addition to the effect of material properties, the thickness (mass) of pot also changes the heating characteristics. Thicker pots tend to allow more uniform heat distribution; however, they take longer to heat. The size and placement of the heating element with respect to the pot is also of concern.

6.3.1 Metals

Copper has the highest conductivity among all common cooking materials. Copper pans are highly treasured due to their ability to distribute heat evenly. However, copper tends to oxidize, leaving a black tarnish on its surface which also reduces its conductivity. To prevent oxidation, copper pots need constant cleaning and polishing.

In addition, copper can be toxic if it diffuses into food in large amounts. Copper pans are often lined with tin to overcome these difficulties. The high costs of copper pans keep them from being used in majority of households.

Table 6.2 Properties of Common Cooking Materials [99]

Material	ρ (kg/m^3)	k (W/mK)	c_p (J/kgK)	a ($10^{-6}m^2/s$)
Aluminum	2780	170	880	70
Cast iron	7870	70	450	21
Copper	8900	400	385	117
Stainless steel	8000	15	480	3.7
Glass	2600	4	800	1.9

Aluminum pans have the second highest thermal conductivity, next to copper, and are available at much lower cost. Aluminum is non-toxic and non-reactive, and also lightweight. Anodized aluminum has a thin coating of aluminum oxide (Al_2O_3) on the surface. Aluminum oxide forms as a result of aluminum reacting with oxygen at high temperature, and is a very hard ceramic suitable for protection from scratches.

Stainless steel is an alloy of iron, chromium, and nickel, and is desired due to its strength and resistance to corrosion. However, it is a relatively poor conductor, and often must be lined with copper or aluminum to improve the heat distribution. Cast iron is typically iron alloyed with a small amount of carbon to increase strength. Cast iron pans are very prone to corrosion, and must be "seasoned" to prevent rusting. Seasoning a pan involves coating it with oil, then heating at moderate heat for a few hours. This fills up the small pores on the surface of the pan. Cast iron pans are generally heavy duty, allowing even heating despite the low conductivity and an ability to retain heat well.

7.3.2 Ceramics

Ceramic is usually a compound of metallic and non-metallic elements. They are poor conductors of heat, but are excellent at retaining heat once heated. They are very resistant to corrosion and are non-toxic. Due to their ability to retain heat, dishes made of thick ceramic materials will keep foods warm longer than metallic serving dishes of comparable shape and size.

A common problem with most ceramics is their tendency to crack due to thermal stress. Since they are such poor conductors of heat, there may be a large temperature difference between one side of the pan and the other. In such case, the warmer side expands more than the other, causing the pan to crack. Ceramic pans are seldom used on stovetops for this reason; ovens allow even heating from all sides, preventing large thermal gradients.

6.3.3 Coating Materials

Two common materials used for coating are Teflon (non-stick coating) and glass enamel. Teflon is a polymer which covers small roughness on pan surfaces and forms a very smooth finish, preventing food from sticking. Teflon coated pans are popular for low fat cooking; however, the coating is easily scratched by metal utensils. Glass enamel is formed by fusing glass powders to pan surfaces. The enamel improves the chemical resistance of the pan and prevents corrosion; however, they may crack when exposed to sudden changes in temperature.

All of these methods require that the food must first be raised to cooking temperature, and then kept at this temperature for a sufficient period to effect the softening, drying, decomposing, coagulating or other change required. The quantities of heat necessary for most of these physical and chemical changes involved in cooking are small as the chemical heats of reaction or conversion are unimportant in comparison with the heat for increasing the food's temperature and the heat losses.

The majority of foods contain a high proportion of water, and heating them to cooking temperatures necessitates 4.2kJ/ kg/°C. The higher the heat input rate to the food and container the faster the food will heat to cooking temperature. Except where water vaporization is a necessary part of the cooking process as in bread baking, the speed of cooking is practically independent of heat rate as long as the temperature is maintained by a heat input rate equal to the thermal losses. It is therefore generally true that differences in the time required for cooking similar quantities of food on cookers having various heat supply capacities are due mainly to the different durations of the heating up periods. This implies that cookers of low and high heat supply rates may not show large differences in the time required for foods that have to be cooked for several hours.

The largest form of cooking heat loss is usually the heat consumed in vaporizing water present in the food or added for, followed by convection losses from utensils and oven walls.

If the energy source has a limited capacity such as the solar input, control of these losses becomes important. Lof [97] estimates that the energy used in boiling food for one hour assuming a quarter of the water boils away is distributed as follows:

Heating food to 100°C	25%
Convection losses from vessel	45%
Vaporization of water	35%

According to his estimates, the hourly convection loss is about 6800 kJ/m2 of cooking utensil; hence an average size pot of 0.2m diameter and 0.1m height would lose 240 W by convection, requiring a total input of 530 W. Swet [98, 99] estimates that 2kWh is required to cook a family meal, so that approximately four hours of cooking time is required with an input of 530 W.

The required food temperatures needed for cooking do not fluctuate to a great degree because starches and proteins are gelatinized and denatured respectively in the region of 65°C to 75°C. However, the time required to complete cooking is not linearly related to temperature as cooking at 75°C may take five to ten times longer than at 100°C. Even though a temperature of 75°C or greater will initiate the cooking process, the temperature of the heat supply depends greatly on the type of cooking. Direct fire involves temperatures of up to 1000°C making high heat transfer rates possible whereas oven cooking requires temperatures of approximately 200°C, so the heat transfer rates are lower and longer cooking periods are required.

Solar cookers of the practical variety should provide a heat supply rate equal to that commonly used. Hotplates average at one kilowatt capacity, a rate capable of boiling two litres of water in ten minutes. For a solar unit to provide this power at least two square metres of collector area is required. If less than this is used, either longer cooking times must be accepted, smaller quantities of food used, or heat conservation practiced [100]

6.4 Types of Cook Tops

Cook tops, also called hotplates, are small stoves with one or more burners at the top. Unlike regular stoves, they consist simply of burners and do not include grills and ovens. They are usually placed on countertops and connected to an underwater gas tank or power socket.

For most people, availability of a gas hookup will partly determine whether they ultimately go with a gas or electric cook top.

6.4.1 Gas Burners

Quick response time and easily adjustable, provide good temperature control and consumption varies according to the size of the burner and setting.

6.4.2 Electric Hotplates

There are three types of electric hotplates available - coil, solid and ceramic. Efficiency varies between different types as shown in the Table 6.3.

Table 6.3 Efficiency of different types of hotplates [101]

Type of electric hotplate	Efficiency (%)
Coil	55 – 65
Solid	50 – 55
Ceramic – Standard	55 – 60
Ceramic – Halogen	45 – 50
Ceramic – Induction	80 – 85

6.4.2.1 Radiant Coil Hotplates

Quick response time and easily adjustable, more efficient than solid and ceramic hotplates, generally hinge up so that spillage bowls can be cleaned (some models have plug-in elements which can be removed for easier cleaning and replacement).

6.4.2.2 Solid Hotplates

- Fixed to the hob and do not need to be moved for cleaning.
- Slightly less efficient and have a slower response time than coil hot plates.
- Retain heat longer than coil plates so they can be switched off before cooking is finished to save energy.
- Require regular cleaning to maintain their efficiency and appearance.

6.4.2.3 Ceramic Cook Tops

- Have elements concealed under a flat, glass surface.
- Provide stylish appearance and are easier to clean than coil and solid hotplates.

- Less efficient and have a slower response time than coil and solid hotplates.
- Generally more expensive to purchase than coil or solid hotplates.

Should have a light to indicate when there is residual heat in the cook top. Cook tops of the ceramic variety can also use halogen elements. These have precise and time to cool down once switched off. They are less energy efficient than other electric accurate heat control with an almost instant response time but take a relatively long hotplate.

6.4.2.4 Induction Cooking

Electromagnetic technology is used in induction cooking to heat the cooking utensil and its contents with very little energy wasted on heating the ceramic cooking surface. Power is supplied via an electronic circuit and electronically controls an inductor coil inside the appliance. This coil generates a magnetic field when a saucepan is placed in contact with the hob's surface causing induction currents to flow through the base of the pan. The cook top surface stays cool, and spillages don't get baked on, making cleaning easier.

This form of cooking also provides immediate response and precise temperature control. It is a relatively new technology and is considered to be the most efficient type of electric hotplate. Induction cook tops can only be used in conjunction with certain types of cookware. These include cast iron, iron, enameled steel and certain types of glass with an iron-alloy base inset. Standard glass, aluminum, copper based, stainless steel (unless with an iron core) and earthenware cooking vessels are unsuitable.

6.5 Hotplate Temperatures

There is an absence of data on hotplate temperatures required to cook food within satisfactory times. At this juncture a distinction must be made between the quantity of heat energy available and the temperature of this energy. A cooker might be able to supply One kilowatt at 100°C, but as the pot nears 100°C, the heat input will drop considerably because of the thermal contact resistance, and the time taken per unit temperature rise will increase substantially. If a continuous kilowatt is supplied to a hotplate, the temperature of the hotplate will rapidly rise to 300-400°C whilst the water in the pot comes up to boil.

For the purposes of obtaining order of magnitude figures for hotplate temperatures, a 150mm diameter electric hotplate had a thermocouple inserted at the centre of its top surface as

shown in Figure 6.8, and a 150mm diameter aluminum pot containing one liter of water was used to represent the cooking utensil. The lid was kept on the pot throughout the tests.

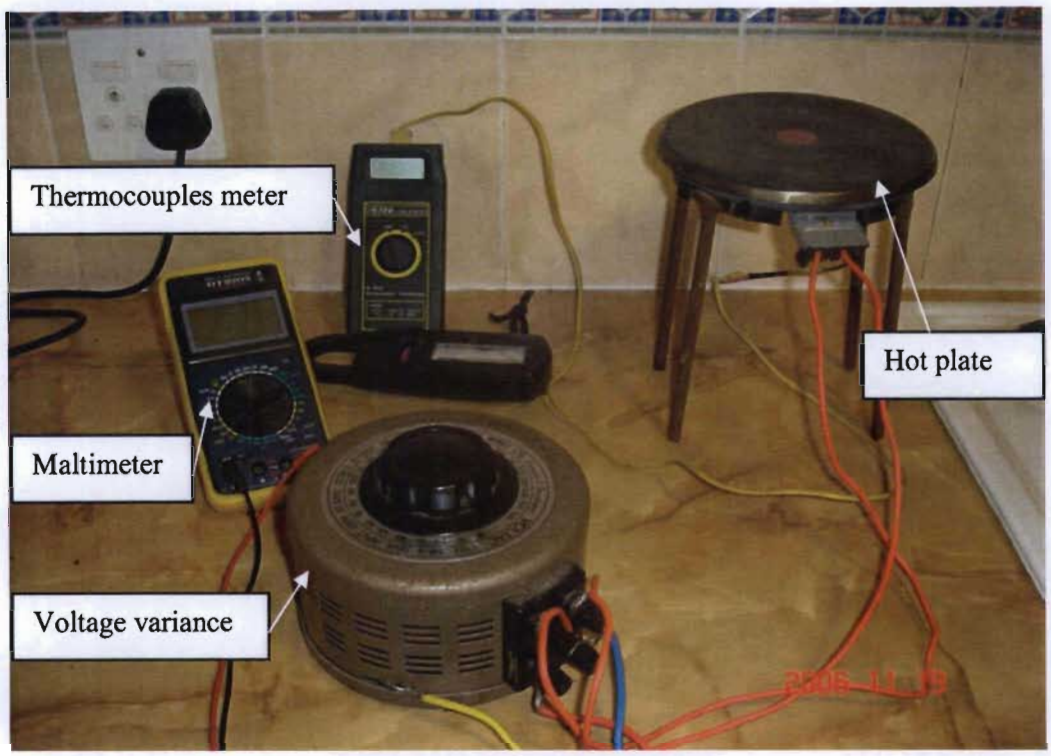

Figure 6.8 Hotplate Temperature Test Rig

Investigations included two different energy input modes, namely constant heat energy input and constant hotplate temperature. For the first mode, the hotplate was connected through a wattmeter, and the energy input controlled by a variable voltage source, whilst the constant hotplate temperature tests used a Eurotherm temperature controller to monitor the thermocouple in the centre of the hotplate.

Dual energy inputs of 300 watts and 900 watts on a constant basis gave times to boiling from 21° C of 75 minutes and 17 minutes respectively. However, even though the hotplate temperatures were initially at ambient the temperatures at the point of boiling were 255°C and 410°C respectively.

Whilst the water was boiling, the 300W input temperature remained at 255°C and the 900W input increased to 470°C. For the constant temperature case, hotplate temperatures of 150, 200, 250 and 300°C were used. The average times to boil which obtained from several experiments are given in Table 6.4.

A dramatic time increase occurs with lower hotplate temperatures, but it must be noted that these times would be considerably less if a pot with a larger base was used. For the purpose of estimating the losses from the pot at 100°C and the contact resistance between the pot and hotplate, the hotplate temperature was lowered until the water in the pot was just boiling. This was found to occur at 115°C with a power input of 140W.

Table 6.4 Boiling Times

Temperature (°C)	Pot (a) Aluminum Average Time (mins)	Pot (b) stainless steel Average Time (mins)
300	20	17
250	28	21
200	43	38
150	89	79

Alternatively the losses can be found by the rate at which the pot cools near 100 °C, and the energy balance is given by:

Heat energy lost from pot = heat lost by water + heat lost by aluminum

The one liter pot of water at 100° C was removed from the hotplate and placed on a surface of low thermal conductance. With the lid kept on, the average temperature dropped from 98°C to 90° C in four minutes, and substituting these values into the equation yields a loss of 151W which corresponds to the measured loss above.

Through already established data on the losses at boiling, and the minimum temperature difference required to keep the water boiling, the contact resistance can be calculated,

$$q = h_t A(T_2 - T_1) \quad \text{.....6.6}$$

Where h_t = Contact Coefficient

A = Contact Area

T_2 = Temperature of hotplate

T_1 = Temperature of pot

6.6 Energy Storage Materials Selection

It is essential that the heat store operating temperature be in the region of 200 °C to 300 °C in order to provide a suitable heating rate of the food to be cooked. Water is unsuitable as the heat transfer fluid because it vaporizes at 100 °C at atmospheric pressure, although it has a high specific heat. Pressurizing the system will increase the boiling point, but even increasing the pressure to 15 bars will only raise the boiling point to 200 °C. Furthermore, high pressure piping and tanks would be required which are expensive and the unit could explode showering users with scalding water.

To draw the figures 6.9, 6.10, 6.13 and 6.14 we used Equation 2.1 in chapter 2 to calculate the sensible heat storage, and using Equation 2.2 in chapter 2 to calculate the latent heat tstorage per unit mass and The heat storage capacity per unit mass and per unit volume for water (20 - 99.9 °C), molten salt (60% sodium nitrate,40% potassium nitrate), sodium nitrate and potassium nitrate, oil, Scrap Iron, scrap aluminum and rock at temperature from 25 to 325 °C are shown in Figure 6.9 and Figure 6.10. The reference temperature is 25 °C. Because water evaporates over 100 °C less than 1 atm pressure, the upper limit for the water temperature is usually less than 100 °C. Figures 6.9 and 6.10 were shown that molten salt has very high heat storage capacity. For the temperature range from 20 °C to 320 °C, the heat storage capacities per unit mass and per unit volume of molten salt are 3.15 and 2.94 times that of rock, respectively.

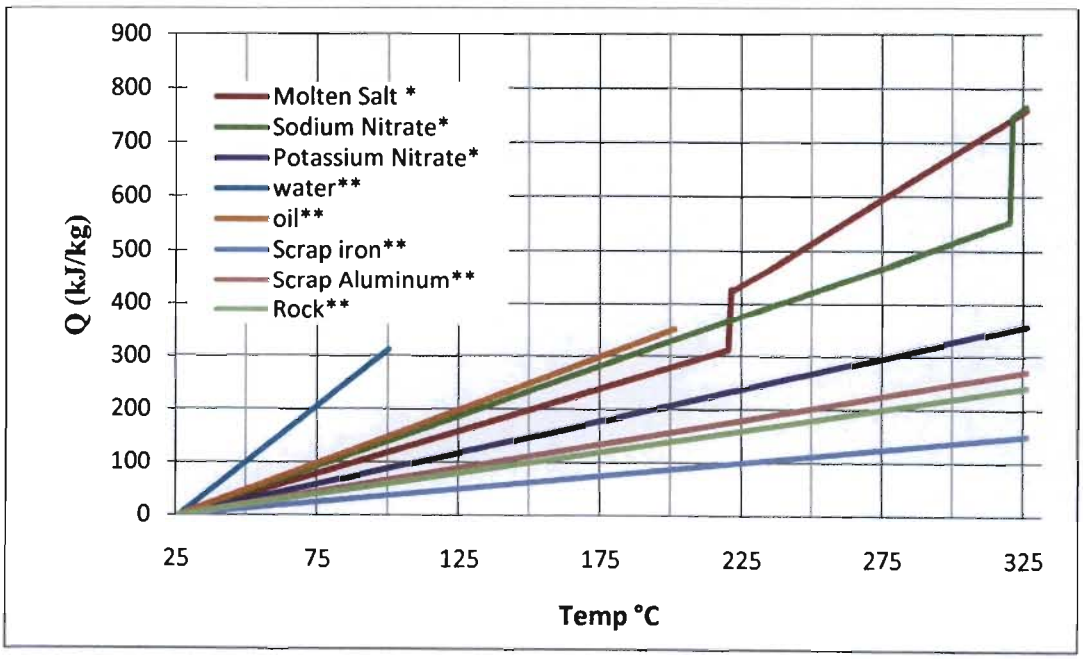

* Abdul's experiments, ** drawn using data from appendix T

Figure 6.9 Heat Storage Capacity per Unit Mass

Compared with water, the heat storage capacity of molten salt is much higher because of the greater temperature range available and the latent heat of molten salt. The heat storage capacity per unit mass and per unit volume of molten salt (20 – 320 °C) are 2.36 and 4.85 times that of water (20 – 99.9 °C), respectively.

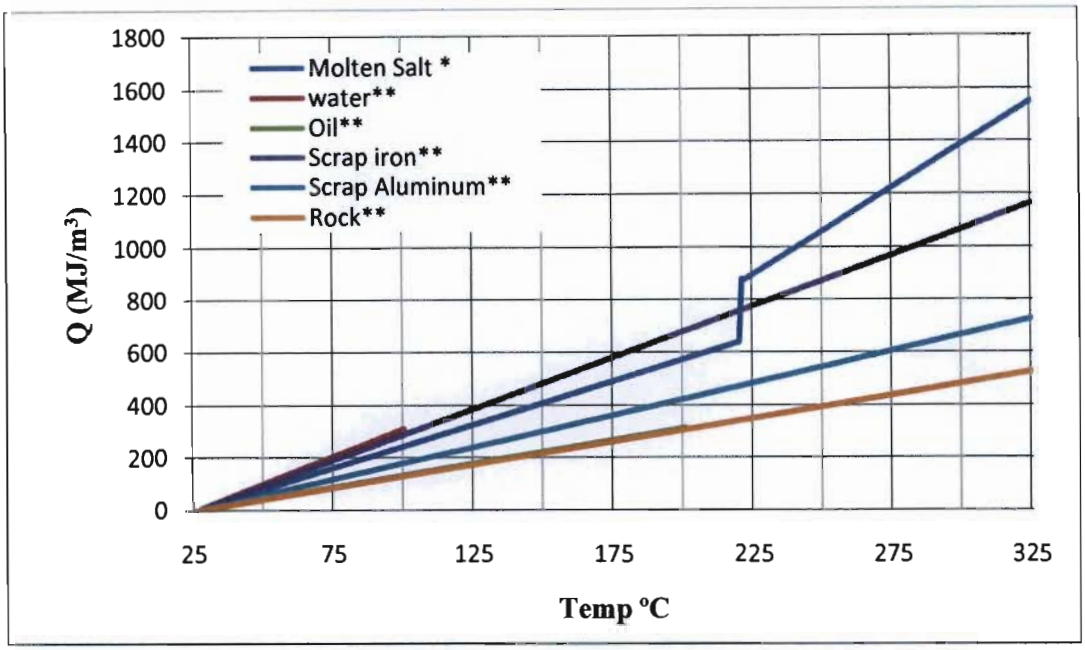

Figure 6.10 Heat Storage Capacity per Unit Volume

Through a number of experiments, visual testing at different temperature of Sodium Nitrate, Potassium Nitrate and molten salt the mixture of both (60% sodium nitrate,40% potassium nitrate) as shown in Figures 6.11 and 6.12. Figure 6.13 shows until 290 °C there are no changes in phase of sodium nitrate and potassium nitrate. Sodium nitrate: colorless transparent crystals or white granules or powder, with saline, slightly bitter taste, deliquesces in moist air.

Potassium nitrate: colorless transparent prisms or white, granular or crystalline powder with cooling, saline pungent taste.

Figure 6.14 shows the phase change and melting of molten salt; it just started at 218°C.
In Figures 6.9 – 6.12, curves denoted by * were obtained from authors experiments and ** are drawn using past data from Table T.18 in appendix T.

In order to observe the behaviour of sodium nitrate and potassium nitrate the sample of 200 g of sodium nitrate and 200g of potassium nitrate were put in kiln. By controlling the temperature from 0 to 290 °C, maximum temperature was 290 °C, increment 1 °C for a period of 2 hrs. The result was that till 290 °C no changes in phase both stay in solid phase, just a little bit changing in colour of potassium nitrate as shown in Figure 6.11.

Figure 6.11 Sodium Nitrate and Potassium Nitrate tests at 290°C

For the reason that the maximum temperature of heat transfer fluid which were used was 320°C and heat loss from the system, the operating temperature was from 250 °C to 290 °C. For all that to reduce the melting point the Sodium Nitrate and Potassium Nitrate were mixed, following that the mixture were put in kiln to observe their behaviour. As shown in Figure 6.12 at 218°C, the mixture partially melted.

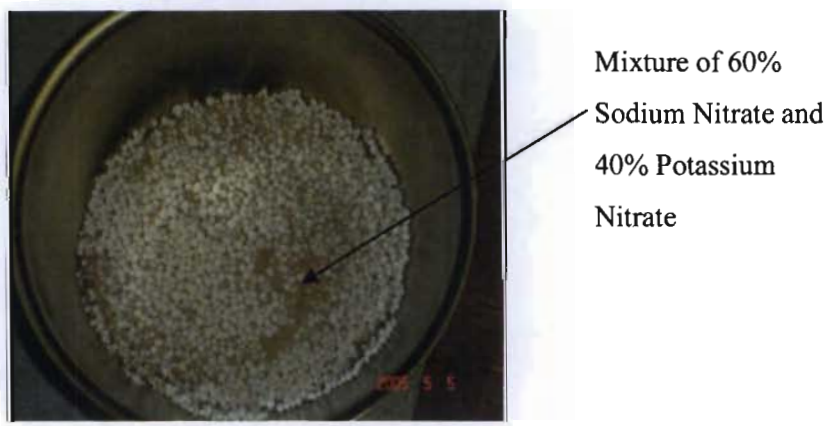

Figure 6.12 Mixtures of Sodium Nitrate and Potassium Nitrate Tests at 218°C

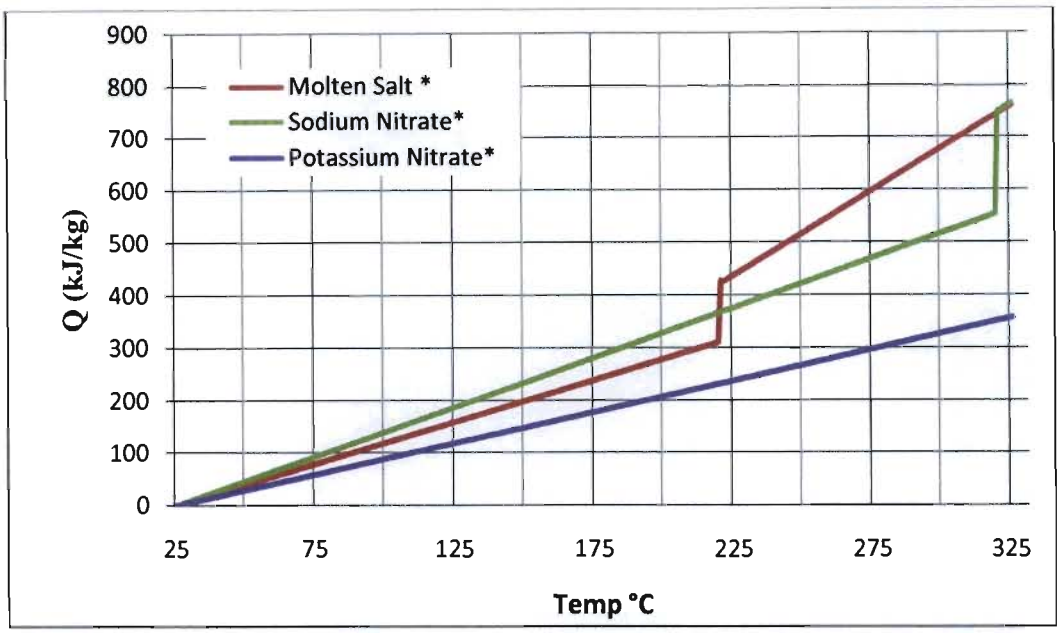

Figure 6.13 Heat Storage Capacities per Unit Mass for Molten Salt, Sodium Nitrate and Potassium Nitrate

In Figure 6.13 the heat storage capacity of molten salt (60% of Sodium Nitrate and 60% of Potassium Nitrate), Potassium Nitrate and Sodium Nitrate were compared. The figure shows that the molten salt has a higher heat storage capacity and a lower melting point, at 224 °C. The heat storage capacity per unit mass of molten salt is greater than Sodium Nitrate and Potassium Nitrate by 1.20 and 1.8 times respectively.

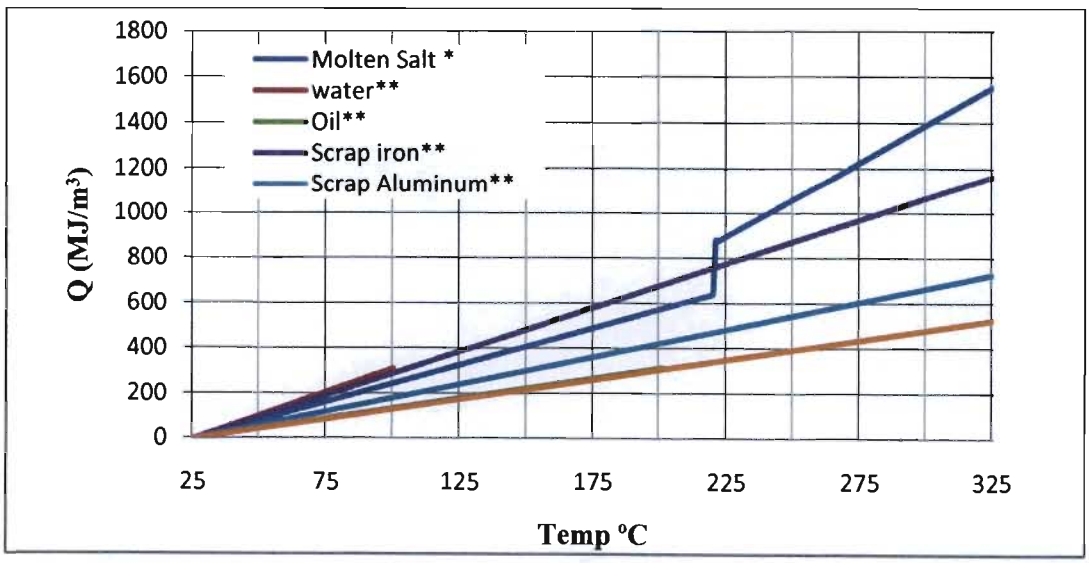

Figure 6.14 Heat Storage Capacities per Unit Mass for Molten Salt, Sodium Nitrate and Potassium Nitrate

6.7 Summary

In this chapter energy consideration and material selection have been carried out. A procedure for incorporating phase-change thermal storage materials in heat storage and modes of heat transfer, cooking methods, cooking materials, was explored. Performance evaluations of the types of cook tops, hotplate temperatures, were presented and results are used as a guide in selecting appropriate phase-change materials (PCMs) for the heat storage systems. This temperature provides the lead to the selection of appropriate PCMs for heat storage unit in heat systems, especially those powered by solar energy. From experiments result Molten salt, therefore, are best suited for such operations. This chapter shows that the selection of appropriate PCMs can be determined purely from theoretical thermodynamic considerations and experiments.

CHAPTER 7
EXPERIMENTAL DESIGN AND SETUP

Central to the design of a thermal energy storage system is its thermal capacity or in other words the amount of energy that it can store and provide. However, selection of the appropriate system is related to various cost-benefit considerations.

The cost of a TES system mainly depends on the following items:

- The storage material itself
- The heat exchanger for charging and discharging the system
- The cost for the space and/or enclosure for the TES

From a technical point of view, the crucial requirements are:

- High energy density (per-unit mass or per-unit volume) in the storage material
- Good heat transfer between heat transfer fluid (HTF) and the storage medium
- Mechanical and chemical stability of storage material
- Compatibility between HTF, heat exchanger and/or storage medium
- Complete reversibility for a large number of charging/discharging cycles
- Thermal losses
- Ease of control

All these factors have to be considered when deciding on the type and the design of a thermal storage system. Figures D.1–D.12 in Appendix D shows the experiments design drawing.

7.1 Design of an experimental apparatus to determine the physical properties of locally available industrial grade heat storage materials.

Two experimental facilities designed to determine the physical properties of locally available industrial grade of Sodium Nitrate and potassium Nitrate have been chosen.

7.1.1 Heat Storage Calorimeter

The first design set of experiments were carried out in a 114 mm diameter x 750 mm height cylindrical heat storage container which was constructed from steel pipe as shown in Figure 7.2 and Figure 7.3. A stainless steel convoluted hose as shown in Figure 7.1 which used as

heat transfer tube was installed at the center of the storage unit having a dimension of 30 mm-ID x 550 mm height, with 0.086 m^2 surface area. This tube was used as a heating element as shown in Figure 7.3, its two ends connected to the power from the welding machine through electric varies resistance. To control heat loss from the heat storage tank, a heat insulation box was equipped and surrounded the tank. The PCM was inserted in the space between the inner and outer tubes with the quantity being 10 kg. Twelve J-type thermocouples (0.3 mm) were imbedded in the PCM in the radial (5, 15, 25, 35, 45 and 55 mm from the heat transfer tube) and in the longitudinal (55, 110, 140, 185, 350 and 450 mm from the bottom of the container) positions as shown in Table 7.1 and the thermocouples were fitted on bottom and top heat storage tank. The temperature histories during the thermal cycles were recorded by a thermocouple thermometer as shown in Figure 6.4.

Table 7.1 Radial and longitudinal position of Heat Storage Calorimeter Thermocouples

Radial Distance From heat transfer pipe	Longitudinal Distance From the bottom of the heat storage calorimeter	Thermocouples No.
5 mm	55 mm	T6
15 mm	110 mm	T5
25 mm	140 mm	T4
35 mm	185 mm	T3
45 mm	350 mm	T2
55 mm	450 mm	T1

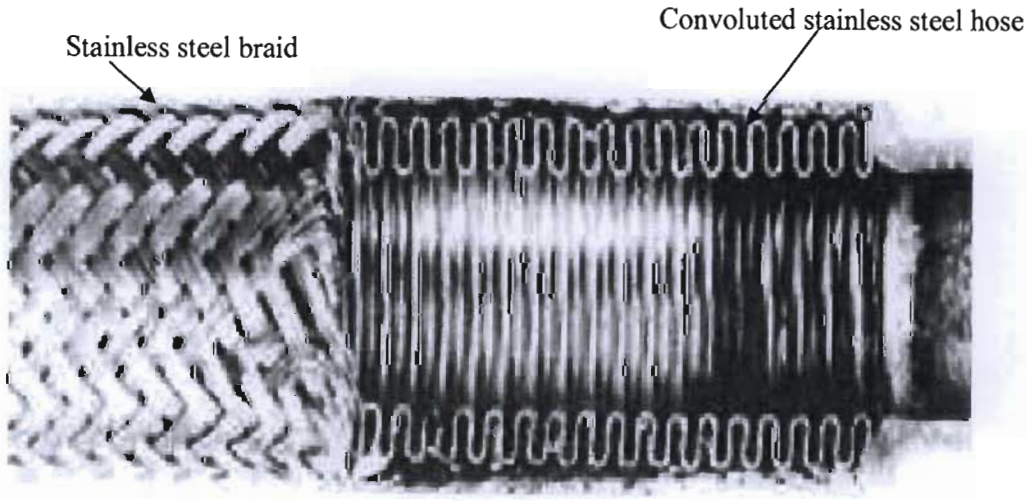

Figure 7.1 Convoluted hose which was used as heating element

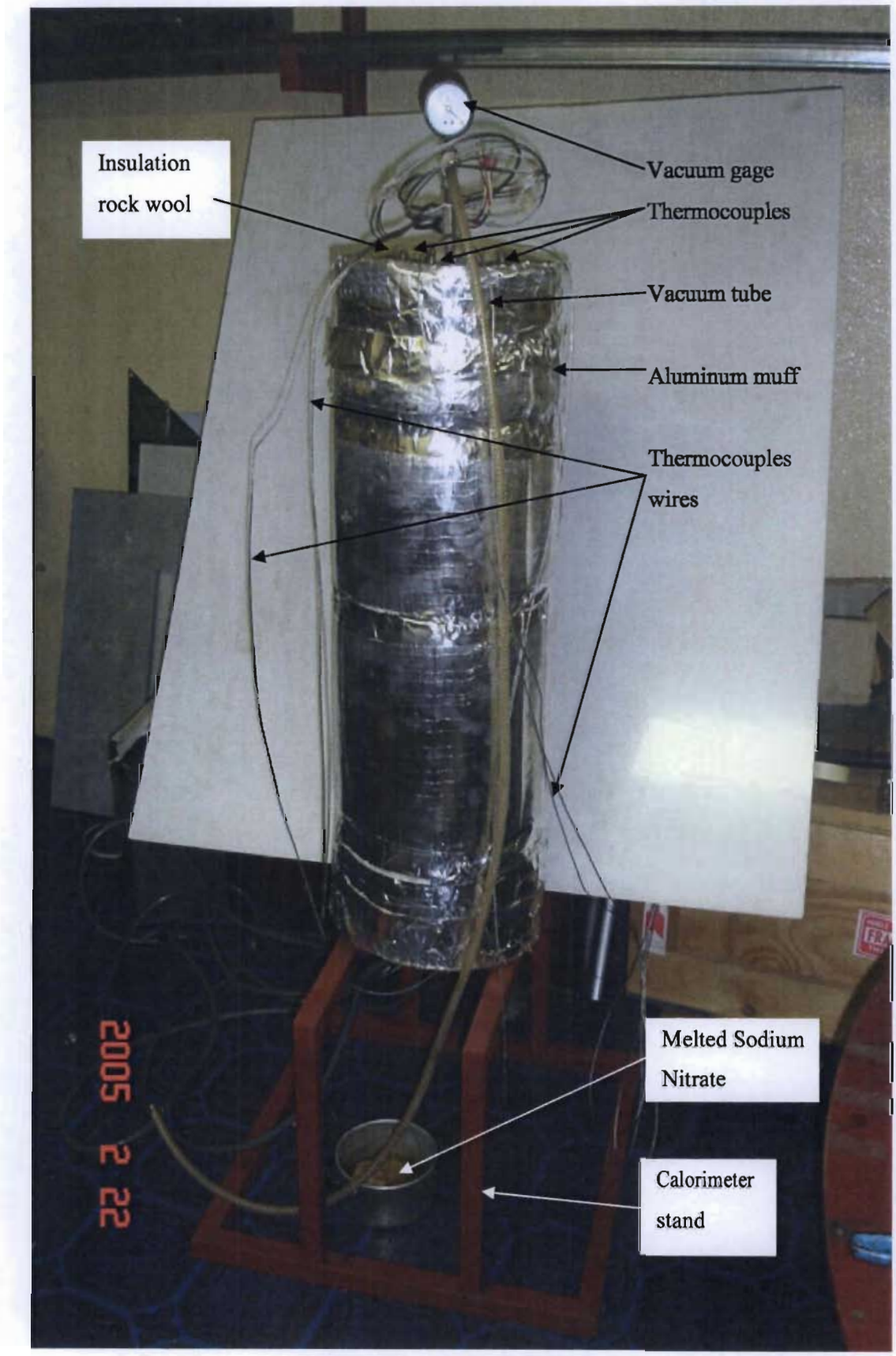

Figure 7.2 Heat Storage Calorimeter

Figure 7.3 shows the top of heat storage calorimeter with vacuum pump to suck the air from inside the heat storage container and avoid any burning of the heat storage material inside the storage tank.

Figure 7.3 Top of heat storage calorimeter with vacuum gage

Figure 7.4 Shows a cut view of the heat storage calorimeter consisting in the middle the convoluted heat transfer pipe having a dimension of 30 mm-ID x 550 mm height, with 0.086 m^2 surface area. In the middle lies an 8 mm steel bar with the top end welded in top of the convoluted heat transfer pipe, and the bottom end fixed through the bottom of the heat storage calorimeter and insulated from touching the body of the calorimeter. The bottom of the steel bar was connected to the terminal of the welding machine which is shown in Figure 7.5.

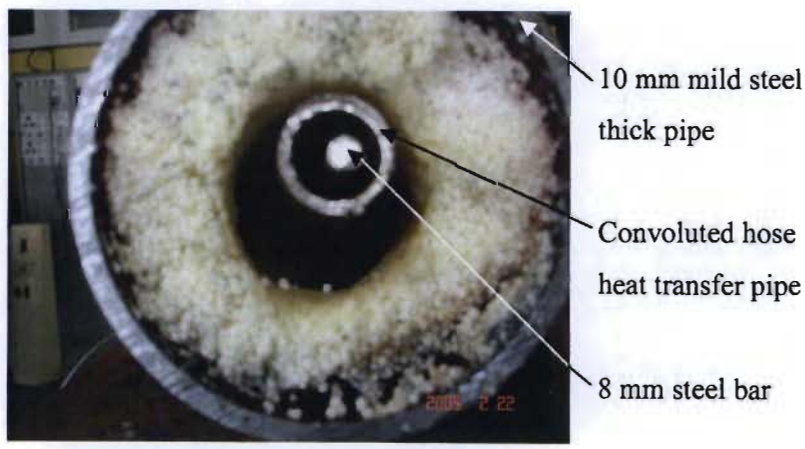

Figure 7.4 Cut view of a heat storage calorimeter

Figure 7.5 shows the welding machine which was used as power supplier to get high current with low voltage. For cooling, protection and to reduce overheating of the welding machine, 3m of ½ inch copper pipes was used to circulate the oil from the bottom of the welding machine to the top to keep it cooled.

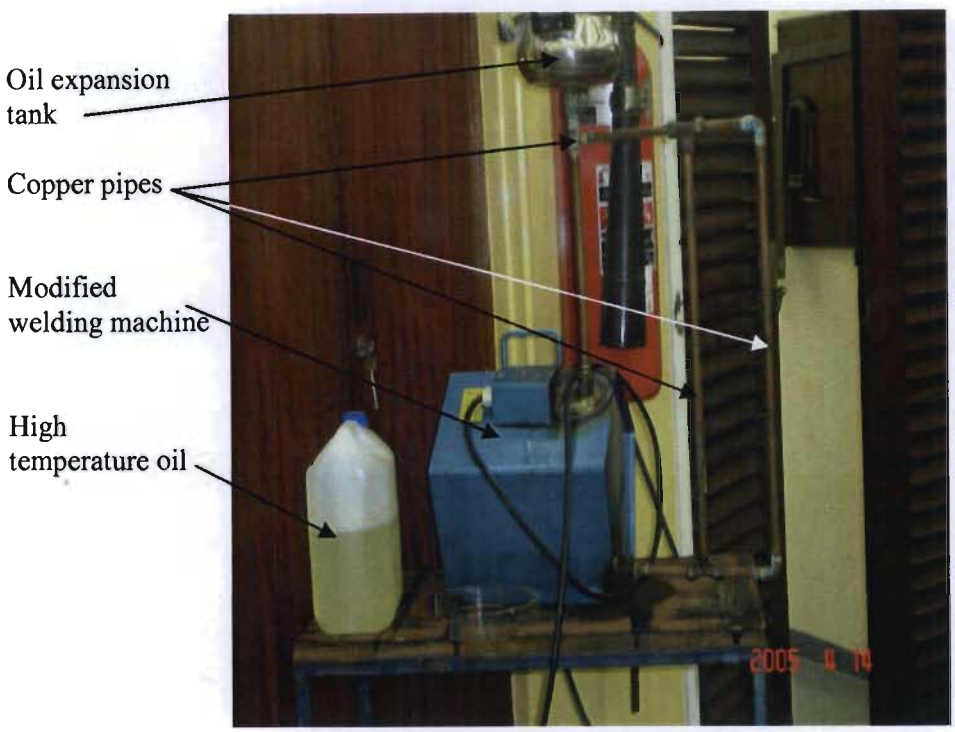

Figure 7.5 Welding machine and the cooling system

7.1.2 Physical Properties of Heat Storage Material

To determine the physical properties of the heat storage material, second design Experiments were carried out in a 180 mm diameter x 150 mm height cylindrical heat storage container which was constructed from a steel pipe as shown in Figure 7.6. A steel heat transfer tube with four fins as shown in Figure 7.7 was installed at the center of the storage unit having a dimension of 28 mm-ID x 3 mm thickness. This storage container was surrounded by 2 kV electrical heater elements.

Twelve K-type thermocouples (0.3 mm) were imbedded in the PCM in the radial (6, 16, 26, 36, 46 and 56 mm from the heat transfer tube) and in the longitudinal (15, 35, 55, 75,95 and 125 mm from the bottom of the container) positions, and the thermocouples were fitted by using compression fitting on the surface of the heat transfer tube. Two K-type thermocouples were placed at the inlet and outlet of the Heat Transfer Fluid (HTF). The temperature

histories during the thermal cycles were recorded by Data logger and these data were stored in a computer. To reduce heat loss from the heat storage tank, a heat insulation box as shown in Figure 7.8 equipped surrounded the tank. The PCM was inserted in the space between the inner and outer tubes with the quantity being 4 kg.

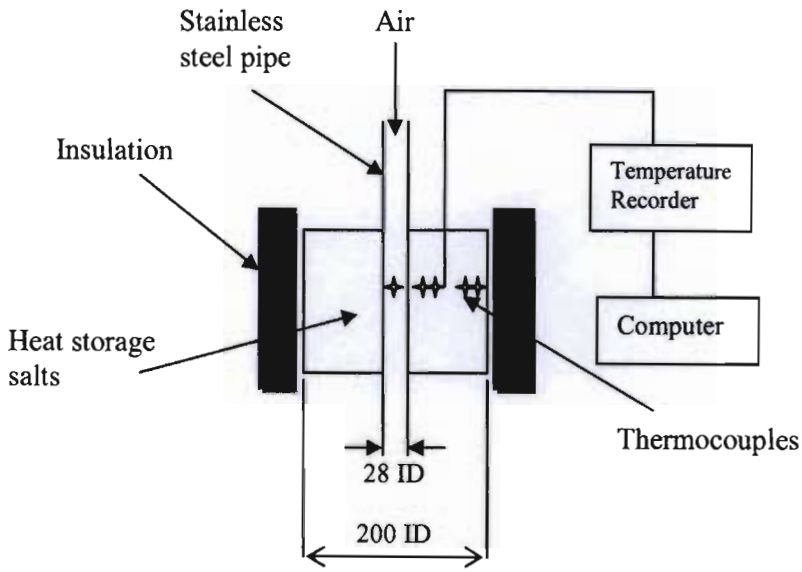

Figure 7.6 Calorimeter to determine physical properties of industrial grade heat storage material.

Figure 7.7 Primary construction of heat storage calorimeter

Table 7.2 Radial and longitudinal position of Thermocouples

Radial Distance From heat transfer pipe	Longitudinal Distance From the bottom of the heat storage calorimeter	Thermocouples No.
6 mm	15 mm	T1, T12
16 mm	35 mm	T3, T10
26 mm	55 mm	T2, T11
36 mm	75 mm	T4, T9
46 mm	95 mm	T5, T8
56 mm	125 mm	T6, T7

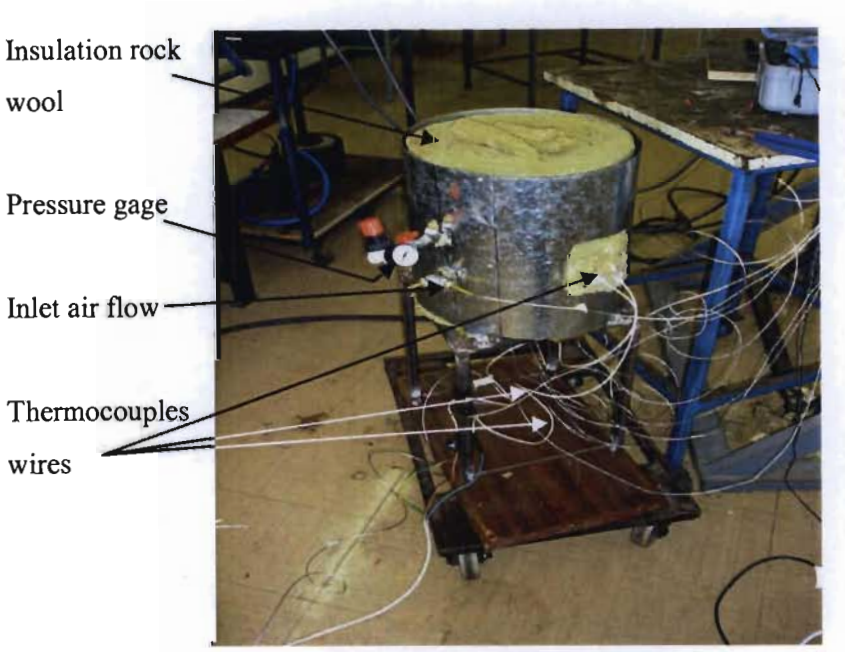

Figure 7.8 Final construction of heat storage calorimeter

7.1.3 Heat Transfer Characteristics of Proposed Design

Different stages of the manufacturing and assembly process of the heat storage tank are shown in Figures 7.9-7.20. The third design Experiments were carried out in a 265 mm diameter 610 mm height, 10 mm thickness cylindrical heat storage container which was constructed from a steel pipe as shown in Figure 7.9. A stainless steel 304l heat transfer tube with four fins as shown in Figure 7.10 was installed at the center of the storage unit and welded in the top flange having a dimension of 20.96 mm-ID, 26.7 mm-OD.

Two stainless steel 304l convoluted hose pipes 1.36m and 1.22m long on both sides were welded to connect a 3/8 inch standard wall stainless steel pipe which was used as a heating element with a total surface area of 0.129 m^2 as shown in Figure 7.9. The two ends of the convoluted hose pipe were connected together in series and fixed in the top flange, insulated from touching the flange by using four small flanges and gas kit as shown in Figure 7.11. The heating element was powered through the modified and fabricated welding machine to get a high current with low voltage.

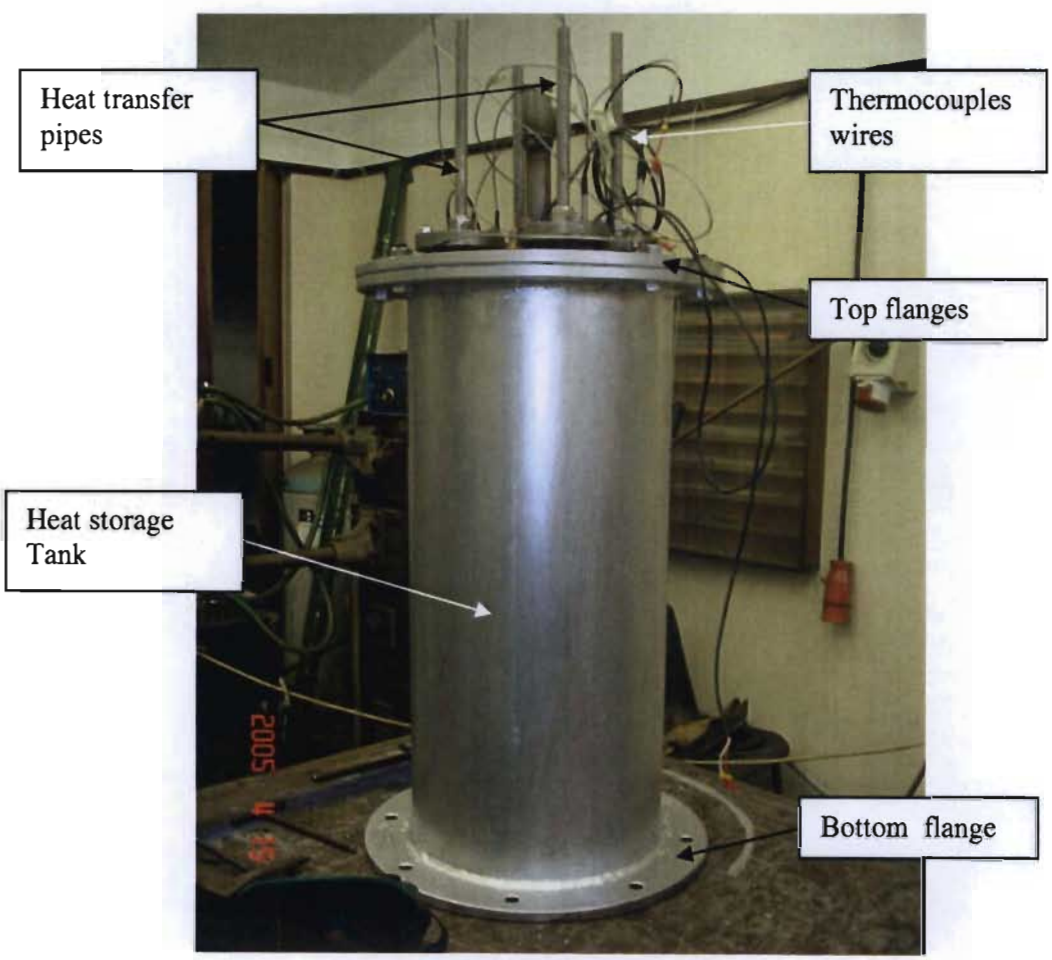

Figure 7.9 Heat Storage Tank

Twelve K-type thermocouples (0.3 mm) were imbedded in the PCM in the radial (6, 16, 26, 36, 46 and 56 mm from the heat transfer tube) and in the longitudinal (15, 35, 55, 75,95 and 125 mm from the bottom of the container) positions, and the thermocouples were soldered on the surface of the heat transfer tube. Two K-type thermocouples were placed at the inlet and outlet of the Heat Transfer Fluid (HTF).

The temperature histories during the thermal cycles were recorded by Data logger and these data were stored in a computer. To reduce heat loss from the heat storage tank, a heat insulation box were equipped surrounded the tank. The PCM heat storage tank was filled at the beginning with 40kg of mixture of 24kg Sodium Nitrate ($NaNO_3$) and 16 kg Potassium Nitrate (KNO_3).

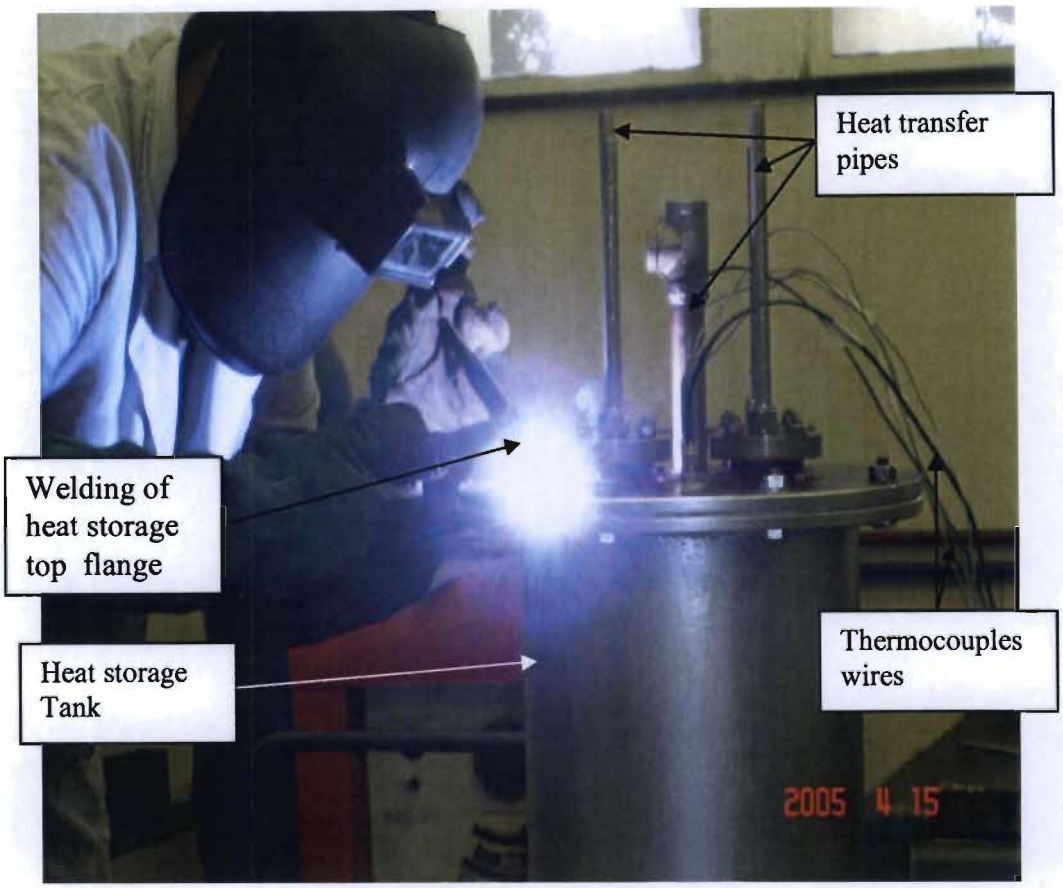

Figure 7.10 Welding of heat storage tank

Figure 7.10 shows a part of welding process of the top flange of the heat storage tank which done in the Mechanical Engineering workshop. Figure 7.11 shows heat transfer longitudinal fins and fitting of convoluted heat pipes in the top flange of the heat storage tank through 4 small flanges which were fitted using 4 bolts each and insulated from touching the body of the heat storage tank by using high heat gaskets.

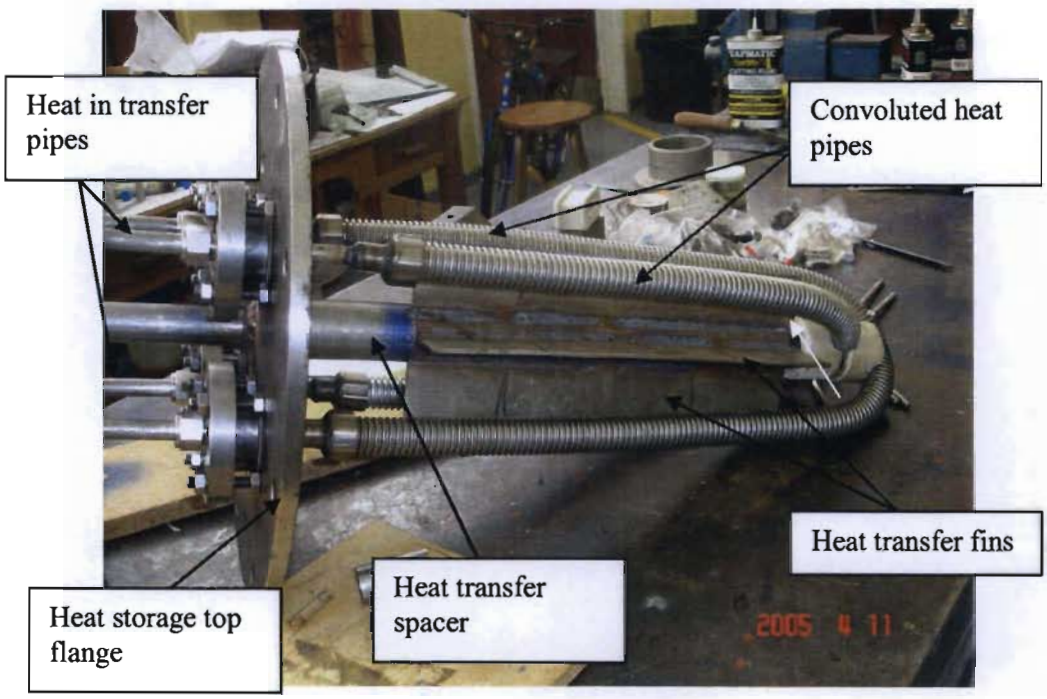

Figure 7.11 Fitting of convoluted heat pipes in the top flange

Figure 7.12 shows aassembly of heat storage tank and fitting of convoluted heat pipes in the top flange the heat storage tank through 4 small flanges which are fitted using 4 bolts each and insulated from touching the body of the heat storage tank.

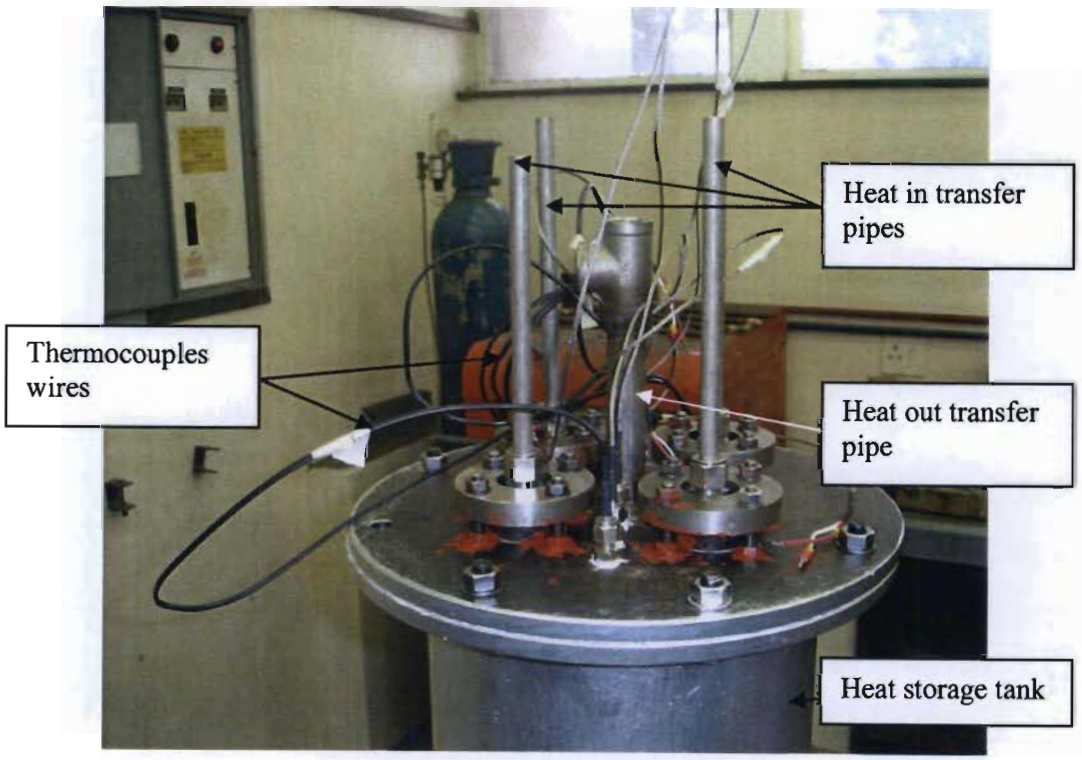

Figure 7.12 Assembly of heat storage tank

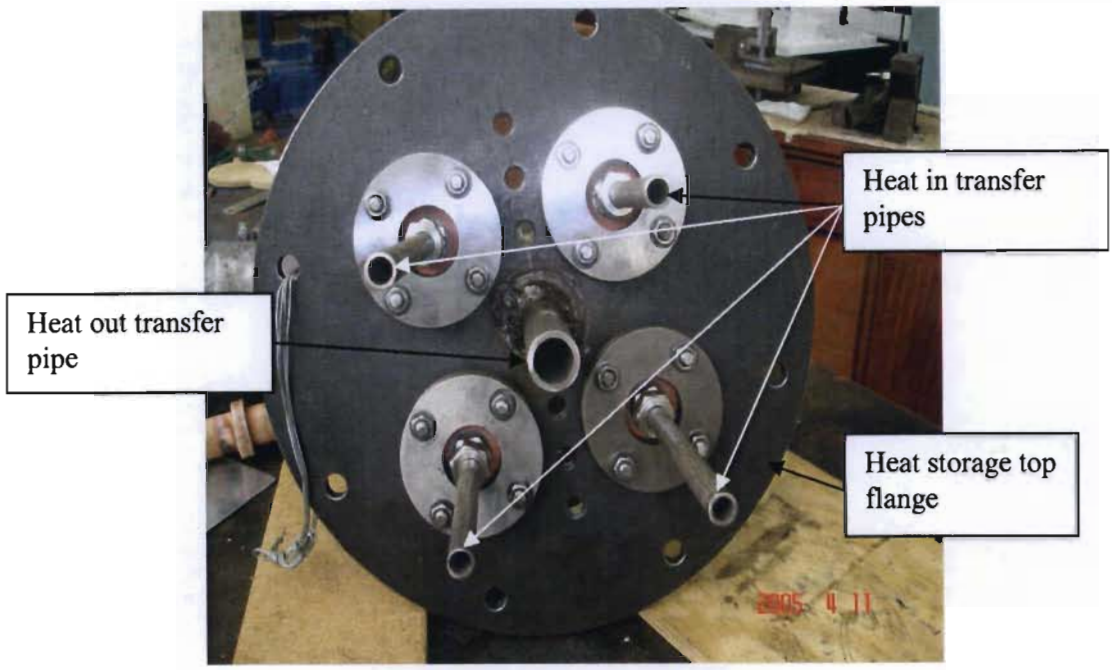

Figure 7.13 Assembly of heat transfer pipes

Figure 7.13 shows the heat transfer pipe which is made from stainless steel pipe and welded in the middle of the heat storage top flange, and four stainless steel tubes which are fitted by using compression fittings and insulated by double layers of high temperature gaskets from touching the body of the heat storage tank.

Figure 7.14 shows filling the heat storage tank from the bottom by turning the whole tank upside down with 40 kg of a mixture of sodium nitrate and potassium nitrate (60% and 40% respectively)

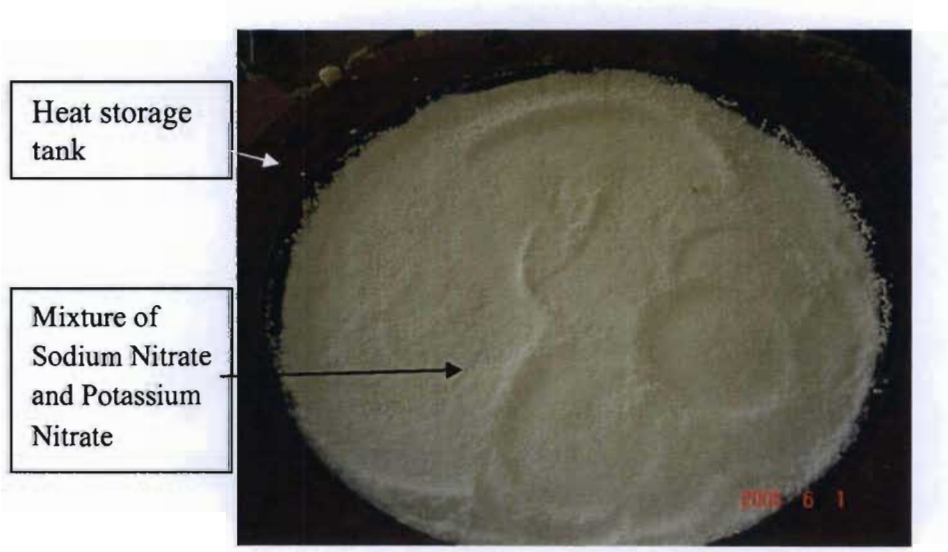

Figure 7.14 Filling Mixed of Sodium Nitrate and Potassium Nitrate Heat Storage Salt

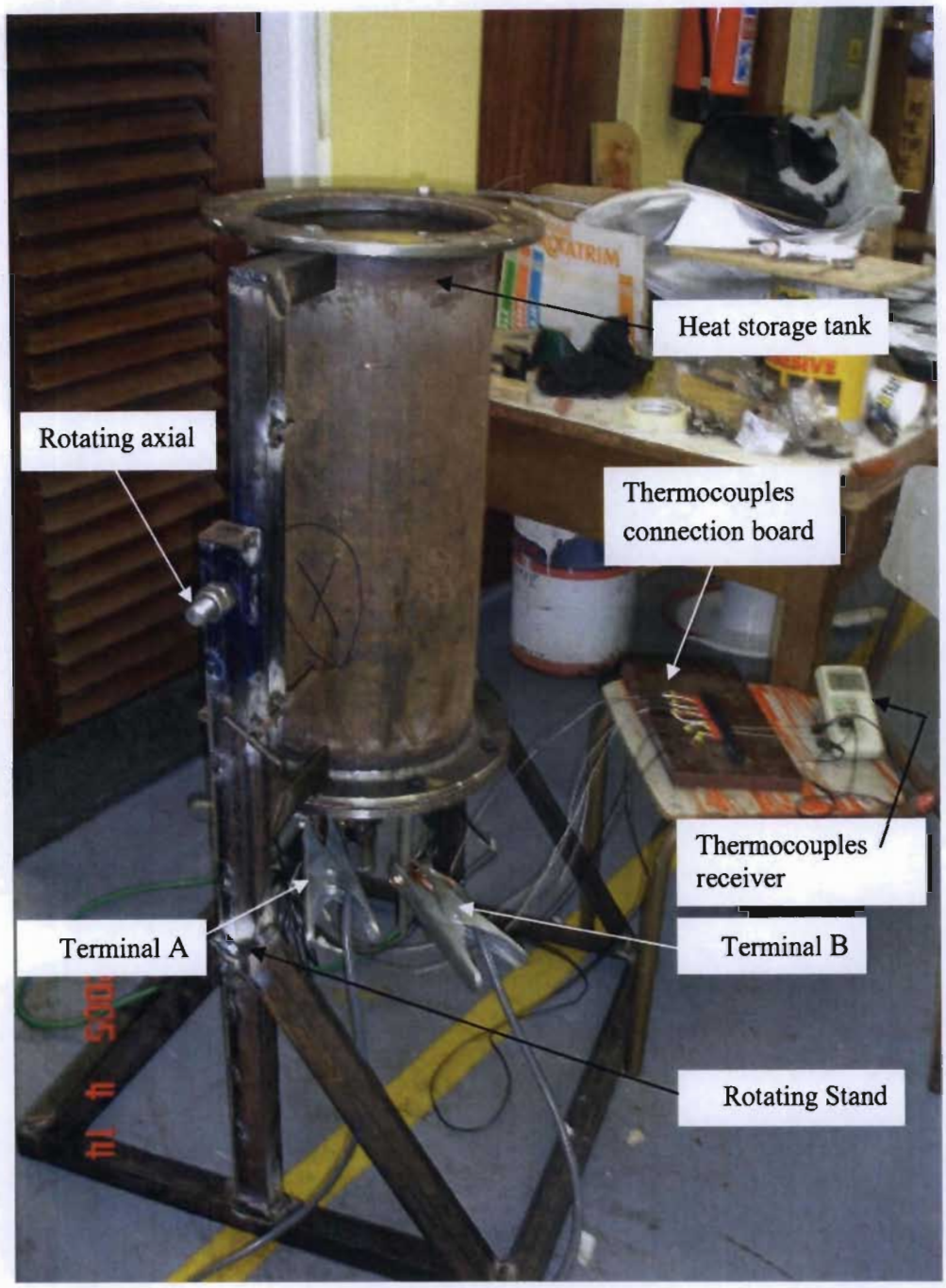

Figure 7.15 Testing heating element by heating water

Figure 7.15 shows the testing rig of the heat storage tank using water by rotating the tank upside down and filling it with water and tested by boiling the water. Both terminal A and B are connected to the power through the welding machine to get low voltage with high amperes; 20 A and 10 V will give us 200 W to run the test with.

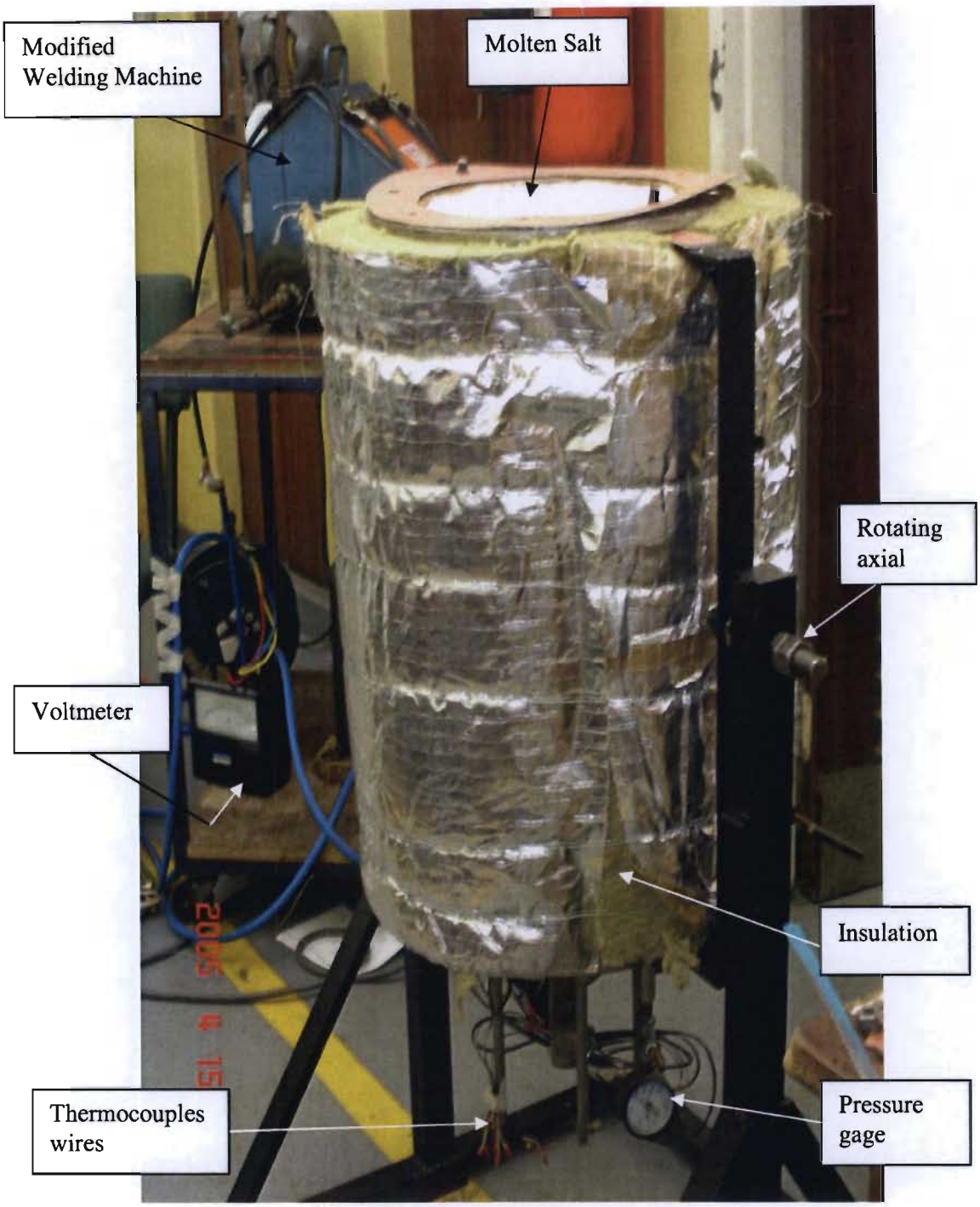

Figure 7.16 Insulating and setup of heat storage system

Figure 7.16 shows the electric low voltage heat storage tank, in an upside down position and filled with heat storage materials before closing the bottom flange. And show the modified welding machine (low voltage power resource).

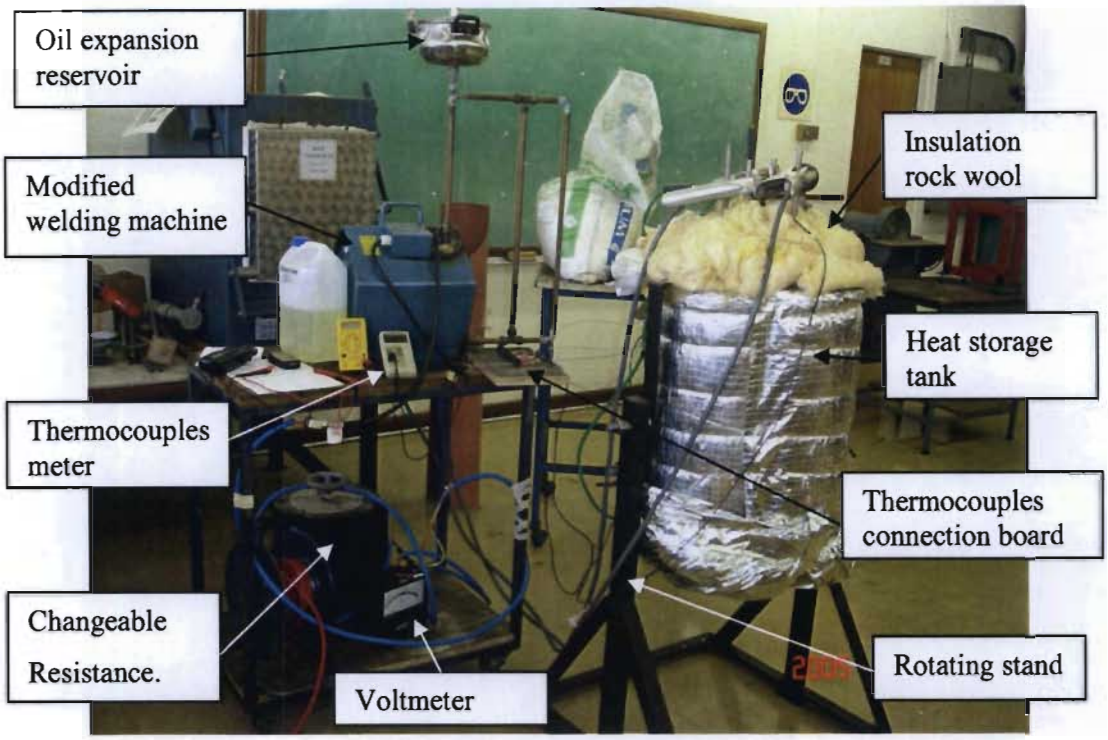

Figure 7.17 Setup of Heat Storage system

The setup of heat storage tank shown in Figure 7.17 consist of Heat storage tank which insulated with high-temperature insulation wool, rotating stand, modified welding machine which was used as low voltage power source, oil expansion reservoir for cooling the welding machine during the charging process, thermocouples meter, ammeter, voltmeter, changeable resistance.

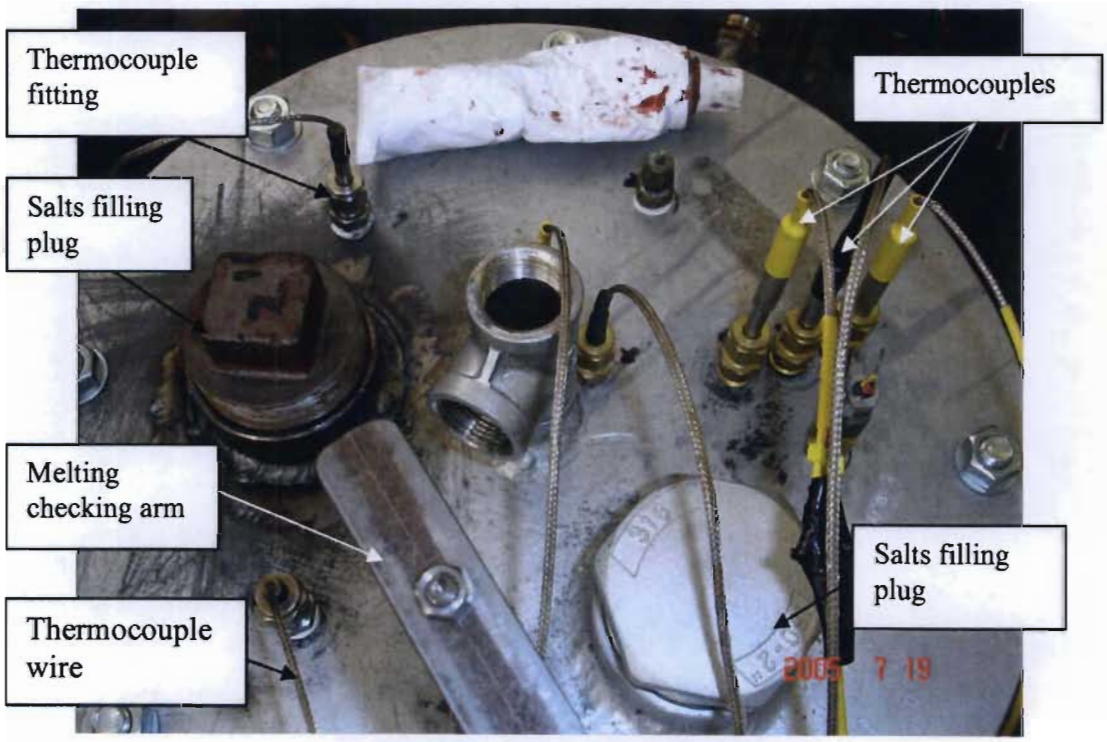

Figure 7.18 Plugs for Filling of Heat Storage Salt

figure 7.18 shows the top flange of heat storage tank consist of 2 salts filling plugs, thermocouples fitting and checking arm to check the states of phase of the salts mixture.

Figure 7.19 Bottom of Heat Storage Tank after the Salts Melted

Figure 7.19 shows the bottom of heat storage tank after rotated upside down to observe what happen to the heat storage salts mixture. As you can see from the picture in figure 7.19, two colours appear yellow brown and white. The brown colour indicated that the mixture melted and become solid again by solidification process, the white colour for the unchanged phase salts.

Figure 7.20 shows assembly of oil gear pump with driving motor which used to circulate the oil through the heating element pipe to the coil pipe inside the heat storage tank to transfer the heat through the heating salt.

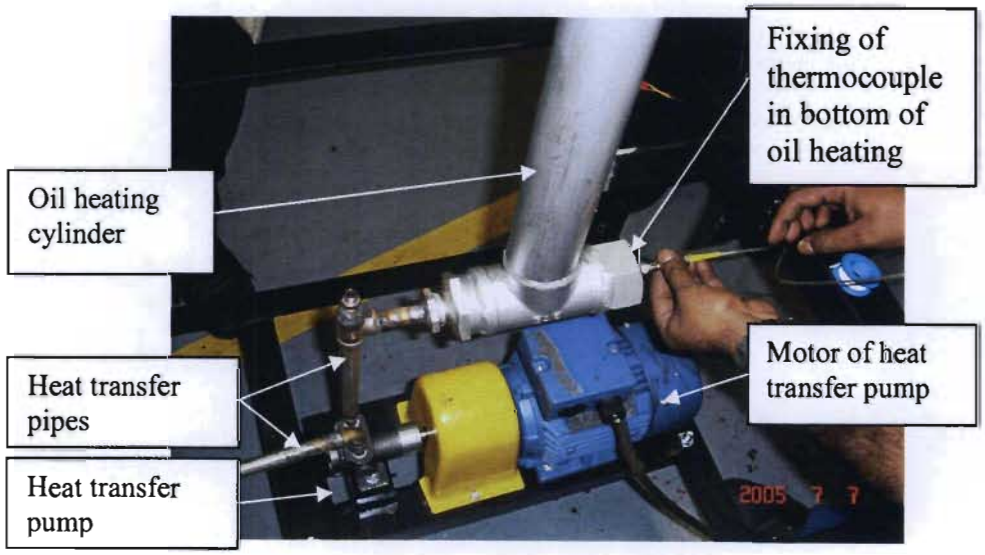

Figure 7.20 Assembly of oil circulating pump

7.2 Oil Heat Transfer System

Forth design set of experiments as shown in figure 7.21 and Figure D.2 in appendix D, were carried out in a 265 mm diameter 490 mm height, 10 mm thickness cylindrical heat storage container which was constructed from a steel pipe and four flanges as shown in Figure 7.9. A heat transfer coil pipe 3/8 inch standard wall as shown in Figure D.2 and Figure D.4 in appendix D were mounted to the top and bottom of inside wall of heat storage cylinder to transfer the heat collected to heat storage phase change materials. Four longitudinal fins having a dimension 3mm x 360mm x 40mm as shown in Figure D.4 in appendix D were mounted to the middle of heat transfer coil to transfer the heat collected to heat storage phase change material during the charging process.

A 3/4 inch stainless steel (304 L) heat transfer pipe was mounted to the underside of heat storage top flange to transfer the heat collected to storage cylinder. 4 longitudinal fins having a dimension 3mm x 242mm x 60mm as shown in Figure D.3 and Figure D.6 in appendix D were mounted to the side of heat transfer pipe to transfer the heat from the heat storage materials to outside the heat storage cylinder to cooking pot during discharging process.

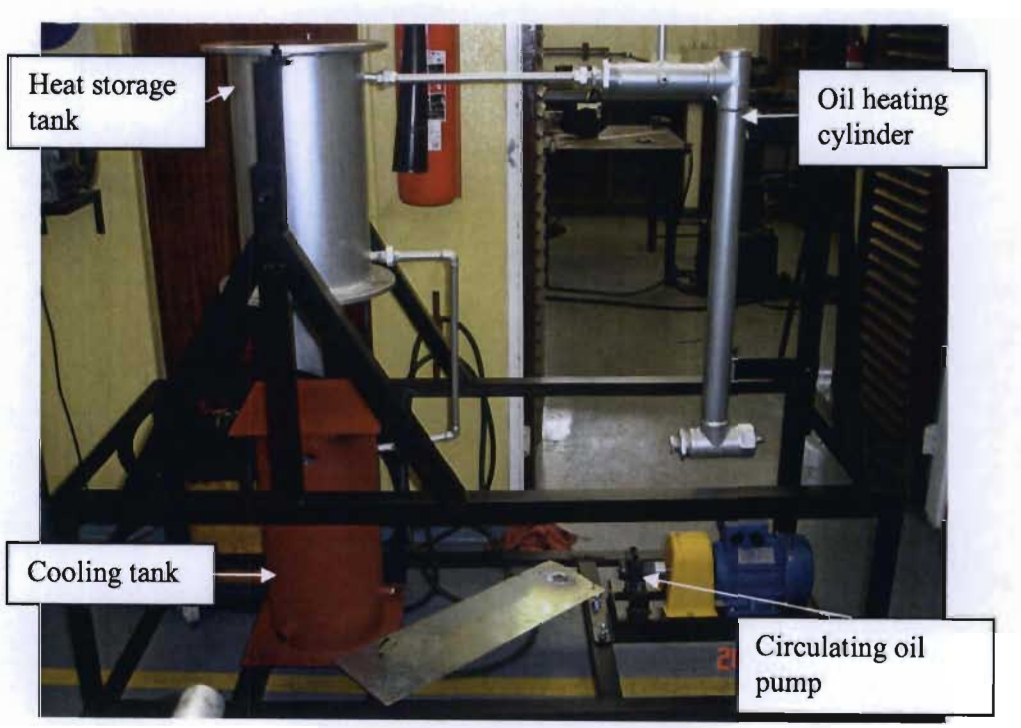

Figure 7.21 Oil Heat Storage Tank Rag under Construction

The second part is a cooling tank having a dimension of 265 mm-ID, its design the same as the heating storage tank which is used for cooling the hot oil by circulating tap water over

the coil pipe to reduce the oil temperature to 150°C to go back to the heater through the circulating pump. This process drops the temperature from 300°C to 150°C in order to protect the oil gear pump from high temperatures while the heat loss is about 50% of the input power.

The third part is the gear circulating pump which is connected to the system through a ½ inch pipe and circulates the hot oil from the heater to the coil pipe of the heat storage tank and from the heat storage tank to the cooling process to reduce the temperature to 150°C.

The fourth component is the 2kW heating element having a length of 750mm and 2 inch fitting tread which was installed inside a 2 inch pipe with 800 mm length used to heat the oil to 300°C. The expansion reservoir is used for oil expansion, and the bleeding point uses the lowest point plug. The heating element was modified by fitting 8 semi circular fins to it for heating the oil faster as seen in Figure 7.22.

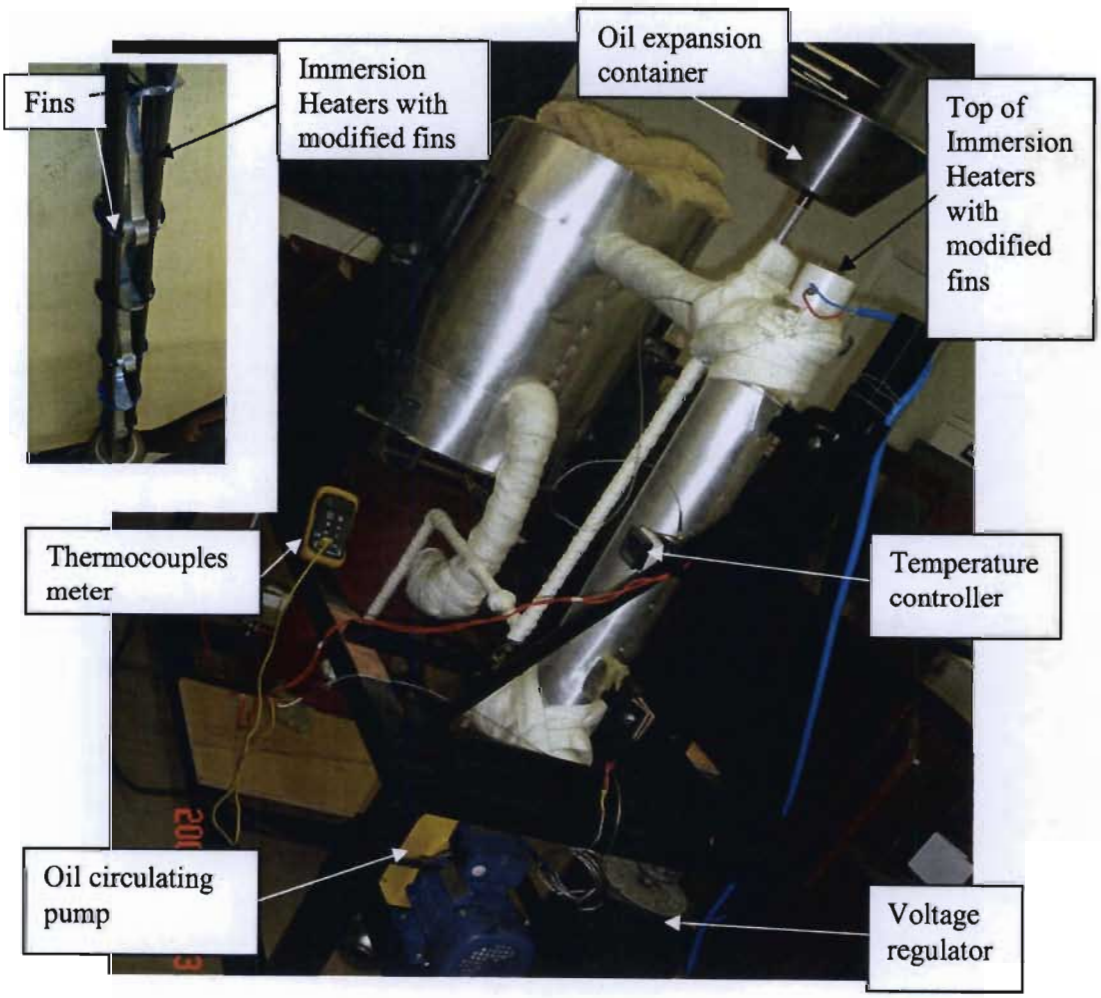

Figure 7.22 Immersion Heaters with modified fins fixed in the Heat Storage System

7.3 Discharging of Electric Heat Storage System

7.31 Steam Discharging Unit

One of the methods which were used by dropping water inside the heat transfer pipe after at least 4 hours of full charging of the heat storage system; 3.2 liters of water was converted to dry steam at 2.6 bar pressure which can be used as cooking power to cook different types of food. The system is shown in Figure 7.23.

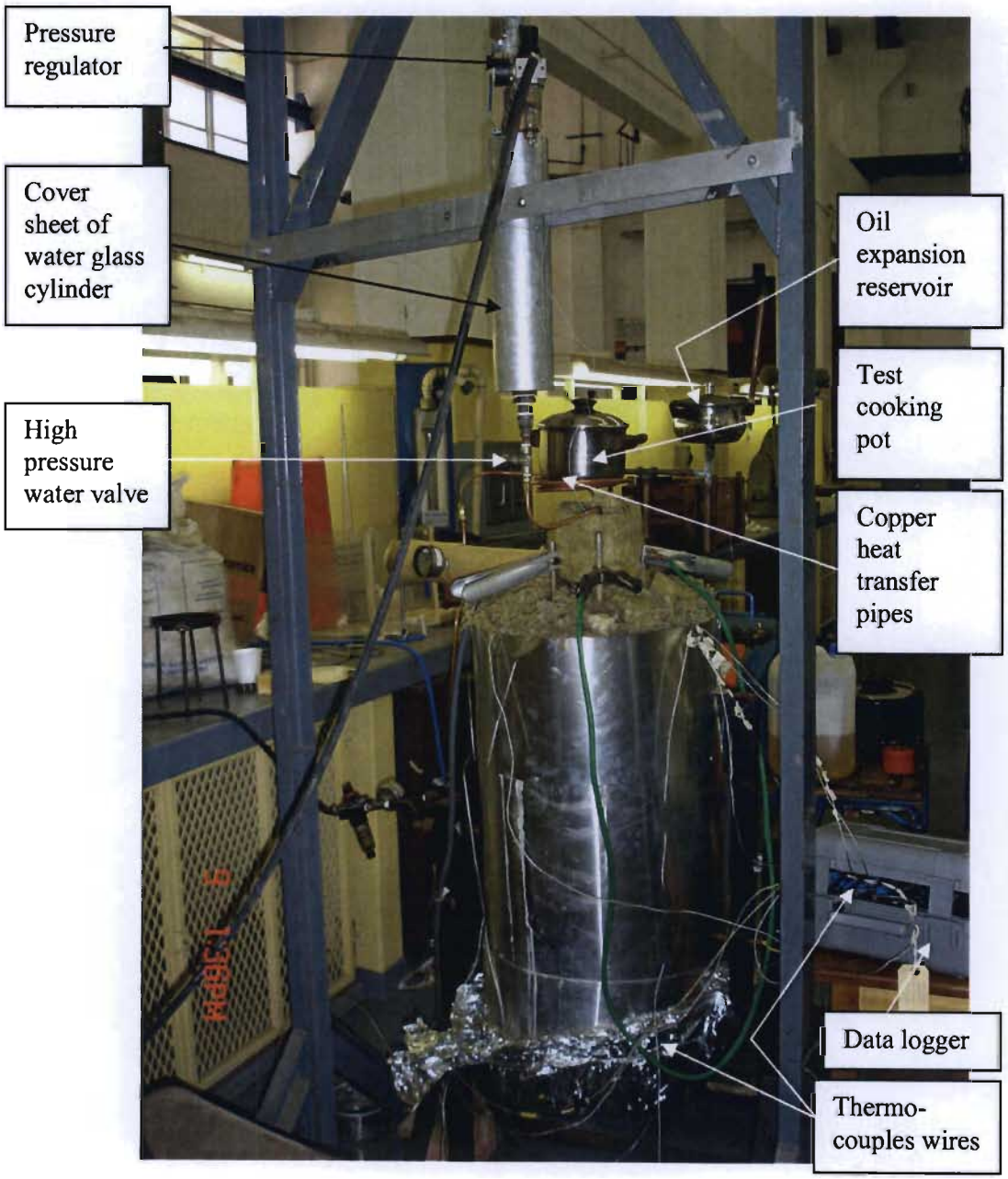

Figure 7.23 Water Drop Discharging System by Using 8 mm Copper Coils for Cooking.

7.3.2 Air Discharging Unit

This was achieved by pushing air under 2 bar pressure through the inlet of heat pipe inside the heat storage tank to outside of heat storage tank to cooking pan.

7.4 Backup Liquid Petroleum Gas Burner for Solar Cooker

Backup liquid petroleum gas (LPG) burner for a solar cooker is used when the temperature of the heat storage unit is lower than the melting point of the heat storage salt. This is done by mixing hot air from the heat storage unit with LPG to reduce the gas consumption as shown in Figure 7.24 It is assumed that on a bad weather day the max hot air temperature available from the thermal storage unit is approximately 150 °C.

The air temperature has to be constantly monitored, the reason being that the higher the airflow rate the cooler the element becomes. The added advantage of the solar cooker is the stovetop is at a higher temperature than ambient, this was assumed to be 100 °C.

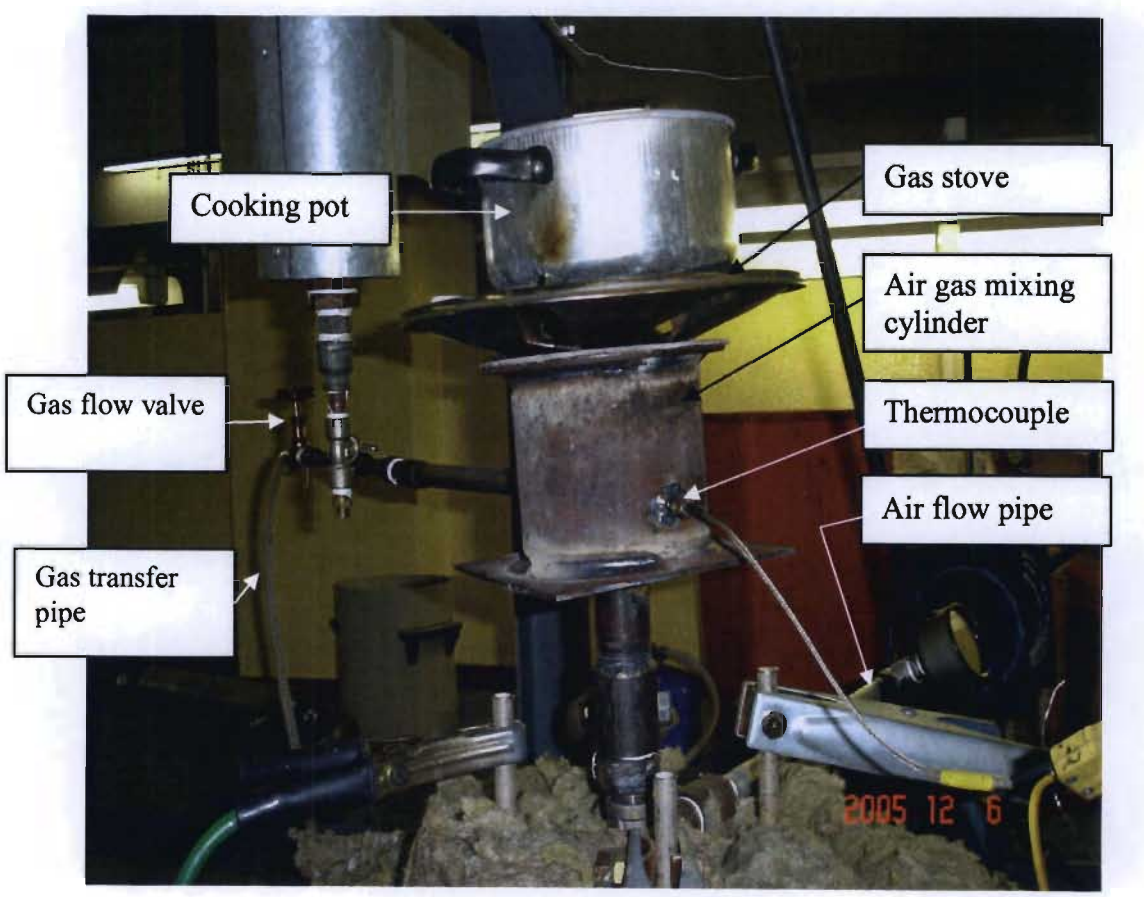

Figure 7.24 Backup Liquid Petroleum Gas Burner

7.5 Summary

This chapter has provided a suggested procedure based on the amount of energy that can be stored and provided. Since the experimental design and set up are the most significant part of the project, this chapter has been dedicated to design of an experimental apparatus to determine the physical properties of locally available industrial grade heat storage materials. The uses of heat storage calorimeter, physical properties of heat storage materials and heat transfer characteristics of proposed design have been examined. Several systems, like oil heat transfer system, electric heat storage system, and backup liquid petroleum gas burner for solar cooker have been analyzed. These systems and units presented demonstrate the methodology for development of our thermal energy storage and cooker model for the solar energy project.

CHAPTER 8
RESULTS AND DISCUSSION

8.1 First Calorimeter Results

To determine the physical properties of locally available industrial grade heat storage materials. The results of the calorimetric measurements are presented in temperature-time[§§] diagrams for charging and discharging process.

8.1.1 Charge Process

A typical radial temperature history during a heat storage stage of sodium nitrate versus time is shown in Figure 8.1 which is obtained from data in Table T.19 in Appendix T. Since the system is heated from the middle of the heat storage tank, the temperature near to the heating element rises rapidly and the phase transition occurs at the temperature range 310 to 350 °C. As can be seen, the temperature of the melted PCM increases sharply until the radial temperature distribution becomes uniform due to the convection in the liquid after the PCM has melted.

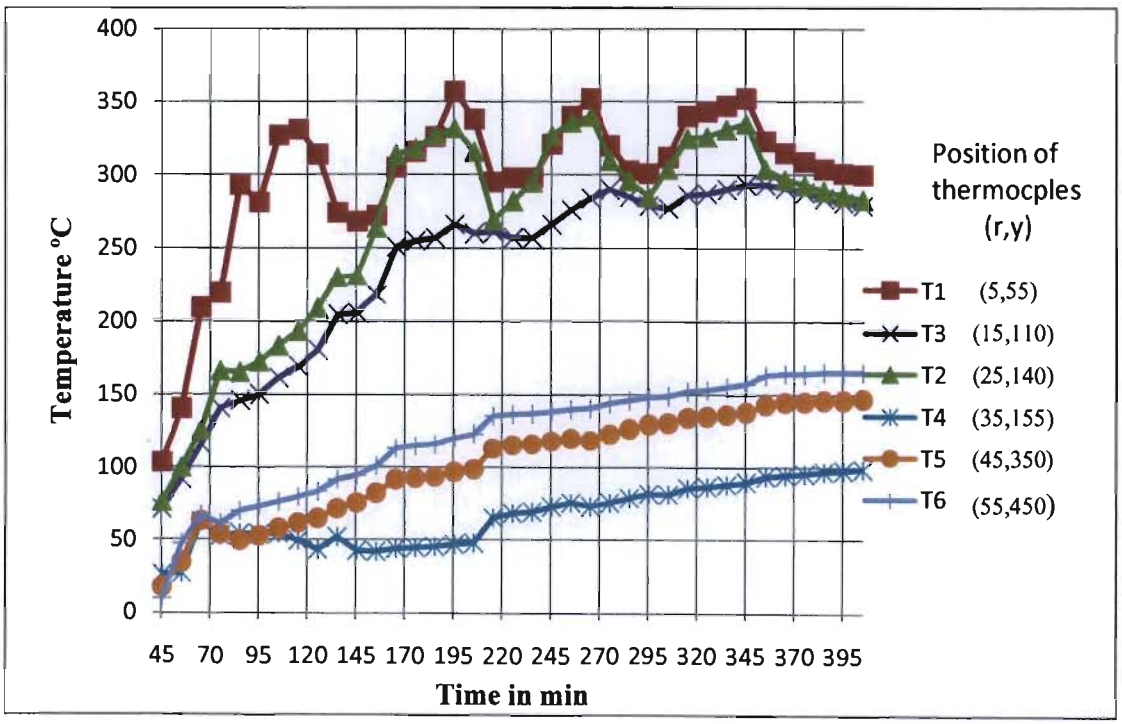

Figure 8.1 Temperature histories during a heat storage stage.

([§§] In this chapter and thereafter, minutes, hours or days have been used for times which conversions are known).

The PCM melted around the heating temperature as shown in Figure 8.2, and at the bottom of the tank melted completely as shown in Figure 8.3. Conversely, in the top of heat storage tank melting didn't occur due to the fact that the heat distribution around the heating element melted fast and left a gap between the heating element and PCM which worked as insulation as shown in Figure 8.4. Some corrosion appeared in the bottom of the heat storage tank as shown in Figure 8.5; elsewhere inside the tank it did not appear as shown in Figure 8.6.

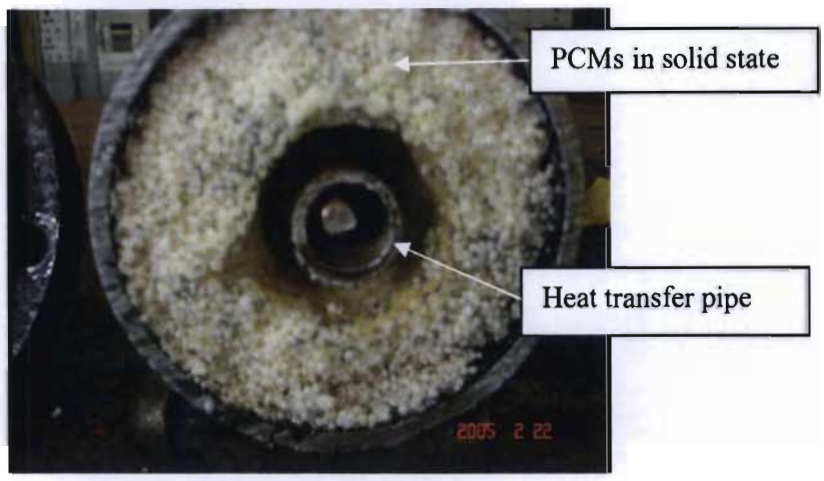

Figure 8.2 Section cut in ¾ length of heat storage tank after 6 months

After of a period of six months the first calorimeter was disassembled. In order to see what had happened inside the heat storage calorimeter were cut it into pieces. Figure 8.2 and figure 8.3 show views of a cut section and can been observed that the storage material near or touching the heat transfer pipe (convoluted pipe) had melted but in other places it hadn't melted. At the 1/4 length position from the bottom of the heat storage tank it had completely melted at different temperatures.

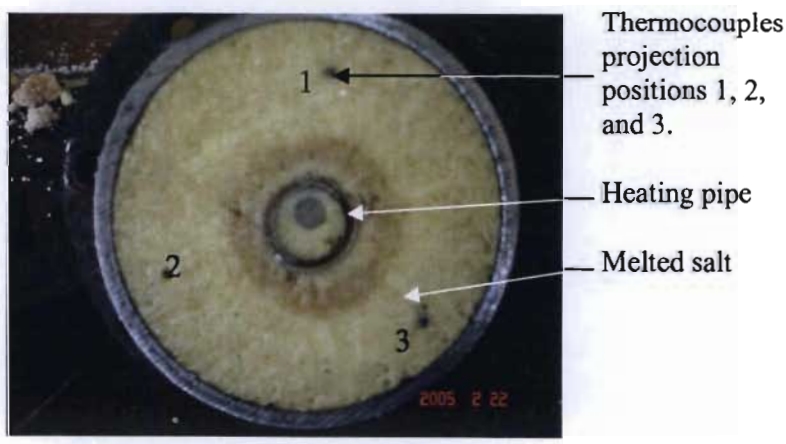

Figure 8.3 Section cut in 1/4 length from bottom of heat storage tank after 6 months

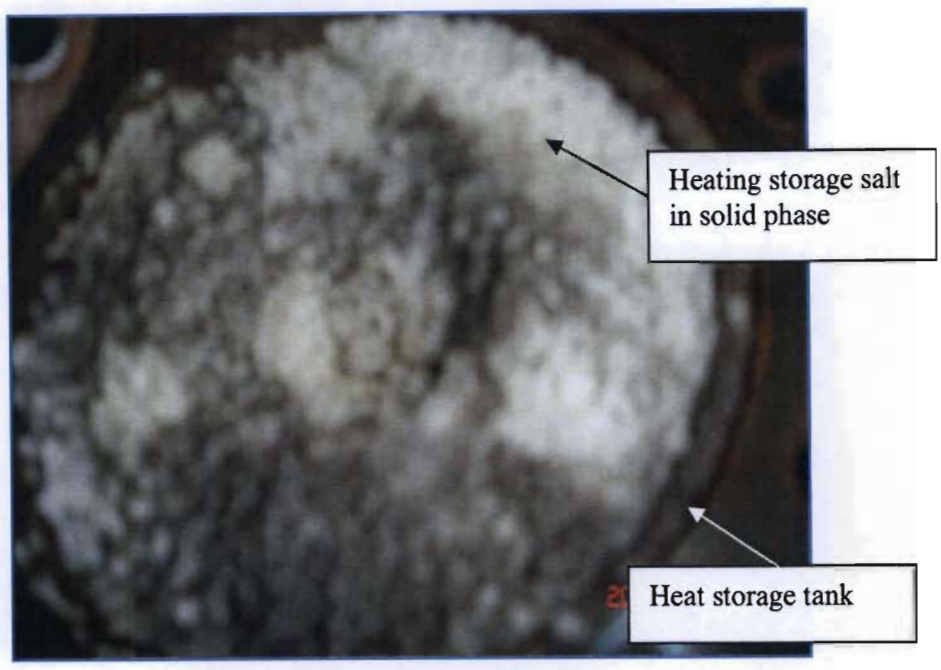

Figure 8.4 Heating storage salts in solid phase

Figure 8.4 shows the top of the heat storage calorimeter and as you can see the storage salt is still in a solid phase with darkened color because of the corrosion from the bottom flange.

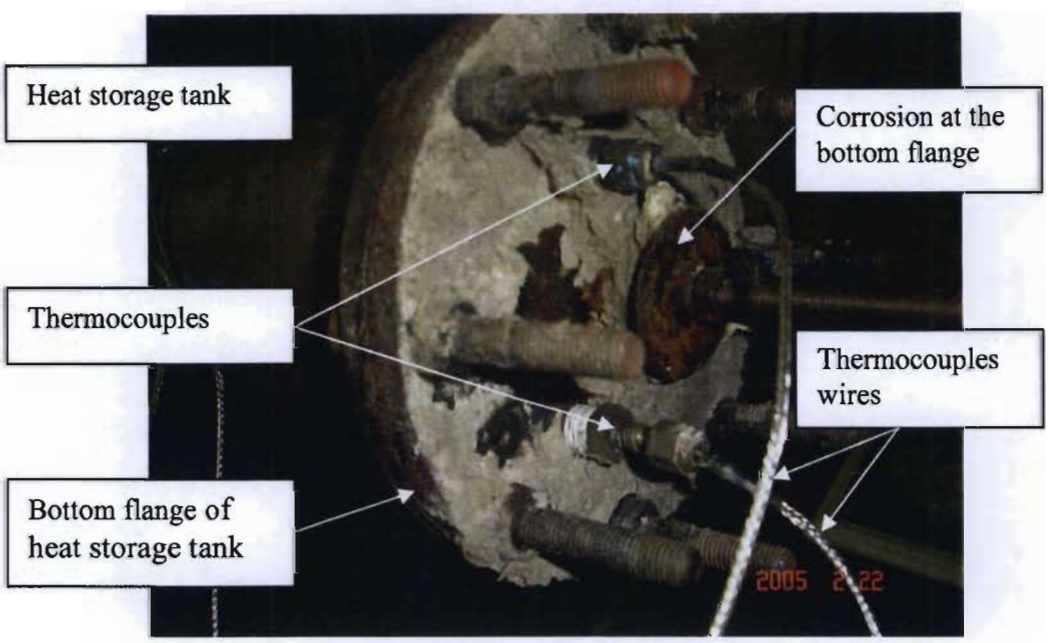

Figure 8.5 Bottom of heat storage tank after 6 months

Leaking of the heat storage salts from the bottom of the heat storage calorimeter (as shown in figure 7.2 in chapter 7) which caused corrosion as shown in Figure 8.5.

Figure 8.6 Horizontal cut in heat storage tank.

8.1.2 Discharge Process

A typical radial temperature history during a heat discharge stage of sodium nitrate versus time is shown in Figure 8.7 which was obtained from data in Table T.20 in Appendix T. The temperature of the melted PCM at the beginning of the phase transition is around 310 °C which is the phase transition temperature of the PCM. As the system was lifted without insulation the heat dropped down sharply after 149 min.

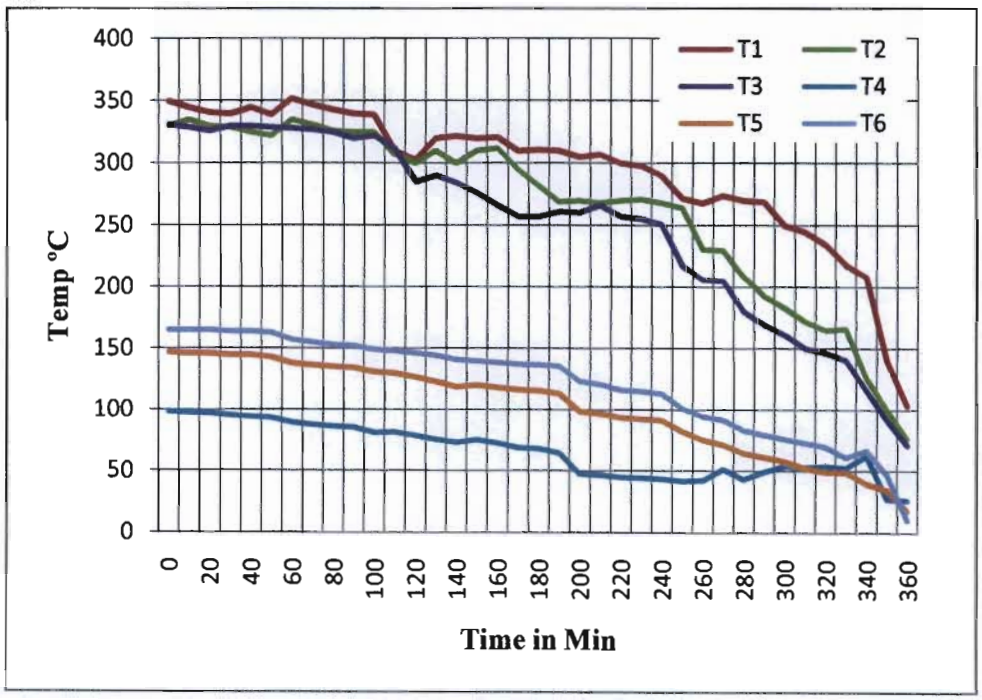

Figure 8.7 Discharging temperature of heat storage calorimeter

8.2 Second Calorimeter Results

A typical radial temperature history during a heat storage stage of mixture of 60% Sodium Nitrate and 40% of Potassium Nitrate versus time is shown in Figure 8.8. Since the system is heated from the shell-side of heat storage tank, the temperature at shell side rises rapidly and the phase transition occurs at the temperature range 210 °C to 250 °C. As can be seen, the temperature of the melted PCM increases sharply until the radial temperature distribution becomes uniform due to the convection in the liquid after the PCM has melted.

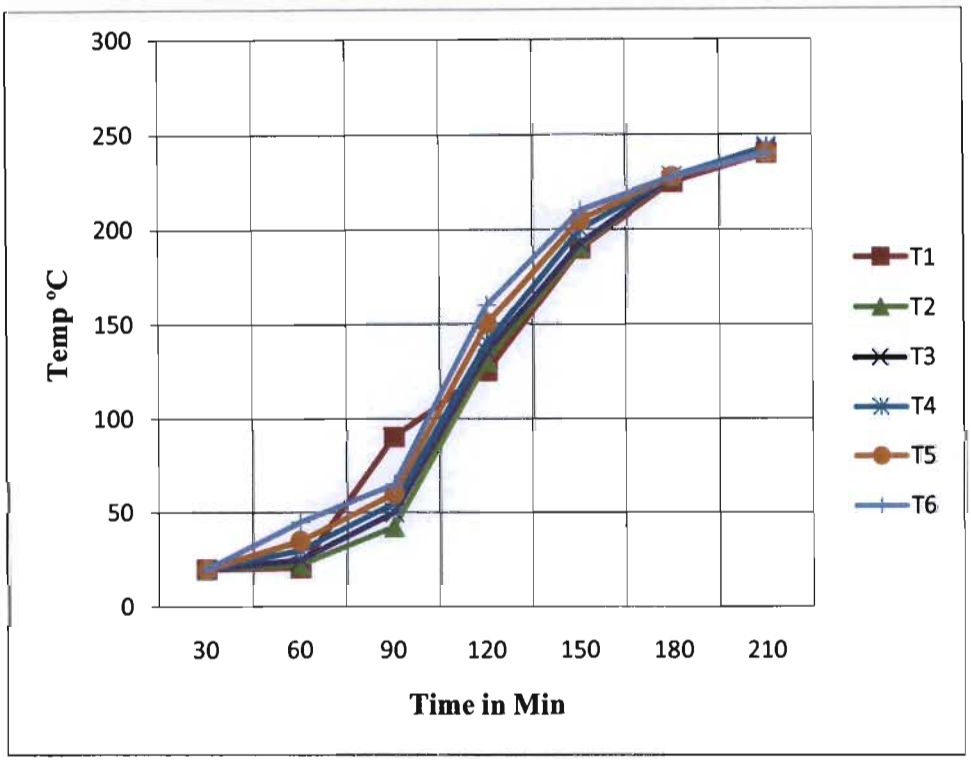

Figure 8.8 Temperature histories during a heat storage stage.

After an hour of stopping charging the system, the discharging process of the system was started by air (as heat transfer fluid) at 1.5 atm. At the heat discharging stage, a typical temperature history in the radial direction is shown in Figure 8.9. When the system is cooled by air, the temperature is uniformly distributed in the radial direction until the temperatures reach the phase transition temperature 220 - 250 °C.

The temperature around the heat transfer tube decreases linearly with time. However, a distinct phase transition without the super cooling across the radius can be found near the heat transfer tube. Thereafter the temperature drops sharply. The total amount of heat recovery, Q, during the heat release stage can be calculated from Equation 2.2 in chapter 2.

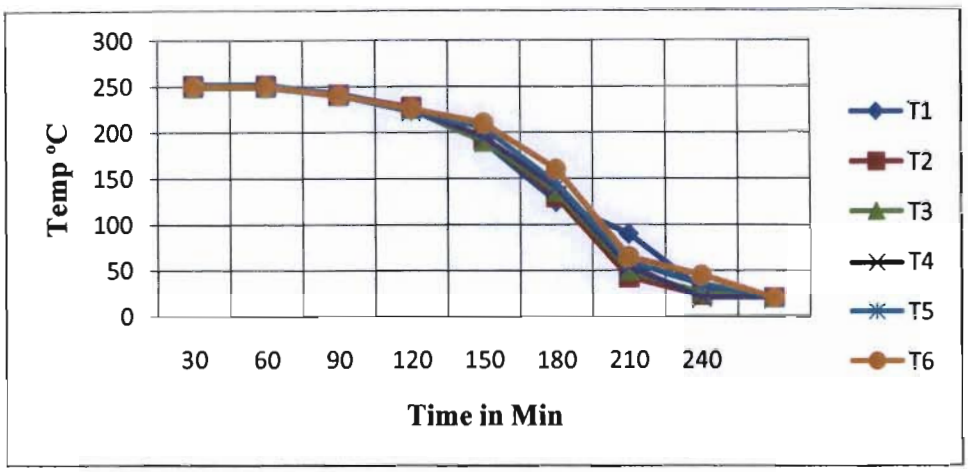

Figure 8.9 Temperature histories during a heat discharge stage.

8.3 Charging of Electric Heat Storage System

Figure 8.10 shows the temperature histories during a heat storage stage of electric heat storage for 2 days at 300W charging power. Overlapping was occurred because the system was tested without proper insulation and due to this gap can be seen clearly between the Tt which presents the average temperatures near to the top, surrounding the middle of the heat storage tank and Tb present the average temperature of the heat sensor near to the bottom which far from the heating source; because of the big heat loss the difference in ΔT becomes more by increasing the charging of the system. When the heat in middle and top of the heat storage reach melting point, the salt surrounding, near the wall of heat storage tank starts to work as insulation.

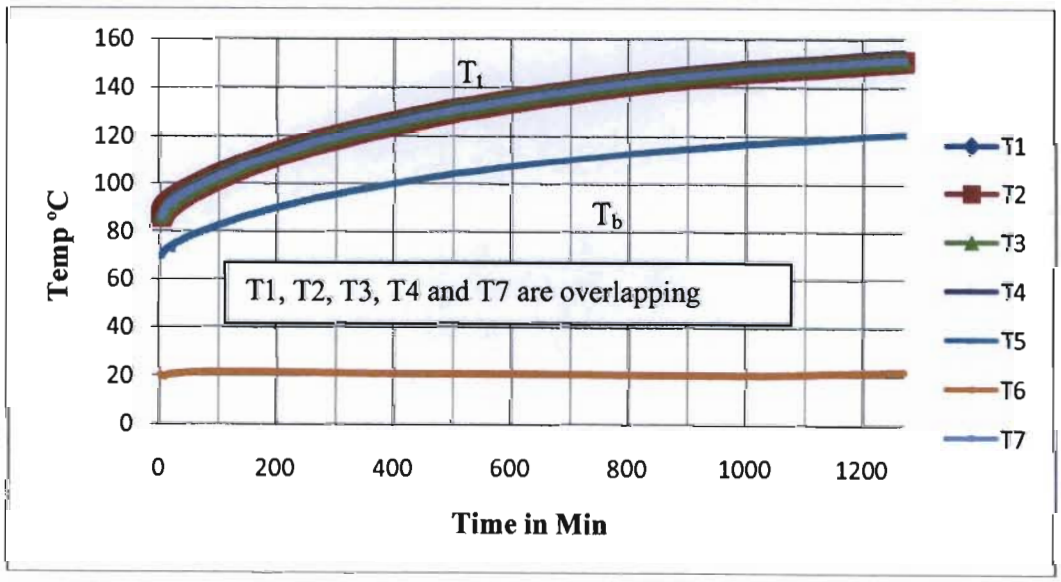

Figure 8.10 Temperature histories during a heat storage stage of electric heat storage

8.4 Discharging of Electric Heat Storage System

Two different methods were used to discharge the heat storage tank. The first was steam discharge unit, and the second method was an air discharging unit

8.4.1 Steam Discharging Unit

One of the methods was used by dropping water inside the heat transfer pipe after at least 4 hours of full charge of heat storage 3.2l was converted to dry steam at 2.6 bar pressure which can be used for cooking different types of food.

8.4.2 Air Discharging Unit

Discharging of electric heat storage system done by pushing air under two bar pressure through the heat pipe inside heat storage tank, Figure 8.11 shows the temperature histories of the slow charging of an electric heat storage tank which was obtained from the data taken by a data logger and a graph drawn using Microsoft Excel software. Since the system is heated from inside by convoluted heating pipes, the temperature of the heating pipes side rises rapidly and the phase transition occurs at the temperature range 210 °C to 250 °C. As can be seen, the temperature of the mixture salts sodium nitrate and potassium nitrate rises without any phase change until the temperature reaches above 220 °C and the temperature of melted PCM increases sharply until the radial temperature distribution becomes uniform due to the convection in the liquid after the PCM has melted.

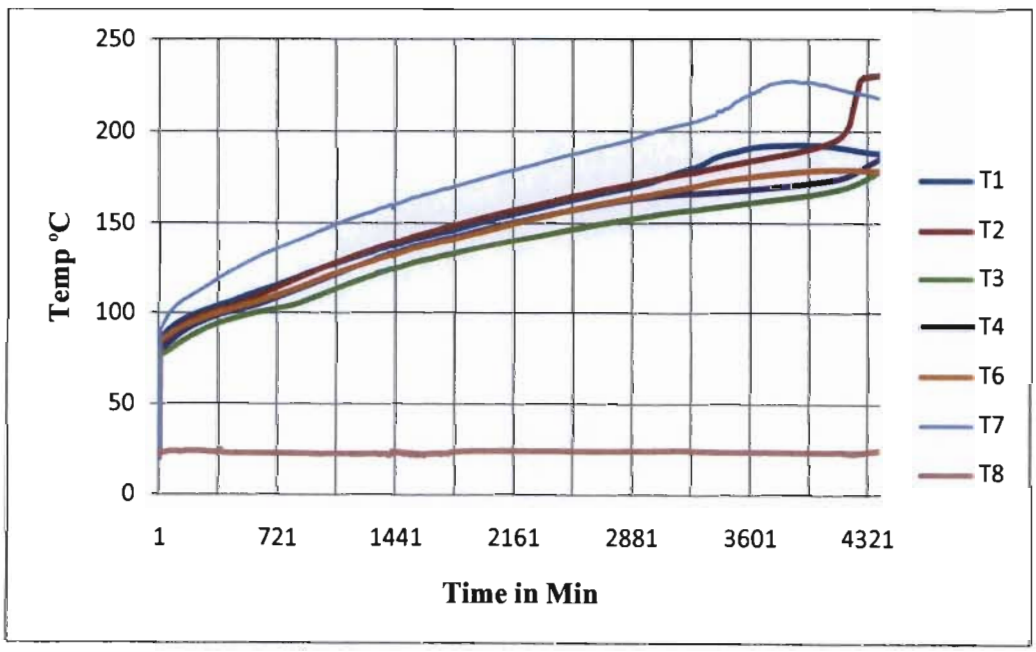

Figure 8.11 Charging temperature for 3 days at 300W charging power.

8.5 Backup Liquid Petroleum Gas Burner for Solar Cooker

It is assumed that on a bad weather day the maximum hot air temperature available from the thermal storage unit is approximately 150°C. In this case the air temperature has to be constantly monitored, the reason being that the higher the airflow rate the cooler the element becomes.

The added advantage of the solar cooker is the stovetop is at a higher temperature than ambient, this was assumed to be 100 °C. The initial temperature of the stovetop was set at 100 °C. Tests were also conducted with the stovetop at room temp; this to compare directly with a test conducted on a Cadac Handi Stovetop cooker.

A Cadac Handi Cooker was used to determine the gas consumption from a normal home use perspective. Results show that at full throttle the Handi Cooker takes approximately seven minutes to bring a liter of water to the boil. This is at a gas flow rate of 227 g/h, using 26 g of LPG.

Table 8.1 Averages Gas Consumption

Gas Consumption (g)	**Time Taken to reach boiling point**	**Gas Consumption (g/h)**
26 g	412 Sec (7 Min)	227.185 g/h
The ambient air temperature and initial water temperature were		
Ambient air temperature		26.5°C
Initial Water temperature		23.4°C

In order to compare our cooking system operation with that in Table 4.3 [13] a several experiments of cooking operation were done and the average cooking operation time is shown in Table 8.2.

Table 8.2 Cooking Times for Steam Heated Cook Top

No	Cooking operation	Energy store Temperature	Hot plate Temperature	Time required Minutes
1	Cook 0.5kg rice in 0.75kg water	230°C	160°C	40
2	Fry 3 eggs and 0.25kg onions	230°C	160°C	21
3	Steam 1 kg rice in 1.3kg water	240°C	175°C	36
4	Fry 0.5kg rice, 0.25kg green beans and 0.25kg shrimps	250°C	180°C	32
5	Fry 1kg sausages	250°C	180°C	21
6	Fry 4 eggs and 0.25kg onions	250°C	180°C	15
7	Fry 0.8kg beef	260°C	185°C	30
8	Fry omelette, 3 eggs, 0.25kg onions	260°C	185°C	15

Table 8.2 shows the time required for cooking different cooking operations taking much longer than what was found in reference [13] when using very high pressure. The temperature curves of different parts of the heat storage system are shown in Figure 8.13 to Figure 8.16, and it can be seen that there are two stages of one cycle. One is power on, and the other is power off. In the first stage, the time of sensible heat storage was about 3 days.

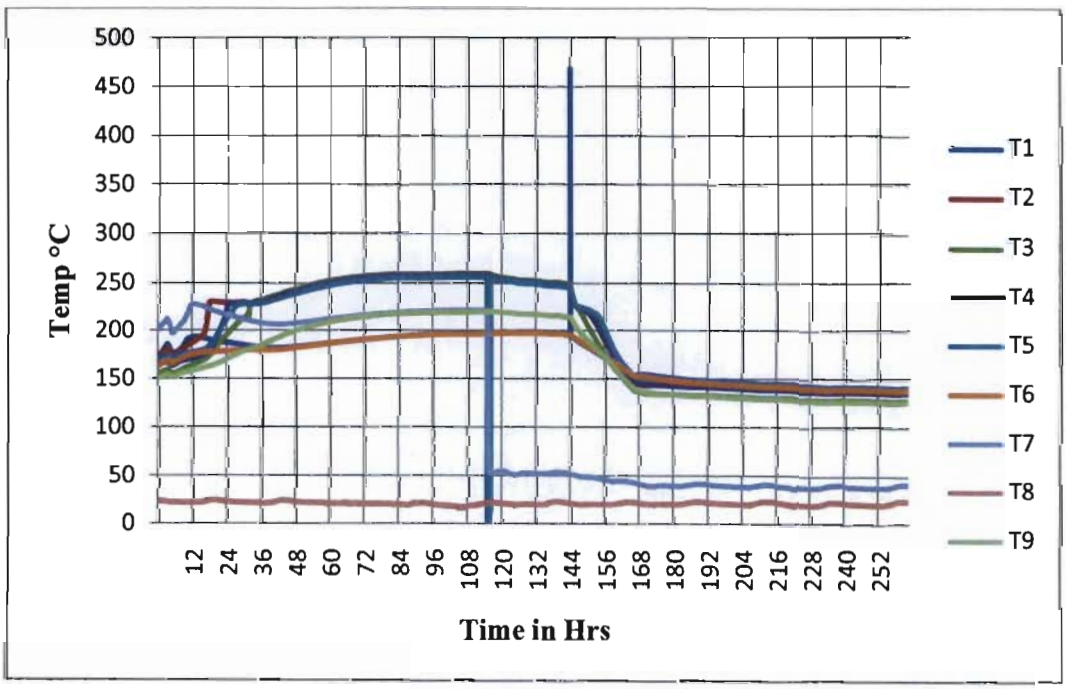

Figure 8.12 Charging and discharging the system for 10 days

After 3 days of charging the system as shown in Figure 8.11, the temperature distribution during melting of the mixture of sodium nitrate and potassium nitrate started changing its phase from solid phase to liquid phase. The melting process curve shows that T1 and T6 have similar behaviour due to the radial position of the thermocouples.T1 at point 144 had a reading of 468.84 which is out of normal range; this might be due to the sensor reading incorrectly because at point 145 it had a value of 211.12, temperature T5 at point 114 gives a value of 255, at point 115 it reads 3.0355, at point 116 it displays 255.73 which shows that the sensor appears to be reading incorrectly.T7 at point 114 had a reading of 222.15, at point 115 it was 221.15, at point 129 it recorded 52.376, and at point 177 a value of 39.749 was reached. T8 represented the ambient temperature and T9 represented the reading of the thermocouple inside the middle of the heat storage pipe. At point 48 it had a value of 199.28 and at point 120 the recorded value was 223.

From Figure 8.12 one can clearly see that during the period from point 24 to point 144, the salt mixture had completely melted; this was also confirmed by viewing the melting checking bar which was moving smoothly in all directions. The discharging process took place 4 hours after cutting off the power at point 140 till point168 by draping water inside the heat transfer pipes which was at 225°C to get 3kw dry steam above 170 °C.

Figure 8.13 shows the melting behaviour of the mixture of sodium nitrate and potassium nitrate during the charging process at 250 watt. As seen from the charging curve T2, T3, T4 and T5 all behave differently at the beginning of the heat transaction at 210°C of the phase change period. However, because of heat distribution and their position inside the heat storage tank, their temperature fluctuates within a range of ± 45 °C, at 240°C, and later they start to behave similarly due to their radial positions and the heat storage material around them which completely melts. When T1 and T6 are still at a temperature range below melting point, the salts at these points are still in a solid phase need more power to change their phase. T7 near the heat storage tank surfaces and T8 are the ambient temperature.

Figure 8.14 shows the temperature distribution during melting of the mixture of sodium nitrate and potassium nitrate as it started changing its phase from a solid phase to a liquid phase at a charging power of 250 watt and the power cut off. Upon any of the thermocouples reaching 280°C, and after being cut 440 min from reaching 250 °C, the charging curve shows that T2, T3, T4 and T5 all behave similarly as a result of their radial positions. T1 and T6 at

sub-melting point still maintain the salts in a solid phase as they need more power to change to a liquid phase. T7 near the heat storage tank surfaces and T8 are the ambient temperature.

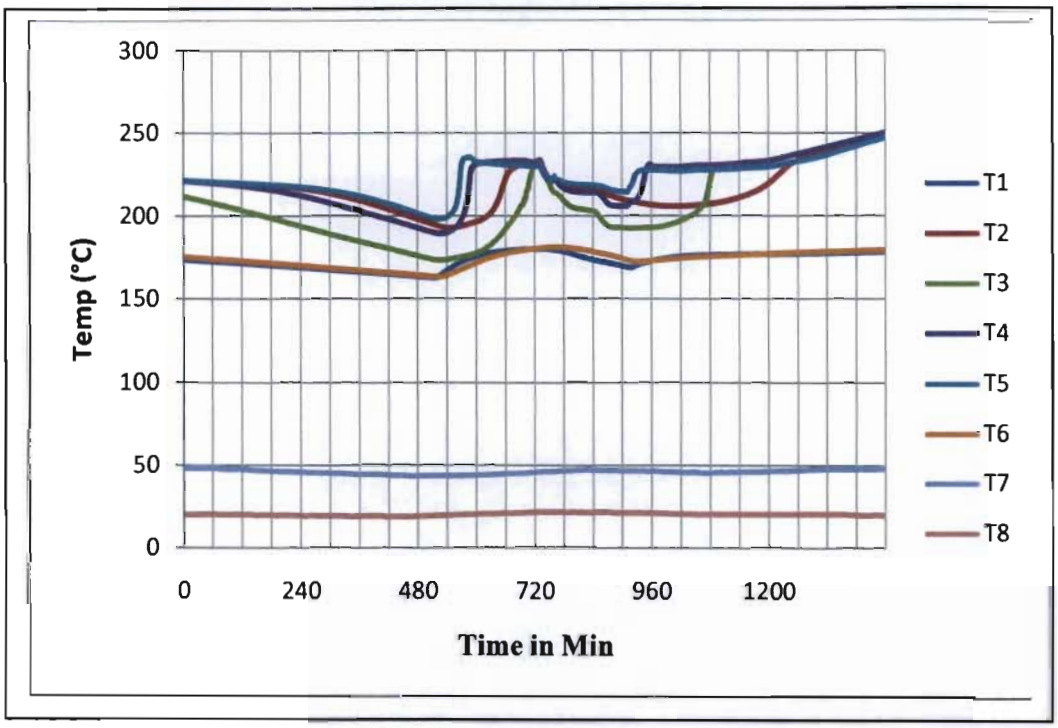

Figure 8.13 Temperature distributions during melting of the mixture salts

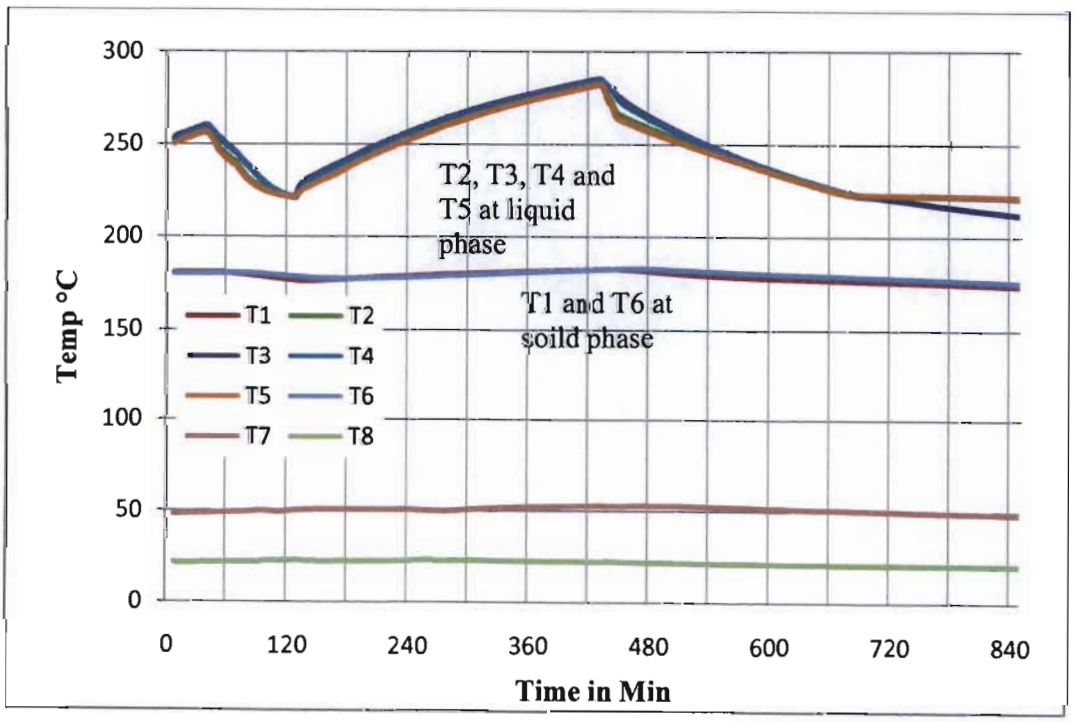

Figure 8.14 Temperature distributions during melting of the mixture salt at charging power 250 Watt

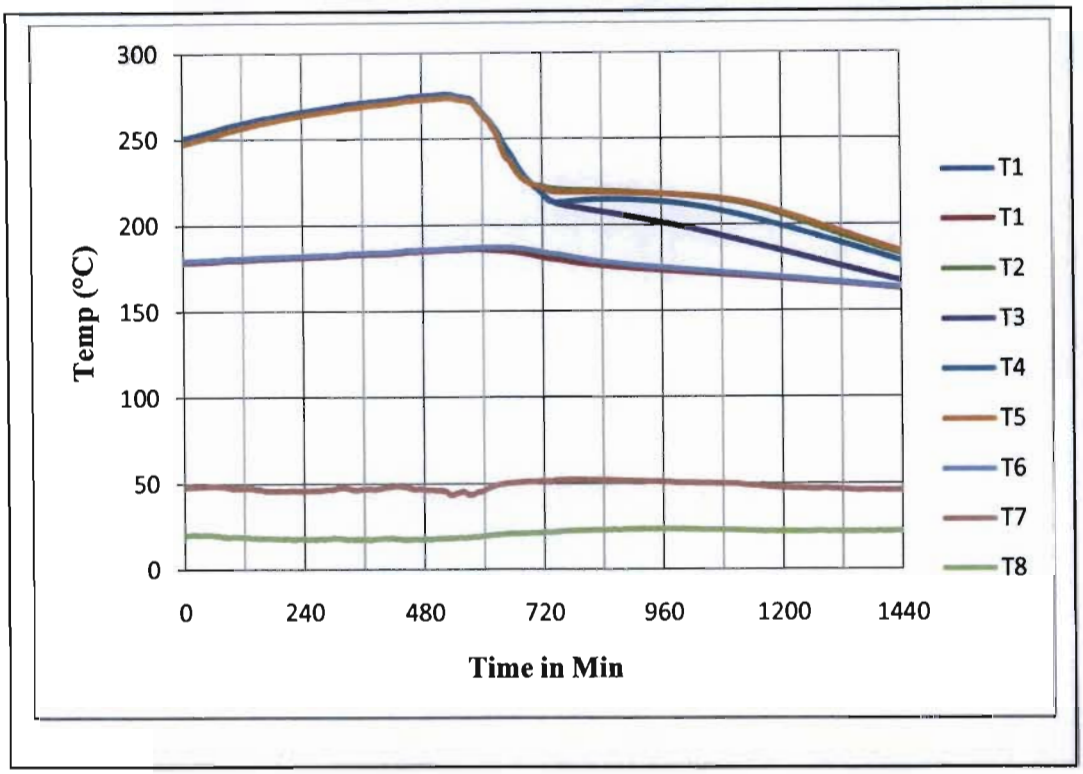

Figure 8.15 Charging and discharging the system

Figure 8.15 shows the temperature distribution during melting of the mixture of sodium nitrate and potassium nitrate started changing its phase from solid phase to liquid phase at charging power 250 watt. Initially, the solid-liquid PCMs T_2, T_3, T_4 and T_5 behave like sensible heat storage (SHS) materials; their temperature rises as they absorb heat. Unlike conventional SHS, however, when PCMs reach the temperature at which they change phase (their melting temperature) they absorb large amounts of heat at an about 220 °C almost constant temperature. The PCM continues to absorb heat without a significant rise in temperature until all the material is transformed to the liquid phase. The two phases above and below the phase transition can be distinguished from each other in terms of some ordering that takes place in the phase below the transition temperature. In the liquid-solid transition, the molecules of the liquid get "ordered" in space when they form the solid phase. In a paramagnet, the magnetic moments on the individual atoms can point in any direction (in the absence of an internal magnetic field), but in the ferromagnetic phase the moments are lined up along a particular direction, which is then the direction of ordering. Thus in the phase above the transition, the degree of ordering is smaller than in the phase below the transition.

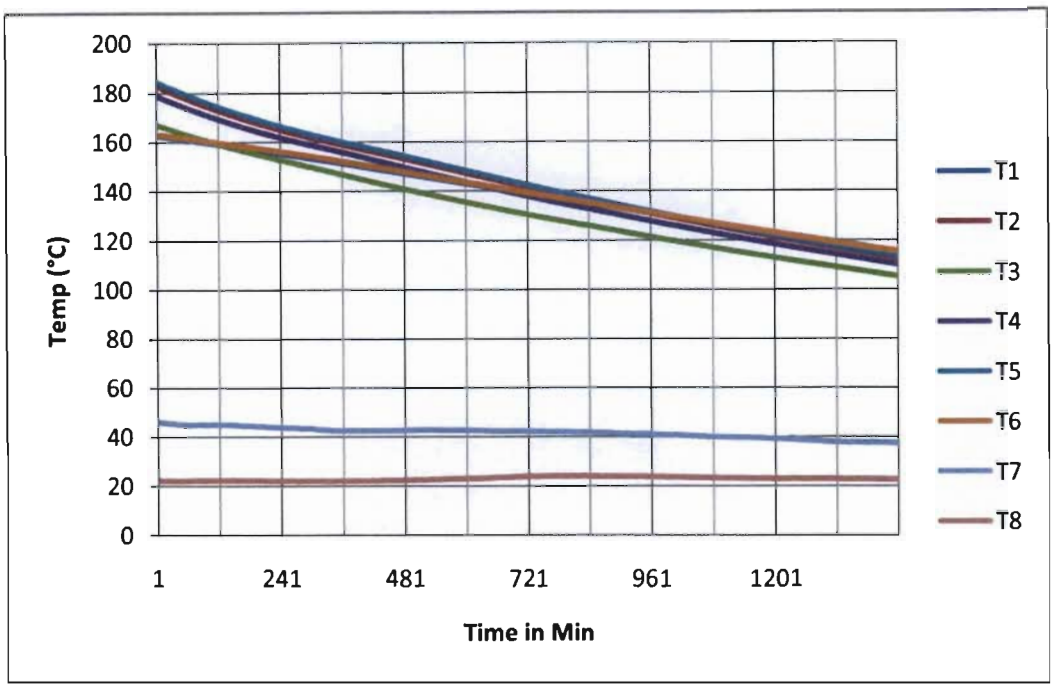

Figure 8.16 Continue discharging of the system from 180°C

Figure 8.16 is a continuation of figure 8.15 shows the discharging process of heat storage unit at air flow rate 1kg/min.

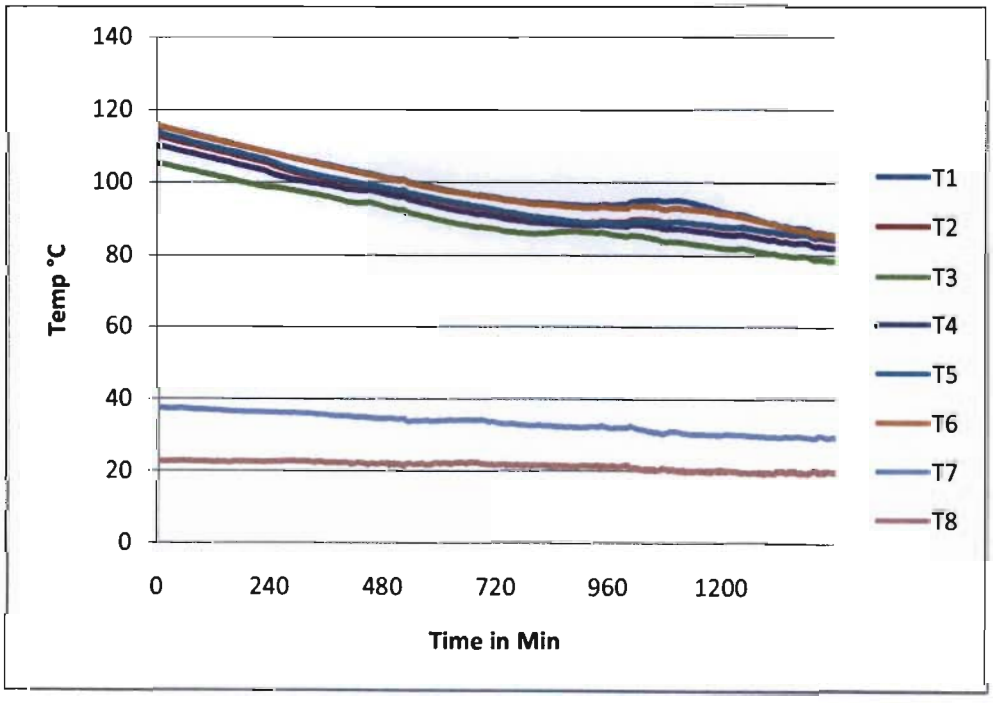

Figure 8.17 Continue discharging of the system from 120°C

Figure 8.17 and Figure 8.18 a continuation of figure 8.16 shows the discharging process of heat storage unit at air flow rate 1kg/min till the temperature become 70°C.

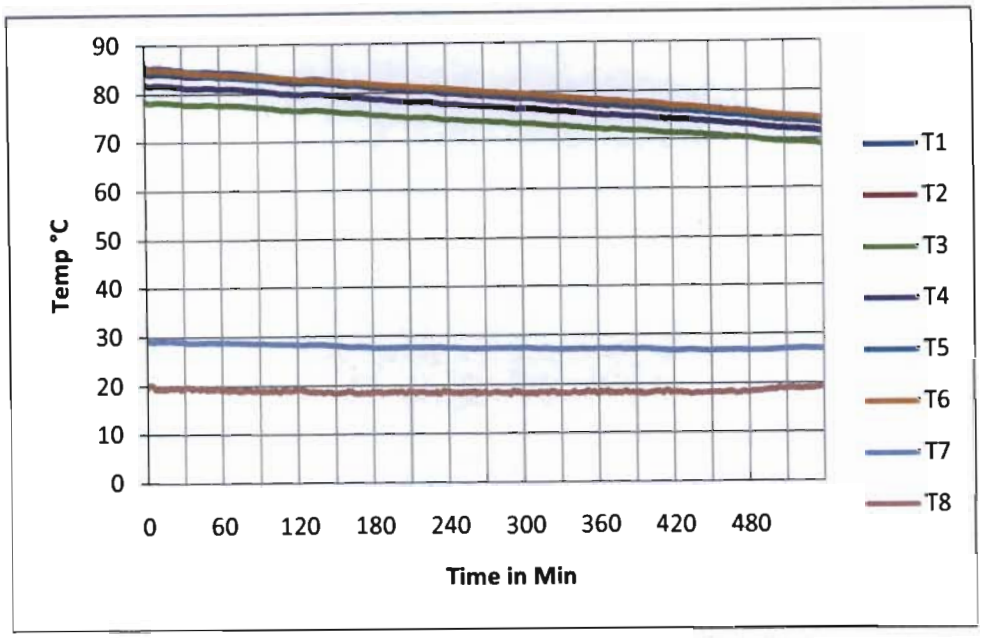

Figure 8.18 Continue discharging of the system till 70°C

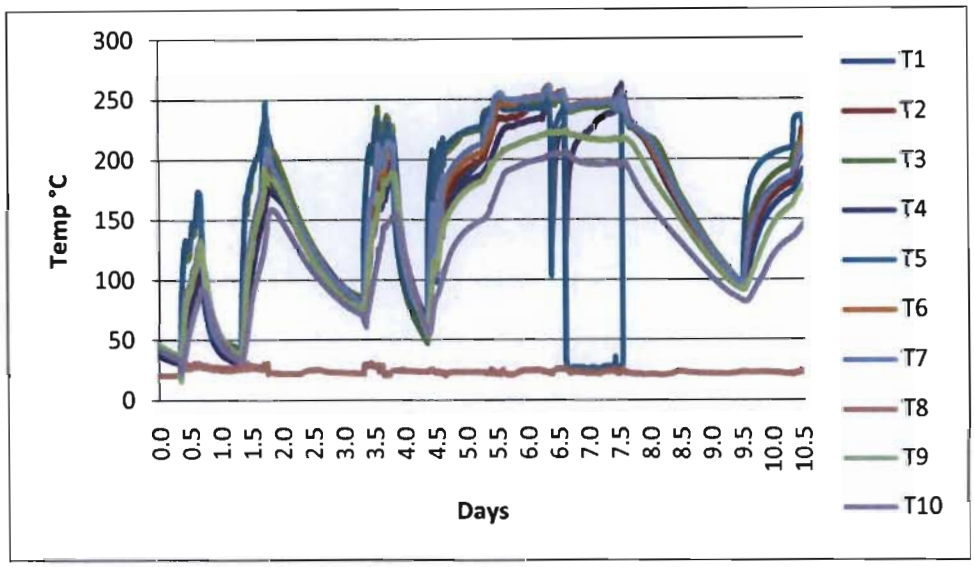

Figure 8.19 Charging and discharging of oil heat transfer heat storage system

To understand the long-duration behaviour of thermal energy storage a mixture of sodium nitrate and potassium nitrate salts were repeated charging and discharging at different charging rate as shown in Figure 8.19 to observe behaviour of sensible heat and latent heat till the system were stabled at temperature 260 °C and the PCMs were completely melted in

temperatures range of 220 °C to 260 °C. Such data, which have never been obtained before, have direct application to solar cooking power systems.

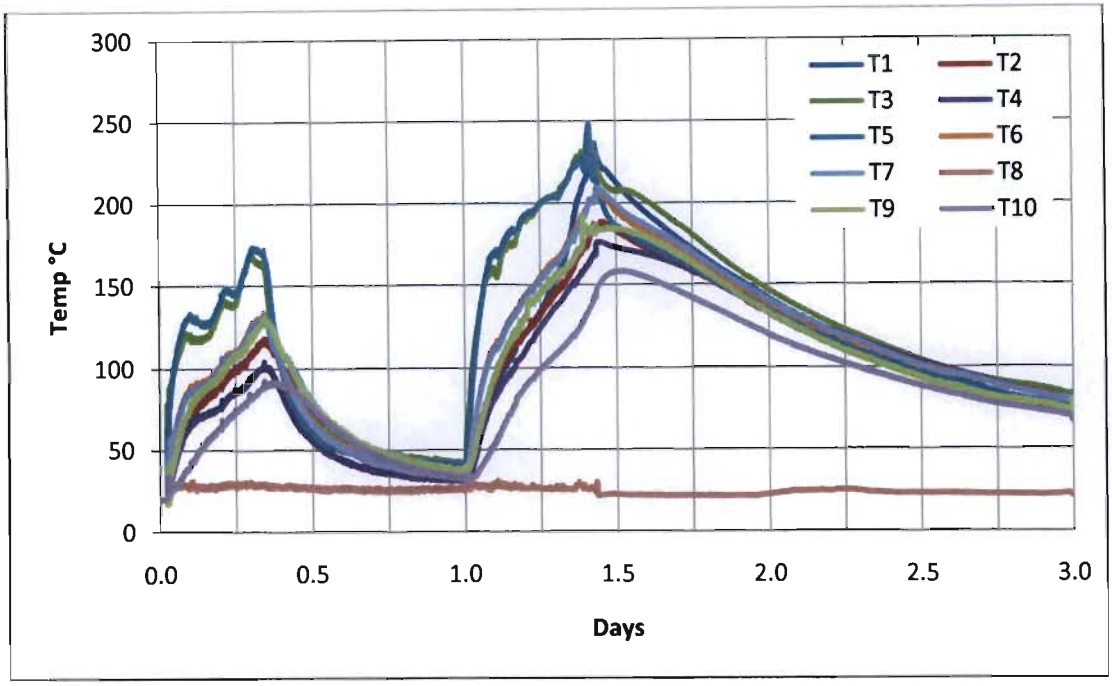

Figure 8.20 Charging and discharging of the oil system

Figure 8.20 shows charging and discharging of the oil heat transfer heat storage system during solidification of the mixture of heat storage salts (60% Sodium Nitrate and 40% Potassium Nitrate).

As can be seen from the heat charging and discharging curves, phase salt temperature T3 and T5 behave similarly, as do T6 and T7 and also T2 and T9. This is due to their radial and longitudinal positions in the heat storage system tank. A fundamental requirement for the charging of the heat storage system is a higher temperature than can be obtained in the course of discharge, since heat transport/flux necessitates a temperature difference. The quality of the heat is dependent on the temperature at which it is available: the higher the temperature, the more diverse the uses to which the heat may be put. For this reason, it is desirable for the temperature level in the course of storage to fall as little as possible. Heat pipe temperature T10 after 1.5 days had a maximum value of 160°C inside the heat transfer pipe which is a very low temperature for transferring it to the hot plate for cooking purposes. Despite this, it is adequate for heating water, and that is why at this stage the backup LPG system was used.

In the case of sensible heat storage system, as can be seen from Figure 8.21 the input of heat is associated with gradual heating of the storage material (and vice versa during discharge), whereas latent heat is stored and discharged at the melting temperature of the PCM. Latent heat storage therefore has the advantage over sensible heat storage in that the temperature loss is limited to the loss during heat transport from and to the storage system.

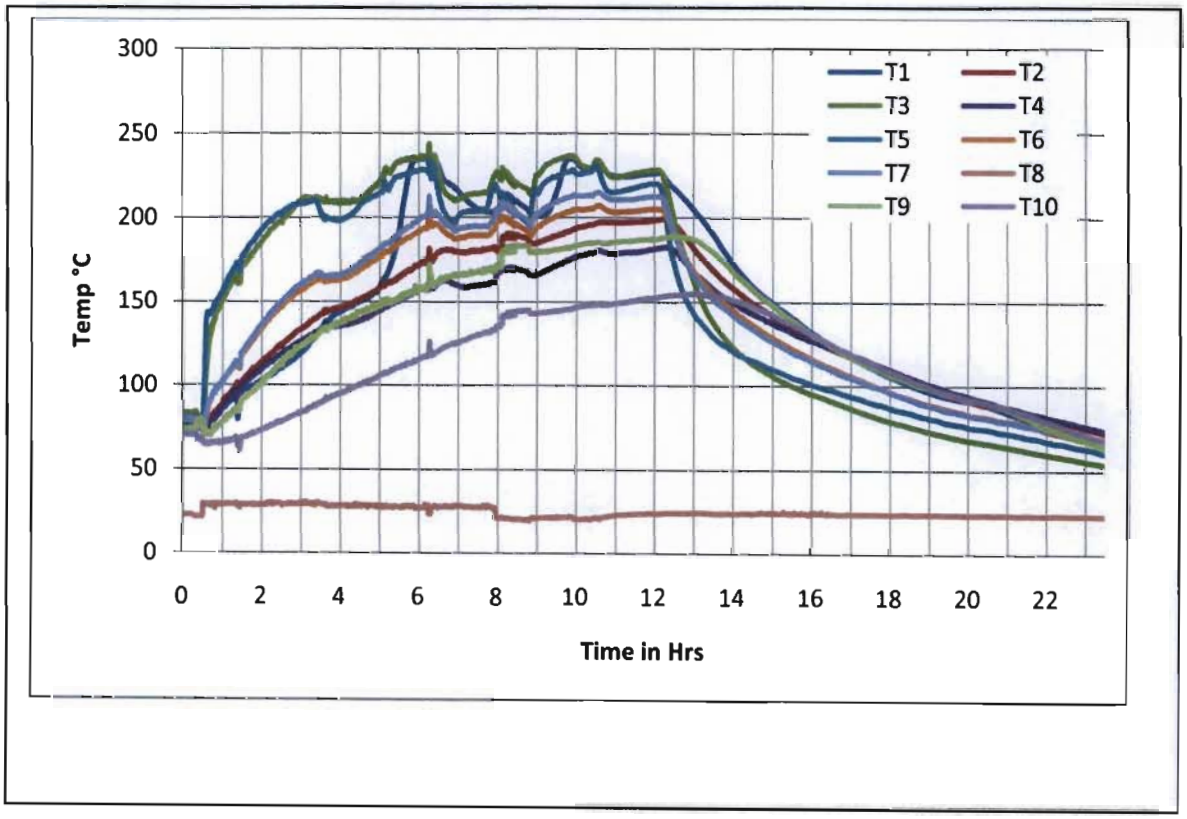

Figure 8.21 Sensible and latent heat Charging and discharging of the system

To see the effect of the flow rate and inlet fluid temperature on the outlet fluid temperature distribution, the flow rate was increased to 10 l/min and the inlet fluid temperature to 310 °C. This means that the duration of the heat charge decreases with the increasing flow rate or increasing inlet fluid temperature.

Figure 8.22 shows the charging and discharging of the oil heat transfer latent heat storage system which were repeated over 90 times for a period of 3.5 years. From an enormous number of experiments carried out over a long period, it was established that the system was stable. During charging, the storage outlet temperature is limited by the heat transfer oil maximum operation temperature.

With the introduction of an expensive synthetic heat transfer oil, capable of increasing the operating temperature from the former 310 °C up to 400 °C, the direct storage technology becomes uneconomical. During discharging, the storage outlet temperature is limited by the inlet temperature.

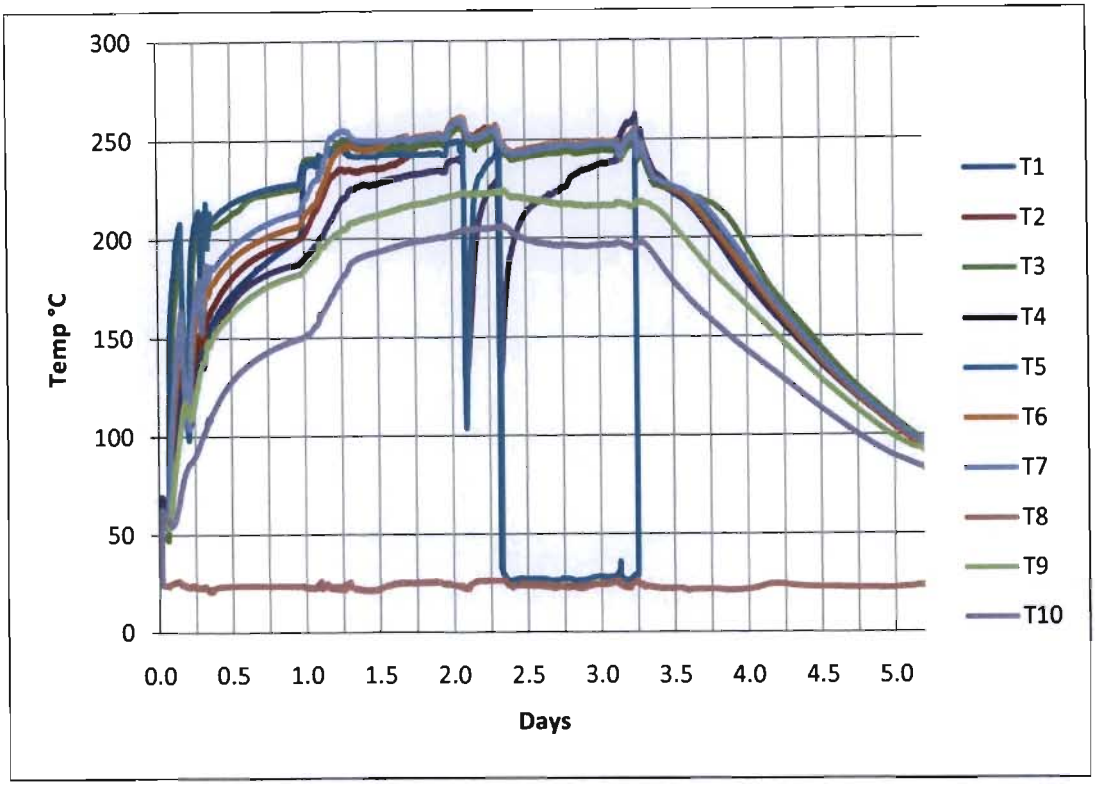

Figure 8.22 Charging and discharging of the oil system latent heat storage

8.6 Discussion over all Results

Initially, the solid-liquid PCMs behave like sensible heat storage (SHS) materials; their temperature rises as they absorb heat. Unlike conventional SHS, however, when PCMs reach the temperature at 220°C to 260°C which they change phase they absorb large amounts of heat at an almost constant temperature. The PCM continues to absorb heat without a significant rise in temperature until all the material is transformed to the liquid phase. When the ambient temperature around a liquid material falls, the PCM solidifies, releasing its stored latent heat.

The two phases above and below the phase transition can be distinguished from each other in terms of some ordering that takes place in the phase below the transition temperature. In the

liquid-solid transition, the molecules of the liquid get "ordered" in space when they form the solid phase. In a paramagnet, the magnetic moments on the individual atoms can point in any direction (in the absence of an internal magnetic field), but in the ferromagnetic phase the moments are lined up along a particular direction, which is then the direction of ordering. Thus in the phase above the transition, the degree of ordering is smaller than in the phase below the transition. One measure of the amount of disorder in a system is its entropy, which is the negative of the first derivative of the thermodynamic free energy with respect to temperature. This change in entropy can be continuous or discontinuous at the transition temperature.

Discontinuous transitions involve a discontinuous change in the entropy at the transition temperature. A familiar example of this type of transition is the freezing of water into ice. As water reaches the freezing point, order develops without any change in temperature. Thus there is a discontinuous decrease in the entropy at the freezing point. This is characterized by the amount of latent heat that must be extracted from the water for it to be "ordered" into the solid phase (ice). Discontinuous transitions are also called first-order transitions.

In a continuous transition, entropy changes continuously, and hence the growth of order below transition temperature is also continuous. There is no latent heat involved in a continuous transition. Continuous transitions are also called second-order transitions. The paramagnet to ferromagnetic transition in magnetic materials is an example of such a transition.

The degree of ordering in a system undergoing a phase transition can be made quantitative in terms of an order parameter. At temperatures above the transition temperature the order parameter has a value zero, and below the transition it acquires some nonzero value. For example, in a ferromagnet the order parameter is the magnetic moment per unit volume (in the absence of an externally applied magnetic field). It is zero in the paramagnetic state since the individual magnetic moments in the solid may point in any random direction. Below the transition temperature, however, there exists a preferred direction of ordering, and as the temperature is lowered below phase transition temperature, more and more individual magnetic moments start to align along the preferred direction of ordering, leading to a continuous growth of the magnetization or the macroscopic magnetic moment per unit volume in the ferromagnetic state. Thus the order parameter changes continuously from zero above to some nonzero value below the phase transition temperature. In a first-order transition, the order parameter would change discontinuously at the transition temperature.

In this latent heat storage system, the solid-liquid interface moves away from the heat transfer surface during phase change. During this process, the surface heat flux decreases due to the increasing thermal resistance of the growing layer thickness of the molten solidified medium. In the case of solidification, conduction is the only transport mechanism, and in most cases, it is very poor. In the case of melting, natural convection can occur in the molten layer and this generally increases the heat transfer rate compared to the solidification process.

However, the generally low heat transfer rate can be increased considerably by using a suitable heat transfer enhancement technique. There are several methods to enhance the heat transfer in latent heat storage system. The finned tubes with different configurations were used to improve the charge/discharge capacity of heat storage system in this project.

8.7 Summary

This chapter has placed a strong emphasis on the results and discussions of some the major findings of the project. It is important to emphases the need to carefully areas the potential impact of The Thermal Energy Storage (TES). TES experiments are designed to provide data to help researchers understand the long-duration behaviour of thermal energy storage a mixture of sodium nitrate and potassium nitrate salts that undergo repeated melting and freezing. Such data, which have never been obtained before, have direct application to solar cooking power systems. These power systems will store solar energy in a thermal energy salt, such as a mixture of sodium nitrate and potassium nitrate salts (which melts at a lower temperature). The energy was stored as the latent heat of fusion when the salt is melted by absorbing solar thermal energy. The stored energy will then be extracted during the shade portion, enabling the solar cooking power system to provide constant power for cooking.

Details of several sets of experiments results were given in this chapter to provide the data necessary to validate the solar cooking system. The first two experiments, First Calorimeter and Second Calorimeter, were developed to obtain data on TES material behaviour in cylindrical heat storage containers. Results of charging and discharging of electric heat storage system, oil heat transfer heat storage system, steam discharging unit, air discharging unit and backup liquid petroleum gas burner for solar cooker were given and discussed in details in this chapter.

CHAPTER 9

CONCLUSIONS AND RECOMMENDATIONS

9.1 Conclusions

Primary experiments using a mixture of sodium nitrate and potassium nitrate as a PCM (selected because of its high fusion temperature and thermal conductivity properties when storing thermal energy) were carried out, and matching ratios of the two chemical compounds and the relevant phase change temperature and the heat of fusion were studied. Throughout the experiments, a relevant container material was chosen to withstand corrosion and high efficiency thermal insulation material was also used.

A prototype module of a high temperature phase change materials heat storage system was developed, which together as a system provided the essential domestic power requirements including power for cooking and hot water for a family remote from the national grid. The thermal performance of the system was studied by experiments and the results show:

1. With high heat of fusion and thermal conductivity, a mixture of NaO_3 and KNO_3 is both a feasible and suitable heat storage medium.
2. The heat storage ratio of the cooker is relatively high and increases proportionately with higher heating power levels through the heat pipes.
3. During the phase change process, the heat storage cooker can provide a stable heat discharge rate and meet the demand for indoor thermal comfort to an acceptable extent.
4. With a high heat storage ratio and small size, the cooker is economical for domestic use because of its low operating cost. Encouragingly, the initial experimental results provide positive data for further modeling and optimization of such high temperature phase change storage heaters.

The following conclusions were established:

1. The results of heat charge/discharge experiments using a vertical heat exchange unit showed that the available enthalpy bounding the phase conversion temperature range was not quantitatively affected by the way the temperature of the thermal medium varied during heat charge and discharge. However, rapid cycles of heat charging and discharging showed big differences in available enthalpy. To allow adequate heat

flow during rapid cycles of heat charging and discharging the heat transfer coefficient between the thermal medium and PCM needs to be increased.

2. The physical properties of this mixture of the heat transfer between a PCM and a heat exchanger including natural convection of a PCM in the storage tank were measured, and as a result of discharging the storage system, the evidence shows that 3kw can be obtained as dry steam which is enough to cook a family meal during night time.
3. Corrosion test results revealed that SUS316 can be used as the construction material for heat transfer pipe storage tanks and heat exchangers for this mixture.
4. In terms of material cost, all materials are expensive compared to water, ranging from pure Sodium Nitrate costing about R50/kg to commercial Sodium Nitrate at about R5/kg, and Potassium Nitrate more expensive than Sodium Nitrate. This particular heating storage system used commercial grade sodium nitrate and potassium nitrate, which is 10 times cheaper than the pure materials.
5. A mixture of sodium nitrate and potassium nitrate as latent heat storage offers an advantage compared to other heat stores, particularly when the cycling temperature is close to the phase change temperature and the phase change can be used quite often.
6. In terms of safety under normal conditions, nitrates are stable compounds. However, at higher temperatures they decompose, and may be explosive at extreme conditions (high temperature and pressure). A temperature controller was used to control the temperature throughout the heat storage tank.

9.2 Recommendations

When using a heat pipe involving working fluid water and air pressure at a maximum of three bars as a heat transfer technique, improving the heat transfer from inside the storage tank can be obtained by using Sulfur.

This recommendation is based on the heat pipe being composed of a stainless-steel cylinder housing a Sulfur working fluid, and at the active temperatures for this application, 126°C to 526°C, the Sulfur becoming saturated.

As a chemical element, Sulfur is abundant, inexpensive, and relatively nontoxic, especially compared to other liquids like mercury and toluene which can also be used in this temperature range. Sulfur has the disadvantage of having too high a viscosity for normal heat

pipe use. However, for this application its high viscosity may actually be an advantage. Many heat pipes need to function under low hydraulic pressure gradients, that is, when they are nearly level. However, in this case, the heat pipe is only needed to function when it is vertical, i.e. when the hydraulic pressure is at its maximum, as that's the operating condition under which cooking is being done. To reduce the cost of using an oil heat pump which costs about R8000, using a car oil pump which only costs a few hundred Rand is further recommend.

Finally, it is concluded that the work presented in this thesis will provide adequate guidelines for the design of future thermal energy storage units and cooking systems, especially those pertaining to the experimental and analytical models which will in turn lead to greater accuracy and confidence in the design procedure adopted by future designers of thermal energy storage units.

9.3 Summary

The objectives of this research project were achieved by providing a model of heat storage system based upon phase change salts (Sodium Nitrate and Potassium Nitrate). The most important fundamental conclusions were made in this chapter. Selected conclusions include: for the development of Phase Change Thermal Energy Storage system, the choice of suitable Phase Change Material (PCM) plays an important role in addition to heat transfer mechanism; due to PCM having a slow heat transfer rate as a result of variations in thermal conductivity, experimental methods have been adopted to increase the heat transfer rate in order to increase its applicability and faster charging/discharging times. Given that energy utilised for cooking plays an important role in sustainable energy management worldwide, when it comes to heat storage units, food can be cooked even in the late evening which means that solar cookers with storage units are extremely beneficial for humans as well as for energy conservation. Finally important recommendations were made.

APPENDIX D

SYSTEM DESIGN DRAWING

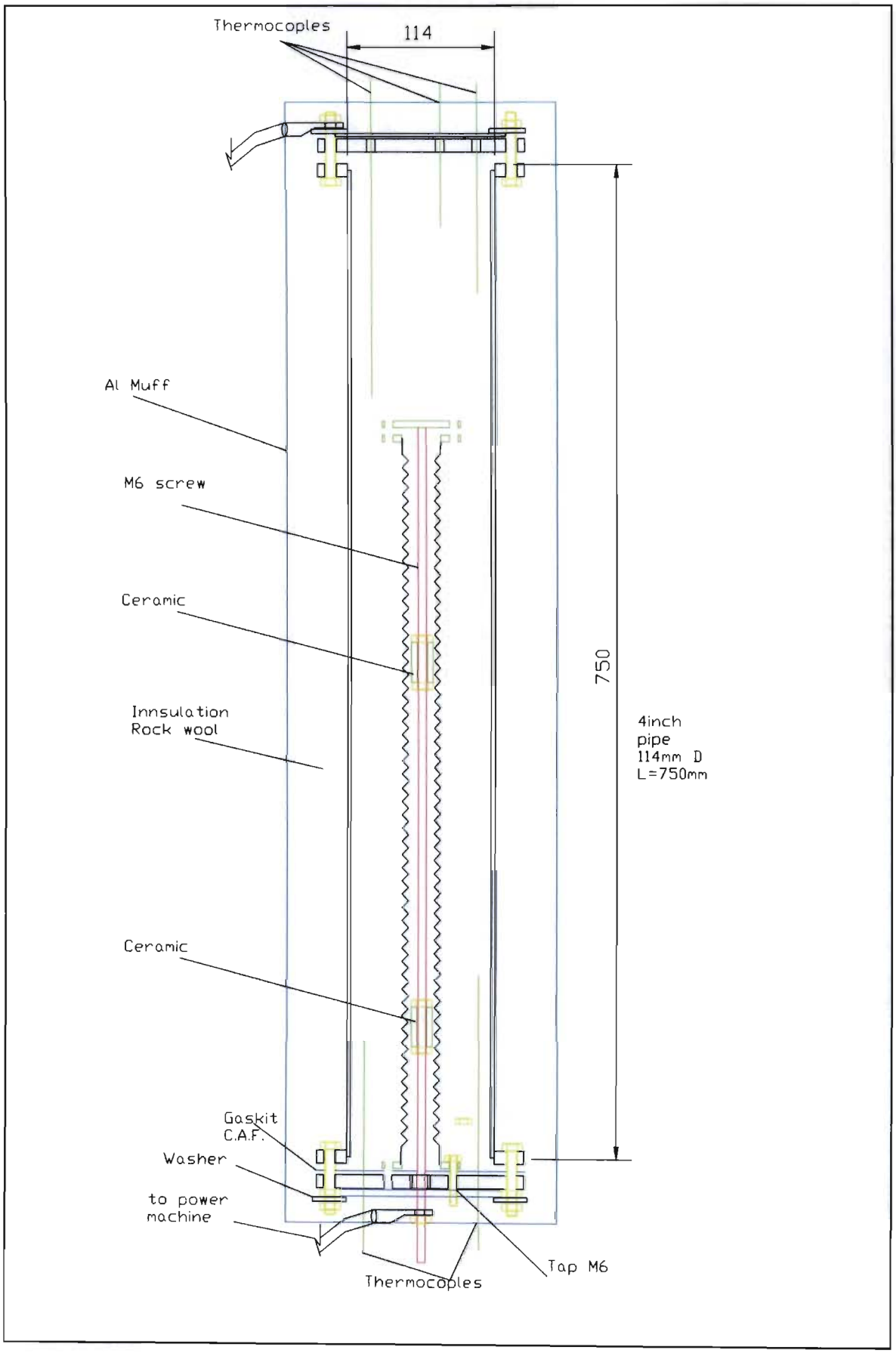

Figure D.1 Drawing Design of First Heat Storage Calorimeter

- All Dimensions in Figure D.1 – D.12 in mm, unless otherwise specified.

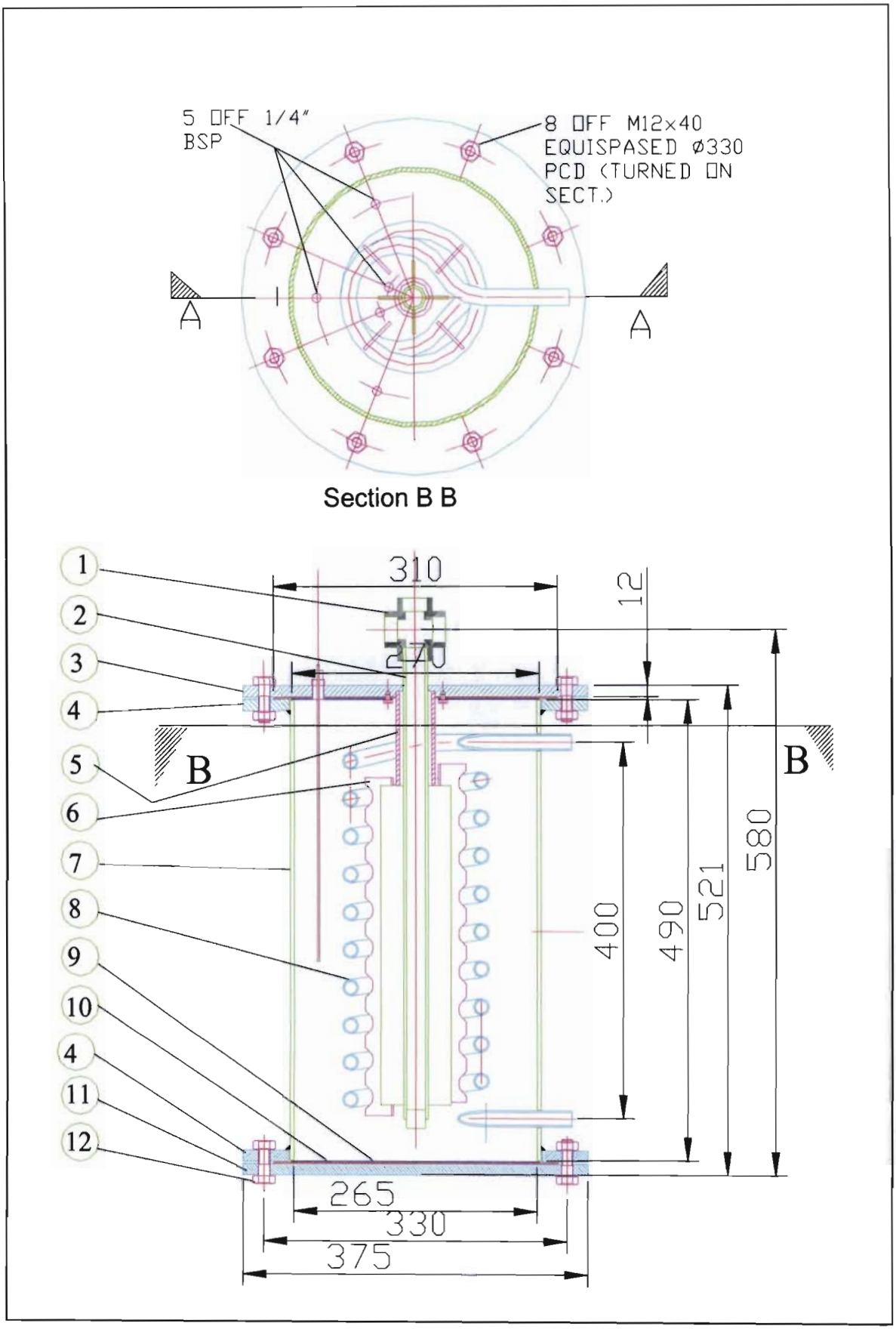

Figure D.2 Drawing Design of Second Heat Storage Calorimeter

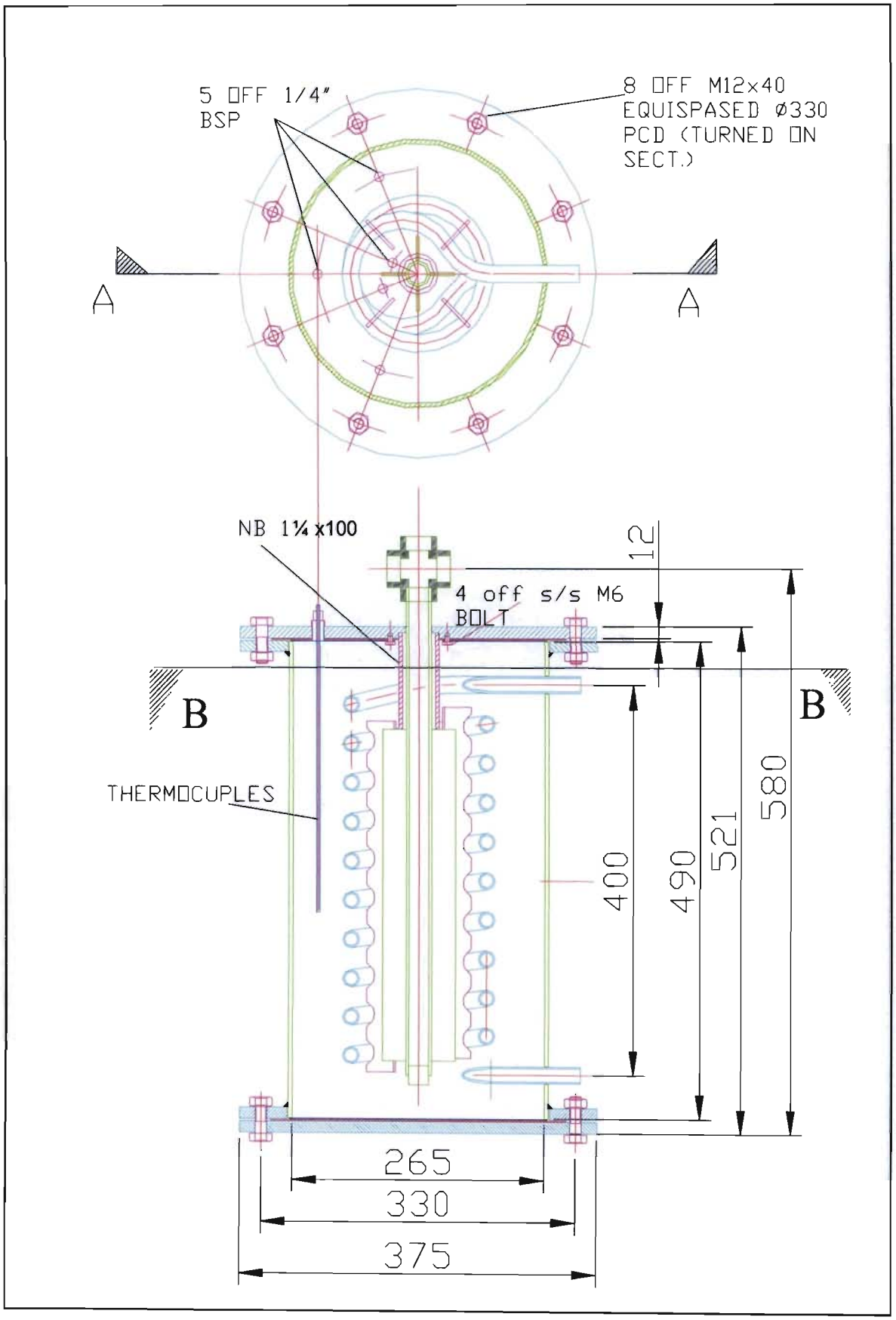

Figure D.3 Details Drawing Design of Second Heat Storage Calorimeter

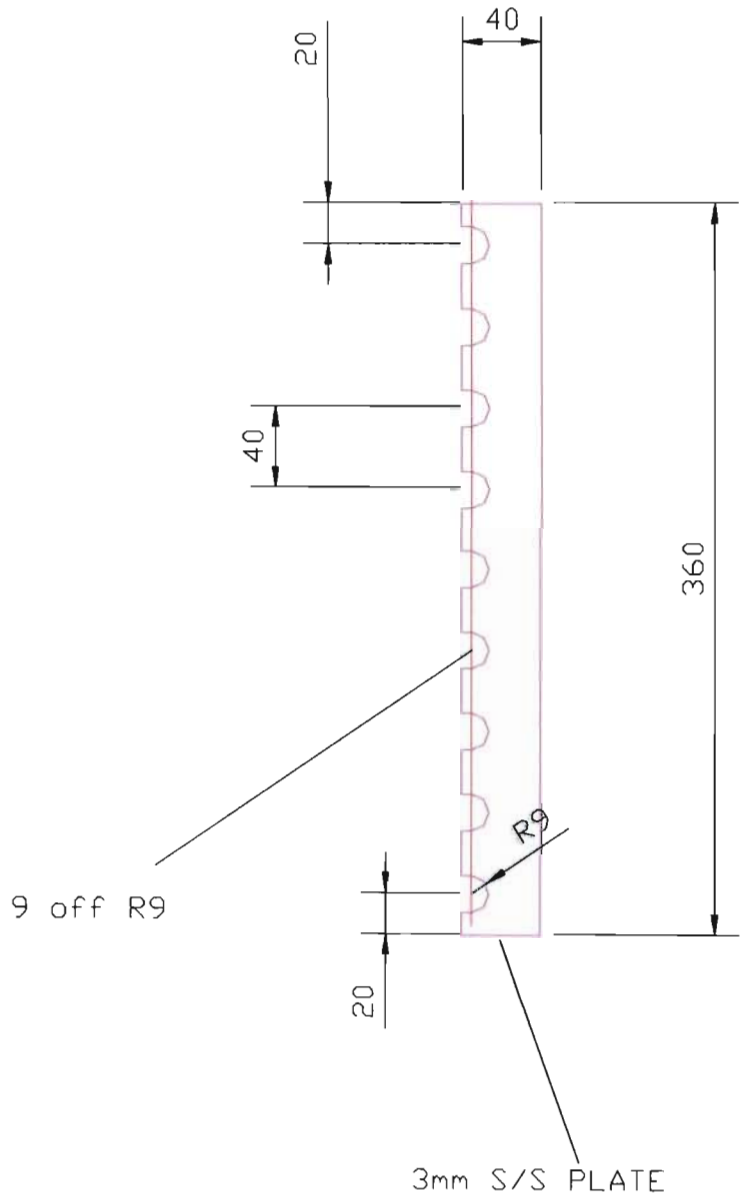

Figure D.4 Drawing Design of Heat Pipe Fins

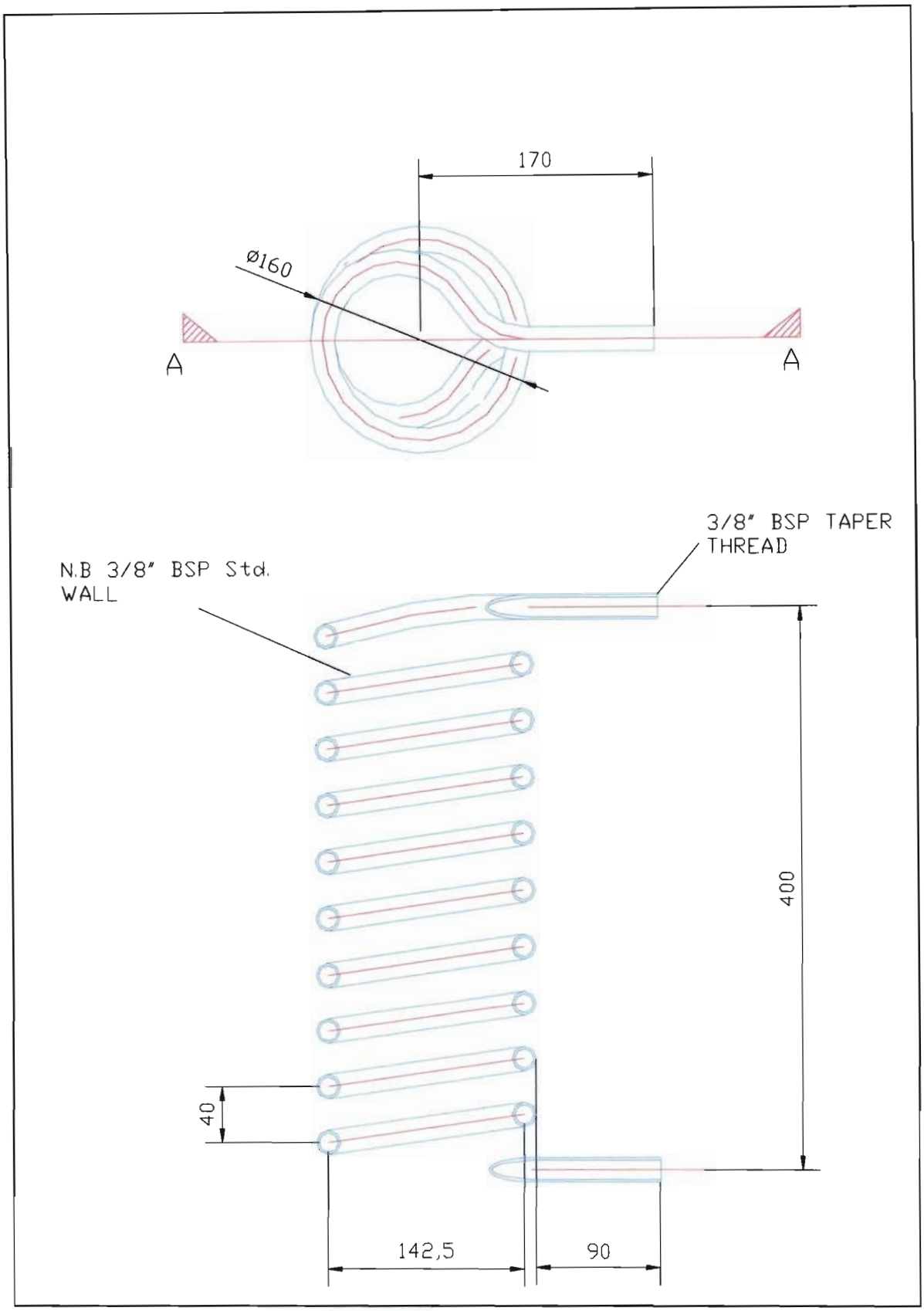

Figure D.5 Drawing Design of the Heat Transfer Coil Pipe

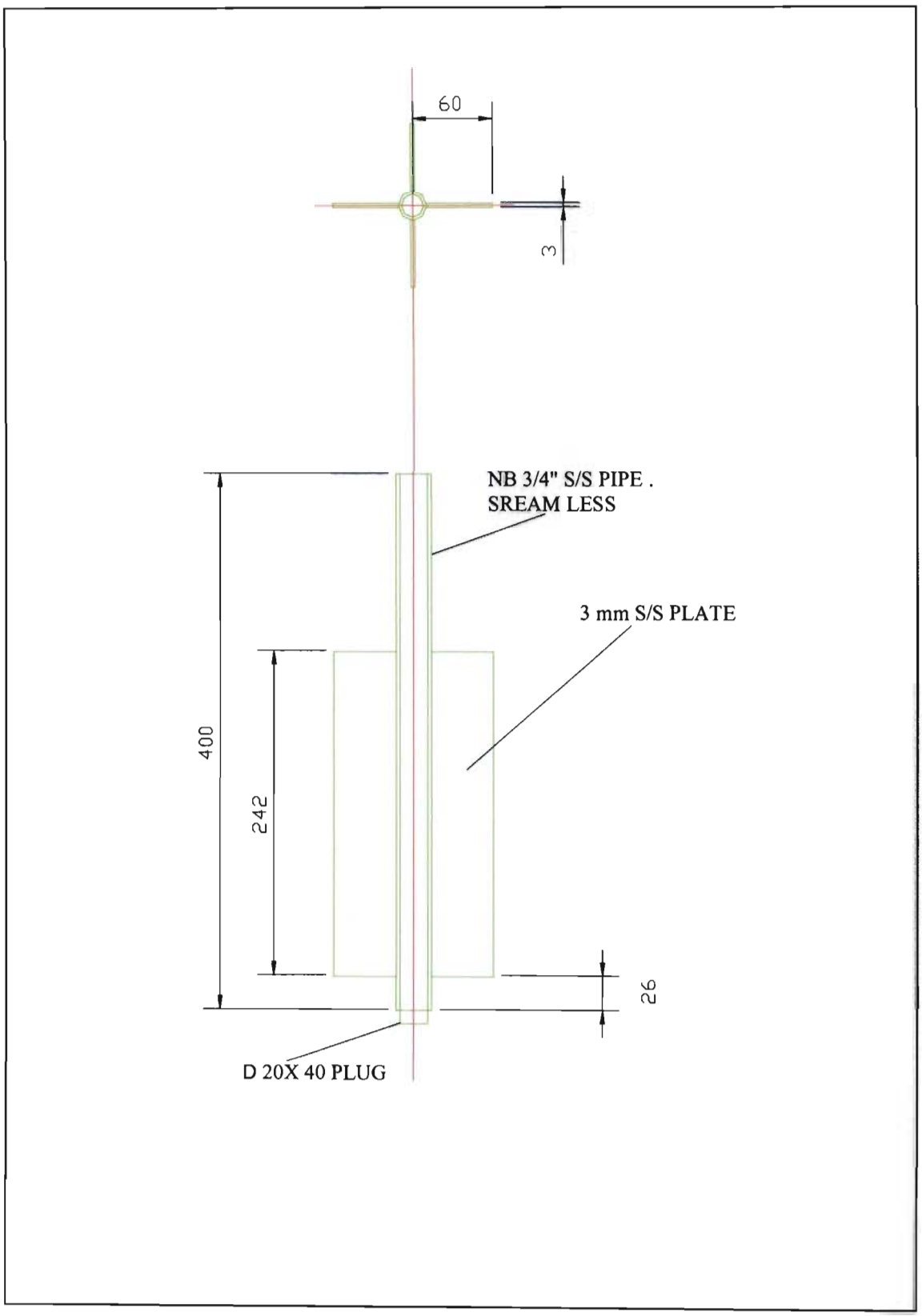

Figure D.6 Drawing Design of Fined Heat Transfer Pipes

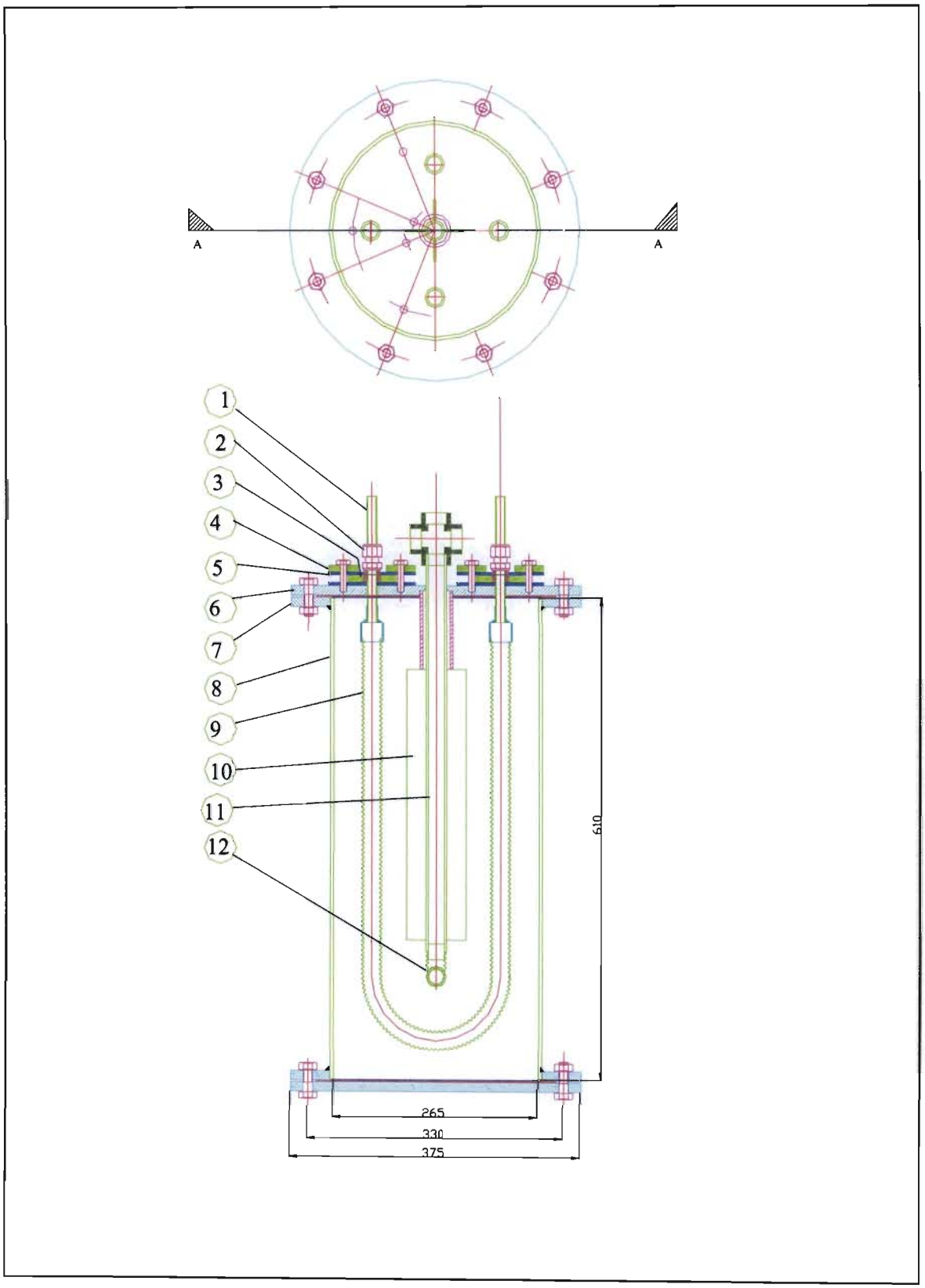

Figure D.7 Drawing Design the Electric Heat Storage Calorimeter

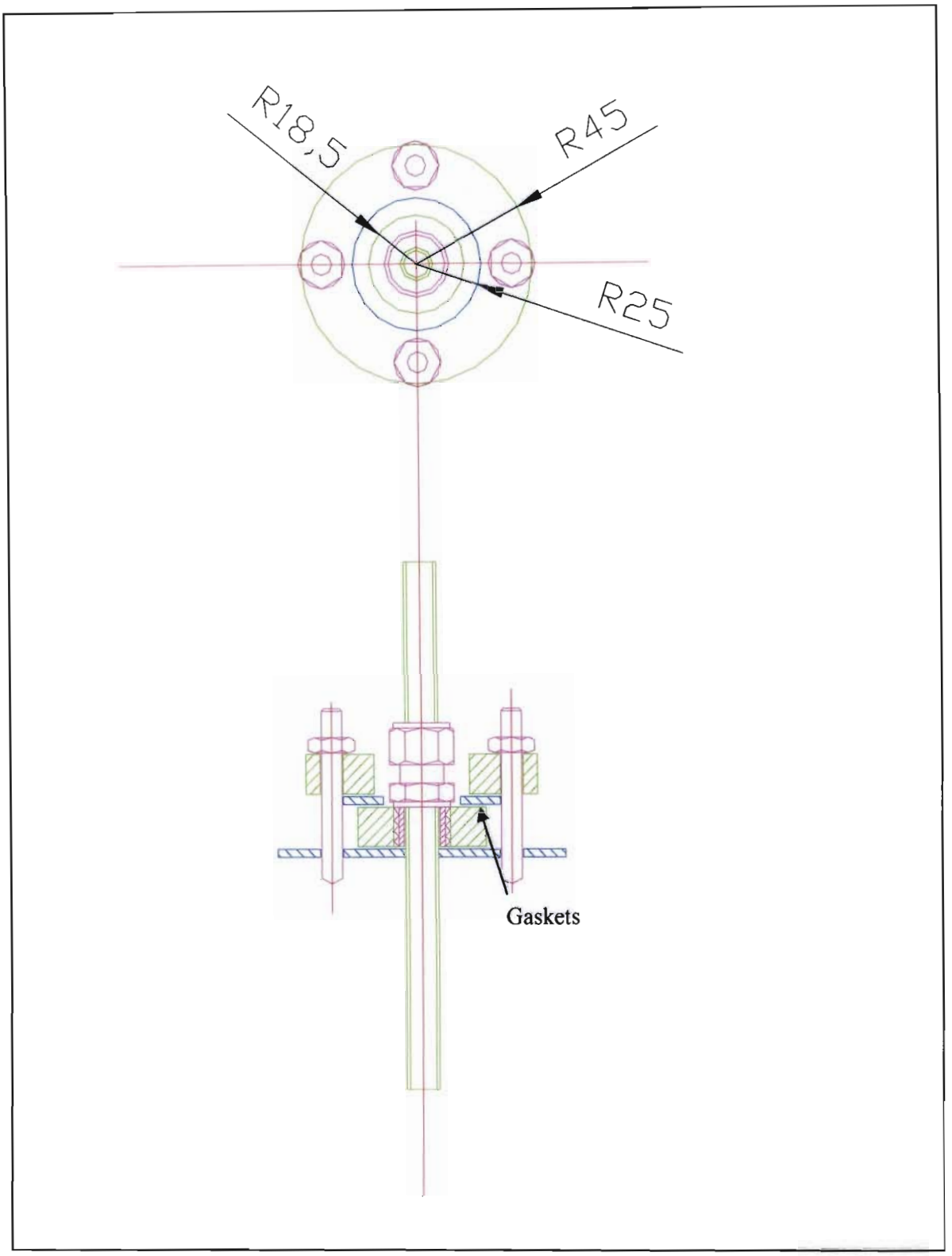

Figure D.8 Drawing Design of the Ends of Convoluted Heat Transfer Pipes

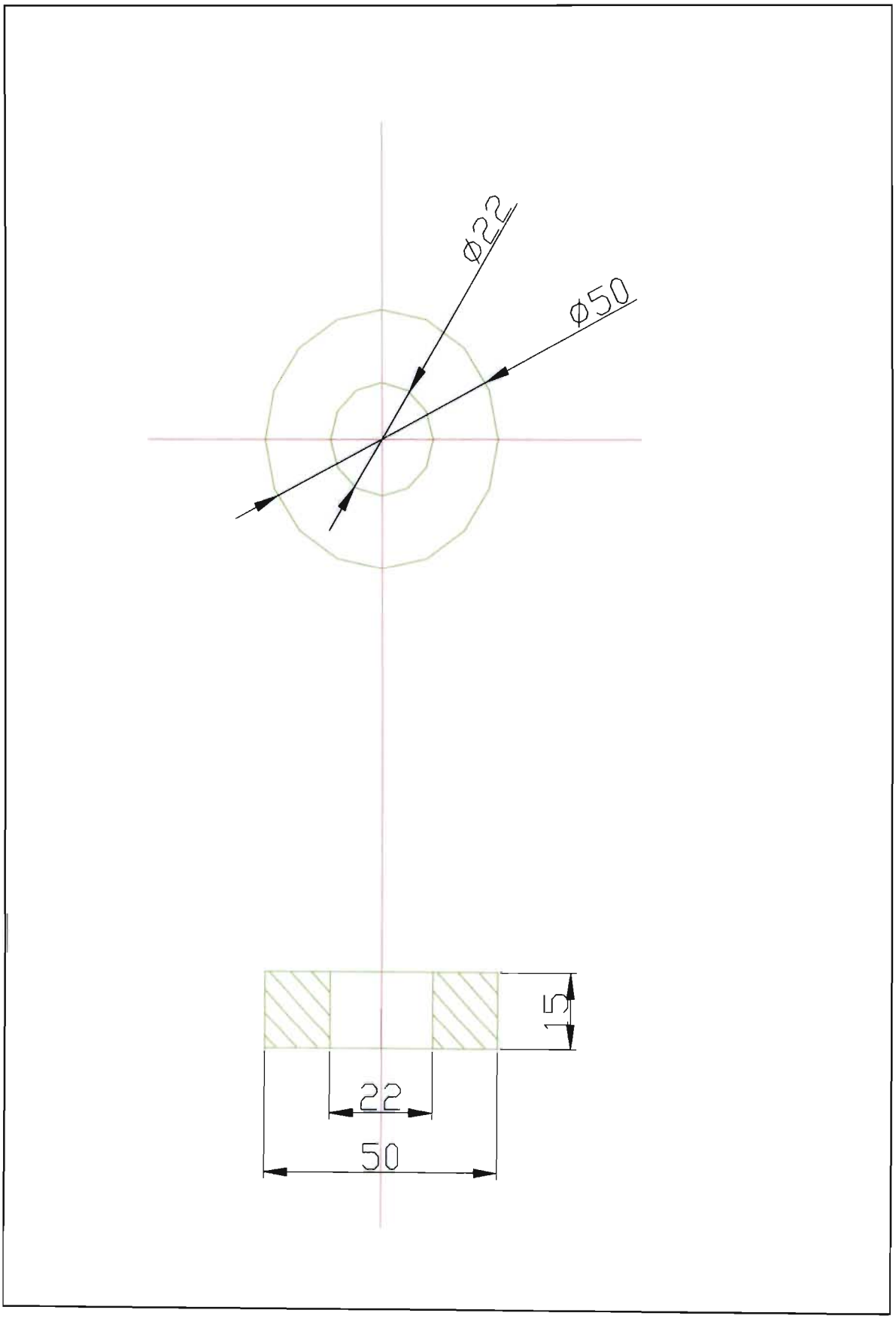

Figure D.9 Drawing Design of the Small Flanges of Convoluted Heat Transfer Pips

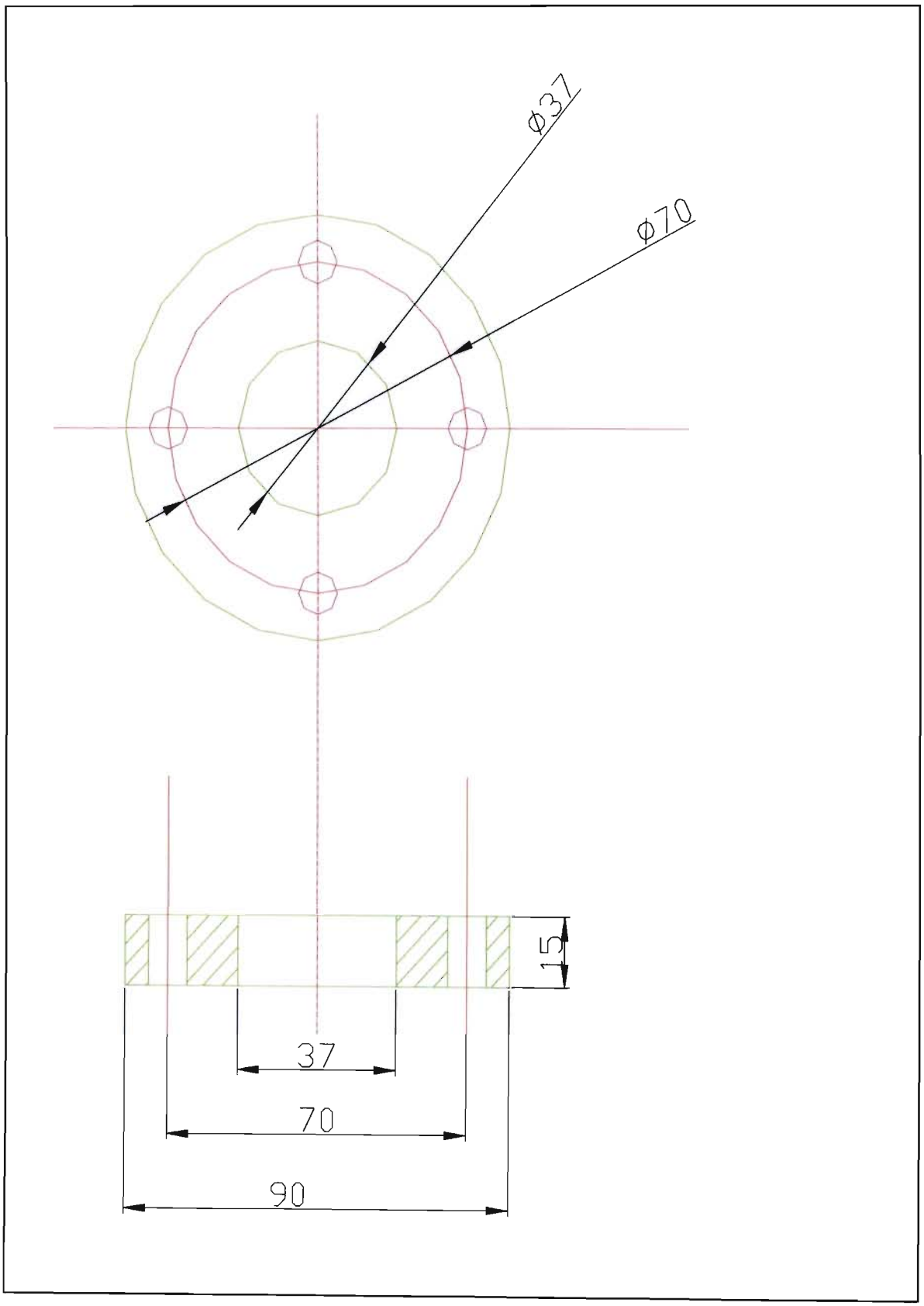

Figure D.10 Drawing Design of the Flanges of Convoluted Heat Transfer Pips

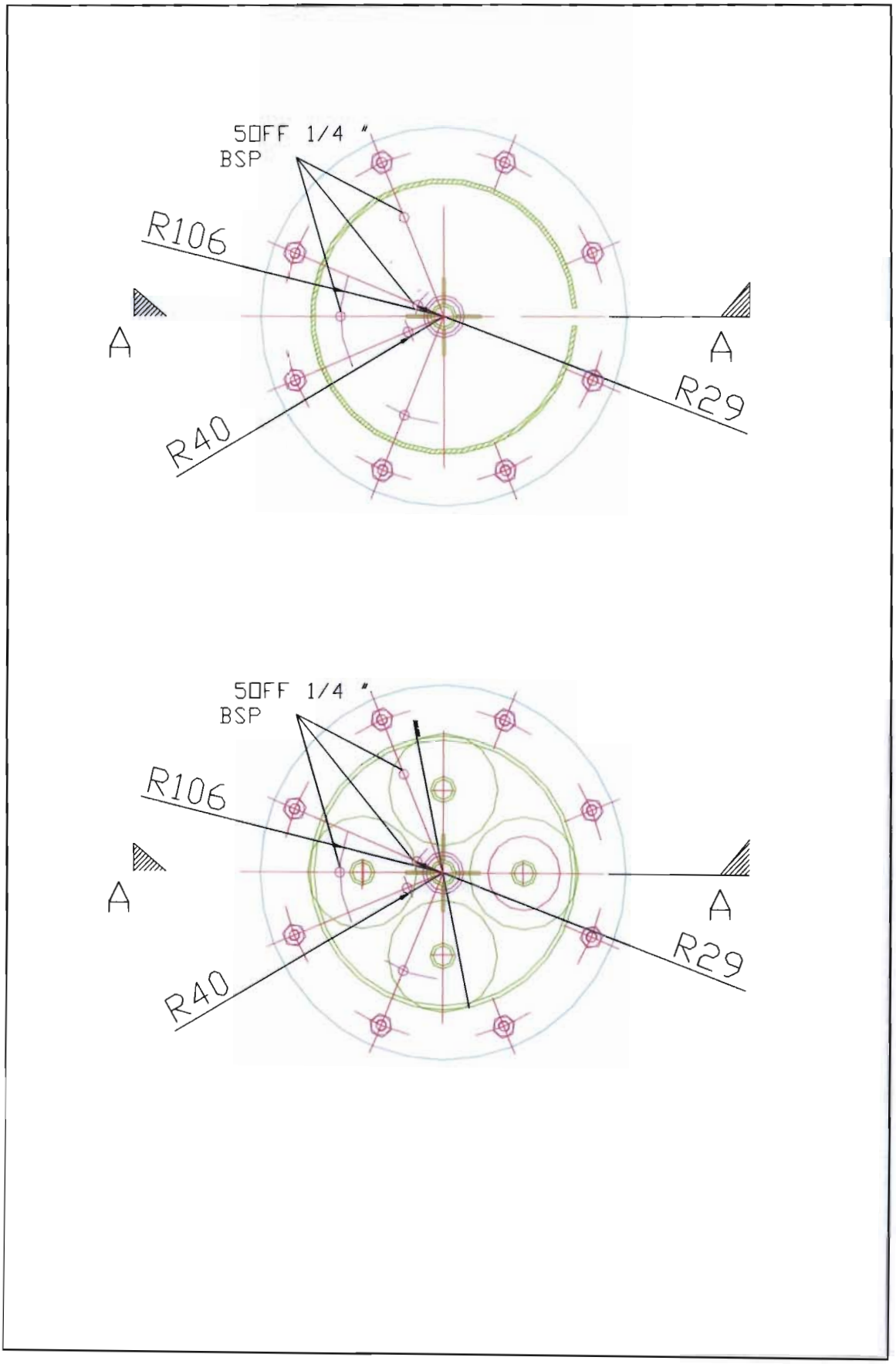

Figure D.11 Drawing Design of the Bottom and Top Flanges of the Electric Heat Storage Tank

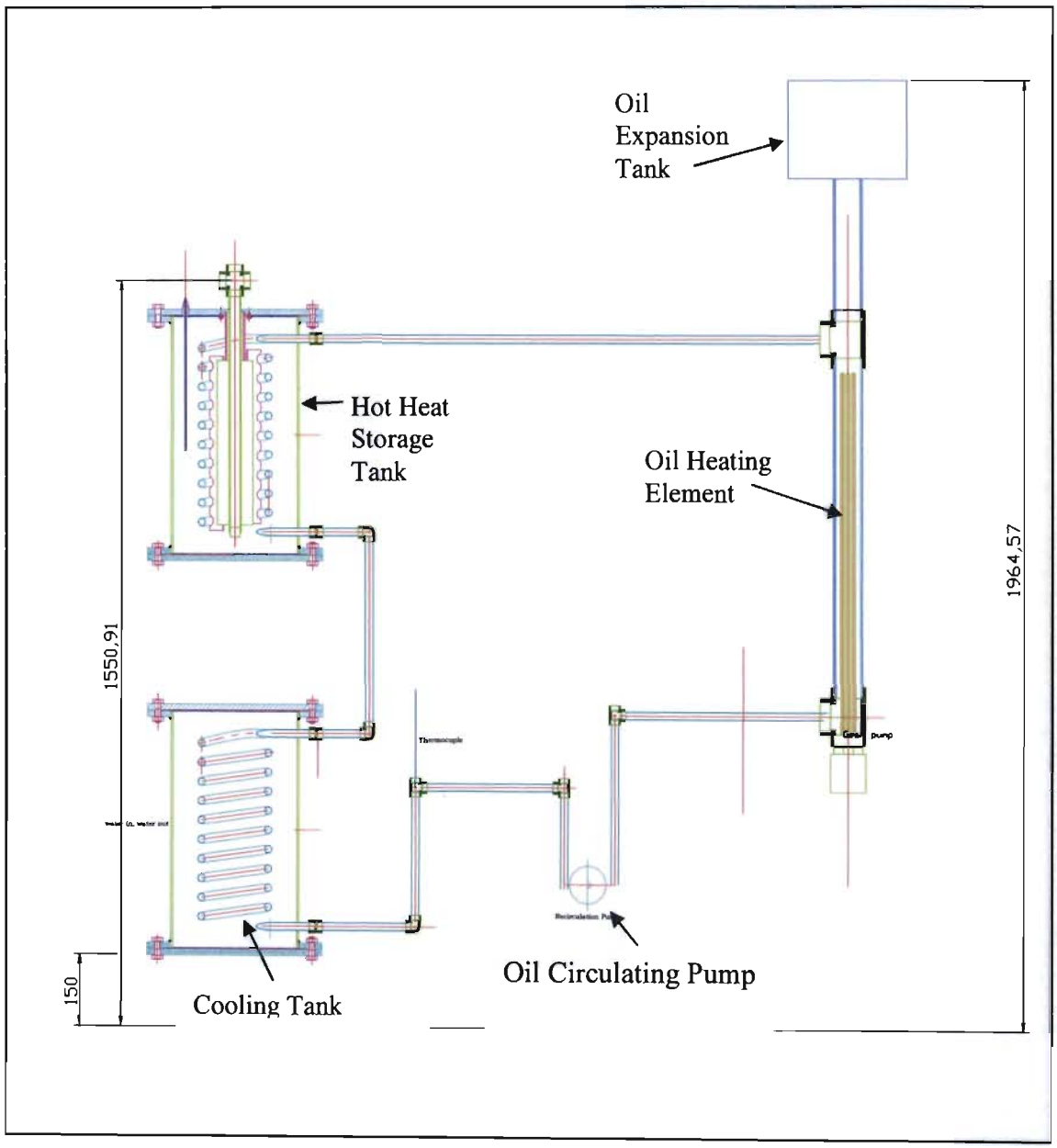

Figure D.12 Drawing Design of the Oil Heat Storage Tank

APPENDIX T

TABLES

Table T.1 Commercially Available Phase Change Materials [24]

PCM	Melting Point °C	Heat of fusion, cal/g	Density, liquid, g/cm^3
Coolness storage			
Na_2S0_4 . $10H_2O$ - NH_4Cl-KCl	8	29	1.49 gel
PE Glycol	11	24	1.12
$CaCl_rCaBr_2$-$6H_20$-KBr	12	32	1.78 gel
Heat buffers and sinks			
$CaCl_2$-$CaBr_2$-$6H_20$	15-34	34	1.78 gel
Na_2S0_4 - $10H_2O$-NaCl	18	35	1.48 gel
$CaCl_2$ - $6H_20$	27	46	1.56
Moderate temperature			
Na_2S0_4 - $10H_2O$	32	60	1.48 solid
$CaBr_2$. $6H_20$	34		1.96
Neopentyl glycol	43	31	
$Na_2S_20_3$. $5H_20$	48	48	1.67
Paraffin wax	50	64	0.76
Intermediate temperature			
$MgCl_2$-$Mg(N0_3)_2$-$6H_20$	58	32	1.52
$NaC0_2CH_3$. $3H_20$	58	54	1.28
$Na_4P_20_7$ - $10H_2O$	70	44	1.80 gel
$Mg(N0_3)_2$ - $6H_20$	89	39	1.55
$NH_4A1(S0_4)_2$ - $12H_20$	95	64	1.65 solid
High temperature			
$MgCl_2$. $6H_20$	114	40	1.45
Polyethylene	132	48	0.96 solid

Conversion factor: 1 cal/g = 4.181 kJ/kg.

Table T.2 Commercial PCMs available in the market [20]

PCM name	Type of product	Melting temperature (°C)	Heat of fusion (kJ/kg)	Density (kg/m^3)	Source
SN33	Salt solution	-33	245	1.24	Cristopia [41]
TH-31	n.a.	-31	131	n.a.	TEAP [42]
SN29	Salt solution	-29	233	1.15	Cristopia [41]
SN26	Salt solution	-26	268	1.21	Cristopia [41]
TH-21	n.a.	-21	222	n.a.	TEAP [42]
SN21	Salt solution	-21	240	1.12	Cristopia [41]
STL-21	Salt solution	-21	240	1.12	Mitsubishi Chemical
SN18	Salt solution	-18	268	1.21	Cristopia [41]
TH-16	n.a.	-16	289	n.a.	TEAP [42]
STL-16	n.a.	-16	n.a.	n.a.	Mitsubishi Chemical
SN15	Salt solution	-15	311	1.02	Cristopia [41]
SN12	Salt solution	-12	306	1.06	Cristopia [41]
STLN10	Salt solution	-11	271	1.05	Mitsubishi Chemical
SNIO	Salt solution	-11	310	1.11	Cristopia [41]
TH-10	n.a.	-10	283	n.a.	TEAP [42]
STL-6	Salt solution	-6	284	1.07	Mitsubishi Chemical
SN06	Salt solution	-6	284	1.07	Cristopia [41]
TH-4	n.a.	-4	286	n.a.	TEAP [42]
STL-3	Saltsolution	-3	328	1.01	Mitsubishi Chemical
SN03	Saltsolution	-3	328	1.01	Cristopia [41]
ClimSel C	n.a.	7	130	n.a.	Climator [44]
RT5	Paraffin	9	205	n.a.	Rubitherm GmbH
ClimSel C	n.a.	15	130	n.a.	Climator [44]
ClimSel C	Salt hydrate	23	148	1.48	Climator [44]
RT25	Paraffin	26	232		Rubitherm GmbH
STL27	Salt hydrate	27	213	1.09	Mitsubishi Chemical
S27	Salt hydrate	27	207	1.47	Cristopia [41]
RT30	Paraffin	28	206	n.a.	Rubitherm GmbH
TH29	Salt hydrate	29	188	n.a.	TEAP [42]
ClimSel C	Salt hydrate	32	212	1.45	Climator [44]
RT40	Paraffin	43	181	n.a.	Rubitherm GmbH
STL47	Salt hydrate	47	221	1.34	Mitsubishi Chemical
ClimSel C	n.a.	48	227	1.36	Climator [44]
STL52	Salt hydrate	52	201	1.3	Mitsubishi Chemical
RT50	Paraffin	54	195	n.a.	Rubitherm GmbH
STL55	Salt hydrate	55	242	1.29	Mitsubishi Chemical
TH58	n.a.	58	226	n.a.	TEAP [42]
ClimSel C	n.a.	58	259	1.46	Climator [44]
RT65	Paraffin	64	207		Rubitherm GmbH
ClimSel C	n.a.	70	194	1.7	Climator [44]
PCM72	Salt hydrate	72	n.a.	n.a.	Merck KgaA [6]
RT80	Paraffin	79	209	n.a.	Rubitherm GmbH
TH89	n.a.	89	149	n.a.	TEAP [42]
RT90	Paraffin	90	197	n.a.	Rubitherm GmbH
RT110	Paraffin	112	213	n.a.	Rubitherm GmbH [45]

Table T.3 Inorganic substances with potential use as PCM [20]

Compound	Melting temperature (°C)	Heat of fusion (kJ/kg)	Thermal conductivity (W/mK)	Density (kg/m^3)
H_20	0 [1,5]	333 [1]	0.612 (liquid, 20° C)[l]	998 (liquid, 20 °C) [1]
		334 [5]	0.61 (30 °C) [5]	996 (30 °C) [5]
				917 (solid, 0 °C) [1]
$LiC10_3 \cdot 3H_20$	8.1 [6,7]	253 [6]	n.a.	1720 [6]
$ZnCl_2 \cdot 3H_26$	10 [8]	n.a.	n.a.	n.a.
$K_2HP0_4 \cdot 6H_20$	13 [8]	n.a.	n.a.	n.a.
$NaOH\text{-}3½H_20$	15 [8]	n.a.	n.a.	n.a.
	15.4 [7]			
$Na_2Cr0_4 \cdot 10H_2O$	18 [8]	n.a.	n.a.	n.a.
$KF\text{-}4H_20$	18.5 [1,6,7,9]	231 [1,6,9]	n.a.	1447 (liquid, 20 °C) [1]
				1455 (solid, 18 °C) [1]
				1480 [6]
$Mn(N0_3)_2 \cdot 6H_20$	25.8 [18]	125.9 [10]	n.a.	1738 (liquid, 20 °C) [10]
				1728 (liquid, 40 °C) [10]
				1795 (solid, 5 °C) [10]
$CaCl_2 \cdot 6H_20$	29 [4,11]	190.8 [4,11]	0.540 (liquid, 38.7 °C) [4,11]	1562 (liquid, 32 °C) [4,11]
	29.2 [7]	171 [1,9]	0.561 (liquid, 61.2 °C) [11]	1496 (liquid) [1]
	29.6 [6]	174.4 [12]	1.088 (solid, 23 °C) [4,11]	1802 (solid, 24 °C) [4,11]
	29.7 [1,9]	192 [6]		1710 (solid, 25 °C) [1]
	30 [8] 29-39 [12]			1634 [12] 1620 [6]
$LiN0_3 \cdot 3H_20$	30 [6]	296 [6]	n.a.	n.a.
$Na_2S0_4 \cdot 10H_2O$	32.4 [1,7,9]	254 [1,9]	0.544 [1]	1485 (solid) [1]
	32 [13] 31-32 [12]	251.1 [12]		1458 [12]
$Na_2C0_3 \cdot 10H_2O$	32-36 [12]	246.5 [12]	n.a.	1442 [12]
	33 [6,7]	247 [6]		
$CaBr_2 \cdot 6H_20$	34 [4,7,11]	115.5 [4,11]	n.a.	1956 (liquid, 35 °C) [4,11]
				2194 (solid, 24 °C) [4,11]
$Na_2HP0_4 \cdot 12H_20$	35.5 [8]	265 [12]	n.a.	1522 [12]
	36 [12]	280 [6]		
	35[6,9]	281 [9]		
	35.2 [7]			
$Zn(N0_3)_2 \cdot 6H_20$	36 [4,7,11]	146.9 [4,11]	0.464 (liquid, 39.9 °C) [4,11]	1828 (liquid, 36 °C) [4,11]
	36.4 [1,9]	147 [1,9]	0.469 (liquid, 61.2 °C) [7]	1937 (solid, 24 °C) [4,11]
				2065 (solid, 14 °C) [1]
$KF \cdot 2H_20$	41.4 [7]	n.a.	n.a.	n.a.
$(CH_3COO)½H_20$	42 [8]	n.a.	n.a.	n.a.
$K_3P0_4 \cdot 7H_20$	45 [8]	n.a.	n.a.	n.a.
$Zn(N0_3)_2 \cdot 4H_20$	45.5 [8]	n.a.	n.a.	n.a.
$Ca(NO_s)_2 \cdot 4H_20$	42.7[7]	n.a.	n.a.	n.a.
	47 [8]			
$Na_2HPQ_4 \cdot 7H_20$	48 [7]	n.a.	n.a.	n.a.

(continued on next page)

Table T.3 (*continued*)

Compound	Melting temperature (°C)	Heat of fusion (kJ/kg)	Thermal conductivity (W/mK)	Density (kg/m^3)
$Na_2S_2O_3 \cdot 5H_2O$	48 [1,6-8]	201 [1]	n.a.	1600 (solid) [1]
	48-49 [12]	209.3 [12] 187 [6]		1666 [12]
$Zn(NO_3)_2 \cdot 2H_2O$	54 [8]	n.a.	n.a.	n.a.
$NaOH \cdot H_2O$	58.0 [7]	n.a.	n.a.	n.a.
$Na(CH_3COO) \cdot 3H_2O$	58 [6,13] 58.4 [7,14-	264 [14-20] 226 [6]	n.a.	1450 [6]
$Cd(NO_3)_2 \cdot 4H_2O$	59.5 [7]	n.a.	n.a.	n.a.
$Fe(NO_3)_2 \cdot 6H_2O$	60 [8]	n.a.	n.a.	n.a.
NaOH	64.3 [6]	227.6 [6]	n.a.	1690 [6]
$Na_2B_4O_7$ - $10H_2O$	68.1 [7]	n.a.	n.a.	n.a.
$Na_3PO_4 \cdot 12H_2b$	69 [7]	n.a.	n.a.	n.a.
$Na_2P_2O_7 \cdot 10H_2O$	70 [6]	184 [6]		n.a.
$Ba(OH)_2 \cdot 8H_2O$	78 [1,4,6,7,11,13]	265.7 [4,11] 267 [1] 280 [6]	0.653 (liquid, [4,11] 85.7°C) 0.678 (liquid, [11] 98.2°C) 1.255 (solid, 23°C) [4,11]	1937 (liquid, 84°C) [4,11]2070 (solid, 24°C) [4,6,11]2180 (solid) [1]
$AlK(SO_4)_2 \cdot 12H_2O$	80 [8]	n.a.	n.a.	n.a.
$KAl(SO_4)_2 \cdot 12H_2O$	85.8 [7]	n.a.	n.a.	n.a.
$Al_2(SO_4)_3 \cdot 18H_2O$	88 [7]	n.a.	n.a.	n.a.
$Al(NO_3)_3 \cdot 8H_2O$	89 [8]	n.a.	n.a.	n.a.
$Mg(NO_3)_2 \cdot 6H_2O$	89 [4,6,11]	162.8 [4,11]	0.490 (liquid, [4,11] 95 °C	1550 (liquid, 94°C) [4,11]
	90 [7,8]	149.5 [6]	0.502 (liquid, [11] 11 0°	1636 (solid, 25°C) [4,11]
			0.611 (solid, 37°C) [4,11] 0.669 (solid, 55.6°C) [11]	1640 [6]
$(NH_4)Al(SO_4) \cdot 6H_2O$	95 [6,8]	269 [6]	n.a.	n.a.
Na_2S-5±H_2O	97.5 [8]	n.a.	n.a.	n.a.
$CaBr_2 \cdot 4H_2O$	110 [8]	n.a.	n.a.	n.a.
$Al_2(SO_4)_3 \cdot 16H_2O$	112 [8]	n.a.	n.a.	n.a.
$MgCl_2 \cdot 6H_2O$	117 [4,6,7,11]	168.6 [4,11]	0.570 (liquid, [4,11] 12 0°	1450 (liquid, 120°C) [4,11]
	115 [8]	165 [1,6]	0.598 (liquid, [11] 14 0	1442 (liquid, 78°C) [1]
	116 [1]		0.694 (solid, 90 °C) [4,11]	1569 (solid, 20°C)
			0.704 (solid, 1 11	1570 (solid, 20°C) [1]
$Mg(NO_3) \cdot 2H_2O$	130 [8]	n.a.	n.a.	n.a.
$NaNO_3$	307 [21]	172 [21]	0.5 [22]	2260 [21]
	308 [22,23]	174 [23] 199 [22]		2257 [22]
KNO_3	333 [22]	266 [22] 116 [23]	0.5 [23]	2.110 [23]
KOH	380 [22]	149.7 [22]	0.5 [22]	2.044 [22]
$MgCl_2$	714 [21]	452 [21]	n.a.	2140 [21]
NaCl	800 [21]	492 [21] 466.7 [22]	5 [22]	2160 [21,22]
Na_2CO_3 KF K_2CO_3	854 [22] 857 [21] 897 [22]	275.7[22] 452 [21] 235.8[22]	2[22] na 2 [22]	2.533 [22] 2370 [21] 2.290 [22]

n.a.: not available.

Table T.4 List of Organic PCMs [100]

Material	Melting Point (°C)	Latent Heat (kJ/ kg)	Material	Melting Point (°C)	Latent Heat (kJ/ kg)
N-Tetradecane	5.5	226	N-Pentacosane	53.7	164
Formic acid	7.8	247	Myristic acid	54.0	199
N-Pentadecane	10.0	205	Oxolate	54.3	178
Acetic acid	16.7	273	Tristearin	54.5	191
N-Hexadecane	16.7	237	O-Xylene dichloride	55.0	121
Caprilone	40.0	260	ß Chloroacetic acid	56.0	147
Docasyle bromide	40.0	201	N-Hexacosane	56.3	255
N-Henicosane	40.5	161	Nitro naphthalene	56.7	103
Phenol	41.0	120	a Chloroacetic acid	61.2	130
N-Lauric acid	43.0	183	N-Octacosane	61.4	134
P-Joluidine	43.3	167	Palmitic acid	61.8	164
Cynamide	44.0	209	Bees wax	61.8	177
N-Docosane	44.5	157	Glyolic acid	63.0	109
N-Tricosane	47.6	130	P-Bromophenol	63.5	86
Hydrocinnamic acid	48.0	118	Azobenzene	67.1	121
Cetyl alcohol	49.3	141	Acrylic Acid	68.0	115
O-Nitroaniline	50.0	93	Dintro toluene (2,4)	70.0	111
Camphene	50.0	239	Phenylacetic acid	76.7	102
Diphenyl amine	52.9	107	Thiosinamine	77.0	140
P-Dichlorobenzene	53.1	121	Benzylamine	78.0	174

Hale et al., 1971; Lane, 1983; Garg et al., 1985; Buddhi, 1994; Sharma, 1999; Gustafsson et al., 1998; Zalba et al., 2003; Farid et al., 2004.

Table T.5 List of Inorganic PCMs [26].

Name	Melting Point (°C)	Latent Heat (kJ/kg)	Name	Melting Point (°C)	Latent Heat (kJ/kg)
H_2O	0.0	333	BI_3	31.8	10
$POCl_3$	1.0	85	$SO_3(ß)$	32.3	151
D_2O	3.7	318	$TiBr_4$	38.2	23
$SbCl_5$	4.0	33	$H_4P_2O_6$	55.0	213
H_2SO_4	10.4	100	SO_3 (γ)	62.1	331
IC l (ß)	13.9	56	$SbCl_3$	73.4	25
MOF_6	17.0	50	$NaNO_3$	307	199
SO3(a)	17.0	108	KNO_3	380	266
IC l (a)	17.2	69	KOH	380	149
P_4O_6	23.7	64	$MgCl_2$	800	492
H_3PO_4	26.0	147	NaCl	802	492
Cs	28.3	15	Na_2CO_3	854	275
Ga	30.0	80	KF	857	452
$AsBr_3$	30.0	38	K_2CO_3	897	235
$SnBr_4$	30.0	28			

Lane, 1983; Abhat, 1983; Garg et al., 1985; Buddhi, 1994; Hale et al., 1971; Sharma, 1999.

Table T.6 Melting Point and Latent Heat of Fusion of Paraffins [26].

Name	No. of "C" Atoms	Melting Point (°C)	Density (kg/m^3)	Thermal Conductivity (W/mK)	Latent Heat (kJ/kg)
n - Dodecane	12	-12	750	0.21^S	n.a.
n - Tridecane	13	-6	756		n.a.
n - Tetradecane	14	4.5–5.6	771		231
n - Pentadecane	15	10	768	0.17	207
n - Hexadecane	16	18.2	774	0.21^S	238
n - Heptadecane	17	22	778		215
n - Octadecane	18	28.2	814^S [14], 775^L [14]	0.35^S [14], 0.149^L[14]	245
n - Nonadecane	19	31.9	912^S, 769^L	0.21^S	222
n - Eicosane	20	37			247
n - Heneicosane	21	41			215
n - Docosane	22	44			249
n - Tricosane	23	47			234
n - Tetracosane	24	51			255
n - Pentacosane	25	54			238
Paraffin wax	n.a.	32	785^S [15], 749^L [15]	0.514^S [15], 0.224^L [15]	251[15]
n - Hexacosane	26	56	770	0.21^S	257
n - Heptacosane	27	59	773		236
n - Octacosane	28	61	910^S, 765^L		255
n - Nonacosane	29	64			240
n - Triacontane	30	65			252
n - Hentriacontane	31	n.a.	930^S, 830^L		n.a.
n - Dotricontane	32	70			n.a.
n - Tritricontane	33	71			189

S: solid; L: liquid; n.a.: not available.
Lane, 1983; Abhat, 1983; Garg et al., 1985; Buddhi, 1994; Hale et al., 1971; Sharma, 1999.

Table T.7 Melting Point and Latent Heat of Fusion of Non – paraffin [26].

Name	Melting Point (°C)	Density (kg/m^3)	Latent Heat (kJ/ kg)
Formic acid	7.8	1226.7^{15C}	247
Acetic acid	16.7	1050^{20C}	187
Glycerin	17.9	1260^{20C}	198.7
Lithium chloride ethanolate	21	n.a.	188
Polyethylene glycol 600	20–25	1100^{20C}	146
D – Lattic acid	26	1249^{15C}	184
1-3 Methyl pentacosane	29	n.a.	197
Camphenilone	39	n.a.	205
Docasyl bromide	40	n.a.	201
Caprylone	40	n.a.	259
Heptadecanone	41	n.a.	201
1-Cyclohexylooctadecane	41	n.a.	218
4-Heptadacanone	41	n.a.	197
Cyanamide	44	1080^{20C}	209
Methyl eicosanate	45	851^{79C}	230
3-Heptadecanone	48	n.a.	218
2-Heptadecanone	48	n.a.	218
Camphene	50	842^{54C}	238
9-Heptadecanone	51	n.a.	213
Methyl behenate	52	n.a.	234
Pentadecanoic acid	52.5	n.a.	178
Hypophosphoric acid	55	n.a.	213
Chloroacetic acid	56	1580^{20C}	130
Trimyristin	33–57	862^{20C}	201–213
Heptaudecanoic acid	60.6	n.a.	189
Bee wax	61.8	950	177
Glycolic acid	63	n.a.	109
Oxazoline wax-TS 970	74	n.a.	
Arachic acid	76.5	n.a.	227
Bromcamphor	77	1449^{81C}	174
Durene	79.3	838^{20C}	156
Acetamide	81	1159	241
Methyl brombrenzoate	81	n.a.	126
Alpha napthol	96	$1095^{98.7C}$	163
Glautaric acid	97.5	1429	156
p-Xylene dichloride	100	n.a.	138.7
Methyl Fumarate	102	1045	242
Catechol	104.3	1370^{15C}	207
Quinone	115	1318^{20C}	171
Acetanilide	115	1210^{4C}	142
Succinic anhydride	119	1104	204
Benzoic acid	121.7	1266^{15C}	142.8
Stibene	124	1164^{15C}	167
Benzamide	127.2	1341	169.4
Phenacetin	137	n.a.	136.7
Alpha glucose	141	1544	174
Acetyl – p- toluidene	146	n.a.	180
Phenylhdrazone benzaldehyide	155	n.a.	134.8
Salicylic acid	159	1443^{20C}	199
Benzanilide	161	n.a.	162
O-Mannitol	166	1489^{20C}	294
Hydroquinone	172.4	1358^{20C}	258
p-Aminobenzoic acid	187	n.a.	153

Lane, 1983; Abhat, 1983; Garg et al., 1985; Buddhi, 1994; Hale et al., 1971; Sharma, 1999.

Table T.8 Melting Point and Latent Heat of Fusion of Fatty Acids [26].

Name	Melting Point (°C)	Density (kg/m^3)	Thermal Conductivity (W/mK)	Latent Heat (kJ/kg)
Propyl palmiate	10	n.a.	n.a.	186
Isopropyl palmiate	11	n.a.	n.a.	100
Oleic acid	13.5–16.3	863^{60C}	n.a.	n.a.
Isopropyl stearate	14–19	n.a.	n.a.	140–142
Caprylic acid	16	901^{30C}	0.149^{39C}	148
	16.3	862^{80C} 981^{13C} 1033^{10C}	0.145$^{67.7C}$, 0.148^{20C}	149
Butyl stearate	19	n.a.	n.a.	140 123–200
Dimethyl sabacate	21	n.a.	n.a.	120–135
Vinyl stearate	27–29	n.a.	n.a.	122
Methyl palmitate	29	n.a.	n.a.	205
Capric acid	32	878^{45C}	0.153$^{38.5C}$	152.7
	31.5	886^{40C}, 1004^{24C}	0.152$^{55.5C}$, 0.149^{40C}	153
Erucic acid	33	853^{70C}	n.a.	n.a.
Methyl-12-hydroxy-stearate	42–43	n.a.	n.a.	120–126
Lauric acid	42–44	862^{60C}, 1007^{24C}	n.a.	178
Elaidic acid	47	851^{79C}	n.a.	218
Pelargoinc acid	48	n.a.	n.a.	n.a.
Myristic acid	49–51	861^{55C}	n.a.	205
	54	844^{80C}		187
Palmitic acid	64	850^{65C}	0.162$^{68.4C}$	185.4
	61	847^{80C}	0.159$^{80.1C}$	203.4
Stearic acid	69	848^{70C}	0.172^{70C}	202.5
	60–61	965^{24C}		186.5
Valporic acid	120	n.a.	n.a.	n.a.

Lane, 1983; Abhat, 1983; Garg et al., 1985; Buddhi, 1994; Hale et al., 1971; Sharma, 1999.

Table T.9 Melting Point and Latent Heat of Fusion of Salt Hydrates [26]

Name	Melting Point (°C)	Density (kg/m³)	Thermal Conductivity (W/m K)	Latent Heat (kJ/kg)	Melting Behavior[a] [13]
$LiClO_3.3H_2O$	8	n.a.	n.a.	253	c
$NH_4Cl.Na_2SO_4.10H_2O$	11	n.a.	n.a.	163	n.a.
$K_2HO_4.6H_2O$	14	n.a.	n.a.	108	c
$NaCl.Na_2SO_4.10H_2O$	18	n.a.	n.a.	286	n.a.
$KF.4H_2O$	18	n.a.	n.a.	330	c
$K_2HO_4.4H_2O$	18.5	1447^{20C}, 1455^{18C}, 1480^{6C}	n.a.	231	n.a.
$Mn(NO_3)_2.6H_2O$	25	1738^{20C}[12],	n.a.	148	n.a.
	25.8	1728^{40C}[12], 1795 [12]		125.9[12]	
$LiBO_2.8H_2O$	25.7	n.a.	n.a.	289	n.a.
$FeBr_3.6H_2O$	27	n.a.	n.a.	105	n.a.
$CaCl_2.6H_2O$	29–30	1562^{32C}, 1802^{24C}	$0.561^{61.2C}$, 1.008^{23C}	170–192	ic
$LiNO_3.3H_2O$	30	n.a.	n.a.	189–296	c
$Na_2SO_4.10H_2O$	32	1485^{24C}	0.544	251–254	ic
$Na_2CO_3.10H_2O$	33–36	1442	n.a.	247	ic
$KFe(SO_4)_2.12H_2O$	33	n.a.	n.a.	173	ic
$CaBr_2.6H_2O$	34	1956^{35C}, 2194^{24C}	n.a.	115–138	n.a.
$LiBr.2H_2O$	34	n.a.	n.a.	124	ic
$Na_2HPO_4.12H_2O$	35	1522	n.a.	256–281	ic
$Zn(NO_3)_2.6H_2O$	36	1828^{36C}, 1937^{24C}, 2065^{14C}	$0.464^{39.9C}$, $0.469^{61.2C}$	134–147	c
$Mn(NO_3)_2.4H_2O$	37	n.a.	n.a.	115	n.a.
$FeCl_3.6H_2O$	37	n.a.	n.a.	223	c
$CaCl_2.4H_2O$	39	n.a.	n.a.	158	ic
$CoSO_4.7H_2O$	40.7	n.a.	n.a.	170	n.a.
$CuSO_4.7H_2O$	40.7	n.a.	n.a.	171	n.a.
$KF.2H_2O$	42	n.a.	n.a.	162–266	c
$MgI_2.8H_2O$	42	n.a.	n.a.	133	n.a.
$CaI_2.6H_2O$	42	n.a.	n.a.	162	n.a.
$Ca(NO_3)_2.4H_2O$	43–47	n.a.	n.a.	106–140	c
$Zn(NO_3)_2.4H_2O$	45	n.a.	n.a.	110	n.a.
$K_3PO_4.7H_2O$	45	n.a.	n.a.	145	n.a.
$Fe(NO_3)_3.9H_2O$	47	n.a.	n.a.	155–190	ic
$Mg(NO_3)_3.4H_2O$	47	n.a.	n.a.	142	n.a.
$Na_2SiO_3.5H_2O$	48	n.a.	n.a.	168	n.a.
$Na_2HPO_4.7H_2O$	48	n.a.	n.a.	135–170	ic
$Na_2S_2O_3.5H_2O$	48	1600	n.a.	209	n.a.
$K_2HPO_4.3H_2O$	48	n.a.	n.a.	99	n.a.
$MgSO_4.7H_2O$	48.4	n.a.	n.a.	202	n.a.
$Ca(NO_3)_2.3H_2O$	51	n.a.	n.a.	104	n.a.
$Na(NO_3)_2.6H_2O$	53	n.a.	n.a.	158	n.a.
$Zn(NO_3)_2.2H_2O$	55	n.a.	n.a.	68	c
$FeCl_3.2H_2O$	56	n.a.	n.a.	90	n.a.
$CO(NO_3)_2.6H_2O$	57	n.a.	n.a.	115	n.a.
$Ni(NO_3)_2.6H_2O$	57	n.a.	n.a.	168	n.a.
$MnCl_2.4H_2O$	58	n.a.	n.a.	151	n.a.

Table T.9 Continued

Name	Melting Point (°C)	Density (kg/m^3)	Thermal Conductivity (W/m K)	Latent Heat (kJ/kg)	Melting Behavior[a] [13]
$CH_3COONa.3H_2O$	58	n.a.	n.a.	270–290	ic
$LiC_2H_3O_2.2H_2O$	58	n.a.	n.a.	251–377	n.a.
$MgCl_2.4H_2O$	58.0	n.a.	n.a.	178	n.a.
$NaOH.H_2O$	58	n.a.	n.a.	272	n.a.
$Na(CH_3COO).3H_2O$	58	n.a.	n.a.	n.a.	n.a.
$Cd(NO_3)_2.4H_2O$	59	n.a.	n.a.	98	n.a.
$Cd(NO_3)_2.1H_2O$	59.5	n.a.	n.a.	107	n.a.
$Fe(NO_3)_2.6H_2O$	60	n.a.	n.a.	125	n.a.
$NaAl(SO_4)_2.12H_2O$	61	n.a.	n.a.	181	ic
$FeSO_4.7H_2O$	64	n.a.	n.a.	200	n.a.
$Na_3PO_4.12H_2O$	65	n.a.	n.a.	168	n.a.
$Na_2B_4O_7.10H_2O$	68	n.a.	n.a.	n.a.	n.a.
$Na_3PO_4.12H_20$	69	n.a.	n.a.	n.a.	n.a.
$LiCH_3COO.2H_2O$	70	n.a.	n.a.	150–251	c
$Na_2P_2O_7.10H_2O$	70	n.a.	n.a.	186–230	ic
$Al(NO_3)_2.9H_2O$	72	n.a.	n.a.	155–176	ic
$Ba(OH)_2.8H_2O$	78	1937^{84C}, 2070^{24C}, 2180	$0.653^{85.7C}$, $0.678^{98.2C}$, 1.255^{23C}	265–280	c
$Al_2(SO_4)_3.18H_2O$	88	n.a.	n.a.	218	ic
$Sr(OH)_2.8H_2O$	89	n.a.	n.a.	370	ic
$Mg(NO_3)_2.6H_2O$	89–90	1550^{94C}, 1636^{25C}	0.490^{95C}, 0.502^{110C}, 0.611^{37C}, $0.669^{55.6C}$	162–167	c
$KAl(SO_4)_2.12H_2O$	91	n.a.	n.a.	184	n.a.
$(NH_4)Al(SO_4).6H_2O$	95	n.a.	n.a.	269	n.a.
$Na_2S.51/2H_2O$	97.5	n.a.	n.a.	n.a.	n.a.
$LiCl.H_2O$	99	n.a.	n.a.	212	ic
$CaBr_2.4H_20$	110	n.a.	n.a.	n.a.	n.a.
$Al_2(SO_4)_2.16H_2O$	112	n.a.	n.a.	n.a.	n.a.
$MgCl_2.6H_2O$	115–117	1450^{120C}, 1442^{78C}, 1569^{20C}, 1570^{20C}	0.570^{120C}, 0.598^{140C}, 0.694^{90C}, 0.704^{110C}	165–169	n.a.
$NaC_2H_3O_2.3H_2O$	137	1450	n.a.	172	n.a.

n.a.: not available; c: congruent melting; ic: incongruent melting.
Lane, 1983; Abhat, 1983; Garg et al., 1985; Buddhi, 1994; Hale et al., 1971; Sharma, 1999.

Table T.10 List of Organic and Inorganic Eutectics [26].

Name	Composition (wt %)	Melting Point (°C)	Latent Heat (kJ/ kg)
Na_2SO_4+NaCl+KCl+H_2O	31+13+16+40	4	234
Na_2SO_4+NaCl+NH_4Cl+H_2O	32+14+12+42	11	n.a.
$C_5H_5C_6H_5$+ $(C_6H_5)_2O$	26.5+73.5	12	97.9
Na_2SO_4+NaCl+H_2O	37+17+46	18	n.a.
Na_2S_4+$MgSO_4$+H_2O	25+21+54	24	n.a.
$C_{14}H_{28}O_2$+$C_{10}H_{20}O_2$	34+66	24	147.7
$Ca(NO)_3.4H_2O$+$Mg(NO)_3.6H_2O$	47+53	30	136
NH_2CONH_2+NH_4 NO_3	–	46	95
$Mg(NO_3)_2.6H_2O$+NH_4 NO_3	61.5+38.4	52	125.5
$Mg(NO_3)_2.6H_2O$+$MgCl_2.6H_2O$	58.7+41.3	59	132.2
$Mg(NO_3)_2.6H_2O$+$Al(NO_3)_2.9H_2O$	53+47	61	148
$Mg(NO_3)_2.6H_2O$+$MgBr_2.6H_2O$	59+41	66	168
Napthalene + Benzoic Acid	67.1+32.9	67	123.4
$AlCl_3$+NaCl+$ZrCl_2$	79+17+4	68	234
$AlCl_3$+NaCl+KCl	66+20+14	70	209
NH_2CONH_2+NH_4Br	66.6+33.4	76	151
$LiNO_3$ + NH_4 NO_3+$NaNO_3$	25+65+10	80.5	113
$AlCl_3$+NaCl+KCl	60+26+14	93	213
$AlCl_3$+NaCl	66+34	93	201
$NaNO_2$+$NaNO_3$+KNO_3	40+7+53	142	n.a.

n.a.: not available. Lane, 1983; Abhat, 1983; Garg et al., 1985; Buddhi, 1994; Hale et al., 1971; Sharma, 1999.

Table T.11 Melting Point and Latent Heat of Fusion of Some Selected Solid - Solid PCMs [24]

Name	Melting Point (°C)	Latent Heat (kJ/kg)
38.2%NPG/61.8%PE	26–32	18–75
38.2%NPG/61.8%TAM	22–35	27–33
76.4%NPG/33.6%TAM	28–38	75–80
76.4%NPG/33.6%PE	31–37	35–46
91%NPG/9%PE	31–36	68
91%NPG/9%TAM	30–39	143–150
Neopentyl glycol (NPG)	43	130
Diamnopentacrythritol	68	184
2-Amino - 2 - methyl - 1, 3 - propanediol	78	264
2 - Methyl - 2 - mtro - 1, 3 - propanediol	79	201
Trumethylolethane	81	192
Pentaglycerin	81	192
2-Hydroxymethyl-2-methyl-1, 3 - propanediol	81	192
Monoaminopentaerythritol	86	192
Cross-linked polyethylene	110–115	125–146
Tris(Hydroxymethyl)acetic acid	124	205
2-Amino-2-hydroxymethyl-1, 3 - propanediol	131	285
Cross-linked HDPE	125–146	167–201
2,2-Bis(Hydroxymethyl) Propionic acid	152	289
38.2%NPG/61.8%PE	170	147
Penterythritol (PE)	185	303

Lane, 1983; Abhat, 1983; Garg et al., 1985; Buddhi, 1994; Hale et al., 1971; Sharma, 1999.

Table T.12 List of Commercially Available PCMs (0 °C–118 °C) [26]

Name	Melting Point (°C)	Latent Heat (kJ/kg)	Density (kg/m^3)	Manufacturer
TH 0	0	334	n.a.	TEAP (www.teappcm.com)
A 4	4	227	766	EPS Ltd. (www.epsltd.co.uk)
Witco 85010-1	4	129.6	n.a.	Witco
RT 2	6	156	860	Rubitherm (www.rubitherm.com)
TH 7	7	189	n.a.	TEAP (www.teappcm.com)
RT 5	7	156	860	Rubitherm (www.rubitherm.com)
E 7	7	120	1540	EPS Ltd. (www.epsltd.co.uk)
C 7	7	162	1420	Climator (www.climator.com)
RT 6	8	174	860	Rubitherm (www.rubitherm.com)
E 8	8	140	1470	EPS Ltd. (www.epsltd.co.uk)
A 8	8	220	770	EPS Ltd. (www.epsltd.co.uk)
E 10	10	140	1520	EPS Ltd. (www.epsltd.co.uk)
E 13	13	140	1780	EPS Ltd. (www.epsltd.co.uk)
C 15	15	130	n.a.	Climator (www.climator.com)
E 21	21	150	1480	EPS Ltd. (www.epsltd.co.uk)
RT 20	22	172	870	Rubitherm (www.rubitherm.com)
A 22	22	220	770	EPS Ltd. (www.epsltd.co.uk)
C 24	24	216	1480	Climator (www.climator.com)
RT 26	25	131	880	Rubitherm (www.rubitherm.com)
TH 25	25	159	n.a.	TEAP (www.teappcm.com)
Witco 45 A	26.3	167.2	n.a.	Witco
S 27	27	207	1470	Cristopia (www.cristopia.com)
STL 27	27	213	1090	Mitsubishi Chemical
RT 27	28	179	870	Rubitherm (www.rubitherm.com)
GR 27	28	72	750	Rubitherm (www.rubitherm.com)
PX 27	28	112	640	Rubitherm (www.rubitherm.com)
A 28	28	245	790	EPS Ltd. (www.epsltd.co.uk)
TH 29	29	188	1540	TEAP (www.teappcm.com)
E 30	30	201	1300	EPS Ltd. (www.epsltd.co.uk)
C 32	32	302	1450	Climator (www.climator.com)
E 32	32	186	1460	EPS Ltd. (www.epsltd.co.uk)
RT 35	35	157	880	Rubitherm (www.rubitherm.com)
RT 42	43	174	880	Rubitherm (www.rubitherm.com)
GR 41	43	63	750	Rubitherm (www.rubitherm.com)
FB 41	43	117	750	Rubitherm (www.rubitherm.com)
RT 41	43	152	880	Rubitherm (www.rubitherm.com)
STL 47	47	221	1340	Mitsubishi Chemical
E 48	48	201	1670	EPS Ltd. (www.epsltd.co.uk)
C 48	48	324	1360	Climator (www.climator.com)
STL 52	52	201	1300	Mitsubishi Chemical
PX 52	53	103	640	Rubitherm (www.rubitherm.com)
STL 55	55	242	1290	Mitsubishi Chemical
FB 54	55	135	750	Rubitherm (www.rubitherm.com)
RT 54	55	179	900	Rubitherm (www.rubitherm.com)
E 58	58	226	1280	EPS Ltd. (www.epsltd.co.uk)
C 58	58	364	1460	Climator (www.climator.com)
TH 58	58	226	1290	TEAP (www.teappcm.com)
RT 65	64	173	910	Rubitherm (www.rubitherm.com)
C 70	70	194	1700	Climator (www.climator.com)
PX 80	77	91	640	Rubitherm (www.rubitherm.com)
GR 80	79	71	750	Rubitherm (www.rubitherm.com)
FB 80	79	132	750	Rubitherm (www.rubitherm.com)
RT 80	79	175	920	Rubitherm (www.rubitherm.com)

Table T.13 Physical Properties of Organic Heat-Transfer Fluids [24].

	Dowtherm					Syltherm	Therminol	
Fluid	A	G	LF	J	HT	800	VP-1	66
Composition	Mixture DPO – DP[a]	Mixture of di- and triaryl ether	Aromatic blend	Alkylated aromatic	Hydrogenated terphenyl	Dimethyl siloxane	Mixture DPO – DP[a]	Hydrogenated terphenyl
Temperature use range								
Liquid, °F (min/max)	60/750	20/700	−40/650	−100/600	25/650	−40/750	60/750	15/650
Vapor, °F (min/max)	495/750	....	....	358/600	....	....	495/750	
Minimum pumping temperature, °F[d]	53.6[e]	−4	−50	<−100	31	<−50	53.6[e]	30
Flash Point, °F (COC)[f]	255	285	275	145	355	320	240	350
Fire Point, °F (COC)[f]	275	295	295	155	375	350	260	380
Autoignition temperature, °F ASIM D-2155 (new ASIM method E-669-78)	(1139)	(1083)	(932)	(788)	(662)	725	1150	705
Liquid physical properties at 600°F								
Vapor pressure, lb/in² gage (mm Hg)	30.6	9.5	17.3	159.8	(386)	50.0	31.0	(434)
Thermal conductivity, Btu/h · ft · °F	0.061	0.059	0.054	0.0627	0.062	0.052	0.056	0.0545
Specific heat, Btu/lb · °F	0.579	0.540	0.590	0.721	0.630	0.49	0.564	0.628
Density, lb/ft³	49.29	53.94	48.93	35.46	49.58	42.00	49.78	50.30
Viscosity, cP	0.19	0.30	0.24	0.10	0.38	0.43	0.183	0.40
Price range[h]	C	D	D	C	D	E	C	D

[a]Generic chemical equivalent fluids:

Diphenyl-diphenyloxide	Hydrogenated terphenyls	Manufacture
Dowtherm A	Dowtherm HT	Dow Chemical Company
Therminol VP-1	Therminol 66	Monsanto Company
Diphyl		Bayer Leverkusen
Therm S 300	Therms S 900	Nippon Steel
Gilotherm DO	Gilotherm TH	Rhône Poulenc
Thermex		ICI/England
Santotherm VP1	Santotherm 66	Monsanto/Europe

Table T.13 (*continued*)

				Mobiltherm						
60	55	Caloria HT43	Texatherm	600	603	605	Marlotherm S	Diphyl DT	Therm S 600	Gilotherm ALD
Polyaromatic	Synthetic hydro carbon	Parafinic oil	Parafinic oil	Mineral oil	Mineral oil	Mineral oil	Isomeric dibenzyl toluenes	Isomeric dimethyl diphenyl oxide	Alkyl diphenyl	Alkyl benzene
-60/600	0/600	15/600	5/600	5/600	25/550	5/550	-4/662	-4/626	-39/707	32/590
-50	4	>15	>5	35	>25	20	-18	-46	-22	-49
310	350	390	430	350	380	400	374	275	266	358
320	410	430	ND[g]	ND	ND	ND	ND	ND	ND	367
835	675	670	675	ND	ND	ND	932	1013	ND	ND
6.9	(341)	(110)	(150)	(210)	(160)	(120)	(134)	15.3	11.3	(310)
0.0540	0.0535	0.046	0.064	0.060	0.065	0.065	0.0644	0.0534	0.0569	0.0609
0.622	0.699	0.70	0.70	0.70	0.67	0.670	0.608	0.552	0.625	0.645
49.05	42.71	44.42	42.4	47.30	42.43	42.43	50.85	49.79	47.96	43.70
0.30	0.36	0.40	0.54	0.45	0.43	0.47	0.38	0.273	0.322	0.35
D	A	A	A	A	A	A	ND	ND	ND	ND

[b] All reported physical property data were received from the fluid manufacturers after May 1985. The manufacturers and their respective trademarks are: Dowtherm (Dow Chemical Company), Syltherm (Dow Corning Corporation), Therminol (Monsanto Company), Caloria (Exxon Company), Texatherm (Texaco Incorporated), Mobiltherm (Mobil Oil Corporation), Diphyl (Farbenfabriken Bayer AG, Leverkusen, Germany), Gilotherm (Rhône-Poulenc, Paris, France), Marlotherm (Chemische Werke Hülls AG, Germany), Therm S (Nippon Steel Chemical Company, Tokyo, Japan).

[c] Eutectic mixture of 26.5% diphenyl (DP) and 73.5% diphenyl oxide (DPO).

[d] Temperature where fluid viscosity = 1000 cP.

[e] Freeze point.

[f] (COC)—Cleveland open cup.

[g] ND—No data available from manufacturer.

[h] Price range, $/gal: A = $2.00–5.00; B = $5.00–$10.00; C = $10.00–$15.00; D = $15.00–$20.00; E–over $20.00.

CONVERSION FACTORS: °C = (°F − 32)/1.8; bar = mm Hg/750.2; W/m · °C = 1.7307 Btu/h · ft · °F; kJ/kg · °C = 4.1868 Btu/lb · °F; kg/m^3 = 16.021 lb/ft^3; mPa · s = 1.00 cP.

Table T.14 Comparison of Heat-Transfer Fluid Engineering Properties [24].

Fluid	Maximum use Temperature,*		Film coefficient at 600°F, Btu/h. ft2 .°F		Pressure drop at600°F, lb/in 2		Film coefficient at 315.5°C, W/m2.°C		Pressure drop at 315.5°C, mbar/m	
			Velocity***		Velocity***		Velocity***		Velocity***	
	°F/°C	MPT,** °F/°C	5.0 ft/s	7.0 ft/s	3.0 ft/s	7.0 ft/s	1.52 m/s	2.13 m/s	0.91 m/s	2.13 m/s
Dowtherm A	750/399	53.6/12	464	607	1.3	6.9	2630	3450	2.9	15.6
Therminol VP-1	759/399	53.6/12	449	588	1.3	7.0	2550	3340	2.9	15.8
Syltherm 800	750/399	<-50/<-45	239	313	1.2	6.2	1360	1780	2.7	14.0
Dowtherm G	700/371	-4/-20	387	506	1.5	7.6	2200	2870	3.4	17.2
Dowtherm HT	650/343	30/-1	353	462	1.4	7.2	2000	2620	3.2	16.3
Therminol 66	650/343	30/-1	319	417	1.4	7.3	1810	2370	3.2	16.5
Dowtherm LF	650/343	-50/ -45	384	503	1.3	6.9	2180	2860	2.9	15.6
Dowtherm J	600/316	<-100/<-73	522	684	0.9	4.9	2960	3880	2.0	11.1
Therminol 60	600/316	-50/-45	355	465	1.4	7.0	2020	2640	3.2	15.8
Therminol 55	600/316	4/-15	302	395	1,2	6.2	1710	2240	2.7	14.0
Caloria HT 43	600/316	>15§/>-9	268	351	1.3	6.5	1520	1990	2.9	14.7
Texatherm	600/316	>5§/>-15	280	367	1.3	6.4	1590	2080	2.9	14.5
Mobiltherm 600	600/316	35/2	319	417	1.4	7.0	1810	2370	3.4	15.8
Mobiltherm 603	600/316	>20§/>-7	310	406	1.3	6.3	1760	2310	2.9	14.3
Mobiltherm 605	600/316	20/-7	298	390	1.3	6.3	1690	2210	2.9	14.3
Marlotherm S	662/350	-18/ -28	366	479	1.4	7.4	2080	2720	3.2	16.6
Diphyl DT	626/330	-46/-43	359	469	1.4	7.1	2040	2660	3.2	16.0
Therm S 600	707/375	-22/-30	350	458	1.4	6.9	1990	2600	3.2	15.5
Gilotherm ALD	590/310	-49/-45	330	433	1.3	6.4	1870	2460	2.9	14.4

* Manufacturer's maximum recommended use temperature.
** MPT = minimum pump temperature, where viscosity reaches 1000 cP.
*** Velocity in 1-in schedule 40 pipe.
§ Reported pour-point temperature.

Table T.15 Physical properties of Molten HTS and Drawsalt [24].

	HTS		Drawsalt	
	Physical property	Reference	Physical property	Reference
Liquidus, °F (±5°F)*	$446.8 - 6.0769C + 0.18341C^2 - 0.0033042C^3$	3*b*, pp. 786–795	473 ± 1	8
Volume change on melting $\Delta V_m/V$, %	4.0 ± 0.5	7	4.6 ± 0.5	3*a*, pp. 396–411
Heat of fusion ΔH_m, Btu/lb	≈35	1	49	8
Heat capacity C_p, Btu/lb · °F	0.37 ± 0.03	1	0.38 ± 0.02	†
Thermal conductivity k, Btu/ft · h · °F	0.29 ± 0.12	9	0.31 ± 0.07	3*a*, pp. 396–411
Viscosity η, cP (±5%)‡*	$\exp[-1.404 + 1747.7/(T + 116.8)]$			
Surface tension γ, lb/ft (±1%)*	$0.0092 - 2.4 \times 10^{-4} T$	§	$0.0108 - 2.4 \times 10^{-5} T$	3*a*, pp. 396–411
Density ρ, lb/ft³*	$131 - 0.0256T$	11	$129 - 9.6 \times 10^{-4} T^2$	¶

* C is nitrite as % by weight $NaNO_2$; $0\% < C < 40\%$; T is in °F.

† Determined to 800°F.[3]

‡ Recent values[10] are lower. Those shown summarize previous HTS[1,11] and recent eutectic drawsalt[12] data. It seems viscosities of the two salts are very close.[12] Viscosities for noneutectic (60/40) drawsalt may be 3 to 5% lower than shown here (Ref. 3*a*, pp. 396–411).

§ Values shown are for eutectic drawsalt, which seem to be very close to HTS values.[12]

¶ ±1% (Ref. 3*a*, pp. 396–411). There are also recent values for the eutectic drawsalt.[12]

CONVERSION FACTORS: 2.326 kJ/kg = 1 Btu/lb; 4.187 kJ/kg · K = 1 Btu/lb · °F; 1.731 J/m · s · K = 1 Btu/ft · h · °F, 1 mPa · s = 1 cP; 68.54 mN/m = 1 lb/ft; 16.018 kg/m³ = 1 lb/ft³ = 0.13368 lb/gal.

SOURCE: Adapted from the references cited.

Table T.16 IEC-ISA-Designated Thermocouple Alloys [24]

Thermo		Typical	Base	Applications	
Type	Elements	Alloy	Composition	Atmosphere	Maximum Temperature
J	JP	Iron	Fe	Oxidizing, reducing,	760°C
	JN	Constantan (J)	45%Ni-55%Cu	inert	
K	KP	Chromel	90%Ni-10%Cr	Oxidizing, inert	1260°C
	KN	Alumel	94%Ni-Al,Mn,Fe		
N	NP	Nicrosil	Ni-14%Cr-1.4%Si	Oxidizing, inert	1260°C
	NN	Nisil	Ni-4.4%Si-0.1%Mg		
T	TP	Copper	OFHC Cu	Mild oxidizing,	370°C
	TN	Constantan (T)	45%Ni-55%Cu	reducing, inert	
E	EP	Chromel	90%Ni-10%Cr	Oxidizing, reducing	870°C
		Constantan (T)	45%Ni-55%Cu	inert	
R	RP	Pt-Rh	87%Pt-13%Rh	Oxidizing, inert	1480°C
	RN	Pt	Pt		
S	SP SN	Pt-Rh	90%Pt- 10%Rh Pt	Oxidizing, inert	1480°C
B	BP	Pt-Rh	70%Pt-30%Rh	Oxidizing, inert	1700°C
	BN	Pt-Rh	94%Pt-6%Rh		

Table T.17 Seebeck Coefficient For Various Thermocouples [100].

Temperature [°C]	E µV/°C	J µV/°C	K µV/°C	R µV/°C	S µV/°C	T µV/°C
-200	25.1	21.9	15.3	-	-	15.7
-100	45.2	41.1	30.5	-	-	28.4
100	58.7	50.4	39.5	5.3	5.4	38.7
200	67.5	54.3	41.4	7.5	7.3	46.8
300	74.0	55.5	40.0	8.8	8.5	53.1
400	77.9	55.4	41.4	9.7	9.1	58.1
500	80.0	55.1	42.2	10.4	9.6	61.8
600	80.9	56.0	42.6	10.9	9.9	-
700	80.7	58.5	42.5	11.3	10.2	-

Table T.18 Phase Change Materials [100].

Material	*Tm [°C]*	*ρ_s [kg/m^3]*	*ρ_l [kg/m^3]*	*Δhm [kJ/kg]*	*$\rho\Delta hm$ [MJ/m^3]*	*Cps [kJ/kg.k]*	*Cpl [kJ/kg.k]*	*ks [w/m.k]*	*Ref.*
H_20	0	917	1000	335	307	2.1	4.2	2.2	1
$ZnCI_2/3H_20$	10	-	-	-	-	-	-	-	2
$K_2HP0_4/6H_20$	13	-	-	-	-	-	-	-	2
$NaOH/15.5H_20$	15	-	-	223	-	-	-	-	2
$Na_2Cr0_4/10H_20$	16	-	-	183	-	-	-	-	2
Polyethylene Glycol 600	20-25	-	-	147	-	-	-	-	3
Sasol wax C_2,H_M	29-33	-	-	-	-	-	-	-	4
n-Octodecane	30	1710	-	171	293	1.45	-	-	2,5
$CaCI_2/6H_20$	30	1710	-	171	293	1.45	-	-	2,5
Na_2SO_4-$10H_2O$	32	1485	1453	254	377	1.92	3.26	1.85-2.12	3,6
Na_2HP0_4-$14H_20$	35	1520	1442	281	430	1.70	-	-	5
Na_2HP0_4-$12H_20$	36.1	1520	1442	279	424	1.68	1.93	1.54-2.12	2,6
$Zn(N0_3)_2$-$6H_20$	36.4	2065	-	148	305	1.34	-	-	5
$K(CH_3COO)/5.5H_20$	42	-	-	-	-	-	-	-	2
Carbowax 1540	±43	1000	-	155	155	-	-	0.26	7
Laurie acid	44	870	-	178	155	1.60	-	-	5
Suntech P116, Paraffin wax	±44	790	748	226	179	2.51	-	0.2	8
$K_3P0_4/7H_20$	45	-	-	-	-	-	-	-	2
$Na_2S_20_3/5H_20$	45	1600	-	201	322	1.47	-	-	2,5
Wax-ester	45-49	950	825	183	151	1.68	-	-	5
$Ca(N0_3)_2/4H_20$	47	-	-	163	-	-	-	-	2
Paraffin (Sunoco 116)	47.2	817	786	210	172	2.89	2.89	0.497	3,6
$Zn(N0_3)_2/4H_20$	48	-	-	159	-	-	-	-	2
$Na_2S_20_2$-$5H_20$	49	-	-	200	-		-	-	3
$Ni(N0_3)_2/6H_20$	53	-	-	166	-		-	-	2

Table T.18 (*continued*)

Material	*Tm [°C]*	*ρs [kg/m³]*	*ρl [kg/m³]*	*Δhm [kJ/kg]*	*ρΔhm [MJ/m³]*	*Cps [kJ/kg.k]*	*Cpl [kJ/kg.k]*	*ks [w/m.k]*	*Ref.*
Shell paraffin wax	53.5	865	781	249	215	1.8	-	0.23	9
$Zn(N0_3)_2$-$2H_20$	54	-	-	-	-	-	-	-	2
$(Mg(N0_3)_2$-$6H_20)/(Mg(N0_3)_2$-$2H_20)$	55.5	-	-	-	-	-	-	-	2
n-Paraffin wax	56	910	822	195	177	1.77	1.77	0.21	10
Tristerearin 133	56	-	-	191	-	-	-	-	3
$Fe(N0_3)_2$-$6H_20$	60	-	-	126	-	-	-	-	2
FRP 140/145 wax	62	917	777	236	216	1.93	-	0.23	11
Stearic acid	69	-	-	199	-	-	-	-	3
$CH_3(CH_2)_{le}$-COOH	69.4	941	847	203	191	1.69	2.35	1.67	6
$92(Ba(OH)_2$-$8H_20)/8H_20$	78	2100	1800	275	578	-	-	-	12
Hi-Mic 1070 wax	79.4	921	797	167	154	1.90	-	0.23	11
Pentaglycerine	81	-	-	193	-	-	-	-	3
$Ba(OH)_2$-$8H_20$	82	-	-	266	-	-	-	-	3
Propionamide	84	-	-	168	-	-	-	-	3
$NH_4Al(S0_4)_2$-$12H_20$	93.5	1640	-	268	440	-	-	-	13
$(COOH)_2$-$2D_20$	94	-	-	348	-	-	-	-	13
$LiCI0_4$-$3H_20$	95	1835	-	280	514	-	-	-	13
Polyethylene	100-140	-	-	160-180	-	-	-	-	3
$(COOH)_2$-$2H_20$	101.5	1640	-	394	646	-	-	-	13
Form Stable HDPE	127	880	-	192	168	2.54	2.61	0.25	14
$CO(NH_2)_2$	133	-	-	251	-	-	-	-	15
Polyethylene	135	-	-	209	-	-	-	-	15
$7NaOH/40NaN0_2/53KN0_3$	142	-	-	82	-	1.34	1.86	-	16
Nylon type 12	179	-	-	-	-	-	-	-	3
Pentaerythritol	188	-	-	322	-	-	-	-	15
64KOH/36NaOH	190	2060	-	233	480	-	-	-	17

Table T.18 (*continued*)

Material	*Tm [°C]*	*ρs [kg/m³]*	*ρl [kg/m³]*	*Δhm [kJ/kg]*	*ρΔhm [MJ/m³]*	*Cps [kJ/kg.k]*	*Cpl [kJ/kg.k]*	*ks [w/m.k]*	Ref.
AI_2Cl_6	192	-	-	262	-	-	-	-	15
Nylon type 6	216	-	-	105 -	-	-	-	-	3
$NaCl0_3$	225	-	-	212	-	-	-	-	15
Cellulose acetate	229	-	-	-	-	-	-	-	3
P-chlorbenzoic acid	240	-	-	206	-	-	-	-	15
KOH	249	-	-	261	-	-	-	-	3
UNO,	252	2310	1776	530	941	2.03	2.04	1.35	1
$51KCl/49ZnCl_2$	260	2480	-	198	491	-	-	-	17
27LiCl/63LiOH	262	1640	-	316	518	-	-	-	18
Nylon type 6/6	265	-	-	105-	-	-	-	-	3
$NaN0_2$	271	-	-	329	-	2.06	2.08	-	16
$7.8NaCl/6.4NaC0_3/85.8NaOH$	282	2100	-	316	-	-	-	-	18
ZnCI,	283	2260	-	169	382	-	-	-	17
$FeCl_3$	304	-	-	288	-	-	-	-	15
$NaN0_3$	307	1900	-	171	324	1.871	1.885	0.553	19
NaOH	318	2130	1780	160	285	2.461	2.342	0.837	1,19
NaSCN	323	-	-	288	-	-	-	-	15
Polytetrafluoroethylene-Teflon	327	-	-	-	-	-	-	-	3
$KN0_3$	334	1870	-	106	198	1.192	1.218	0.498	19
Na_20_2	349	-	-	315	-	-	-	-	3
KOH	360	1730	-	149	258	1.277	1.486	-	19
$24.5NaCl/20.5KCl/55MgCl_2$	385-393	1800	-	410	738	-	-	1.0	1
$20KCl/50MgCl_2/30NaCl$	396	2250	-	412	927	-	-	-	17
$32Li_2C0_3/35K_2C0_3/33Na_2C0_3$	397	2300	2140	277	593	1.68	1.63	-	1
80LiOH/20LiF	427	1600	-	427	683	-	-	-	18
$38MgCl_2/62NaCl$	435	2160	-	328	708	-	-	-	17
Na_2Mo0_4	440	-	-	296	-	-	-	-	15

Table T.18 (*continued*)

Material	*Tm [°C]*	*ρs [kg/m³]*	*ρl [kg/m³]*	*Δhm [kJ/kg]*	*ρΔhm [MJ/m³]*	*Cps [kJ/kg.k]*	*Cpl [kJ/kg.k]*	*ks [w/m.k]*	*Ref.*
48NaCl/52$MgCl_2$	450	2225	1610	431	694	0.92	1.0	-	1
B_2O_3	460 to 470	1840	-	330	607	-	-	-	17
Li OH	471	1425	1385	1080	1500	3.3	3.9	1.3	1
$KMgCl_3$	487	-	-	313	-	-	-	-	15
23UF/67KF	492	2530	-	668	1690	-	-	-	18
33NaCl/67$CaCl_2$	500	2160	1900	282	536	0.84	1.0	-	1
35Li_2C0_3/65K_2C0_3	505	2265	1960	345	676	1.34	1.76	-	1
$KCl0_4$	527	-	-	1254	-	-	-	-	3
52I\laCI/48I\liCI$_2$	570	2840	-	558	1585	-	-	-	18
88AI/12Si	579	2553	2445	515	1259	1.49	1.27	high	1
52LiF/35NaF/13CaF_2	615	2630	-	630	1657	-	-	-	18
46LiF/44NaF/10MgF_2	632	2610	-	858	2239	-	-	-	3,18
LiF/NaF	652	2480	-	816	2024	-	-	-	18
Al	660	2560	2370	400	948	0.92	-	200	1
LiH	699	-	-	2680	-	-	-	-	3
54LiF/48MgF_2	710	2920	-	782	2283	-	-	-	18
$MgCl_2$	714	2410	-	452	1089	-	-	-	17
67KF/33NaF	721	2285	-	586	1339	-	-	-	18
Li_2C0_3	725	2110	-	605	1277	-	-	-	18
Li_2C0_3	726	2114	1810	607	1100	-	-	1.45	1
$Na_2B_40_7$	740	2300	2630	530	1220	1.75	1.77	-	1
67UF/33MgF_2	741	-	-	900	2000	-	-	-	1
54NaF/23CaF_2/23MgF_2	745	2760	-	574	1584	-	-	-	18
55LiF/45CaF_2	765	2880	-	747	2151	-	-	-	18
NaCl	800	2160	-	492	1062	-		-	17
62.5NaF/22.5MgF_2/15KF	809	2630	-	607	1596	-	-	-	18
67NaF/33MgF_2	832	2690	2190	618	1353	1.42	1.38	4 to 12	1
$LiB0_2$	835	1400	-	698	977	-	-	-	18

Table T.18 (*continued*)

Material	*Tm [°C]*	*ρs [kg/m³]*	*ρl [kg/m³]*	*Δhm [kJ/kg]*	*ρΔhm [MJ/m³]*	*Cps [kJ/kg.k]*	*Cpl [kJ/kg.k]*	*ks [w/m.k]*	*Ref.*
LiF	848	1714	-	1050	1800	-	-	-	1
Na_2C0_3	854	2530	-	311	787	-	-	-	17
Na_2S0_4	884	2700	-	202	545	-	-	-	17
NaF	933	-	-	750	-	-	-	-	3
51CaF/49MgF	944	3090	-	650	2009	-	-	-	18
Be	1265	-	-	1210	-	-	-	-	3
MgF_2	1271	-	-	979	-	-	-	-	3
Si	1415	-	-	1654	-	-	-	-	3

Table T.19 Temperature histories during a heat storage stage.

Time (Min)	T1 (°C)	T2 (°C)	T3 (°C)	T4 (°C)	T5 (°C)	T6 (°C)	Power
45	103.5	76.4	71.2	26.5	18	10.3	On
55	140.4	100.1	91.8	27.5	34.8	47.5	On
65	209	126	115.7	62.5	63.1	67	On
75	219	166	140.6	52.8	53.9	61.2	Off
85	293	165	146	54.2	49.3	69.9	Off
95	281	172	150	53.5	52.6	73	Off
105	327	183	161	54.3	58	76.3	On
115	331	193	169	49.4	61.6	79.7	On
125	314	209	180	43.4	64.8	83.4	Off
135	274	230	205	51.9	71.6	91.7	Off
145	268	231	206	42.7	75.6	94.6	On
155	272	264	218	42	82.4	101	On
165	305	314	251	44	91.7	113.2	On
175	316	318	255	44.7	92.7	115	On
185	326	327	257	45.3	93.7	116	On
195	357	332	266	46.9	96.9	120.4	Off
205	338	316	260	47.9	98.8	123.2	Off
215	295	269	261	65.1	113.2	135.5	Off
225	298	282	257	68.3	115.7	136.58	On
235	298	295	257	69.3	116.3	137	On
245	321	327	266	72.8	118.3	138.4	On
255	340	336	276	75.6	120	139.8	On
265	352	340	284	73.3	118.8	140.7	On
275	320	310	290	75.7	123	144.1	Off
285	303	296	285	78.9	126.8	146	Off
295	301	285	279	81.8	129.9	148	Off
305	312	304	277	81.4	130.8	149	On
315	340	325	286	85.8	134.4	152	On
325	343	326	287	86.6	135.1	153	On
335	347	331	290	88	136.4	155	On
345	352	335	293	89.7	138	157	On
355	323	304	293	93.7	143.1	163	Off
365	315	297	291	94.6	144.8	164	Off
375	309	293	288	95.6	145	164	Off
385	304	289	284	97	146	165	Off
395	301	286	281	97.7	146	165	Off
405	300	283	279	98.7	147	165	Off

Table T.20 Discharging of Heat Storage Tank without any Load

Time (Min)	T1 (°C)	T2 (°C)	T3 (°C)	T4 (°C)	T5 (°C)	T6 (°C)
0	350	330	331	98.7	147	165
10	345	335	329	97.7	146	165
20	341	330	326	97	146	165
30	340	329	330	95.6	145	164
40	345	325	330	94.6	144.8	164
50	339	322	329	93.7	143.1	163
60	352	335	328	89.7	138	157
70	347	331	327	88	136.4	155
80	343	326	325	86.6	135.1	153
90	340	325	320	85.8	134.4	152
100	339	325	322	81.4	130.8	149
110	310	307	312	81.8	129.9	148
120	303	300	285	78.9	126.8	146
130	320	310	290	75.7	123	144.1
140	322	300	284	73.3	118.8	140.7
150	320	310	276	75.6	120	139.8
160	321	312	266	72.8	118.3	138.4
170	310	295	257	69.3	116.3	137
180	311	282	257	68.3	115.7	136.58
190	310	269	261	65.1	113.2	135.5
200	305	270	260	47.9	98.8	123.2
210	307	268	266	46.9	96.9	120.4
220	300	270	257	45.3	93.7	116
230	298	271	255	44.7	92.7	115
240	290	268	251	44	91.7	113.2
250	272	264	218	42	82.4	101
260	268	231	206	42.7	75.6	94.6
270	274	230	205	51.9	71.6	91.7
280	270	209	180	43.4	64.8	83.4
290	269	193	169	49.4	61.6	79.7
300	250	183	161	54.3	58	76.3
310	245	172	150	53.5	52.6	73
320	235	165	146	54.2	49.3	69.9
330	219	166	140.6	52.8	49	61.2
340	209	126	115.7	62.5	40	67
350	140.4	100.1	91.8	27.5	34.8	47.5
360	103.5	76.4	71.2	26.5	18	10.3

REFERENCES

1. Duffie J.A. and Beckman W.A., "Solar Engineering of Thermal Processes", 2nd edition, John Wiley and Sons, New York, pp.382-412, (1991).
2. Claude du Plessis, "Experimental and Theoretical Assessment of Ice Storage in Air Conditioning", Master Thesis, Department of Mechanical Engineering, University of Natal, Durban, South Africa, (1994).
3. Beckmann G., Gilli. PV., "Thermal Energy Storage", Springer-Verlag/Win, New York, pp. 272-290, (1984).
4. Tomlinson J. J. and Kannberg L. D., "Thermal Energy Storage", Mechanical Engineering 112, pp. 68-72, September, (1990).
5. Lynch R., "an Energy Overview of the Republic Of South Africa", U.S. Department of Energy Office of Fossil Energy, Washington, D.C. 20585-1290 USA, telephone: 1-301-903-2617.
6. Di J.F., "Solar Stove With Downward Heat Transport System" Master Thesis, School of Mechanical and Manufacturing Engineering, University of New South Wales, Sydney Australia, (1992).
7. Gaunt T., "Electrification technology and processes to meet economic and social objectives in South Africa", Department of Electrical Engineering, May, (2003).
8. Howellsa M.I., Alfstada T., Victorb D.G., Goldsteinc G., Remmed U., "A Model of Household Energy Services in A Low-Income Rural African Village", Energy Policy 33, pp.1833-1851, (2005).
9. Lloyd P., Dick A., Howells M., Alfstad T., "A Baseline Study for Nkweletsheni". Energy Research Institute, University of Cape Town, (2002).
10. Eberhard A., Van Hooren C., "Poverty and Power", Pluto Press, (1995).
11. Van den Heetkamp R. R. J., "The Development of Small Solar Concentrating Systems with Heat Storage for Rural Food Preparation", Physica Scripta. T97, pp. 99-106, (2002).
12. Naumann R. and Emons H.H., "Results of Thermal Analysis for Investigation of Salt Hydrates as Latent Heat-Storage Materials", J. Thermal Analysis, 35, pp. 1009–1031, (1989).

13. Tiwari G.N., Suneja S.,"Solar Thermal Engineering System", New Delhi, Narosa Publishing House, pp. 11-120, (1997).

14. Morrison G. L., Di. J., "Mills D. R., Development of a Solar Thermal Cooking System", School of physics, University of Sydney, (1993).

15. Ercan O., "Storage of Thermal Energy, in Energy Storage Systems", EOLSS, (2006). *www.bjpu.edu.cn/sci/hn/client_c/lunwen/2004_52.pdf*

16. Abhat A., "Low Temperature Latent Heat Thermal Energy Storage: Heat Storage Materials", Solar Energy 30, 313–332, (1983).

17. Lane G. A., "Solar Heat Storage: Latent Heat Materials", vol. I, Background and Scientific Principles, CRC Press, Boca Raton, Fla., (1983).

18. Lane G.A., "Solar Heat Storage: Latent Heat Material", vol. II, Technology, CRC Press, Florida, (1986).

19. Dincer I., Rosen M.A., "Thermal Energy Storage, Systems and Applications", John Wiley & Sons, Chichester (England), (2002).

20. Zalba B., Marín J.M., Cabeza L.F. and Mehling H., "Review On Thermal Energy Storage with Phase Change: Materials, Heat Transfer Analysis and Applications", Appl. Therm. Eng. **23**, pp. 251–283, (2003).

21. Husnain S.M., "Review On Sustainable Thermal Energy Storage Technologies, Part 1: Heat Storage Materials and Techniques", Energy Convers Manage **39**, pp. 1127–1138, (1998).

22. Garg H.P., Mullick S.C., Bhargava A.K., "Solar Thermal Energy Storage", Holland: Reidel Publishing Company, pp. 668, (1985).

23. Jing Li, Zhongliang Liu, Chongfang Ma, "An Experimental Study on the Stability and Reliability of the Thermal Properties of Barium Hydroxide Octahydrate as a Phase Change Material", (2004). www.bjpu.edu.cn/sci/hn/client_c/lunwen/2004_52.pdf

24. Eric C. Guyer, David L. Brownell, "Hand book of applied thermal design", Hamilton Printing Co, Castleton, NY, (1999).

25. Telkes M., "Nucleation of Supersaturated Inorganic Salt Solutions," Ind. Eng. chem., 44, pp.1308, (1952).

26. Sharma S.D. and Sagara K., "Latent Heat Storage Materials and Systems: a Review", International Journal of Green Energy, 2: 1–56, (2005).

27. Lane G.A., Kott A.C., Warner G.L., Hartwick P. B., and Rossow H.E., "Macro-Encapsulation of Heat Storage Phase Change Materials for Use in Residential Buildings", Report OROV 5217/8, The Dow Chemical Co., Midland, Mich., (1978).

28. Kohler J. and Lewis D., "Phase Change Products for Passive Homes", Solar Age, 8, pp.65, (1983).

29. Crank J., "Free and Moving Boundary Problems", Clarendon Press, Oxford, (1984).

30. Carslaw H.S. and Jaeger J.C., "Conduction of Heat in Solids", 2nd Edition, Oxford University Press, Oxford, (1986).

31. Price P.H. and M.R. Slack "The Effect of Latent Heat on Numerical Solutions of the Heat Flow Equation", Br. J. appl. Phys, 5, pp.285-287, (1954).

32. Eyres N.R., Hartree D.R., Ingham J., Jackson R., Sarjant R.J., and Wagstaff S.M., "The Calculation of Variable Heat Flow in Solids", Phil. Trans. R. Soc, A240, 1-57, (1946).

33. Eckert E.R.G., Goldstein R.J., Ibele W.E., Patankar S.V., Simon T.W., Strykowski P.J., Tamma K.K., Kuehn T.H., Bar-Cohen A., and others, "Heat Transfer-a Review of 1994 Literature", Int. J. Heat Trasfer 40, pp.3729–3804, (1997).

34. London A.L., Seban R.A., "Rate of ice formation", Trans. ASME 65, pp.771–778, (1943).

35. Shamsundar N., Srinivasan R., "Analysis of Energy Storage by Phase Change with an Array of Cylindrical Tubes, In: Thermal Energy Storage and Heat Transfer In Solar Energy Systems, American Society of Mechanical Engineers, vol. 35, New York, (1978).

36. Lazaridis A., "A Numerical Solution of the Multidimensional Solidification (or Melting) Problem", Int. J. Heat Mass Transfer 13, 1459–1477, (1970).

37. Shamsundar N., Sparrow E.M., "Analysis of Multidimensional Conduction Phase Change via the Enthalpy Model", J. Heat Transfer, Trans. ASME, pp.333–340, August (1975).

38. Shamsundar N., Sparrow E.M., "Effect of Density Change on Multidimensional Conduction Phase Change", J. Heat Transfer, Trans. ASME 98, pp.550–557, (1976).

39. Goodling J.S., Khader M.S., Results of the numerical solution for outward solidification with flux boundary conditions, J. Heat Transfer, Trans. ASME 97, pp. 307–309, (1975).

40. Meyer G.H., "The Numerical Solution of Multidimensional Stefan Problems-A Survey, in: Moving Boundary Problems", Academic Press, (1978).

41. Marshall R., "Studies Of Natural Convection Effects in an Annulus Containing A Phase Change Material", Proceedings of the UK International Solar Energy Society on Storage in Solar Energy Systems, London, pp. 11, (1978).

42. Bathelt A.G., P.D. Van Buren, R. Viskanta, Heat transfer during solidification around a cooled horizontal cylinder, AIChE Symp. Series 75 pp.103-111, (1979).

43. Sparrow E.M., C.F. Hsu, Analysis of two-dimensional freezing on the outside of a coolant-carrying tube, Int. J. Heat Mass Transfer 24 (8), pp.1345–1357, (1981).

44. Shamsundar N., Similarity rule for solidification heat transfer with change in volume, J. Heat Transfer, 103, pp.173, (1981).

45. Shamsundar N., Formulae for freezing outside a circular tube with axial variation of coolant temperature, Int. J. Heat Mass Transfer, 25 (10) pp.1614–1616, (1982).

46. Achard P., Lecomte D., Mayer D., Etude des transferts thermiques dans un stockage par chaleur latente utilisant un echangeur tubulaire immerge, Revue Generale de thermique Fr. (254), pp.169–175, (1983).

47. Hunter L.W., Kuttler J.R., The enthalpy method for heat conduction problems with moving boundaries, J. Heat Transfer, Trans. ASME 111, pp.239–242, (1989).

48. Amdjadi M., B. Fabre, C. Meynadier, Résolution unidimensionnelle d'un problème de Stefan par une méthode à pas de temps variable: application à une bille de chliarolithe, Revue générale de thermique Fr. (339), pp.129–134, (1990).

49. Banaszek J., Domanski R., Rebow M., El-Sagier F., Experimental study of solid–liquid phase change in a spiral thermal energy storage unit, Appl. Thermal Eng. 19, pp.1253-1277, (1999).

50. Bathelt A.G., Viskanta R., Leidenfrost W., An Experimental Investigation of Natural Convection In the Melted Region Around a Heated Horizontal Cylinder, J. Fluid Mech. 90, 227–239, (1979).

51. Gobin D., Role de la convection thermique dans les processus de fusion-solidification, Ecole d'ete, GUT-CET, Modélisation numérique en thermique, Institut d'etudes scientifiques de Cargèse, (1992).

52. Özisik M.N., Phase-Change Problems. In: *Heat Conduction*, Wiley–Interscience (1993).

53. Ismail K.A.R., Stuginsky R., A parametric study on possible fixed bed models for PCM and sensible heat storage, Appl. Thermal Eng. 19, pp.757–788, (1999).

54. Ismail K.A.R., A. Batista de Jesus, Modeling and solution of the solidification problem of PCM around a cold cylinder, Numer. Heat Transfer, Part A 36, pp.95–114, (1999).

55. Furzerland R.M., A comparative study of numerical methods for moving boundary problems, J. Inst. Math. Appl. 26, pp.411–429, (1980).

56. Abhat A., Aboul-Enein S., Malatidis N., Heat of fusion storage systems for solar heating applications, in: C. Den Quden (Ed.), Thermal Storage of Solar Energy, Martinus Nijhoff, (1981).

57. Ismail K.A.R., Alves C.L.F., M.S. Modesto, Numerical and experimental study on the solidification of PCM around a vertical axially finned isothermal cylinder, Appl. Thermal Eng. 21, pp.53–77, (2001).

58. Siegel R., Solidification of low conductivity material containing dispersed high conductivity particles, Int. Heat Mass Transfer 20, pp.1087–1089, (1977).

59. Sharma S.D., Buddhi D., Sawhney R.L. and Sharma A. Design, development and performance evaluation of a latent heat storage unit for evening cooking in a solar cooker, Energy Convers Manage 41, pp. 1497–1508, (2000).

60. Buddhi D., Sharma S.D., Sharma A. Thermal performance evaluation of a latent heat storage unit for late evening cooking in a solar cooker having three reflectors. Energy Convers Manage; 44,pp.809-17, (2003).

61. Shukla A., Buddhi D., Sharma S.D., Sagara K. Accelerated thermal cycle test of erythritol for the latent heat storage application. In: Proceedings of the EM4 Indore workshop IEA ECES IA annex 17, 21–24 Apri, Indore, India, (2003).

62. Das T.C.T, Karmakar S., Rao D.H. Solar box-cooker: part II-analysis and simulation. Sol Energy;52(3), pp.273–82, (1994).

63. Ahmed B. Users and disusers of box solar cookers in urban India-implications for solar cooking projects. Sol Energy;69(Suppl. 6), pp.209, (2001).

64. Algifri A.H., Al-Tawaie HA. Efficient orientation impacts of box-type solar cooker on the cooker performance. Sol Energy;70(2), pp.165–70, (2001).

65. Balzar A, Stumpf P, Eckhoff S, Ackerman H, Grupp M. A solar cooker using vacuum-tube collectors with integrated heat pipes. Sol Energy, (1996).

66. Biermann E, Grupp M, Palmer R. Solar cooker acceptance in South Africa: results of a comparative fieldtest. Sol Energy,66(6), pp.401–7, (1999).

67. Das T.C.T, Karmakar S, Rao DH. Solar box-cooker: part I-modelling. Sol Energy, 52(3), pp.265–72, (1994).

68. Funk PA. Evaluating the international standard procedure for testing solar cookers and reporting performance. Sol Energy, 68(1), pp.1-7, (2000).

69. Habeebullah M.B., Khalifa A.M., Olwi I. The oven receiver: an approach toward the revival of concentrating solar cookers. Sol Energy, 54(4), pp.227-37, (1995).

70. Khalifa A.M.A., Taha M.M.A., Akyurt M. Design, simulation, and testing of a new concentrating type solar cooker. Sol Energy;38(2), pp.77-88, (1987).

71. Esen M., Thermal performance of a solar cooker integrated vacuum-tube collector with heat pipes containing different refrigerants. Sol Energy;76(6), pp.751-7, (2004).

72. Kumar R., Adhikari R.S., Garg H.P., Kumar A. Thermal performance of a solar pressure cooker based on evacuated tube solar collector. Appl Therm Eng; 21, 1699–706, (2001).

73. Mullick S.C., Kandpal T.C., Kumar S. Testing of box-type solar cooker: second figure of merit F2 and its variation with load and number of pots. Sol Energy ;57(5), pp.409–13, 1996.

74. Nyahoro P.K., Johnson R.R., Edwards J. Simulated performance of thermal storage in a solar cooker. Sol Energy; 59(1–3):pp.11–7, (1997).

75. Rao A.V.N., Subramayan S. Solar cookers-part I: cooking vessel on lugs. Sol Energy;75(3):181–5, (2003).

76. Rao A.V.N., Subramayan S. Solar cookers-part II: cooking vessel with central annual cavity. Sol Energy; 78 (1):19–22, (2005).

77. Suharta H., Abdullah K., Sayigh A. The solar oven: development and field-testing of user-made designs in Indonesia. Sol Energy; 64 (4-6):121-32, (1998).

78. El-Sebaii A.A., Domanski R., Jaworski M. Experimental and theoretical investigation of a box-type solar cooker with multi-step inner reflectors. Energy; 19 (10):1011-21, (1994).

79. Domanski R., El-Sebaii AA, Jaworski M. Cooking during off-sunshine hours using PCM as storage media. Energy; 20(7):607-16, (1995).

80. Buddhi D., Sahoo L.K. Solar cooker with latent heat storage: design and experimental testing. Energy Convers Manage;38(5):493-8, (1997).

81. Ozturk H.H., Experimental determination of energy and exergy efficiency of the solar parabolic-cooker. Sol Energy; 77(1): 67-71, (2004).

82. Schwarzer K., de Silva MEV. Solar cooking system with or without heat storage for families and institutions. Sol Energy; 75(1): 35-41, (2003).

83. Sharma S.D., Sagara K. Solar cooker for evening cooking using latent heat storage material based on evacuated tube solar collector. In: Proceedings of 6th workshop IEA ECES IA annex 17, 8–9 June, Arvika, Sweden, (2004).

84. Sharma S.D., Iwata T., Kitano H, Kakuichi H, Sagara K. Experimental results of evacuated tube solar collector for use in solar cooking with latent heat storage. In: Proceedings of the EM4 Indoor workshop IEA ECES IA annex 17, India, 21–24 April, (2004).

85. Sharma S.D., Iwata T., Kitano H, Sagara K. Thermal performance of a solar cooker based on an evaluated tube solar collector with a PCM storage unit. Sol Energy; 78(3):416–26, (2005).

86. Kirst W.E. Nagel W.M., and Casmer 1. B., A New heat Transfer Medium for High Temperatures, Am. lnst. Chem. Eng. Trans.. 36, pp.371-394, (1940).

87. "Olin Hitec® Heat Transfer Salt," Tech. Brochure, Olin Corp. Stamford, CT, (1984).

88. Janz G. J., Allen C. B., Bansal N. P., Murphy R. M., and Tompkins R., "Physical Properties Data Compilations Relevant to Energy Storage," pts. II and IV, NSRDS-NBS 61, Superintendent of Documents, U.S. GPO, Washington, DC. (a) pt. II, pp.442, (1979). (b) pt. IV, pp.870, (1981).

89. Janz G. J., Molten Salts Handbook, Academic Press, New York, (1967).

90. Nissen D. A., and Meeker D. E., "Nitrate/Nitrite Chemistry in NaN03-KN03 Melts," Inorg. Chem., 22, pp.716-721, (1983).

91. HITEC heat transfer salt, Coastal Chemical Co., L.L.C, Brenntag Company, 5300 Memorial Drive, Houston, TX 77007, Phone: 713-865-8787, Fax: 713-865-8788.

92. Anthony F. Mills, Basic Heat & Mass Transfer, Second Edition, Irwin, (1999).

93. Incropera, F.P. and De Witt, D.P., Introduction to Heat Transfer, Second Edition, John Wiley & Sons, New York, NY, (1990).

94. Horn, J., Cooking A to Z: The Complete Culinary Reference Source, New and Revised Edition, Cole Group, Santa Rosa, CA, (1997).

95. Wolke, R.L., What Einstein Told His Cook, W.W. Norton & Company, New York, (2002).

96. McGee, H., On Food and Cooking: The Science and Lore of the Kitchen, Simon and Schuster, New York, NY, (1984).

97. Lof G.Q.G. "Use of solar energy for heating purposes: Solar Cooking", Agenda item III.C.4, United Nations conference on new sources of energy, Rome, (1961).

98. Hall C.A., Swet C.J, and Temanson L.A. "Cooking with stored solar heat", Sun, mankind's future source of energy, p.547, Pergamon Press, (1978).

99. Swet C.J., "A prototype solar kitchen", Mechanical Engineering, p.35, August, (1974).

100. Hofmann J., Low Temperature Thermal Energy Storage Utilising Shell and Tube Technology, Master Thesis, Department of Mechanical Engineering, University of Natal, Durban, South Africa, (1993).

101. Efficiency of different types of hotplates, Government of Western Australia, Sustainable Energy Development Office.

http://www1.sedo.energy.wa.gov.au/pages/cooktops.asp